Mechanistic Studies of Vertebrate Hedgehog Signaling

Dissertation advisor: Dr. Adrian Salic Hanna Tukachinsky

Mechanistic Studies of Vertebrate Hedgehog Signaling

Abstract

Metazoans use Hedgehog signaling to direct many stages of embryonic development, and deregulation of this pathway is implicated in many types of cancer. I investigated several steps of Hedgehog pathway transduction that were poorly understood in mechanistic terms.

The mature Hedgehog ligand is produced by a self-proteolysis reaction that covalently attaches a cholesterol molecule to the signaling half of the protein. I showed that the catalytic cysteine forms a disulfide bridge that is essential for the folding and function of the C-terminal tail of Hedgehog, and identified two protein disulfide isomerases that remodel this bridge to free the catalytic thiol group after folding is complete. Using pulse chase assays to follow Hedgehog processing, I demonstrated that the self-proteolysis reaction takes place in the endoplasmic reticulum, that the cleaved C-terminal tail of Hedgehog is degraded before moving to the Golgi, and that Hedgehog mutants defective in processing get degraded in their entirety by the same route.

Lipidated Hedgehog ligand requires the transmembrane protein Dispatched for secretion. I devised a system to test Dispatched function in cultured cells, and showed that some inactive Dispatched mutants fail to bind Hedgehog, while others bind more tightly than the wild type protein. Scube2 was implicated as a Hedgehog pathway component in zebrafish genetic studies. I showed that Scube2 is a secreted protein that binds Hedgehog via its cholesterol adduct and solubilizes it in aqueous media. Dispatched and Scube2 bind Hedgehog on opposing faces, and they function synergistically to release it from the membrane.

Vertebrate Hedgehog signaling relies on intraflagellar transport through an antenna-like organelle called the primary cilium. The Hedgehog receptor Patched and transducer protein Smoothened localize to primary cilia in a mutually exclusive pattern, depending on Hedgehog ligand presence. I showed that cytoplasmic components of the pathway Suppressor of Fused (SuFu, a pathway inhibitor) and Glioma-associated oncogene transcription factors (the Gli family, the effectors of the pathway) localize to primary cilia and accumulate there when Smoothened is activated. SuFu and Gli form a complex that dissociates when the pathway is turned on, and this dissociation depends on trafficking through the cilium.

Table of Contents

List of Figures and Tables

Acknowledgments

Firstly, I would like to thank my parents, Alexander and Galia, for many things, not least of which is bringing me to the United States where I suspect my prospects are better than where we were born. I want to thank them for financially supporting me until I began graduate school, and still supporting me over the phone nowadays. I'd also like to thank my brothers Eli and Ari, who were still very much children when I began graduate school but are now a source of support and advice. I'd like to thank my sister Tali who was only a year old when I left for college and somehow managed to grow up into one of my best friends.

I'd like to thank my best friend from college, Elspeth Reed, who has written stories I'll never forget, planned out great vacations, and has given me a *raison d'etre* several times over these years. I'd like to thank my close friends from my graduate school class, Michael Chao and William Pastor. Their friendship got me through the first year of graduate school, and although like every BBS group our meetings dwindled in frequency over the years I always knew I had two people I could count on to put me in a better mood. I'll always cherish Will's slightly absurd impulses to go on adventures and drunken trivia talents, and Mike's love of the outdoors and knack for just the right amount of skeptical sarcasm to be hilarious instead of depressing.

To say members of my lab have been like family is understatement, given how much time I've spent with them. I'd like to thank Lyle Lopez for being here with me all these years. I want to thank him for recommending Adrian's lab, for collaborating with me on our First Real Paper (TM), for filling me in on 80's and 90's rock, and for being the most amazing combination of conscientious and chill that I've ever met. I also want to thank him for always managing to find the time to help me out when I most needed it, including during the writing of this dissertation. I'd like to thank Cindy Jao. I always admired and tried to emulate the careful way

she did experiments and her no-nonsense approach to solving problems. I'll always remember our movie nights, our tongue in cheek (right?) discussions of celebrity gossip, and the few times she managed to inspire me to go to yoga together. I miss her. I'd like to thank Daniel Nedelcu, who was my late night lab buddy and fellow energy drink connoisseur. Although many of our conversations have sounded like arguments over the years, I was always happy to have someone to talk to at night. I'd like to thank Ryan Kuzmickas with whom I collaborated on a project and who made postseason baseball a lot more fun through our pseudorivalry. I'd like to thank Kostadin Petrov who has been my go-to for informed opinions on fashion, anime, and the latest paper published in our field.

I'd like to also thank my dissertation committee-- Drs. Randy King, Tom Rapoport and Malcolm Whitman-- for providing fresh perspectives on scientific problems I was trying to solve. I would especially like to thank Tom who afforded me the opportunity to work on a paper with some of his lab members, which led me to a whole new set of experiments that turned into a story. I'd like to thank several collaborators from outside my laboratory: Xin Chen for her generosity, Sol Schulman for helpful experimental advice, and Wilhelm Haas for patiently doing many iterations of mass spectrometry experiments.

Last but certainly not least, I want to thank my advisor, Adrian Salic, with whom I have had the privilege to spend a lot of time. Among a myriad of things to be grateful for, I'd especially like to thank Adrian for keeping our young lab well-funded, for teaching me to be a good scientist at the bench (by example!), for refining my scientific taste, and for being that witty, fun person in the next bay over all these years. I can only hope some of his talent and work ethic has rubbed off on me.

CHAPTER ONE:

GENERAL INTRODUCTION

Overview of Hedgehog Signaling Roles in Metazoans

Higher metazoan development is a process in which a single starting cell becomes a complex organism possessing differentiated tissues that will not only carry out different tasks but also be organized in formations that will function as a coherent whole and sustain life. Such a process requires cell-cell communication during embryogenesis, as each genetically identical cell must properly self-identify and carry out division, movement, and differentiation accordingly.

The role of Hedgehog in *Drosophila* segmentation

The body plans of higher animals are constructed from repeating segments, and the genes that establish and define these segments were first discovered in *Drosophila melanogaster*. Fly embryos establish an anterior/posterior (A/P) and dorsal/ventral axes based on maternally deposited mRNA transcripts, and then proceed to subdivide segments along the A/P axis by a cascade of sequential activation of transcription factors. The opposing gradients of four maternal factors turn on transcription of different gap genes which are translated in different latitudes on the A/P axis. Nearly all gap genes encode transcription factors, which in turn drive the transcription of pair-rule genes. It is the pair-rule genes that subdivide the embryo into seven segments, and turn on segment polarity genes. Much of this process occurs without cell division, but the nuclei divide and eventually become separated into individual cells. The segment polarity genes further divide the embryo into 14 segments, the final number, and maintain each segment identity and boundary. Segment polarity genes can no longer all be transcription factors, because the cells of the embryo are now separated, and communication has to occur intercellularly. In parallel, the homeotic genes activate and endow each equivalent segment with its own identity (Lewis, 1978).

In a classic screen for segmentation mutants, Nusslein-Volhard and Wieschaus used the development of the cuticle as an easy visual readout for mutations that affect embryonic patterning (Nusslein-Volhard and Wieschaus, 1980). Mutants were grouped into the appropriate tier of segmentation genes by the phenotype of segments: mutation of segment polarity genes result in deletions in each segment, mutation of pair-rule genes shows deletions of alternating segments, and mutation of the gap genes shows stretches of segments disappearing. The screen identified, among others, a segment polarity gene they named *hedgehog*, for the stubby appearance of the embryo that was densely covered with denticles instead of having them spaced out in a stripe pattern.

Hedgehog functions as a segment polarity gene in the early stages (9-10) of embryogenesis. It is an intercellular signaling molecule produced in cells that express segment polarity gene and transcription factor Engrailed. The Engrailed stripes are established one step earlier by pair-rule genes. Hedgehog signaling to adjacent anterior cells turns on the Wingless pathway. Cells producing the Wingless signaling molecule in turn signal back and drive Engrailed expression in the adjacent cell. This positive feedback loop maintains the boundary between Hedgehog and Wingless signaling cells, which straddle the parasegment boundary (DiNardo et al., 1988; Martizez Arias et al., 1988). In later stages, Engrailed no longer relies on Wingless signal for expression and both the Wingless and Hedgehog pathways participate in patterning by interacting with homeobox gene expression.

The role of Hedgehog in vertebrate embryogenesis

Mammals and birds use three homologs of *Drosophila* Hedgehog. Sonic hedgehog (Shh) has the broadest role in mammalian embryogenesis, and its mutation results in the most profound

birth defects. Desert Hedgehog (Dhh) is most closely related to the *Drosophila* gene and is important to gonadal development. Mutation of *DHH* results in Swyer syndrome, where genetic males develop as females. Indian Hedgehog (Ihh) directs the growth of cartilage and bone, and its mutation results in brachydactyly. Fish also use Tiggy-Winkle, Echidna, and Qiqihar hedgehog paralogs during embryonic patterning.

The classic example of the prominent role Shh plays in early vertebrate embryogenesis is the patterning of the central nervous system. The notochord is a spinelike organ which mostly serves to coordinate signaling, and is later lost, becoming a part of the intervertebral discs. The notochord is responsible for patterning the neural tube that lies dorsally to it. The ventral side of the neural tube must differentiate into motor neurons, while the dorsal side turns into sensory neurons. During embryonic development, the notochord secretes Shh. The ligand diffuses and establishes a morphogen gradient on the neural tube (Echelard et al., 1993; Krauss et al., 1993; Roelink et al., 1994). The neurons closest to the notochord receive the highest dose and become the floor plate, which also starts secreting Shh ligand (Placzek et al., 1990). Bone morphogenetic factor (Bmp) secreted from the ectoderm forms an opposing gradient. Bmp and Shh establishe the dorsal/ventral axis of the neural tube and specify neurons into different fates depending on their position (Liem et al., 1995).

The role of Shh in craniofacial development is well established. In the absence of Shh signaling, the brain fails to form a ventral midline and separate into two hemispheres, resulting in a condition called holoprosencephaly. Most holoprosencephaly is embryonic lethal. Milder forms may result in the birth of organisms with facial abnormalities like cyclopia, anosmia, a single central incisor, and cleft palate (Chiang et al., 1996).

Shh signaling is also important to patterning of the limb bud, and only one digit forms on each limb in its absence. During development, Hedgehog signal is produced by a region of mesenchyme known as the zone of polarizing activity, which is found on the posterior side of the limb bud. High Shh concentrations specify posterior digits and low concentration specifies the thumb (Riddle et al., 1993; Lopez-Martinez et al., 1995).

Segmentation is much less apparent in vertebrates, and is believed to rely on periodic oscillations of genes rather than transcription factor gradients, but many of the general principles remain. In vertebrates, somites act analogously to arthropod segments. Somites are groups of mesodermic cells that turn into segmented structures like the axial skeleton (sclerotome), skeletal muscles (myotome), and skin (dermomyotome). Hedgehog signaling plays a less obvious role in segmentation of vertebrates, which relies on the pathways Notch and Wnt for boundary establishment. Nevertheless, somitic cells express the Hedgehog receptor Patched, and Sonic hedgehog influences the differentiation of somites of the ventral part of the sclerotome by secretion from the nearby neural tube (Fan and Tessier-Lavigne, 1994; Marigo and Tabin, 1996). In further support of the role of Hedgehog in vertebrate segmentation, its mutation results in defects of the spine and ribs (Chiang et al., 1996).

Hedgehog signaling is also used throughout later stages of embryogenesis, and is involved in the formation of many other organs including the lungs, heart, pancreas, prostate, mammary glands, pituitary gland, and the visual system (reviewed in (McMahon et al., 2003)).

The role of Hedgehog in adult organisms

After the signaling-intensive period of embryogenesis is complete, the Hedgehog pathway is repurposed for directing functions that require cell division and differentiation.

Hedgehog participates in the growth of epithelial structures like hair, nails, scales, and feathers, as well as tooth formation. It supports the function of organs with high turnover, such as the lining of the gastrointestinal tract, as well as differentiation processes like hematopoeisis. Hedgehog is also involved in skin, cartilage, and bone repair and drives differentiation of stem cells in response to trauma. It has also recently been shown to play a role in axonal guidance (reviewed in (McMahon et al., 2003; Sanchez-Camacho and Bovolenta, 2009).

There is intense pharmacological interest in the Hedgehog signaling pathway because of its role in cancer initiation and progression. The types of carcinomas that utilize Hedgehog signaling for proliferation can be grouped into those that tend to be ligand dependent (even if autocrine) and those that are ligand independent, involving components downstream of the Patched receptor. Gliomas (Dierks et al., 2007; Ehtesham et al., 2007), colorectal (Mazumdar et al., 2011), upper gastrointestinal tract cancers (Berman et al., 2003), prostate (Karhadkar et al., 2004; Sanchez et al., 2004), and breast cancers (Kubo et al., 2004) tend to be ligand dependent. On the other hand, medulloblastomas (which involve mutations in *PTCH1, SMO,* or *SUFU)* tend to be ligand independent (Goodrich et al., 1997; Reifenberger et al., 1998; Taylor et al., 2002). Basal cell carcinomas often carry mutations in *PTCH1* and *SMO* (Gailani et al., 1996; Hahn et al., 1996; Lam et al., 1999) whereas cancers of the pancreas carry mutations of *GLI1* and *GLI3* (Thayer et al., 2003). Rhabdomyosarcomas tend to be caused by mutations in *PTCH1* and *SUFU* (Tostar et al., 2006), and in Ewing sarcoma transcription of *GLI1* is directly activated by the Ews-Fli fused transcription factor (Beauchamp et al., 2009).

Ligand dependent tumors or those that result from a mutation in Patched can be treated with antagonists of the most drug-susceptible protein in the pathway, Smoothened. In 2012, Smoothened inhibitor vismodegib (GDC-0449) was approved by the Food and Drug

Administration as a treatment for basal cell carcinoma. Those tumors with inactivating mutations of *SUFU* or activating mutations in *SMO* or *GLI* are more difficult to treat, and any targeted chemotherapeutic agent would have to be cell permeable and inhibit Gli.

Overview of Hedgehog Signal Transduction

Lipid modification of the Hedgehog protein

Hedgehog is synthesized as a 45 kDa precursor protein. After co-translational translocation in the endoplasmic reticulum (ER), the signal sequence is cleaved off (Lee et al., 1992). Hedgehog is palmitoylated on its N-terminus and undergoes a unique self-proteolysis reaction to attach a cholesterol adduct to the C-terminus of the cleaved N-terminal product. The final ligand is a doubly lipidated 19 kDa protein. It is the only protein known to undergo covalent modification with a cholesterol molecule.

Sterolation of the Hedgehog protein

The Hedgehog gene is believed to have evolved from a fusion of two disparate ancient genes. Part of the C-terminal autoprocessing domain resembles an intein. Inteins are defined as segments of proteins that can catalyze their own excision and join back the two pieces of the polypeptide in which they were embedded. True inteins are self-propagating and include a bifunctional homing endonuclease domain inserted into a protein splicing domain (reviewed in (Chevalier and Stoddard, 2001)). In a host that encodes the intein, entry of intein-less alleles can occur via conjugation, transduction, transformation, or sex. The homing endonuclease creates double strand breaks in specific intein-less regions, and DNA repair then converts the wild type allele into the intein-containing allele using the host's other copy of the gene (Gimble and

Thorner, 1992). Intein segments begin with an obligate cysteine or serine residue. In the first step of self-excision, the thiol or hydroxyl sidechain attacks the neighboring carbonyl in the peptide chain, generating a thioester intermediate. The second step involves the same attack by a hydroxyl or thiol group of an amino acid further away, C-terminal to the intein domain. This transesterification reaction produces a branched intermediate. The next step is irreversible and involves the cyclization of the sidechain of an obligate asparagine residue at the end of the intein, resulting in excision of the intein with a five member aminosuccinimide ring on its end. The last step is a spontaneous S-N or O-N shift of the ligated polypeptide to produce a stable protein with no trace of having had a segment inserted into it before (Figure 1.1, left side) (Xu et al., 1994; Shao and Paulus, 1997).

Hedgehog's autoprocessing domain is part of a large family of domains called Hint (Hedgehog intein) that are widespread in single celled organisms in the fungi, protist, eubacteria, and archaebacteria kingdoms. Despite being a degenerate homolog, the Hedgehog C-terminal tail crystal structure aligns with those of self-propagating inteins (Hall et al., 1997). The Hedgehog protein thus represents ancient metazoans harnessing the ability of an intein to ligate surrounding polypeptides, and redirecting its function to attach sterols to a protein.

Hedgehog's self-proteolysis reaction proceeds very similarly. The first step in cleavage is a nucleophilic attack by the sidechain of cysteine on the neighboring glycine carbonyl in a conserved GCF motif. In the transesterification step, it is the 3β hydroxyl group of a cholesterol molecule that attacks the same carbonyl, breaking the thioester bond and generating an ester linkage of the N-terminal half of Hedgehog to cholesterol. This is the active ligand (Figure 1.1, right side) (Porter et al., 1995; Porter et al., 1996a; Porter et al., 1996b).

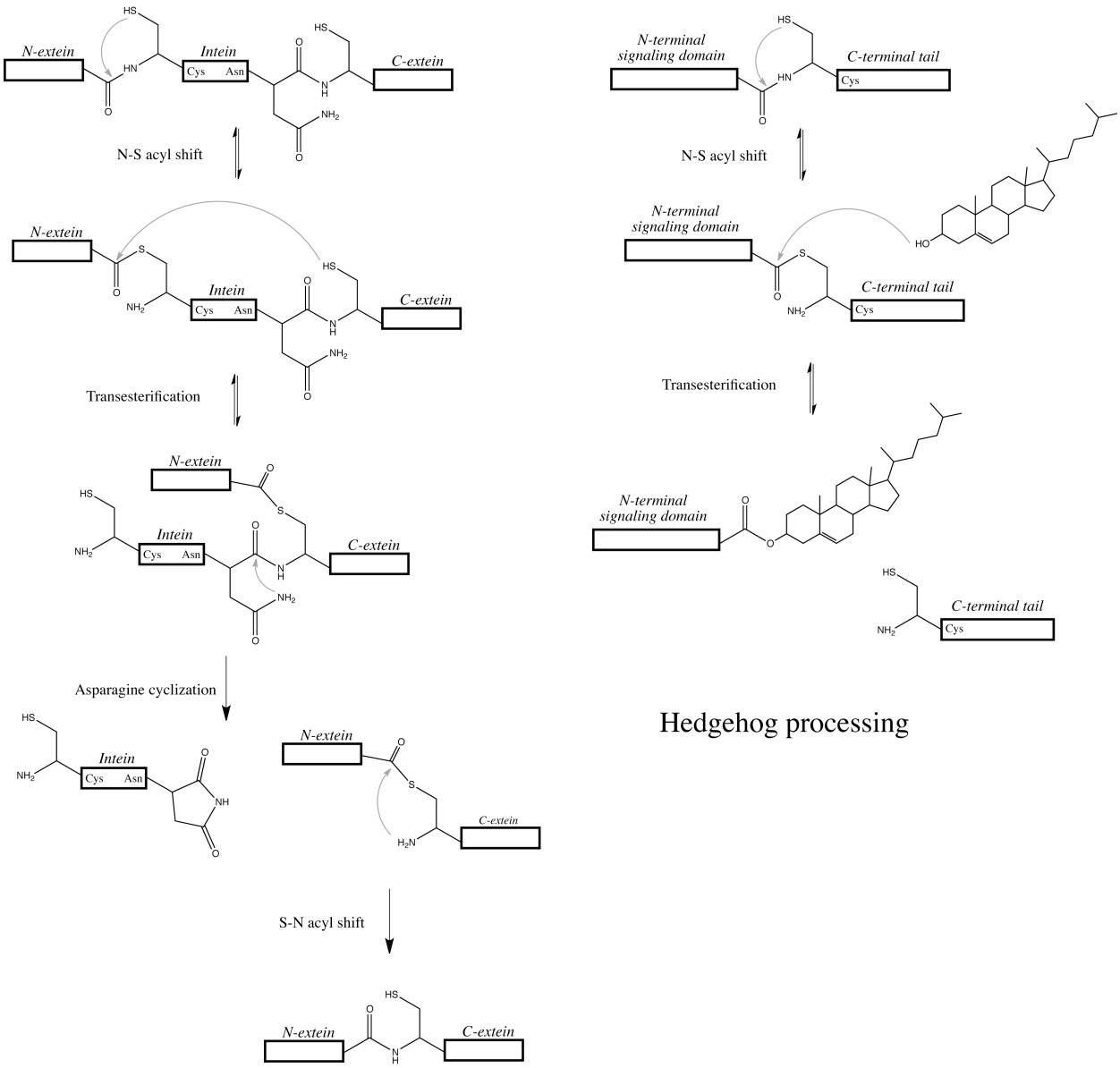

Figure 1.1 Comparison of intein excision and Hedgehog processing mechanism.
Adapted from Xu, Paulus & Chong, 2000 ; Mann & Beachy, 2004.

An important element of the Hedgehog C-terminus is the putative sterol recognition region (SRR) found in other Hog members. The Hedgehog cleavage reaction does not absolutely require cholesterol as it can be carried out in vitro in the presence of reducing reagents such as dithiothreitol, hydroxylamine and glutathione-- resulting in a cleaved Hedgehog protein that is not sterolated. Only the first 145 amino acids of the C-terminal tail are necessary for this

type of cleavage. In contrast, cholesterol addition requires most of the tail (Lee et al., 1994; Porter et al., 1995).

There are other genes in multicellular organisms that include a Hint domain fused to a different N-terminal domain. This group of more closely related Hint domains has been named Hog (for the latter half of Hedgehog). The most notable examples of non-Hedgehog Hog proteins are the Warthog, Ground, and Quahog found in *C. elegans*, an organism which lacks Hedgehog signaling, and uses these genes in unrelated ways for cuticle and extracellular matrix functions such as molting (Burglin, 1996; Aspock et al., 1999; Hao et al., 2006). Although some of the warthog genes are reportedly processed (Porter et al., 1996b), there is no evidence of cholesterol incorporation by any protein other than Hedgehog, despite conservation of the SRR in *C. elegans* hog proteins (Aspock et al., 1999). It is possible that there are other sterols or lipids being attached in the worm.

Palmitoylation of the Hedgehog protein

The common form of palmitoylation involves a cotranslational addition of a palmitate (C16:0) to a cysteine residue of a cytoplasmic protein by thioester linkage (S-palmitoylation). This is a dynamic lipid modification, and its addition and removal can be used to cyclically control a protein's affinity for membranes. Less common is the addition of the palmitate adduct to an N-terminal cysteine of a lumenal protein via a stable amide linkage. This is the type of palmitoylation that Hedgehog undergoes. It is performed in the endoplasmic reticulum by a membrane bound O-acyltransferase (MBOAT) family, discovered by four groups an alternatively named Rasp/Ski/Sit/Cmn in flies, or Hedgehog acetyltransferase (HHAT) in

vertebrates (Amanai and Jiang, 2001; Chamoun et al., 2001; Lee and Treisman, 2001; Micchelli et al., 2002).

The effect of lipid modifications on signaling molecules

It may seem surprising that signaling molecules destined for secretion and diffusion across multiple cells would be modified with hydrophobic adducts that increase their affinity to cell membranes. This section will compare the effects of acylation and sterolation on Hedgehog, Spitz, Wnt, and the hormone ghrelin on diffusion rate, receptor affinity, and ligand potency.

In *Drosophila*, there is another signaling molecule that is modified by the same palmitoyltransferase as Hedgehog: the EGFR ligand Spitz. Spitz is synthesized as a membrane tethered lumenal protein that undergoes proteolytic cleavage by intramembrane protease Rhomboid (Urban et al., 2001) and is subsequently palmitoylated on its N-terminal cysteine by Rasp, the HHAT *Drosophila* homolog (Miura et al., 2006). When Spitz is not palmitoylated, both its secretion rate and diffusion range increase, as might be expected with decreased overall hydrophobicity. In whole animals, *rasp* mutation leads to dysfunctional attenuated Spitz signaling as assayed in retinal patterning. Likewise, when the palmitoylated cysteine of Spitz is mutated to a serine, Spitz is unable to rescue the lethality of *spitz* mutant organisms (Miura et al., 2006). One possible explanation for this is that the palmitate adduct is essential for receptor binding or activation, but the palmitoylated and unpalmitoylated Spitz ligands have the same affinity for the EGF receptor and similar potency to activate it in vitro (Miura et al., 2006). This highlights the notion that increasing the range and diffusion of a morphogen can lead to an inability to signal properly in a physiological context. Spitz is designed as a relatively short-

distance morphogen with a steep gradient, and requires high local concentrations to induce its targets.

The Wnt family of proteins are ligands for the eponymously named pathway, and are homologs of the *Drosophila* segmentation polarity gene *wingless* mentioned earlier. The Wnt proteins are S-palmitoylated on an internal cysteine by the acyltransferase Porcupine (Kadowaki et al., 1996; Tanaka et al., 2000) One of the Wnts, Wnt3a, is also modified with palmitoleate (C16:1) on a serine residue (Takada et al., 2006). It is worth noting that this palmitoylation of a lumenal protein differs from the S-palmitoylation of cytoplasmic proteins, and there is no evidence that the modification is dynamic. Secretion of Wnt ligand is unaffected by mutation of the palmitoylated cysteine (Willert et al., 2003), while Wingless secretion is severely compromised by the protein's resultant misfolding (van den Heuvel et al., 1993). Mutation of the palmitoleated serine of Wnt3a also results in misfolding and retention of the protein in the ER (Takada et al., 2006).

The secreted unpalmitoylated Wnt mutant is not active, however. While it is possible that the palmitate adduct is required for proper folding of the protein, and the secreted Wnt is still slightly misfolded, wild type Wnt that is secreted after palmitoylation and subsequently treated with acyl protein thioesterase-1 is also inactive (Willert et al., 2003). It has since been demonstrated that unpalmitoylated Wnts have reduced binding affinity to their receptors LRP5, LRP6, and Frizzled (Komekado et al., 2007; Kurayoshi et al., 2007).

Ghrelin is a secreted hormone that stimulates growth hormone expression and the appetite in vertebrates. Ghrelin is n-octanoylated on the third serine via an ester bond by an enzyme from the MBOAT family (Kojima et al., 1999; Gutierrez et al., 2008; Yang et al., 2008). Although the majority of circulating ghrelin is not octanoylated, only the octanoylated molecule

has affinity for the growth-hormone secretagogue receptor and activity (Kojima et al., 1999; Hosoda et al., 2000). Perhaps because the hydrophobic chain is short, secretion and diffusion of ghrelin does not appear to be significantly reduced by lipid modifications, but there is some evidence that the octanoylated version requires a saturable transport system to cross the blood-brain barrier, while ghrelin lacking lipid modification diffuses in and out freely (Banks et al., 2002).

Hedgehog secretion is not affected by mutation of HHAT or the cysteine residue that is palmitoylated, but the ligand is inactive in terms of signaling (Pepinsky et al., 1998; Chen et al., 2004). The binding of unpalmitoylated Hedgehog to Patched does not appear to be significantly reduced. In one study, Hedgehog was tethered to the Patched receptor, and the constitutive signaling activity of this fusion was reduced in the absence of *rasp*, the *Drosophila* homolog of HHAT (Miura and Treisman, 2006). Even more convincingly, expression of Hedgehog incapable of being palmitoylated has a slight dominant negative effect in vivo, presumably by competing with wild type Hedgehog for Patched binding (Lee et al., 2001b; Gallet et al., 2006). A direct comparison of binding in a cell culture assay showed that unpalmitoylated Hedgehog binds Patched and competes with palmitoylated Hedgehog binding (Williams et al., 1999). The essential function of the palmitate adduct for signaling activity is not yet understood. It is possible to rescue the signaling activity of Hedgehog lacking palmitate by substituting other lipid modifications at the N terminus, such as myristate, which fully rescues signaling capability, but substitution with a stretch of amino acids with hydrophobic side chains resulted in very little activity (Taylor et al., 2001). Reception of the Hedgehog signal results in Patched internalization and turnover in the lysosome, and the ability of unpalmitoylated Hedgehog to induce this

internalization has not been measured. It is possible that the palmitate adduct is essential for recognition by a factor responsible for internalizing Patched complexed with Hedgehog.

The cholesterol moiety of Hedgehog is essential in that full length Hedgehog mutants that fail to self-proteolyse are inactive and cause holoprosencephaly (Nanni et al., 1999; Maity et al., 2005). In chapter 2 of this dissertation I outline the mechanism by which these mutants are degraded before ever reaching the plasma membrane.

A signaling domain of Hedgehog lacking a cholesterol adduct can be easily generated by truncating the protein at the modified glycine residue. The resultant Hedgehog protein is secreted freely from cells, unlike the wild type dually lipidated version or the palmitoylation site mutant which is still sterolated. This argues that it is cholesterol and not palmitate that is mainly responsible for Hedgehog's strong membrane affinity (Porter et al., 1995). The potency of this truncated ligand is much stronger than that of the unpalmitoylated mutant, but is still significantly less than that of the dually lipidated Hedgehog, despite similar affinity for the Patched receptor, as directly measured in a cell culture assay (Williams et al., 1999). One possible explanation for this reduced potency is that Hedgehog that does not get modified by cholesterol is also less efficiently palmitoylated, either because it migrates faster through the secretory pathway or because it has less affinity for the acyltransferase. This would result in a mixture of Hedgehog ligands with increased numbers of inactive, unpalmitoylated proteins and reduced overall potency. Supporting this explanation, the study that identified the HHAT detected only three species of Hedgehog after transfection into insect cells: unprocessed, sterolated, and dually lipidated (Pepinsky et al., 1998). However, a different study measured [3H]palmitate incorporation into processed and truncated Hedgehog proteins, and found them to

be equal (Chen et al., 2004). Thus, the cholesterol adduct does seem to have a role independent of the palmitate adduct in terms of ligand potency.

	Enzyme	Secretion	Receptor Affinity	Potency
Ghrelin- Loss of octanoylation	GOAT	Similar	Similar	None
Spitz- Loss of palmitoylation	Rasp	Greater	Similar	Similar
Wingless -Loss of palmitoylation	Porc	None	-	-
Wnt - Loss of palmitoylation	Porc	Similar	Low	Low
Hedgehog- Loss of palmitoylation	Rasp/HHAT	Similar	Similar	None
Hedgehog- Loss of cholesterol via truncation	-	Greater	Similar	Lower
Hedgehog- Loss of cholesterol via faulty processing	self-catalysis	None	-	-

Table 1.1. A summary of the consequences of losing lipid adducts on signaling molecules

Unlike the free diffusion of truncated Hedgehog, secretion of cholesterol modified Hedgehog depends on the actions of a twelve pass transmembrane protein called Dispatched, distantly related to the Hedgehog receptor Patched (Burke et al., 1999; Caspary et al., 2002; Kawakami et al., 2002; Ma et al., 2002). The similarity between the proteins, and their relationship to other sterol interacting proteins will be discussed in a later section. Dispatched is not required in the cells receiving the Hedgehog signal, does not affect Hedgehog lipid modification, and is not involved in trafficking cholesterol-modified Hedgehog to the plasma membrane. In fact, *disp-/-* cells can still signal to immediately adjacent cells (Caspary et al., 2002). It is not known what function Dispatched is performing on a molecular level, but its homology to resistance-nodulation-division (RND) permeases in bacteria that form homotrimeric pumps suggests a transporting or flipping action that might drive the cholesterol adduct out of the plasma membrane.

The decreased membrane affinity and concomitant reduction in potency of the uncholesterated Hedgehog has resulted in a contradictory literature about the role of the cholesterol adduct in vivo and in terms of long range signaling. In *Drosophila*, there are reports that Hedgehog without the cholesterol moiety has increased range (Burke et al., 1999; Dawber et al., 2005; Callejo et al., 2006), while in another study, cholesterol modification was required for activating long range targets (Gallet et al., 2006). In the vertebrate limb bud, Hedgehog lacking cholesterol failed to activate long range targets in experiments by one group (Lewis et al., 2001), while a different group saw Hedgehog lacking cholesterol spread further and activate Hedgehog ectopically in the same system (Li et al., 2006).

Models have also been proposed to explain the supposed requirement of cholesterol modification for long range signaling, such as the requirement for cholesterol adducts to form Hedgehog multimers or be incorporated into lipoprotein particles that can travel greater distances than the truncated Hedgehog proteins diffuse (Zeng et al., 2001; Chen et al., 2004; Panakova et al., 2005; Goetz et al., 2006; Callejo et al., 2008). A simpler explanation is that the effects of cholesterol on Hedgehog range may be comparable to the effects of palmitoylation on Spitz--that is, that the lipid adduct is not increasing the range of Hedgehog, but rather allowing it to concentrate and activate targets at the appropriate distances from the secreting cells. The differences between different groups might be attributable to different levels of overexpression of Hedgehog constructs, where experiments performed with higher levels of Hedgehog reveal the longer range of truncated Hedgehog while others do not detect tissue responses of diluted Hedgehog that has spread further.

In the context of whole organisms, lipid modifications are essential for all of the signaling molecules discussed above. Even when the lipid adduct does not contribute to ligand

potency in vitro, it is invariably essential for properly limiting ligand spreading and delivering appropriate dosages to the cells anticipating the signal. It is interesting how fine-tuned these systems appear to be, given that the same type of ligand travels variable physical distances in different organisms, and in different locations within the same organism. Lipid modifications may provide convenient "handles" that can interact with factors at the site of secretion, the site of reception, and anywhere along the intervening journey. This allows for modulation of the steepness and distance of morphogen gradients.

In chapter 3 of this dissertation, I present work on secreted protein Scube2 that interacts with the cholesterol adduct of Hedgehog and dramatically increases its diffusion from cells, providing a possible mechanism for long range movement of cholesterol modified Hedgehog.

Hedgehog receptor Patched

Patched, a twelve pass transmembrane protein, is the main Hedgehog receptor and binds the Hedgehog protein directly (Hooper and Scott, 1989; Ingham et al., 1991; Marigo et al., 1996; Stone et al., 1996). In the absence of Hedgehog, Patched is active and inhibits 7-pass transmembrane protein Smoothened, which is an activator of the pathway. When Hedgehog binds Patched, it is inhibited, and Smoothened is derepressed, activating downstream steps of the pathway (Ingham et al., 1991). In the absence of Patched, the Hedgehog pathway is constitutively activated. Hedgehog binding appears to inhibit Patched activity by triggering its internalization and destruction in the lysosome (Incardona et al., 2000; Gallet and Therond, 2005).

Patched inhibits Smoothened substoichiometrically, arguing that its action is catalytic (Taipale et al., 2002). Like Dispatched, Patched bears resemblance to RND permeases, and is

believed to act as a pump or flippase to control the location of a small molecule that affects Smoothened activity. There may be divergence between vertebrate and arthropod signaling at this step, as *Drosophila* Smoothened does not bind the same small molecules as vertebrate Smoothened. Patched is also a target of the pathway, which acts as a negative feedback loop in which activation of the pathway also produces more of the pathway's negative regulator. In the context of Hedgehog migration across tissue, this negative feedback loop also functions to steepen the Hedgehog gradient, since the cells closest to the source are activated first and produce more receptor in response. (Chen and Struhl, 1996; Gallet and Therond, 2005).

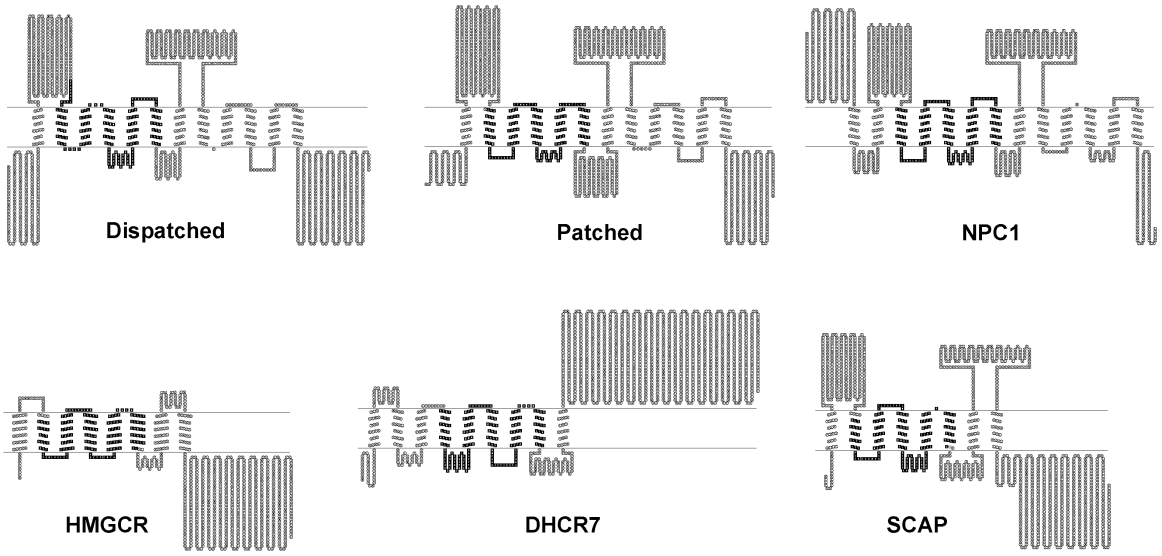

Figure 1.2 Proteins containing sterol sensing domains.
Every protein is oriented with the cytoplasmic face of the membrane on the bottom and the extracellular face on top. Sterol sensing domains are highlighted in bold. Created using UniProt annotations and TOPO2 Transmembrane protein display software. http://www.sacs.ucsf.edu/TOPO2/

Sterol sensing domain proteins

Sterol sensing domains (SSDs) are defined as spans of five consecutive transmembrane helices constituting ~180 amino acids. These domains have no proven function but are conserved among several proteins involved in sterol homeostasis and trafficking, and certain point mutations in these domains dramatically affect the proteins' function. This section will

review the group of proteins that possess this domain before returning to Dispatched and Patched and examining what role the SSD might play in their function.

An SSD is found in HMG-CoA reductase (HMGCR), an eight-pass transmembrane ER-resident protein that converts HMG-CoA to mevalonate. The SSD is not needed for its enzymatic activity but is required for sterol-level induced degradation (Gil et al., 1985; Sever et al., 2003). Another enzyme in the cholesterol biosynthetic pathway that contains an SSD is 9-pass transmembrane protein 7-dehydrocholesterol reductase (DHCR7). DHCR7 converts 7-dehydrocholesterol into cholesterol, and cholest-5,7,34-trienol into desmosterol (which is then converted to cholesterol) in an alternative pathway. Mutation of this enzyme blocks cholesterol production and precursors and their derivatives accumulate. This defect in cholesterol biosynthesis results in Smith-Lemli-Opitz syndrome, which is characterized by many developmental abnormalities affecting virtually every organ system, because of cholesterol's role as an integral component of cell membranes as well as a precursor for bile acids and steroidal hormones (reviewed in (Jira et al., 2003)).

Besides biosynthetic enzymes, SSDs are found in a protein that regulates cholesterol homeostasis. Transcription of cholesterol uptake receptors and cholesterol biosynthetic pathway genes is controlled by cis-acting sterol regulatory elements (SRE), which are activated by the binding of transcription factor SRE binding protein (SREBP). SREBP is normally found in an inactive, membrane-bound state in the ER, and SREBP cleavage activating protein (SCAP) is bound to a resident ER protein Insulin induced gene 1 (Insig1) (Yang et al., 2002). When cholesterol levels in the ER fall, Insig and SCAP dissociate and SCAP binds SREBP and transports it to the Golgi, where enzymes S1P and S2P cleave SREBP and release the transcription factor segment into the cytoplasm (Sato et al., 1994; Wang et al., 1994; Hua et al.,

1996; Sakai et al., 1996). SCAP is an eight pass transmembrane protein that contains an SSD and functions as the cholesterol sensor in the circuit. Mutation of conserved aspartate 443 in the SSD to alanine renders SCAP unresponsive to sterols-- not binding to Insigs in the presence of high cholesterol, and driving transcription of SRE genes constitutively (Yabe et al., 2002).

The SSD is also found in a protein that is involved in intracellular cholesterol transport. Niemann-Pick protein C1 (NPC1) was identified as a locus for the recessive autosomal disease it is named after. Niemann-Pick disease is characterized by aberrant cholesterol trafficking, where unesterified cholesterol that was taken in via LDL particles stays in late endosomes/lysosomes and fails to redistribute to other membranes (Blanchette-Mackie et al., 1988; Sokol et al., 1988). The three organs that are particularly affected are the spleen, the brain, and the liver, which takes up excess cholesterol from the blood. NPC1 is a 13 pass transmembrane protein that resides in endosomes (Garver et al., 2000), and whose SSD is in transmembrane helices 3 through 7. NPC1 has been demonstrated to bind cholesterol directly using a photoactivatable cholesterol analog (Ohgami et al., 2004). This binding activity was dependent on a functional SSD. NPC1, like Patched and Dispatched, shows homology with the RND permease family in prokaryotes. Indeed, Escherichia coli made to express mammalian NPC1 transported acriflavine and oleic acid across membranes (Davies et al., 2000). NPC1 acts together with a partner protein, NPC2, which is a luminal/extracellular small protein that also binds cholesterol directly (Friedland et al., 2003; Ko et al., 2003). NPC2 can shuttle cholesterol between NPC1 and membranes (Infante et al., 2008). The current model for the action of these two proteins is that NPC2 grabs cholesterol freed from LDL particles in the lysosome and hands them off to NPC1, which inserts cholesterol molecules into the membrane, allowing for them to be transported out of the lysosomes to the plasma membrane or ER. Unexpectedly, mutation of conserved SSD aspartate 787 to asparagine

(in a similar position to the aspartate 443 of SCAP mentioned before) results in a gain-of-function mutant of NPC1, which reportedly increases cholesterol trafficking to the plasma membrane and ER (Millard et al., 2005). Other mutations in the SSD do disrupt NPC1 function (Watari et al., 1999).

The SSDs of Patched and Dispatched are clearly required for their function, as mutation of the conserved aspartates result in constitutive signaling in the case of Patched (Strutt et al., 2001; Taipale et al., 2002) and an inability to secrete Hedgehog signal in the case of Dispatched (Ma et al., 2002). Dispatched works to secrete only sterolated Hedgehog, and is thus likely to bind cholesterol directly. Patched, on the other hand, can be easily activated with Hedgehog lacking a cholesterol adduct, and mutation of the SSD does not affect its ability to bind Hedgehog (Strutt et al., 2001). Rather, the SSD of Patched must function in sterol interaction in its catalytic activity of inhibiting Smoothened. The developmental defects in Smith-Lemli-Opitz syndrome resulting from DHCR7 mutation seem to include defects in Hedgehog signaling, and it is believed that the defect is not at the level of Hedgehog ligand sterolation, but rather a faulty response by Smoothened (Koide et al., 2006).

Given the conservation of the SSD in proteins that are known or believed to bind sterols, it is tempting to ascribe direct cholesterol binding activity to this domain. Contrary to expectations, a cholesterol binding site on SCAP was recently mapped to a lumenal loop, and mutating one tyrosine residue to alanine in this loop mimics cholesterol binding—resulting in a constitutively inactive protein that remains bound to Insig (Motamed et al., 2011). This finding raises the possibility that a protein like Dispatched might bind the cholesterol adduct of Hedgehog not with the SSD but an extracellular loop, and thus act to lift lipidated Hedgehog out of the plasma membrane to encourage its secretion.

Accessory Hedgehog receptors

Although Patched binding to Hedgehog is the signal transducing event, there are many cell surface proteins that act as accessory receptors, and in some cases as inhibitory binders that modulate the signal. Identification of these coreceptors has lagged behind that of other pathway components because of functional redundancy, but taken together they play an essential role in Hedgehog signal reception. Cdo and Boc are integral membrane proteins with immunoglobulin and fibronectin-like repeats, the latter of which bind Hedgehog (McLellan et al., 2006; Tenzen et al., 2006; Yao et al., 2006). Gas1 is another Hedgehog binding protein that is GPI anchored in the membrane and binds Hedgehog (Lee et al., 2001a; Martinelli and Fan, 2007). These components were shown to not only limit the range of Hedgehog by soaking it up, but also interact with Patched and form true coreceptors with increased affinity for Hedgehog than Patched alone (Zheng et al., 2010; Izzi et al., 2011). Vertebrates also express a transmembrane protein called Hedgehog interacting protein (Hip) that competitively binds Hedgehog on the same face as Patched and acts as an inhibitor (Chuang and McMahon, 1999; Bishop et al., 2009; Bosanac et al., 2009) Hip is a Hedgehog target and, like Patched, forms a negative feedback loop in the pathway.

In addition to the true receptors listed above, there is evidence that Hedgehog ligand forms at least transient interactions with elements of the extracellular matrix, and these interactions affect its rate of spreading. Heparan sulfate proteoglycans have been shown to have effects on Hedgehog ligand spreading and signaling. The initial observation implicating proteoglycans was the phenotype of the *tout-velu* (*ttv*) mutant in *Drosophila*, where Hedgehog was unable to diffuse to long range targets (Bellaiche et al., 1998). *ttv* encodes an enzyme involved in proteoglycan synthesis (The et al., 1999) and only affects movement of cholesterol-

modified Hedgehog (Callejo et al., 2006). Dally-like protein, a cell surface heparan sulfate proteoglycan, is essential for Hedgehog signaling in *Drosophila* (Lum et al., 2003a). In vertebrates, the role of proteoglycans is more questionable. In contrast to flies, deletion of vertebrate glypican proteins is reported to increase Hedgehog signaling in most cases (Capurro et al., 2008; Williams et al., 2010). Mutations of these glypicans cause phenotypes that might be associated with increased Hedgehog signaling, such as enlarged body size, but there are no profound developmental consequences that would be expected of a core Hedgehog pathway component.

Several other extracellular matrix proteins reportedly affect Hedgehog binding and spreading in vertebrates and flies, including basement membrane heparan sulfate proteoglycan perlecan (Park et al., 2003), secreted glycoprotein vitronectin (Pons and Marti, 2000), and transmembrane receptor of broad specificity LRP2/megalin (McCarthy et al., 2002). Like glypicans, it is unclear if any of these play a crucial role. It is possible that they have essential functions in specific tissue or particular stages of development.

The complexity of the cell surface system that binds Hedgehog probably stems from the multiple roles Hedgehog has in both embryogenesis and later tissue maintenance, and represents tissue adaptations to modulate signals.

Cytoplasmic signal transduction events in *Drosophila*

In *Drosophila*, there is one transcription factor that acts as both repressor and activator of Hedgehog target genes, encoded by segment polarity gene *cubitus interruptus* (*ci*). Ci in its full length form (Ci-155) includes a zinc finger DNA binding domain and a transcriptional activation domain. Ci-155 is partially degraded by the proteasome into a shorter form (Ci-75) that still

includes the DNA binding domain and acts as a repressor for the same genes it activates in its full length form. Activation of Smoothened shifts the balance from Ci-75 to Ci-155, leading to activation of Hedgehog targets. Despite the parsimonious use of one transcription factor, a graded response to Hedgehog signal can be achieved because some target genes are transcribed unless Ci-75 is actively repressing them (*hh*), some are transcribed regardless of Ci-75 and enhanced by activator Ci-155 (*ptc*), and others require the binding of Ci-155 and absence of Ci-75 for activation (*dpp*) (Aza-Blanc et al., 1997; Methot and Basler, 1999).

Ci is generally found in a complex containing kinesin Costal-2 (Cos2), serine/threonine kinase Fused (Fu), and negative regulator of the pathway Suppressor of Fused (SuFu) (Robbins et al., 1997; Sisson et al., 1997). The complex tethers to microtubules via Cos2 and keeps Ci out of the nucleus. Cytoplasmic Ci is subject to a sequence of events that includes phosphorylation by PKA, then CK1, and finally GSK3 (Jiang and Struhl, 1995; Wang et al., 1999; Price and Kalderon, 2002). Phosphorylated Ci is recognized by ubiquitin ligases and marked for degradation by the proteasome (Smelkinson et al., 2007). The Ci-75 form no longer associates with the Cos2 complex and enters the nucleus to repress transcription of target genes. Loss of Cos2 or any of the kinases that initiate the process of Ci degradation result in accumulation of Ci-155 and pathway activation (Wang and Holmgren, 1999; Zhang et al., 2005). Interestingly, it was observed that accumulation of Ci-155 did not correspond with full activation of the pathway, leading to hypotheses that Ci stabilization and activation were separate events and involved posttranslational modifications (Ohlmeyer and Kalderon, 1998). More recent models postulate that activation might simply entail nuclear entry, and that Ci-155 may be protected from partial degradation but still be kept out of the nucleus, perhaps by SuFu, which plays only a small role in *Drosophila* when other pathway components are intact. (reviewed in (Kalderon, 2004)).

Activation of Smoothened increases the rate of Ci entry into the nucleus before conversion to the Ci-75 form (Chen et al., 1999). The mechanism by which this happens is not yet fully understood. There is evidence that Smoothened directly binds the cytoplasmic Ci complex via Cos2, and that this association happens regardless of Hedgehog signal. What changes upon signal activation is that Smoothened and the Ci complex become enriched in the plasma membrane instead of the internal vesicles they favor when the pathway is not active (Jia et al., 2003; Lum et al., 2003b; Ogden et al., 2003; Ruel et al., 2003). Smoothened might induce the phosphorylation and activation of Fu kinase, which in turn phosphorylates Cos2 and SuFu. This leads to a dissociation of Ci from the complex (Liu et al., 2007; Ruel et al., 2007).

Vertebrate cytoplasmic components of the pathway

The function of Cubitus interruptus is split into three related proteins in vertebrates, Gli1, 2, and 3-- named for Gli1's identification as a gene amplified in glioblastomas (Kinzler et al., 1987). Unlike its homologs, Gli1 does not have the N-terminal repressor domain and functions exclusively as an activator of target genes (Sasaki et al., 1999). It does not undergo partial degradation by the proteasome (Dai et al., 1999; Ruiz i Altaba, 1999). Gli1 is only synthesized in response to pathway activation, and so represents a positive feedback mechanism to strengthen the signal. Gli2 and Gli3 are more similar to Ci, in that they can act as both repressors and activators of target genes (Ruiz i Altaba, 1999; Shin et al., 1999). Gli2 is believed to function primarily as an activator. Like Gli1, it is a pathway target, and the partially degraded form is either nonexistent or rare in physiological contexts. Gli3 is primarily a repressor, and is robustly converted by the proteasome into the shorter form (Dai et al., 1999).

Vertebrate Hedgehog signal transduction from Smoothened to the nucleus has diverged from that in *Drosophila*. The homologs of negative regulators Cos2 and Fu do not produce Hedgehog phenotypes when deleted (Chen et al., 2005; Merchant et al., 2005). Meanwhile, SuFu, which is a minor player in *Drosophila*, turns out to be an essential negative regulator of the pathway in mammals (Cooper et al., 2005; Svard et al., 2006). SuFu binds full length Gli proteins and prevents their entry into the nucleus (Pearse et al., 1999; Dunaeva et al., 2003). Interestingly, in the absence of SuFu, the pathway is fully activated, but full length Gli3 and Gli2 are destabilized (Humke et al., 2010). This is somewhat similar to what has been observed in *Drosophila*, with stabilization of Ci-155 not corresponding to full activation of the pathway. It also suggests that full length Gli proteins are stable in the cytoplasm and destabilized after they enter the nucleus and carry out their transcriptional activating function.

The most striking difference between flies and vertebrates is the organization of the vertebrate pathway inside a cell organelle that flies do not possess: the primary cilium.

The primary cilium

Primary cilia are present on most somatic cells in vertebrates. The cilium shaft is 1 to 5 microns long and comprised of nine microtubule doublets which are anchored in the basal body, a root of nine microtubule triplets that is formed from the older of the pair of centrioles since the cell's last division. Euploid cells will thus build only one cilium, and this cilium is resorbed every time the cell undergoes mitosis (Plotnikova et al., 2009). The cilium is built and then dynamically maintained by intraflagellar transport (IFT). Dedicated kinesin 2 motors perform anterograde transport (toward the tip), while retrograde transport back toward the basal body is performed by dynein 1b motors. Disruption of anterograde transport by mutation of kinesins

results in a failure to generate cilia, or a retraction of already established cilia in the case of temperature sensitive mutations shifted after cilium formation (Kozminski et al., 1995; Pazour et al., 2000). Disruption of retrograde transport has similar effects, with formation of a cilium that never reaches full length before retracting (Pazour et al., 1998; Piperno et al., 1998; Pazour et al., 1999). The motors and associated proteins essential for ciliogenesis have been divided into two complexes: IFT-A and IFT-B.

The cilium is ensheathed in a lipid bilayer that is contiguous with the plasma membrane, but the lipid compositions of the cilium and an intermediate transition zone at its base are distinct (Montesano, 1979). Membrane proteins cannot freely diffuse from the surrounding membrane, nor enter the cilium from internal vesicles without being actively allowed in by septins and basal body components (Craige et al., 2010; Hu et al., 2010). Cytoplasmic proteins must likewise be shuttled in, and transition fibers at the base of the cilium are believed to form a flagellar pore complex analogous to the nuclear pore. In fact, the same proteins might participate in nuclear and ciliary import-- importin-beta2 and small GTPase Ran are responsible for entry of KIF17 into the cilium, and some nuclear localization sequences appear to also target cytoplasmic proteins into the cilium (Dishinger et al., 2010). There are also loose consensus sequences for membrane protein import into primary cilia (Jenkins et al., 2006; Berbari et al., 2008; Mazelova et al., 2009). The primary cilium is thus an organelle in every sense, with a distinct composition of proteins and lipids, and regulated entry and exit.

Mutations in IFT components result in ciliopathies. These diseases affect the organs most dependent on primary cilia for their function. Polycystic kidney disease, retinal degenerative disease, and situs inversus are often caused by defects in ciliary transport. Several syndromes that have symptoms clustered in these organs have now been found to be caused by

mutations that affect IFT: Bardet-Biedl syndrome, characterized by renal disease, obesity, diabetes, visual loss, ataxia, mental retardation, and brachydactyly, among many others, Meckel-Gruber syndrome with similar organ systems affected, Joubert syndrome, affecting the balance apparatus, and Kartagener syndrome, affecting cilia in the respiratory tract as well as organ reversal. (reviewed in (Waters and Beales, 2011)) Cilia are also necessary for the function of at least two signaling pathways: Hedgehog and platelet derived growth factor (PDGF) signaling; more controversially, cilia have been implicated in Wnt and Notch signaling. Some of the symptoms of ciliopathies may in fact be caused by perturbations of these signaling pathways.

Hedgehog transduction in the primary cilium

The essential role of ciliary transport in Hedgehog signaling was discovered in a screen for mouse mutants that have neural tube defects, which identified IFT complex B components Kif3a, Ift88, and Ift172 as essential for Hedgehog signaling downstream of Patched (Huangfu et al., 2003). Other IFT-B components were subsequently shown to cause Hedgehog-related defects (Liu et al., 2005; Houde et al., 2006). Mutation of retrograde transport components was also shown to impair Hedgehog signaling (Huangfu and Anderson, 2005; May et al., 2005). The role of cilia in Hedgehog signaling is not restricted by tissue type, nor by organism, as the same dependence was demonstrated in zebrafish (Huang and Schier, 2009; Glazer et al., 2010; Tay et al., 2010), chick (Yin et al., 2009), and frogs (Park et al., 2006).

Trafficking through the primary cilia is also necessary for negative regulation of the Hedgehog pathway. Mutations of retrograde transport machinery Thm1 and Ift122, small GTPases Arl13b and Rab23, and ciliary protein Tulp3 cause ectopic activation of the pathway in at least some tissues (Eggenschwiler et al., 2001; Caspary et al., 2007; Tran et al., 2008; Norman et al., 2009; Patterson et al., 2009; Qin et al., 2011). The severity of ectopic activation by the

above mutation varies, and in many cases, only a subset of Hedgehog target genes get activated, and not all tissues are equally affected. The effect cannot be simplified into anterograde transport regulating the Hedgehog pathway positively and retrograde negatively, because mutation of some retrograde machinery such as the Dync2h1 motor results in loss of Hedgehog signaling, despite a short bulbous ciliary morphology indistinguishable from Thm1 and Ift122 mutants (Ocbina et al., 2011). These observations may explain why many ciliopathies produce symptoms of ectopic Hedgehog activation such as polydactyly.

As would be expected from the striking effects of IFT on signaling, many Hedgehog pathway components congregate at primary cilia in signal-dependent fashion. Patched localizes to the cilium in the pathway's off state, exits upon Hedgehog binding, and Smoothened subsequently accumulates in its place (Rohatgi et al., 2007). This is vaguely analogous to what occurs in flies, where Patched and Smoothened switch localization to the plasma membrane depending on the presence of Hedgehog ligand. Treatment of vertebrate Smoothened with Smoothened Agonist (SAG) sends it to the cilium regardless of the continued presence of Patched there. Given the small size of the compartment and specialized lipids in the cilium, it is tempting to speculate that Patched might be manipulating small hydrophobic molecules to keep Smoothened from accumulating in the cilium. Many other components of the Hedgehog signaling pathway have since been shown to concentrate at primary cilia, including PKA (Barzi et al., 2010), and the cytoplasmic components SuFu and Gli (Haycraft et al., 2005).

Aims of this dissertation

Genetics work in flies, mice, fish, and chick has made great strides in identifying the core and accessory components of the Hedgehog signaling pathway, but a mechanistic understanding of many of its steps remains elusive. Hedgehog is both fascinating and frustrating in how little it resembles other pathways and how many of its steps can only be described in logical circuit terms of inhibition and activation rather than concrete biochemical events. In this dissertation, I describe experiments in the tissue culture system that were used to answer several mechanistic questions: (a) where does Hedgehog processing occur in the cell and why is processing absolutely essential for its function, (b) how does a hydrophobic Hedgehog ligand manage to diffuse from cells secreting it, and (c) how does activated Smoothened at the primary cilium communicate with cytoplasmic components and activate the transcription factor Gli.

References

Amanai, K., and Jiang, J. (2001). Distinct roles of Central missing and Dispatched in sending the Hedgehog signal. *Development* 128, 5119-5127.

Aspock, G., Kagoshima, H., Niklaus, G., and Burglin, T.R. (1999). Caenorhabditis elegans has scores of hedgehog-related genes: sequence and expression analysis. *Genome Res* 9, 909-923.

Aza-Blanc, P., Ramirez-Weber, F.A., Laget, M.P., Schwartz, C., and Kornberg, T.B. (1997). Proteolysis that is inhibited by hedgehog targets Cubitus interruptus protein to the nucleus and converts it to a repressor. *Cell* 89, 1043-1053.

Banks, W.A., Tschop, M., Robinson, S.M., and Heiman, M.L. (2002). Extent and direction of ghrelin transport across the blood-brain barrier is determined by its unique primary structure. *J Pharmacol Exp Ther* 302, 822-827.

Barzi, M., Berenguer, J., Menendez, A., Alvarez-Rodriguez, R., and Pons, S. (2010). Sonic-hedgehog-mediated proliferation requires the localization of PKA to the cilium base. *J Cell Sci* 123, 62-69.

Beauchamp, E., Bulut, G., Abaan, O., Chen, K., Merchant, A., Matsui, W., Endo, Y., Rubin, J.S., Toretsky, J., and Uren, A. (2009). GLI1 is a direct transcriptional target of EWS-FLI1 oncoprotein. *J Biol Chem* 284, 9074-9082.

Bellaiche, Y., The, I., and Perrimon, N. (1998). Tout-velu is a Drosophila homologue of the putative tumour suppressor EXT-1 and is needed for Hh diffusion. *Nature* 394, 85-88.

Berbari, N.F., Johnson, A.D., Lewis, J.S., Askwith, C.C., and Mykytyn, K. (2008). Identification of ciliary localization sequences within the third intracellular loop of G protein-coupled receptors. *Mol Biol Cell* 19, 1540-1547.

Berman, D.M., Karhadkar, S.S., Maitra, A., Montes De Oca, R., Gerstenblith, M.R., Briggs, K., Parker, A.R., Shimada, Y., Eshleman, J.R., Watkins, D.N.*, et al.* (2003). Widespread requirement for Hedgehog ligand stimulation in growth of digestive tract tumours. *Nature* 425, 846-851.

Bishop, B., Aricescu, A.R., Harlos, K., O'Callaghan, C.A., Jones, E.Y., and Siebold, C. (2009). Structural insights into hedgehog ligand sequestration by the human hedgehog-interacting protein HHIP. *Nat Struct Mol Biol* 16, 698-703.

Blanchette-Mackie, E.J., Dwyer, N.K., Amende, L.M., Kruth, H.S., Butler, J.D., Sokol, J., Comly, M.E., Vanier, M.T., August, J.T., Brady, R.O.*, et al.* (1988). Type-C Niemann-Pick disease: low density lipoprotein uptake is associated with premature cholesterol accumulation in the Golgi complex and excessive cholesterol storage in lysosomes. *Proc Natl Acad Sci U S A* 85, 8022-8026.

Bosanac, I., Maun, H.R., Scales, S.J., Wen, X., Lingel, A., Bazan, J.F., de Sauvage, F.J., Hymowitz, S.G., and Lazarus, R.A. (2009). The structure of SHH in complex with HHIP reveals a recognition role for the Shh pseudo active site in signaling. *Nat Struct Mol Biol* 16, 691-697.

Burglin, T.R. (1996). Warthog and groundhog, novel families related to hedgehog. *Curr Biol* 6, 1047-1050.

Burke, R., Nellen, D., Bellotto, M., Hafen, E., Senti, K.A., Dickson, B.J., and Basler, K. (1999). Dispatched, a novel sterol-sensing domain protein dedicated to the release of cholesterol-modified hedgehog from signaling cells. *Cell* 99, 803-815.

Callejo, A., Culi, J., and Guerrero, I. (2008). Patched, the receptor of Hedgehog, is a lipoprotein receptor. *Proc Natl Acad Sci U S A* 105, 912-917.

Callejo, A., Torroja, C., Quijada, L., and Guerrero, I. (2006). Hedgehog lipid modifications are required for Hedgehog stabilization in the extracellular matrix. *Development* 133, 471-483.

Capurro, M.I., Xu, P., Shi, W., Li, F., Jia, A., and Filmus, J. (2008). Glypican-3 inhibits Hedgehog signaling during development by competing with patched for Hedgehog binding. *Dev Cell* 14, 700-711.

Caspary, T., Garcia-Garcia, M.J., Huangfu, D., Eggenschwiler, J.T., Wyler, M.R., Rakeman, A.S., Alcorn, H.L., and Anderson, K.V. (2002). Mouse Dispatched homolog1 is required for long-range, but not juxtacrine, Hh signaling. *Curr Biol* 12, 1628-1632.

Caspary, T., Larkins, C.E., and Anderson, K.V. (2007). The graded response to Sonic Hedgehog depends on cilia architecture. *Dev Cell* 12, 767-778.

Chamoun, Z., Mann, R.K., Nellen, D., von Kessler, D.P., Bellotto, M., Beachy, P.A., and Basler, K. (2001). Skinny hedgehog, an acyltransferase required for palmitoylation and activity of the hedgehog signal. *Science* 293, 2080-2084.

Chen, C.H., von Kessler, D.P., Park, W., Wang, B., Ma, Y., and Beachy, P.A. (1999). Nuclear trafficking of Cubitus interruptus in the transcriptional regulation of Hedgehog target gene expression. *Cell* 98, 305-316.

Chen, M.H., Gao, N., Kawakami, T., and Chuang, P.T. (2005). Mice deficient in the fused homolog do not exhibit phenotypes indicative of perturbed hedgehog signaling during embryonic development. *Mol Cell Biol* 25, 7042-7053.

Chen, M.H., Li, Y.J., Kawakami, T., Xu, S.M., and Chuang, P.T. (2004). Palmitoylation is required for the production of a soluble multimeric Hedgehog protein complex and long-range signaling in vertebrates. *Genes Dev* 18, 641-659.

Chen, Y., and Struhl, G. (1996). Dual roles for patched in sequestering and transducing Hedgehog. *Cell* 87, 553-563.

Chevalier, B.S., and Stoddard, B.L. (2001). Homing endonucleases: structural and functional insight into the catalysts of intron/intein mobility. *Nucleic Acids Res* 29, 3757-3774.

Chiang, C., Litingtung, Y., Lee, E., Young, K.E., Corden, J.L., Westphal, H., and Beachy, P.A. (1996). Cyclopia and defective axial patterning in mice lacking Sonic hedgehog gene function. *Nature* 383, 407-413.

Chuang, P.T., and McMahon, A.P. (1999). Vertebrate Hedgehog signalling modulated by induction of a Hedgehog-binding protein. *Nature* 397, 617-621.

Cooper, A.F., Yu, K.P., Brueckner, M., Brailey, L.L., Johnson, L., McGrath, J.M., and Bale, A.E. (2005). Cardiac and CNS defects in a mouse with targeted disruption of suppressor of fused. *Development* 132, 4407-4417.

Craige, B., Tsao, C.C., Diener, D.R., Hou, Y., Lechtreck, K.F., Rosenbaum, J.L., and Witman, G.B. (2010). CEP290 tethers flagellar transition zone microtubules to the membrane and regulates flagellar protein content. *J Cell Biol* 190, 927-940.

Dai, P., Akimaru, H., Tanaka, Y., Maekawa, T., Nakafuku, M., and Ishii, S. (1999). Sonic Hedgehog-induced activation of the Gli1 promoter is mediated by GLI3. *J Biol Chem* 274, 8143-8152.

Davies, J.P., Chen, F.W., and Ioannou, Y.A. (2000). Transmembrane molecular pump activity of Niemann-Pick C1 protein. *Science* 290, 2295-2298.

Dawber, R.J., Hebbes, S., Herpers, B., Docquier, F., and van den Heuvel, M. (2005). Differential range and activity of various forms of the Hedgehog protein. *BMC Dev Biol* 5, 21.

Dierks, C., Grbic, J., Zirlik, K., Beigi, R., Englund, N.P., Guo, G.R., Veelken, H., Engelhardt, M., Mertelsmann, R., Kelleher, J.F.*, et al.* (2007). Essential role of stromally induced hedgehog signaling in B-cell malignancies. *Nat Med* 13, 944-951.

DiNardo, S., Sher, E., Heemskerk-Jongens, J., Kassis, J.A., and O'Farrell, P.H. (1988). Two-tiered regulation of spatially patterned engrailed gene expression during Drosophila embryogenesis. *Nature* 332, 604-609.

Dishinger, J.F., Kee, H.L., Jenkins, P.M., Fan, S., Hurd, T.W., Hammond, J.W., Truong, Y.N., Margolis, B., Martens, J.R., and Verhey, K.J. (2010). Ciliary entry of the kinesin-2 motor KIF17 is regulated by importin-beta2 and RanGTP. *Nat Cell Biol* 12, 703-710.

Dunaeva, M., Michelson, P., Kogerman, P., and Toftgard, R. (2003). Characterization of the physical interaction of Gli proteins with SUFU proteins. *J Biol Chem* 278, 5116-5122.

Echelard, Y., Epstein, D.J., St-Jacques, B., Shen, L., Mohler, J., McMahon, J.A., and McMahon, A.P. (1993). Sonic hedgehog, a member of a family of putative signaling molecules, is implicated in the regulation of CNS polarity. *Cell* 75, 1417-1430.

Eggenschwiler, J.T., Espinoza, E., and Anderson, K.V. (2001). Rab23 is an essential negative regulator of the mouse Sonic hedgehog signalling pathway. *Nature* 412, 194-198.

Ehtesham, M., Sarangi, A., Valadez, J.G., Chanthaphaychith, S., Becher, M.W., Abel, T.W., Thompson, R.C., and Cooper, M.K. (2007). Ligand-dependent activation of the hedgehog pathway in glioma progenitor cells. *Oncogene* 26, 5752-5761.

Fan, C.M., and Tessier-Lavigne, M. (1994). Patterning of mammalian somites by surface ectoderm and notochord: evidence for sclerotome induction by a hedgehog homolog. *Cell* 79, 1175-1186.

Friedland, N., Liou, H.L., Lobel, P., and Stock, A.M. (2003). Structure of a cholesterol-binding protein deficient in Niemann-Pick type C2 disease. *Proc Natl Acad Sci U S A* 100, 2512-2517.

Gailani, M.R., Stahle-Backdahl, M., Leffell, D.J., Glynn, M., Zaphiropoulos, P.G., Pressman, C., Unden, A.B., Dean, M., Brash, D.E., Bale, A.E.*, et al.* (1996). The role of the human homologue of Drosophila patched in sporadic basal cell carcinomas. *Nat Genet* 14, 78-81.

Gallet, A., Ruel, L., Staccini-Lavenant, L., and Therond, P.P. (2006). Cholesterol modification is necessary for controlled planar long-range activity of Hedgehog in Drosophila epithelia. *Development* 133, 407-418.

Gallet, A., and Therond, P.P. (2005). Temporal modulation of the Hedgehog morphogen gradient by a patched-dependent targeting to lysosomal compartment. *Dev Biol* 277, 51-62.

Garver, W.S., Heidenreich, R.A., Erickson, R.P., Thomas, M.A., and Wilson, J.M. (2000). Localization of the murine Niemann-Pick C1 protein to two distinct intracellular compartments. *J Lipid Res* 41, 673-687.

Gil, G., Faust, J.R., Chin, D.J., Goldstein, J.L., and Brown, M.S. (1985). Membrane-bound domain of HMG CoA reductase is required for sterol-enhanced degradation of the enzyme. *Cell* 41, 249-258.

Gimble, F.S., and Thorner, J. (1992). Homing of a DNA endonuclease gene by meiotic gene conversion in Saccharomyces cerevisiae. *Nature* 357, 301-306.

Glazer, A.M., Wilkinson, A.W., Backer, C.B., Lapan, S.W., Gutzman, J.H., Cheeseman, I.M., and Reddien, P.W. (2010). The Zn finger protein Iguana impacts Hedgehog signaling by promoting ciliogenesis. *Dev Biol* 337, 148-156.

Goetz, J.A., Singh, S., Suber, L.M., Kull, F.J., and Robbins, D.J. (2006). A highly conserved amino-terminal region of sonic hedgehog is required for the formation of its freely diffusible multimeric form. *J Biol Chem* 281, 4087-4093.

Goodrich, L.V., Milenkovic, L., Higgins, K.M., and Scott, M.P. (1997). Altered neural cell fates and medulloblastoma in mouse patched mutants. *Science* 277, 1109-1113.

Gutierrez, J.A., Solenberg, P.J., Perkins, D.R., Willency, J.A., Knierman, M.D., Jin, Z., Witcher, D.R., Luo, S., Onyia, J.E., and Hale, J.E. (2008). Ghrelin octanoylation mediated by an orphan lipid transferase. *Proc Natl Acad Sci U S A* 105, 6320-6325.

Hahn, H., Wicking, C., Zaphiropoulous, P.G., Gailani, M.R., Shanley, S., Chidambaram, A., Vorechovsky, I., Holmberg, E., Unden, A.B., Gillies, S.*, et al.* (1996). Mutations of the human homolog of Drosophila patched in the nevoid basal cell carcinoma syndrome. *Cell* 85, 841-851.

Hall, T.M., Porter, J.A., Young, K.E., Koonin, E.V., Beachy, P.A., and Leahy, D.J. (1997). Crystal structure of a Hedgehog autoprocessing domain: homology between Hedgehog and self-splicing proteins. *Cell* 91, 85-97.

Hao, L., Mukherjee, K., Liegeois, S., Baillie, D., Labouesse, M., and Burglin, T.R. (2006). The hedgehog-related gene qua-1 is required for molting in Caenorhabditis elegans. *Dev Dyn* 235, 1469-1481.

Haycraft, C.J., Banizs, B., Aydin-Son, Y., Zhang, Q., Michaud, E.J., and Yoder, B.K. (2005). Gli2 and Gli3 localize to cilia and require the intraflagellar transport protein polaris for processing and function. *PLoS Genet* 1, e53.

Hooper, J.E., and Scott, M.P. (1989). The Drosophila patched gene encodes a putative membrane protein required for segmental patterning. *Cell* 59, 751-765.

Hosoda, H., Kojima, M., Matsuo, H., and Kangawa, K. (2000). Ghrelin and des-acyl ghrelin: two major forms of rat ghrelin peptide in gastrointestinal tissue. *Biochem Biophys Res Commun* 279, 909-913.

Houde, C., Dickinson, R.J., Houtzager, V.M., Cullum, R., Montpetit, R., Metzler, M., Simpson, E.M., Roy, S., Hayden, M.R., Hoodless, P.A.*, et al.* (2006). Hippi is essential for node cilia assembly and Sonic hedgehog signaling. *Dev Biol* 300, 523-533.

Hu, Q., Milenkovic, L., Jin, H., Scott, M.P., Nachury, M.V., Spiliotis, E.T., and Nelson, W.J. (2010). A septin diffusion barrier at the base of the primary cilium maintains ciliary membrane protein distribution. *Science* 329, 436-439.

Hua, X., Sakai, J., Brown, M.S., and Goldstein, J.L. (1996). Regulated cleavage of sterol regulatory element binding proteins requires sequences on both sides of the endoplasmic reticulum membrane. *J Biol Chem* 271, 10379-10384.

Huang, P., and Schier, A.F. (2009). Dampened Hedgehog signaling but normal Wnt signaling in zebrafish without cilia. *Development* 136, 3089-3098.

Huangfu, D., and Anderson, K.V. (2005). Cilia and Hedgehog responsiveness in the mouse. *Proc Natl Acad Sci U S A* 102, 11325-11330.

Huangfu, D., Liu, A., Rakeman, A.S., Murcia, N.S., Niswander, L., and Anderson, K.V. (2003). Hedgehog signalling in the mouse requires intraflagellar transport proteins. *Nature* 426, 83-87.

Humke, E.W., Dorn, K.V., Milenkovic, L., Scott, M.P., and Rohatgi, R. (2010). The output of Hedgehog signaling is controlled by the dynamic association between Suppressor of Fused and the Gli proteins. *Genes Dev* 24, 670-682.

Incardona, J.P., Lee, J.H., Robertson, C.P., Enga, K., Kapur, R.P., and Roelink, H. (2000). Receptor-mediated endocytosis of soluble and membrane-tethered Sonic hedgehog by Patched-1. *Proc Natl Acad Sci U S A* 97, 12044-12049.

Infante, R.E., Wang, M.L., Radhakrishnan, A., Kwon, H.J., Brown, M.S., and Goldstein, J.L. (2008). NPC2 facilitates bidirectional transfer of cholesterol between NPC1 and lipid bilayers, a step in cholesterol egress from lysosomes. *Proc Natl Acad Sci U S A* 105, 15287-15292.

Ingham, P.W., Taylor, A.M., and Nakano, Y. (1991). Role of the Drosophila patched gene in positional signalling. *Nature* 353, 184-187.

Izzi, L., Levesque, M., Morin, S., Laniel, D., Wilkes, B.C., Mille, F., Krauss, R.S., McMahon, A.P., Allen, B.L., and Charron, F. (2011). Boc and Gas1 each form distinct Shh receptor complexes with Ptch1 and are required for Shh-mediated cell proliferation. *Dev Cell* 20, 788-801.

Jenkins, P.M., Hurd, T.W., Zhang, L., McEwen, D.P., Brown, R.L., Margolis, B., Verhey, K.J., and Martens, J.R. (2006). Ciliary targeting of olfactory CNG channels requires the CNGB1b subunit and the kinesin-2 motor protein, KIF17. *Curr Biol* 16, 1211-1216.

Jia, J., Tong, C., and Jiang, J. (2003). Smoothened transduces Hedgehog signal by physically interacting with Costal2/Fused complex through its C-terminal tail. *Genes Dev* 17, 2709-2720.

Jiang, J., and Struhl, G. (1995). Protein kinase A and hedgehog signaling in Drosophila limb development. *Cell* 80, 563-572.

Jira, P.E., Waterham, H.R., Wanders, R.J., Smeitink, J.A., Sengers, R.C., and Wevers, R.A. (2003). Smith-Lemli-Opitz syndrome and the DHCR7 gene. *Ann Hum Genet* 67, 269-280.

Kadowaki, T., Wilder, E., Klingensmith, J., Zachary, K., and Perrimon, N. (1996). The segment polarity gene porcupine encodes a putative multitransmembrane protein involved in Wingless processing. *Genes Dev* 10, 3116-3128.

Kalderon, D. (2004). Hedgehog signaling: Costal-2 bridges the transduction gap. *Curr Biol* 14, R67-69.

Karhadkar, S.S., Bova, G.S., Abdallah, N., Dhara, S., Gardner, D., Maitra, A., Isaacs, J.T., Berman, D.M., and Beachy, P.A. (2004). Hedgehog signalling in prostate regeneration, neoplasia and metastasis. *Nature* 431, 707-712.

Kawakami, T., Kawcak, T., Li, Y.J., Zhang, W., Hu, Y., and Chuang, P.T. (2002). Mouse dispatched mutants fail to distribute hedgehog proteins and are defective in hedgehog signaling. *Development* 129, 5753-5765.

Kinzler, K.W., Bigner, S.H., Bigner, D.D., Trent, J.M., Law, M.L., O'Brien, S.J., Wong, A.J., and Vogelstein, B. (1987). Identification of an amplified, highly expressed gene in a human glioma. *Science* 236, 70-73.

Ko, D.C., Binkley, J., Sidow, A., and Scott, M.P. (2003). The integrity of a cholesterol-binding pocket in Niemann-Pick C2 protein is necessary to control lysosome cholesterol levels. *Proc Natl Acad Sci U S A* 100, 2518-2525.

Koide, T., Hayata, T., and Cho, K.W. (2006). Negative regulation of Hedgehog signaling by the cholesterogenic enzyme 7-dehydrocholesterol reductase. *Development* 133, 2395-2405.

Kojima, M., Hosoda, H., Date, Y., Nakazato, M., Matsuo, H., and Kangawa, K. (1999). Ghrelin is a growth-hormone-releasing acylated peptide from stomach. *Nature* 402, 656-660.

Komekado, H., Yamamoto, H., Chiba, T., and Kikuchi, A. (2007). Glycosylation and palmitoylation of Wnt-3a are coupled to produce an active form of Wnt-3a. *Genes Cells* 12, 521-534.

Kozminski, K.G., Beech, P.L., and Rosenbaum, J.L. (1995). The Chlamydomonas kinesin-like protein FLA10 is involved in motility associated with the flagellar membrane. *J Cell Biol* 131, 1517-1527.

Krauss, S., Concordet, J.P., and Ingham, P.W. (1993). A functionally conserved homolog of the Drosophila segment polarity gene hh is expressed in tissues with polarizing activity in zebrafish embryos. *Cell* 75, 1431-1444.

Kubo, M., Nakamura, M., Tasaki, A., Yamanaka, N., Nakashima, H., Nomura, M., Kuroki, S., and Katano, M. (2004). Hedgehog signaling pathway is a new therapeutic target for patients with breast cancer. *Cancer Res* 64, 6071-6074.

Kurayoshi, M., Yamamoto, H., Izumi, S., and Kikuchi, A. (2007). Post-translational palmitoylation and glycosylation of Wnt-5a are necessary for its signalling. *Biochem J* 402, 515-523.

Lam, C.W., Xie, J., To, K.F., Ng, H.K., Lee, K.C., Yuen, N.W., Lim, P.L., Chan, L.Y., Tong, S.F., and McCormick, F. (1999). A frequent activated smoothened mutation in sporadic basal cell carcinomas. *Oncogene* 18, 833-836.

Lee, C.S., Buttitta, L., and Fan, C.M. (2001a). Evidence that the WNT-inducible growth arrest-specific gene 1 encodes an antagonist of sonic hedgehog signaling in the somite. *Proc Natl Acad Sci U S A* 98, 11347-11352.

Lee, J.D., Kraus, P., Gaiano, N., Nery, S., Kohtz, J., Fishell, G., Loomis, C.A., and Treisman, J.E. (2001b). An acylatable residue of Hedgehog is differentially required in Drosophila and mouse limb development. *Dev Biol* 233, 122-136.

Lee, J.D., and Treisman, J.E. (2001). Sightless has homology to transmembrane acyltransferases and is required to generate active Hedgehog protein. *Curr Biol* 11, 1147-1152.

Lee, J.J., Ekker, S.C., von Kessler, D.P., Porter, J.A., Sun, B.I., and Beachy, P.A. (1994). Autoproteolysis in hedgehog protein biogenesis. *Science* 266, 1528-1537.

Lee, J.J., von Kessler, D.P., Parks, S., and Beachy, P.A. (1992). Secretion and localized transcription suggest a role in positional signaling for products of the segmentation gene hedgehog. *Cell* 71, 33-50.

Lewis, E.B. (1978). A gene complex controlling segmentation in Drosophila. *Nature* 276, 565-570.

Lewis, P.M., Dunn, M.P., McMahon, J.A., Logan, M., Martin, J.F., St-Jacques, B., and McMahon, A.P. (2001). Cholesterol modification of sonic hedgehog is required for long-range signaling activity and effective modulation of signaling by Ptc1. *Cell* 105, 599-612.

Li, Y., Zhang, H., Litingtung, Y., and Chiang, C. (2006). Cholesterol modification restricts the spread of Shh gradient in the limb bud. *Proc Natl Acad Sci U S A* 103, 6548-6553.

Liem, K.F., Jr., Tremml, G., Roelink, H., and Jessell, T.M. (1995). Dorsal differentiation of neural plate cells induced by BMP-mediated signals from epidermal ectoderm. *Cell* 82, 969-979.

Liu, A., Wang, B., and Niswander, L.A. (2005). Mouse intraflagellar transport proteins regulate both the activator and repressor functions of Gli transcription factors. *Development* 132, 3103-3111.

Liu, Y., Cao, X., Jiang, J., and Jia, J. (2007). Fused-Costal2 protein complex regulates Hedgehog-induced Smo phosphorylation and cell-surface accumulation. *Genes Dev* 21, 1949-1963.

Lopez-Martinez, A., Chang, D.T., Chiang, C., Porter, J.A., Ros, M.A., Simandl, B.K., Beachy, P.A., and Fallon, J.F. (1995). Limb-patterning activity and restricted posterior localization of the amino-terminal product of Sonic hedgehog cleavage. *Curr Biol* 5, 791-796.

Lum, L., Yao, S., Mozer, B., Rovescalli, A., Von Kessler, D., Nirenberg, M., and Beachy, P.A. (2003a). Identification of Hedgehog pathway components by RNAi in Drosophila cultured cells. *Science* 299, 2039-2045.

Lum, L., Zhang, C., Oh, S., Mann, R.K., von Kessler, D.P., Taipale, J., Weis-Garcia, F., Gong, R., Wang, B., and Beachy, P.A. (2003b). Hedgehog signal transduction via Smoothened association with a cytoplasmic complex scaffolded by the atypical kinesin, Costal-2. *Mol Cell* 12, 1261-1274.

Ma, Y., Erkner, A., Gong, R., Yao, S., Taipale, J., Basler, K., and Beachy, P.A. (2002). Hedgehog-mediated patterning of the mammalian embryo requires transporter-like function of dispatched. *Cell* 111, 63-75.

Maity, T., Fuse, N., and Beachy, P.A. (2005). Molecular mechanisms of Sonic hedgehog mutant effects in holoprosencephaly. *Proc Natl Acad Sci U S A* 102, 17026-17031.

Marigo, V., Davey, R.A., Zuo, Y., Cunningham, J.M., and Tabin, C.J. (1996). Biochemical evidence that patched is the Hedgehog receptor. *Nature* 384, 176-179.

Marigo, V., and Tabin, C.J. (1996). Regulation of patched by sonic hedgehog in the developing neural tube. *Proc Natl Acad Sci U S A* 93, 9346-9351.

Martinelli, D.C., and Fan, C.M. (2007). Gas1 extends the range of Hedgehog action by facilitating its signaling. *Genes Dev* 21, 1231-1243.

Martizez Arias, A., Baker, N.E., and Ingham, P.W. (1988). Role of segment polarity genes in the definition and maintenance of cell states in the Drosophila embryo. *Development* 103, 157-170.

May, S.R., Ashique, A.M., Karlen, M., Wang, B., Shen, Y., Zarbalis, K., Reiter, J., Ericson, J., and Peterson, A.S. (2005). Loss of the retrograde motor for IFT disrupts localization of

Smo to cilia and prevents the expression of both activator and repressor functions of Gli. *Dev Biol* 287, 378-389.

Mazelova, J., Astuto-Gribble, L., Inoue, H., Tam, B.M., Schonteich, E., Prekeris, R., Moritz, O.L., Randazzo, P.A., and Deretic, D. (2009). Ciliary targeting motif VxPx directs assembly of a trafficking module through Arf4. *Embo J* 28, 183-192.

Mazumdar, T., Devecchio, J., Agyeman, A., Shi, T., and Houghton, J.A. (2011). Blocking Hedgehog survival signaling at the level of the GLI genes induces DNA damage and extensive cell death in human colon carcinoma cells. *Cancer Res* 71, 5904-5914.

McCarthy, R.A., Barth, J.L., Chintalapudi, M.R., Knaak, C., and Argraves, W.S. (2002). Megalin functions as an endocytic sonic hedgehog receptor. *J Biol Chem* 277, 25660-25667.

McLellan, J.S., Yao, S., Zheng, X., Geisbrecht, B.V., Ghirlando, R., Beachy, P.A., and Leahy, D.J. (2006). Structure of a heparin-dependent complex of Hedgehog and Ihog. *Proc Natl Acad Sci U S A* 103, 17208-17213.

McMahon, A.P., Ingham, P.W., and Tabin, C.J. (2003). Developmental roles and clinical significance of hedgehog signaling. *Curr Top Dev Biol* 53, 1-114.

Merchant, M., Evangelista, M., Luoh, S.M., Frantz, G.D., Chalasani, S., Carano, R.A., van Hoy, M., Ramirez, J., Ogasawara, A.K., McFarland, L.M.*, et al.* (2005). Loss of the serine/threonine kinase fused results in postnatal growth defects and lethality due to progressive hydrocephalus. *Mol Cell Biol* 25, 7054-7068.

Methot, N., and Basler, K. (1999). Hedgehog controls limb development by regulating the activities of distinct transcriptional activator and repressor forms of Cubitus interruptus. *Cell* 96, 819-831.

Micchelli, C.A., The, I., Selva, E., Mogila, V., and Perrimon, N. (2002). Rasp, a putative transmembrane acyltransferase, is required for Hedgehog signaling. *Development* 129, 843-851.

Millard, E.E., Gale, S.E., Dudley, N., Zhang, J., Schaffer, J.E., and Ory, D.S. (2005). The sterol-sensing domain of the Niemann-Pick C1 (NPC1) protein regulates trafficking of low density lipoprotein cholesterol. *J Biol Chem* 280, 28581-28590.

Miura, G.I., Buglino, J., Alvarado, D., Lemmon, M.A., Resh, M.D., and Treisman, J.E. (2006). Palmitoylation of the EGFR ligand Spitz by Rasp increases Spitz activity by restricting its diffusion. *Dev Cell* 10, 167-176.

Miura, G.I., and Treisman, J.E. (2006). Lipid modification of secreted signaling proteins. *Cell Cycle* 5, 1184-1188.

Montesano, R. (1979). Inhomogeneous distribution of filipin-sterol complexes in the ciliary membrane of rat tracheal epithelium. *Am J Anat* 156, 139-145.

Motamed, M., Zhang, Y., Wang, M.L., Seemann, J., Kwon, H.J., Goldstein, J.L., and Brown, M.S. (2011). Identification of luminal Loop 1 of Scap protein as the sterol sensor that maintains cholesterol homeostasis. *J Biol Chem* 286, 18002-18012.

Nanni, L., Ming, J.E., Bocian, M., Steinhaus, K., Bianchi, D.W., Die-Smulders, C., Giannotti, A., Imaizumi, K., Jones, K.L., Campo, M.D.*, et al.* (1999). The mutational spectrum of the sonic hedgehog gene in holoprosencephaly: SHH mutations cause a significant proportion of autosomal dominant holoprosencephaly. *Hum Mol Genet* 8, 2479-2488.

Norman, R.X., Ko, H.W., Huang, V., Eun, C.M., Abler, L.L., Zhang, Z., Sun, X., and Eggenschwiler, J.T. (2009). Tubby-like protein 3 (TULP3) regulates patterning in the mouse embryo through inhibition of Hedgehog signaling. *Hum Mol Genet* 18, 1740-1754.

Nusslein-Volhard, C., and Wieschaus, E. (1980). Mutations affecting segment number and polarity in Drosophila. *Nature* 287, 795-801.

Ocbina, P.J., Eggenschwiler, J.T., Moskowitz, I., and Anderson, K.V. (2011). Complex interactions between genes controlling trafficking in primary cilia. *Nat Genet* 43, 547-553.

Ogden, S.K., Ascano, M., Jr., Stegman, M.A., Suber, L.M., Hooper, J.E., and Robbins, D.J. (2003). Identification of a functional interaction between the transmembrane protein Smoothened and the kinesin-related protein Costal2. *Curr Biol* 13, 1998-2003.

Ohgami, N., Ko, D.C., Thomas, M., Scott, M.P., Chang, C.C., and Chang, T.Y. (2004). Binding between the Niemann-Pick C1 protein and a photoactivatable cholesterol analog requires a functional sterol-sensing domain. *Proc Natl Acad Sci U S A* 101, 12473-12478.

Ohlmeyer, J.T., and Kalderon, D. (1998). Hedgehog stimulates maturation of Cubitus interruptus into a labile transcriptional activator. *Nature* 396, 749-753.

Panakova, D., Sprong, H., Marois, E., Thiele, C., and Eaton, S. (2005). Lipoprotein particles are required for Hedgehog and Wingless signalling. *Nature* 435, 58-65.

Park, T.J., Haigo, S.L., and Wallingford, J.B. (2006). Ciliogenesis defects in embryos lacking inturned or fuzzy function are associated with failure of planar cell polarity and Hedgehog signaling. *Nat Genet* 38, 303-311.

Park, Y., Rangel, C., Reynolds, M.M., Caldwell, M.C., Johns, M., Nayak, M., Welsh, C.J., McDermott, S., and Datta, S. (2003). Drosophila perlecan modulates FGF and hedgehog signals to activate neural stem cell division. *Dev Biol* 253, 247-257.

Patterson, V.L., Damrau, C., Paudyal, A., Reeve, B., Grimes, D.T., Stewart, M.E., Williams, D.J., Siggers, P., Greenfield, A., and Murdoch, J.N. (2009). Mouse hitchhiker mutants have spina bifida, dorso-ventral patterning defects and polydactyly: identification of Tulp3 as a novel negative regulator of the Sonic hedgehog pathway. *Hum Mol Genet* 18, 1719-1739.

Pazour, G.J., Dickert, B.L., Vucica, Y., Seeley, E.S., Rosenbaum, J.L., Witman, G.B., and Cole, D.G. (2000). Chlamydomonas IFT88 and its mouse homologue, polycystic kidney disease gene tg737, are required for assembly of cilia and flagella. *J Cell Biol* 151, 709-718.

Pazour, G.J., Dickert, B.L., and Witman, G.B. (1999). The DHC1b (DHC2) isoform of cytoplasmic dynein is required for flagellar assembly. *J Cell Biol* 144, 473-481.

Pazour, G.J., Wilkerson, C.G., and Witman, G.B. (1998). A dynein light chain is essential for the retrograde particle movement of intraflagellar transport (IFT). *J Cell Biol* 141, 979-992.

Pearse, R.V., 2nd, Collier, L.S., Scott, M.P., and Tabin, C.J. (1999). Vertebrate homologs of Drosophila suppressor of fused interact with the gli family of transcriptional regulators. *Dev Biol* 212, 323-336.

Pepinsky, R.B., Zeng, C., Wen, D., Rayhorn, P., Baker, D.P., Williams, K.P., Bixler, S.A., Ambrose, C.M., Garber, E.A., Miatkowski, K.*, et al.* (1998). Identification of a palmitic acid-modified form of human Sonic hedgehog. *J Biol Chem* 273, 14037-14045.

Piperno, G., Siuda, E., Henderson, S., Segil, M., Vaananen, H., and Sassaroli, M. (1998). Distinct mutants of retrograde intraflagellar transport (IFT) share similar morphological and molecular defects. *J Cell Biol* 143, 1591-1601.

Placzek, M., Tessier-Lavigne, M., Yamada, T., Jessell, T., and Dodd, J. (1990). Mesodermal control of neural cell identity: floor plate induction by the notochord. *Science* 250, 985-988.

Plotnikova, O.V., Pugacheva, E.N., and Golemis, E.A. (2009). Primary cilia and the cell cycle. *Methods Cell Biol* 94, 137-160.

Pons, S., and Marti, E. (2000). Sonic hedgehog synergizes with the extracellular matrix protein vitronectin to induce spinal motor neuron differentiation. *Development* 127, 333-342.

Porter, J.A., Ekker, S.C., Park, W.J., von Kessler, D.P., Young, K.E., Chen, C.H., Ma, Y., Woods, A.S., Cotter, R.J., Koonin, E.V.*, et al.* (1996a). Hedgehog patterning activity: role of a lipophilic modification mediated by the carboxy-terminal autoprocessing domain. *Cell* 86, 21-34.

Porter, J.A., von Kessler, D.P., Ekker, S.C., Young, K.E., Lee, J.J., Moses, K., and Beachy, P.A. (1995). The product of hedgehog autoproteolytic cleavage active in local and long-range signalling. *Nature* 374, 363-366.

Porter, J.A., Young, K.E., and Beachy, P.A. (1996b). Cholesterol modification of hedgehog signaling proteins in animal development. *Science* 274, 255-259.

Price, M.A., and Kalderon, D. (2002). Proteolysis of the Hedgehog signaling effector Cubitus interruptus requires phosphorylation by Glycogen Synthase Kinase 3 and Casein Kinase 1. *Cell* 108, 823-835.

Qin, J., Lin, Y., Norman, R.X., Ko, H.W., and Eggenschwiler, J.T. (2011). Intraflagellar transport protein 122 antagonizes Sonic Hedgehog signaling and controls ciliary localization of pathway components. *Proc Natl Acad Sci U S A* 108, 1456-1461.

Reifenberger, J., Wolter, M., Weber, R.G., Megahed, M., Ruzicka, T., Lichter, P., and Reifenberger, G. (1998). Missense mutations in SMOH in sporadic basal cell carcinomas of the skin and primitive neuroectodermal tumors of the central nervous system. *Cancer Res* 58, 1798-1803.

Riddle, R.D., Johnson, R.L., Laufer, E., and Tabin, C. (1993). Sonic hedgehog mediates the polarizing activity of the ZPA. *Cell* 75, 1401-1416.

Robbins, D.J., Nybakken, K.E., Kobayashi, R., Sisson, J.C., Bishop, J.M., and Therond, P.P. (1997). Hedgehog elicits signal transduction by means of a large complex containing the kinesin-related protein costal2. *Cell* 90, 225-234.

Roelink, H., Augsburger, A., Heemskerk, J., Korzh, V., Norlin, S., Ruiz i Altaba, A., Tanabe, Y., Placzek, M., Edlund, T., Jessell, T.M.*, et al.* (1994). Floor plate and motor neuron induction by vhh-1, a vertebrate homolog of hedgehog expressed by the notochord. *Cell* 76, 761-775.

Rohatgi, R., Milenkovic, L., and Scott, M.P. (2007). Patched1 regulates hedgehog signaling at the primary cilium. *Science* 317, 372-376.

Ruel, L., Gallet, A., Raisin, S., Truchi, A., Staccini-Lavenant, L., Cervantes, A., and Therond, P.P. (2007). Phosphorylation of the atypical kinesin Costal2 by the kinase Fused induces the partial disassembly of the Smoothened-Fused-Costal2-Cubitus interruptus complex in Hedgehog signalling. *Development* 134, 3677-3689.

Ruel, L., Rodriguez, R., Gallet, A., Lavenant-Staccini, L., and Therond, P.P. (2003). Stability and association of Smoothened, Costal2 and Fused with Cubitus interruptus are regulated by Hedgehog. *Nat Cell Biol* 5, 907-913.

Ruiz i Altaba, A. (1999). Gli proteins encode context-dependent positive and negative functions: implications for development and disease. *Development* 126, 3205-3216.

Sakai, J., Duncan, E.A., Rawson, R.B., Hua, X., Brown, M.S., and Goldstein, J.L. (1996). Sterol-regulated release of SREBP-2 from cell membranes requires two sequential cleavages, one within a transmembrane segment. *Cell* 85, 1037-1046.

Sanchez-Camacho, C., and Bovolenta, P. (2009). Emerging mechanisms in morphogen-mediated axon guidance. *Bioessays* 31, 1013-1025.

Sanchez, P., Hernandez, A.M., Stecca, B., Kahler, A.J., DeGueme, A.M., Barrett, A., Beyna, M., Datta, M.W., Datta, S., and Ruiz i Altaba, A. (2004). Inhibition of prostate cancer proliferation by interference with SONIC HEDGEHOG-GLI1 signaling. *Proc Natl Acad Sci U S A* 101, 12561-12566.

Sasaki, H., Nishizaki, Y., Hui, C., Nakafuku, M., and Kondoh, H. (1999). Regulation of Gli2 and Gli3 activities by an amino-terminal repression domain: implication of Gli2 and Gli3 as primary mediators of Shh signaling. *Development* 126, 3915-3924.

Sato, R., Yang, J., Wang, X., Evans, M.J., Ho, Y.K., Goldstein, J.L., and Brown, M.S. (1994). Assignment of the membrane attachment, DNA binding, and transcriptional activation domains of sterol regulatory element-binding protein-1 (SREBP-1). *J Biol Chem* 269, 17267-17273.

Sever, N., Yang, T., Brown, M.S., Goldstein, J.L., and DeBose-Boyd, R.A. (2003). Accelerated degradation of HMG CoA reductase mediated by binding of insig-1 to its sterol-sensing domain. *Mol Cell* 11, 25-33.

Shao, Y., and Paulus, H. (1997). Protein splicing: estimation of the rate of O-N and S-N acyl rearrangements, the last step of the splicing process. *J Pept Res* 50, 193-198.

Shin, S.H., Kogerman, P., Lindstrom, E., Toftgard, R., and Biesecker, L.G. (1999). GLI3 mutations in human disorders mimic Drosophila cubitus interruptus protein functions and localization. *Proc Natl Acad Sci U S A* 96, 2880-2884.

Sisson, J.C., Ho, K.S., Suyama, K., and Scott, M.P. (1997). Costal2, a novel kinesin-related protein in the Hedgehog signaling pathway. *Cell* 90, 235-245.

Smelkinson, M.G., Zhou, Q., and Kalderon, D. (2007). Regulation of Ci-SCFSlimb binding, Ci proteolysis, and hedgehog pathway activity by Ci phosphorylation. *Dev Cell* 13, 481-495.

Sokol, J., Blanchette-Mackie, J., Kruth, H.S., Dwyer, N.K., Amende, L.M., Butler, J.D., Robinson, E., Patel, S., Brady, R.O., Comly, M.E*., et al.* (1988). Type C Niemann-Pick disease. Lysosomal accumulation and defective intracellular mobilization of low density lipoprotein cholesterol. *J Biol Chem* 263, 3411-3417.

Stone, D.M., Hynes, M., Armanini, M., Swanson, T.A., Gu, Q., Johnson, R.L., Scott, M.P., Pennica, D., Goddard, A., Phillips, H*., et al.* (1996). The tumour-suppressor gene patched encodes a candidate receptor for Sonic hedgehog. *Nature* 384, 129-134.

Strutt, H., Thomas, C., Nakano, Y., Stark, D., Neave, B., Taylor, A.M., and Ingham, P.W. (2001). Mutations in the sterol-sensing domain of Patched suggest a role for vesicular trafficking in Smoothened regulation. *Curr Biol* 11, 608-613.

Svard, J., Heby-Henricson, K., Persson-Lek, M., Rozell, B., Lauth, M., Bergstrom, A., Ericson, J., Toftgard, R., and Teglund, S. (2006). Genetic elimination of Suppressor of fused reveals an essential repressor function in the mammalian Hedgehog signaling pathway. *Dev Cell* 10, 187-197.

Taipale, J., Cooper, M.K., Maiti, T., and Beachy, P.A. (2002). Patched acts catalytically to suppress the activity of Smoothened. *Nature* 418, 892-897.

Takada, R., Satomi, Y., Kurata, T., Ueno, N., Norioka, S., Kondoh, H., Takao, T., and Takada, S. (2006). Monounsaturated fatty acid modification of Wnt protein: its role in Wnt secretion. *Dev Cell* 11, 791-801.

Tanaka, K., Okabayashi, K., Asashima, M., Perrimon, N., and Kadowaki, T. (2000). The evolutionarily conserved porcupine gene family is involved in the processing of the Wnt family. *Eur J Biochem* 267, 4300-4311.

Tay, S.Y., Yu, X., Wong, K.N., Panse, P., Ng, C.P., and Roy, S. (2010). The iguana/DZIP1 protein is a novel component of the ciliogenic pathway essential for axonemal biogenesis. *Dev Dyn* 239, 527-534.

Taylor, F.R., Wen, D., Garber, E.A., Carmillo, A.N., Baker, D.P., Arduini, R.M., Williams, K.P., Weinreb, P.H., Rayhorn, P., Hronowski, X.*, et al.* (2001). Enhanced potency of human Sonic hedgehog by hydrophobic modification. *Biochemistry* 40, 4359-4371.

Taylor, M.D., Liu, L., Raffel, C., Hui, C.C., Mainprize, T.G., Zhang, X., Agatep, R., Chiappa, S., Gao, L., Lowrance, A.*, et al.* (2002). Mutations in SUFU predispose to medulloblastoma. *Nat Genet* 31, 306-310.

Tenzen, T., Allen, B.L., Cole, F., Kang, J.S., Krauss, R.S., and McMahon, A.P. (2006). The cell surface membrane proteins Cdo and Boc are components and targets of the Hedgehog signaling pathway and feedback network in mice. *Dev Cell* 10, 647-656.

Thayer, S.P., di Magliano, M.P., Heiser, P.W., Nielsen, C.M., Roberts, D.J., Lauwers, G.Y., Qi, Y.P., Gysin, S., Fernandez-del Castillo, C., Yajnik, V.*, et al.* (2003). Hedgehog is an early and late mediator of pancreatic cancer tumorigenesis. *Nature* 425, 851-856.

The, I., Bellaiche, Y., and Perrimon, N. (1999). Hedgehog movement is regulated through tout velu-dependent synthesis of a heparan sulfate proteoglycan. *Mol Cell* 4, 633-639.

Tostar, U., Malm, C.J., Meis-Kindblom, J.M., Kindblom, L.G., Toftgard, R., and Unden, A.B. (2006). Deregulation of the hedgehog signalling pathway: a possible role for the PTCH and SUFU genes in human rhabdomyoma and rhabdomyosarcoma development. *J Pathol* 208, 17-25.

Tran, P.V., Haycraft, C.J., Besschetnova, T.Y., Turbe-Doan, A., Stottmann, R.W., Herron, B.J., Chesebro, A.L., Qiu, H., Scherz, P.J., Shah, J.V.*, et al.* (2008). THM1 negatively modulates mouse sonic hedgehog signal transduction and affects retrograde intraflagellar transport in cilia. *Nat Genet* 40, 403-410.

Urban, S., Lee, J.R., and Freeman, M. (2001). Drosophila rhomboid-1 defines a family of putative intramembrane serine proteases. *Cell* 107, 173-182.

van den Heuvel, M., Harryman-Samos, C., Klingensmith, J., Perrimon, N., and Nusse, R. (1993). Mutations in the segment polarity genes wingless and porcupine impair secretion of the wingless protein. *Embo J* 12, 5293-5302.

Wang, G., Wang, B., and Jiang, J. (1999). Protein kinase A antagonizes Hedgehog signaling by regulating both the activator and repressor forms of Cubitus interruptus. *Genes Dev* 13, 2828-2837.

Wang, Q.T., and Holmgren, R.A. (1999). The subcellular localization and activity of Drosophila cubitus interruptus are regulated at multiple levels. *Development* 126, 5097-5106.

Wang, X., Sato, R., Brown, M.S., Hua, X., and Goldstein, J.L. (1994). SREBP-1, a membrane-bound transcription factor released by sterol-regulated proteolysis. *Cell* 77, 53-62.

Watari, H., Blanchette-Mackie, E.J., Dwyer, N.K., Watari, M., Neufeld, E.B., Patel, S., Pentchev, P.G., and Strauss, J.F., 3rd (1999). Mutations in the leucine zipper motif and sterol-sensing domain inactivate the Niemann-Pick C1 glycoprotein. *J Biol Chem* 274, 21861-21866.

Waters, A.M., and Beales, P.L. (2011). Ciliopathies: an expanding disease spectrum. *Pediatr Nephrol* 26, 1039-1056.

Willert, K., Brown, J.D., Danenberg, E., Duncan, A.W., Weissman, I.L., Reya, T., Yates, J.R., 3rd, and Nusse, R. (2003). Wnt proteins are lipid-modified and can act as stem cell growth factors. *Nature* 423, 448-452.

Williams, E.H., Pappano, W.N., Saunders, A.M., Kim, M.S., Leahy, D.J., and Beachy, P.A. (2010). Dally-like core protein and its mammalian homologues mediate stimulatory and inhibitory effects on Hedgehog signal response. *Proc Natl Acad Sci U S A* 107, 5869-5874.

Williams, K.P., Rayhorn, P., Chi-Rosso, G., Garber, E.A., Strauch, K.L., Horan, G.S., Reilly, J.O., Baker, D.P., Taylor, F.R., Koteliansky, V.*, et al.* (1999). Functional antagonists of sonic hedgehog reveal the importance of the N terminus for activity. *J Cell Sci* 112 (Pt 23), 4405-4414.

Xu, M.Q., Comb, D.G., Paulus, H., Noren, C.J., Shao, Y., and Perler, F.B. (1994). Protein splicing: an analysis of the branched intermediate and its resolution by succinimide formation. *Embo J* 13, 5517-5522.

Yabe, D., Xia, Z.P., Adams, C.M., and Rawson, R.B. (2002). Three mutations in sterol-sensing domain of SCAP block interaction with insig and render SREBP cleavage insensitive to sterols. *Proc Natl Acad Sci U S A* 99, 16672-16677.

Yang, J., Brown, M.S., Liang, G., Grishin, N.V., and Goldstein, J.L. (2008). Identification of the acyltransferase that octanoylates ghrelin, an appetite-stimulating peptide hormone. *Cell* 132, 387-396.

Yang, T., Espenshade, P.J., Wright, M.E., Yabe, D., Gong, Y., Aebersold, R., Goldstein, J.L., and Brown, M.S. (2002). Crucial step in cholesterol homeostasis: sterols promote binding of SCAP to INSIG-1, a membrane protein that facilitates retention of SREBPs in ER. *Cell* 110, 489-500.

Yao, S., Lum, L., and Beachy, P. (2006). The ihog cell-surface proteins bind Hedgehog and mediate pathway activation. *Cell* 125, 343-357.

Yin, Y., Bangs, F., Paton, I.R., Prescott, A., James, J., Davey, M.G., Whitley, P., Genikhovich, G., Technau, U., Burt, D.W.*, et al.* (2009). The Talpid3 gene (KIAA0586) encodes a centrosomal protein that is essential for primary cilia formation. *Development* 136, 655-664.

Zeng, X., Goetz, J.A., Suber, L.M., Scott, W.J., Jr., Schreiner, C.M., and Robbins, D.J. (2001). A freely diffusible form of Sonic hedgehog mediates long-range signalling. *Nature* 411, 716-720.

Zhang, W., Zhao, Y., Tong, C., Wang, G., Wang, B., Jia, J., and Jiang, J. (2005). Hedgehog-regulated Costal2-kinase complexes control phosphorylation and proteolytic processing of Cubitus interruptus. *Dev Cell* 8, 267-278.

Zheng, X., Mann, R.K., Sever, N., and Beachy, P.A. (2010). Genetic and biochemical definition of the Hedgehog receptor. *Genes Dev* 24, 57-71.

CHAPTER TWO:

PROCESSING AND TURNOVER OF HEDGEHOG IN THE ENDOPLASMIC RETICULUM

The following section contains previously published material from:

Chen X, Tukachinsky H, Huang CH, Jao C, Chu YR, Tang HY, Mueller B, Schulman S, Rapoport TA, Salic A.. Processing and turnover of the Hedgehog protein in the endoplasmic reticulum. *Journal of Cell Biology*. **192(5)**: 825-38 (2011).

Author contributions:

X Chen and I contributed to the manuscript equally. I performed the experiments studying the location of Hedgehog processing and Hedgehog interaction with protein disulfide isomerases. X Chen performed the RNAi experiments demonstrating the involvement of ER-associated degradation machinery in Hedgehog turnover. C Jao performed preliminary studies of Hedgehog processing in vitro, B Mueller performed preliminary experiments to follow Hedgehog processing in cells, S Schulman cloned the library of protein disulfide isomerase mutants I used.

ABSTRACT

The Hedgehog signaling pathway has important functions during metazoan development. The Hedgehog ligand is generated from a precursor by self-cleavage, which requires a free cysteine in the C-terminal part of the protein and results in production of the cholesterol-modified ligand and a C-terminal fragment. Here we demonstrate that these reactions occur in the endoplasmic reticulum (ER). The catalytic cysteine needs to form a disulfide bridge with a conserved cysteine, which is subsequently reduced by protein disulfide isomerase. Generation of the C-terminal fragment is followed by its ER-associated degradation (ERAD), providing the first example of an endogenous luminal ERAD substrate that is constitutively degraded. This process requires the ubiquitin ligase Hrd1, its partner Sel1, the cytosolic ATPase p97, and degradation by the proteasome. Processing-defective mutants of Hedgehog are degraded by the same ERAD components. Thus, processing of the Hedgehog precursor competes with its rapid degradation, explaining the impaired Hedgehog signaling of processing-defective mutants, such as those causing human holoprosencephaly.

INTRODUCTION

The Hedgehog (Hh) signaling pathway is initiated by the binding of the secreted Hh ligand to its cell surface receptor, Patched (Marigo et al., 1996; Stone et al., 1996). This binding event inactivates Patched, resulting ultimately in the activation of a specific transcriptional program, which is important in embryonic development, adult stem cell maintenance and carcinogenesis (Kalderon, 2005; Lum and Beachy, 2004; Ogden et al., 2004). The secreted Hh ligand is generated through a unique process. Hh is synthesized as a precursor that is translocated into the endoplasmic reticulum (ER). The precursor undergoes cholesterol-dependent self-cleavage, resulting in N- and C-terminal fragments (Lee et al., 1994; Porter et al., 1996a; Porter et al., 1995; Porter et al., 1996b) (Supplemental Figure 2.S1). This process is driven by the intein-like activity of the C-terminal fragment in two steps (Hall et al., 1997). In the first step, a conserved catalytic cysteine in the C-terminus attacks the polypeptide backbone and forms a thioester intermediate. In the second step, the 3β-hydroxyl group of a cholesterol molecule displaces the C-terminal fragment, generating an ester linkage with the carboxyl group of the N-terminal fragment. Hh processing and cholesterol modification are critical for normal Hh signaling, and mutations in human Sonic Hedgehog (HShh) that impair processing cause holoprosencephaly, one of the most common congenital malformations of the brain (Maity et al., 2005; Roessler et al., 2009; Traiffort et al., 2004). The cholesterol-modified N-terminal fragment, further modified by pamitylation at its N-terminus (Chamoun et al., 2001), is ultimately released from cells and is responsible for all the signaling effects of the Hh pathway. It is currently unknown where in the secretory pathway the processing of the Hh precursor occurs. In addition, the fate of the C-terminal fragment generated during the processing of the precursor is unclear.

Here we demonstrate that the self-cleavage of the Hh precursor occurs in the ER, requiring the reduction of a disulfide bond between the catalytic cysteine and another conserved cysteine in the C-terminal fragment by protein disulfide isomerase (PDI). After cleavage, the C-terminal fragment is degraded by the ER-associated degradation (ERAD) pathway (Hirsch et al., 2009; Xie and Ng), providing the first example of an endogenous luminal ERAD substrate that is constitutively degraded. Degradation requires key ERAD components previously implicated in the degradation of misfolded ER proteins, including the ubiquitin ligase Hrd1p (Bays et al., 2001a; Bordallo et al., 1998), its interaction partner Sel1 (Gardner et al., 2000; Mueller et al., 2008; Mueller et al., 2006), and the p97 ATPase (Bays et al., 2001b; Jarosch et al., 2002; Rabinovich et al., 2002; Ye et al., 2001). Our results indicate that the generation of the N-terminal signaling domain of Hh in the ER is accompanied by the disposal of the C-terminal fragment by ERAD. We also show that processing-defective mutants of Hh, such as those causing human holoprosencephaly, are quickly degraded by the same ERAD pathway. Our results suggest that ERAD plays a critical role in birth defects caused by Hh precursor mutations.

RESULTS

Purified Hh precursor processing requires a conserved non-catalytic cysteine

We first investigated the in vitro processing of the purified Drosophila Hh precursor (Lee et al., 1994; Porter et al., 1996a). A fusion protein was generated that contains maltose binding protein (MBP), the last 15 amino acids of the N-terminal fragment, and the entire C-terminal fragment of Drosophila Hedgehog (MBP-DHh). The protein was expressed in E. coli and purified as a soluble protein on an amylose affinity column. When incubated with high concentrations of dithiothreitol (DTT) or with low concentration of DTT and cholesterol, MBP-DHh underwent cleavage, generating an N-terminal fragment (MBP-DHh-N) and a C-terminal fragment (DHh-C) (Figure 2.1A), as described (Porter et al., 1996b). The N-terminal fragment was modified with cholesterol, as shown by the change in its electrophoretic mobility compared to the unmodified fragment (Figure 2.1A, lane 4 versus 3), and by the incorporation of ^{3}H-labeled cholesterol (Figure 2.1B).

We noticed that the precursor migrated slower on non-reducing SDS-PAGE gels when treated with even low concentrations of DTT (Figure 2.1A, lane 1 versus 2). Because MBP-DHh contains only two cysteines, this suggests that the catalytically active cysteine (C258) is disulfide bonded with C400. Both cysteines are absolutely conserved among all Hh proteins, across phyla. In the crystal structure of the C-terminal fragment of Drosophila Hh (Hall et al., 1997), C258 is in close proximity to C400, suggesting the possibility of such a disulfide bond. Given that C258 needs to be reduced to act as a nucleophile in Hh processing, this suggests that the disulfide-bonded species is an

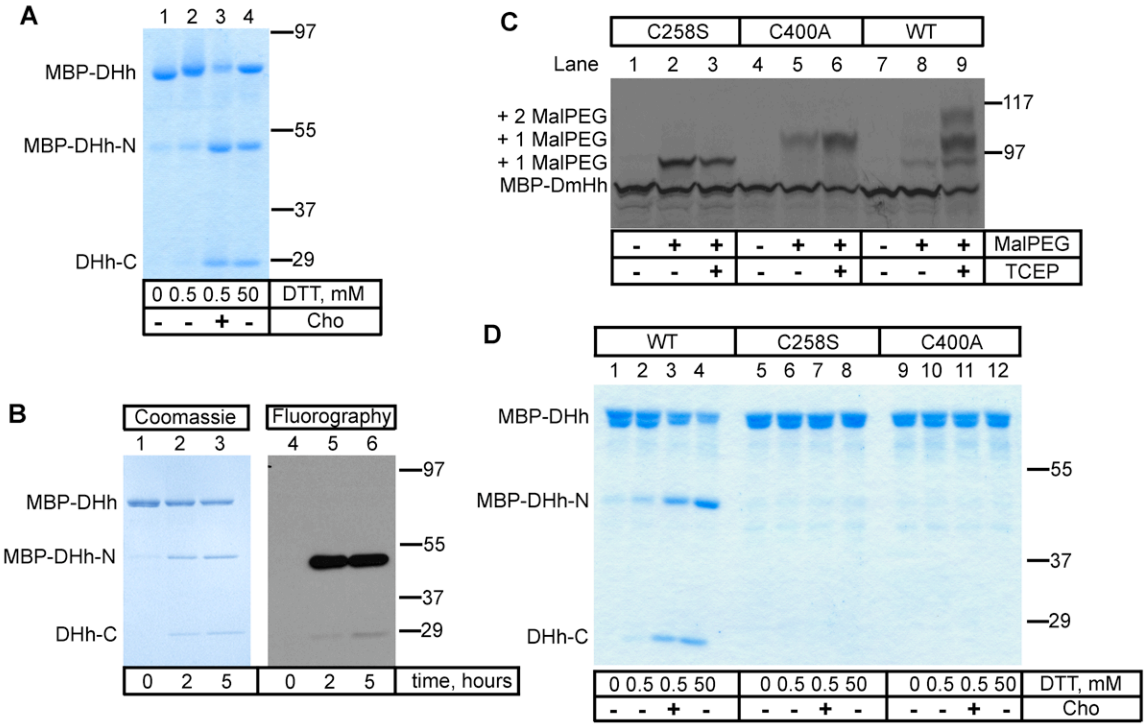

Figure 2.1 Processing of purified Hh precursor.
(A) A fusion was generated between maltose binding protein (MBP), the last 15 amino acids of the N-terminal fragment of Drosophila Hh, and the entire C-terminal fragment of Drosophila Hh (MBP-DHh). The purified protein was incubated for 5 hrs at room temperature with different concentrations of dithiothreitol (DTT) in the absence or presence of cholesterol (Cho). The samples were analyzed by non-reducing SDS-PAGE and Coomassie staining. MBP-DHh-N and DHh-C are the N- and C-terminal fragments generated by Hh processing.
(B) As in (A), but the reaction contained ^{3}H-cholesterol. The samples were analyzed by reducing SDS-PAGE followed by either Coomassie staining (left) or fluorography (right).
(C) In vitro translated, ^{35}S-labeled wild type (WT) MBP-DHh or the indicated Cys mutants were incubated with 5 KDa maleimide polyethylene glycol (Mal-PEG) as indicated, in the presence or absence of the reducing agent tris(2.carboxyethyl)phosphine (TCEP). The samples were analyzed by reducing SDS-PAGE and autoradiography. The positions of singly and doubly Mal-PEG modified species are indicated. The singly modified species have a different mobility, depending on which cysteine is modified.
(D) As in (A), but comparing wildtype MBP-DHh with the two Cys mutants.

inactive precursor; the known requirement of a reducing agent for Hh processing in vitro (Porter et al., 1996b) could be explained by the need to reduce this conserved disulfide bond.

To test whether the two cysteines indeed form a disulfide bridge in MBP-DHh, we expressed the same protein by in vitro translation in reticulocyte lysate and treated it with maleimide-polyethylenglycol (Mal-PEG), a reagent that adds ~5 kDa for each modified free cysteine. Whereas non-reduced wildtype MBP-DHh showed little modification (Figure 2.1C,

lane 8), prior disulfide bond reduction with tris-carboxyethyl phosphine (TCEP) resulted in the appearance of significant levels of singly and doubly Mal-PEG-modified species (lane 9). When either of the two cysteines was mutated, only singly modified protein was detected, even without reduction (lanes 2,3 and 5,6). These data indicate the formation of a disulfide bond between C258 and C400. As expected, mutation of the catalytic C258 completely blocked cleavage of MBP-DHh (Figure 2.1D, lanes 5-8). Interestingly, mutation of the non-catalytic C400 also abolished cleavage, both in the presence of high concentrations of DTT and low concentrations of DTT and cholesterol (lanes 9-12). Thus, despite the presence of a reduced C258, the mutant is inactive, perhaps because a disulfide bond between C258 and C400 is required for the folding of the C-terminus into a catalytically active conformation. In all Hh proteins the non-catalytic cysteine is part of a conserved SCY sequence, and the mutation of the other two residues also abolishes cleavage of DHh (data not shown). Taken together, these experiments suggest that a disulfide bridge needs to form between the conserved cysteines, which subsequently would have to be reduced for generating the thiol group required for intein catalysis.

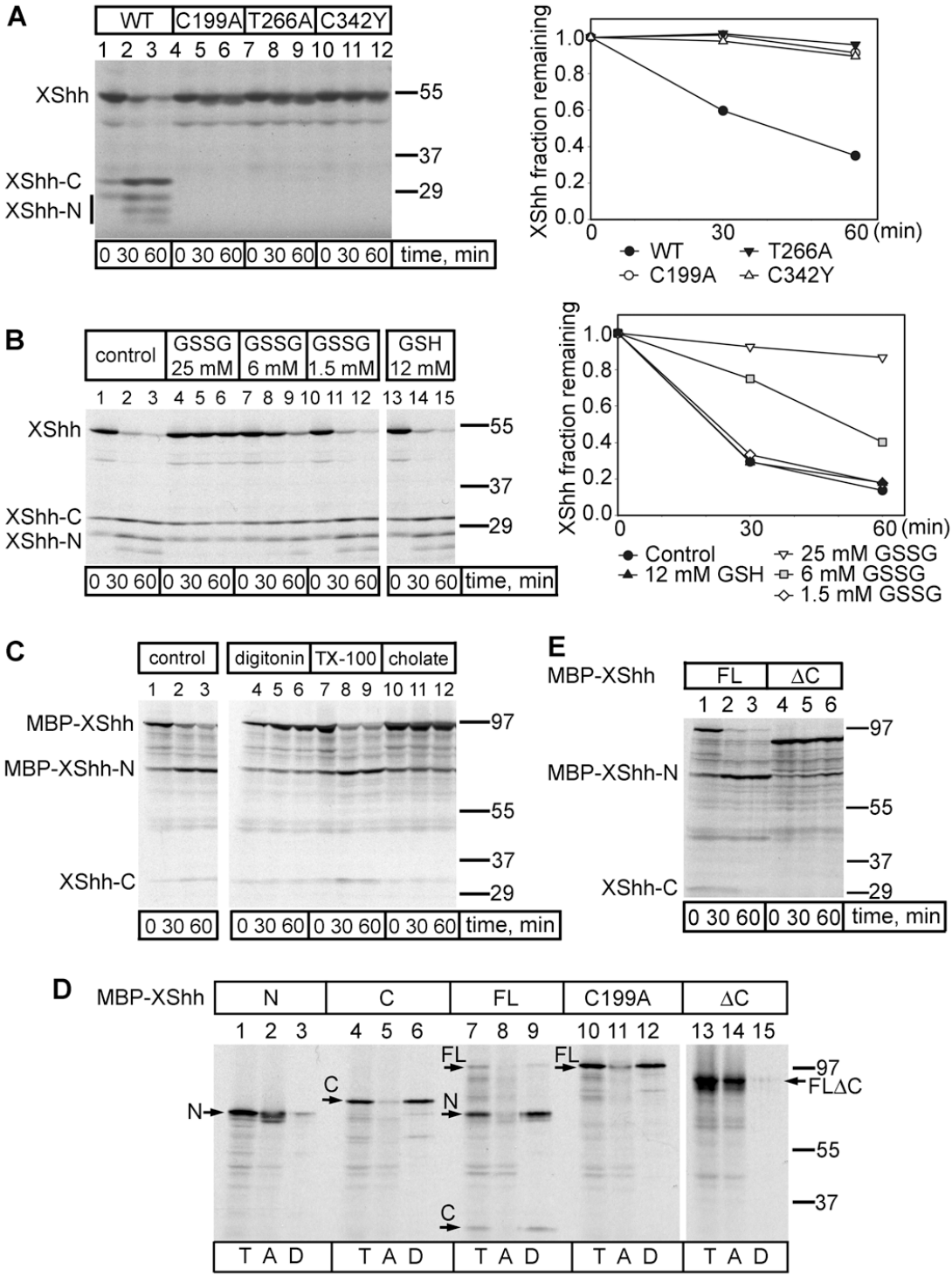

Figure 2.2 Hh processing in Xenopus egg extracts.
(A) In vitro translated, ^{35}S-labeled Xenopus Sonic Hh (XShh) wild type precursor was incubated at room temperature with Xenopus egg extracts for the indicated times. Parallel experiments were performed with three point mutants. The samples were analyzed by SDS-PAGE and autoradiography. The graph shows the quantification of the Hh precursor.

Figure 2.2 (Continued)
(B) As in (A), but the extract was supplemented with the indicated concentrations of oxidized or reduced glutathione (GSSG or GSH).
(C) In vitro translated, ^{35}S-labeled Xenopus Sonic Hh, fused at its N-terminus to the maltose-binding protein (MBP-XShh), was incubated at room temperature with Xenopus egg extracts for the indicated times, in the absence or presence of 0.5% of either the cholesterol-sequestering detergents digitonin or cholate or the control detergent Triton X-100 (TX-100). The samples were analyzed by SDS-PAGE and autoradiography.
(D) In vitro translation was used to generate ^{35}S-labeled fusions of MBP and either the N-terminal fragment of XShh (N), the C-terminal fragment of XShh (C), full-length XShh (FL), full-length XShh with a Cys mutation in the active site (C199A), or XShh lacking the last 93 amino acids (ΔC). The fusions were incubated for 1 hr with Xenopus egg extracts and subjected to Triton X-114 partitioning. Aliquots of the input (T), of the aqueous phase (A), or of the detergent phase (D) were analyzed by SDS-PAGE and autoradiography.
(E) As in (A), but with a MBP fusion of either wild type XShh (FL) or a mutant lacking the last 93 amino acids (ΔC).

Hh processing in extracts and intact cells also requires the conserved, non-catalytic cysteine.

To test whether the conserved, non-catalytic cysteine is essential for the processing of full-length, vertebrate Hh precursor, we established a novel cell-free assay based on Xenopus egg extracts. Radioactively labeled Xenopus Sonic Hedgehog (Lai et al., 1995) (XShh) precursor, generated by in vitro translation in reticulocyte lysate, was efficiently processed when incubated with Xenopus egg extracts (Figure 2.2A, lanes 1-3). As in the purified system, both the catalytic cysteine (C199) and the non-catalytic cysteine (C342) were required for cleavage (lanes 4-6 and 10-12). Mutation of another conserved residue shown to be important for cleavage in DHh (T266) also abolished processing (lanes 7-9). Identical results were obtained with the corresponding DHh constructs, generated by in vitro translation and incubated with Xenopus egg extracts (data not shown). Consistent with our assumption that reduction of the disulfide bridge in the Hh precursor is required for processing, addition of increasing concentrations of oxidized glutathione (GSSG) inhibited XShh precursor cleavage (Figure 2.2B, lanes 1-12).

We next tested whether the N-terminal fragment generated in Xenopus extracts is modified with cholesterol. Indeed, the cleavage reaction was blocked by cholesterol-sequestering

detergents (Figure 2.2C, lanes 4-6 and 10-12 versus lane 1-3 and 7-9). Furthermore, the N-terminal fragment generated in extracts partitioned into the Triton X-114 phase (Figure 2.2D, lanes 7-9), in contrast to the N-terminal fragment generated directly by in vitro translation (lanes 1-3). The C-terminal fragment is also hydrophobic, as it partitioned into the detergent phase, whether alone or contained in the full-length protein (lanes 4-6 and 7-12). Deletion of the last 93 amino acids from full-length XShh (XShhΔC) rendered the protein hydrophilic (lanes 13-15). The deleted region indeed contains a number of hydrophobic amino acids and might interact with cholesterol during the intein reaction (Hall et al., 1997). This deletion greatly delayed, but did not completely abolish, processing of the precursor in Xenopus extracts (Figure 2.2E). Finally, when purified MBP-DHh precursor was added to Xenopus extracts, mass spectrometry identified cholesterol attached to the N-terminal fragment (data not shown). These data demonstrate that cholesterol is properly attached to Hh proteins in Xenopus egg extracts.

To test whether the conserved, non-catalytic cysteine is also essential for the processing of the Hh precursor in intact cells, we stably expressed wild type or cysteine mutants of human sonic Hh (HShh) C-terminally tagged with a hemagglutinin (HA) epitope (HShh-HA) in 293T cells. After inhibiting protein synthesis with cycloheximide, the wild type Hh precursor and the processed C-terminal fragment (HShh-C) were observed at early time points (Figure 2.3A). As in the in vitro system, no processing was observed when either the catalytic cysteine (C198) or the non-catalytic cysteine (C363) was mutated (Figures 2.3B and 2.3C, lanes 1). For both cysteine mutants, the block in processing correlated with a complete absence of active Hh ligand from 293T cell supernatants, as assayed using Hh-responsive NIH-3T3 cells; in contrast, wild type HShh-HA expressed in 293T cells resulted in robust secretion of active Hh ligand (data not shown). Consistent with the postulated role of the two conserved cysteines, a reagent that makes

the ER more oxidizing (diamide) also inhibited Hh precursor processing in mammalian cells, while DTT had the opposite effect, as shown by pulse-chase experiments (Figure 2.3D). These data support the idea that Hh processing requires the formation and subsequent reduction of a disulfide bridge between the conserved cysteines.

We noted that after addition of cycloheximide both the Hh precursor and HShh-C disappeared in a time-dependent manner (Figure 2.3A-C). When the cycloheximide chase of wild type HShh-HA was performed in the presence of the proteasome inhibitor MG132, HShh-C accumulated, indicating that the precursor was efficiently processed and that HShh-C was normally degraded by the cytosolic proteasome (Figure 2.3A, lanes 5,6). Similar experiments with the processing-defective cysteine mutants showed that the Hh precursor is also degraded by the proteasome (Figure 2.3B, C, lanes 5, 6). When HShh-C was expressed by itself, it was also degraded, but at a slower rate (Supplemental Figure 2.S2), indicating that its degradation is most efficient when generated during normal processing.

Hh processing does not require vesicular transport out of the ER

We reasoned that the remodeling of the conserved disulfide bridge in Hh occurs in the ER, the site of all known disulfide bond formation and reduction in the secretory pathway. To test this assumption, we performed pulse-chase experiments after blocking vesicular transport from the ER to the Golgi by brefeldin A (Figure 2.3E). No effect on Hh processing was observed at concentrations that caused the complete disappearance of the Golgi (Supplemental Figure 2.S3), and regardless of whether or not a proteasome inhibitor was present (Figure 2.3E). These results strongly argue that both the processing of the Hh precursor and the degradation of HShh-C occur in the ER.

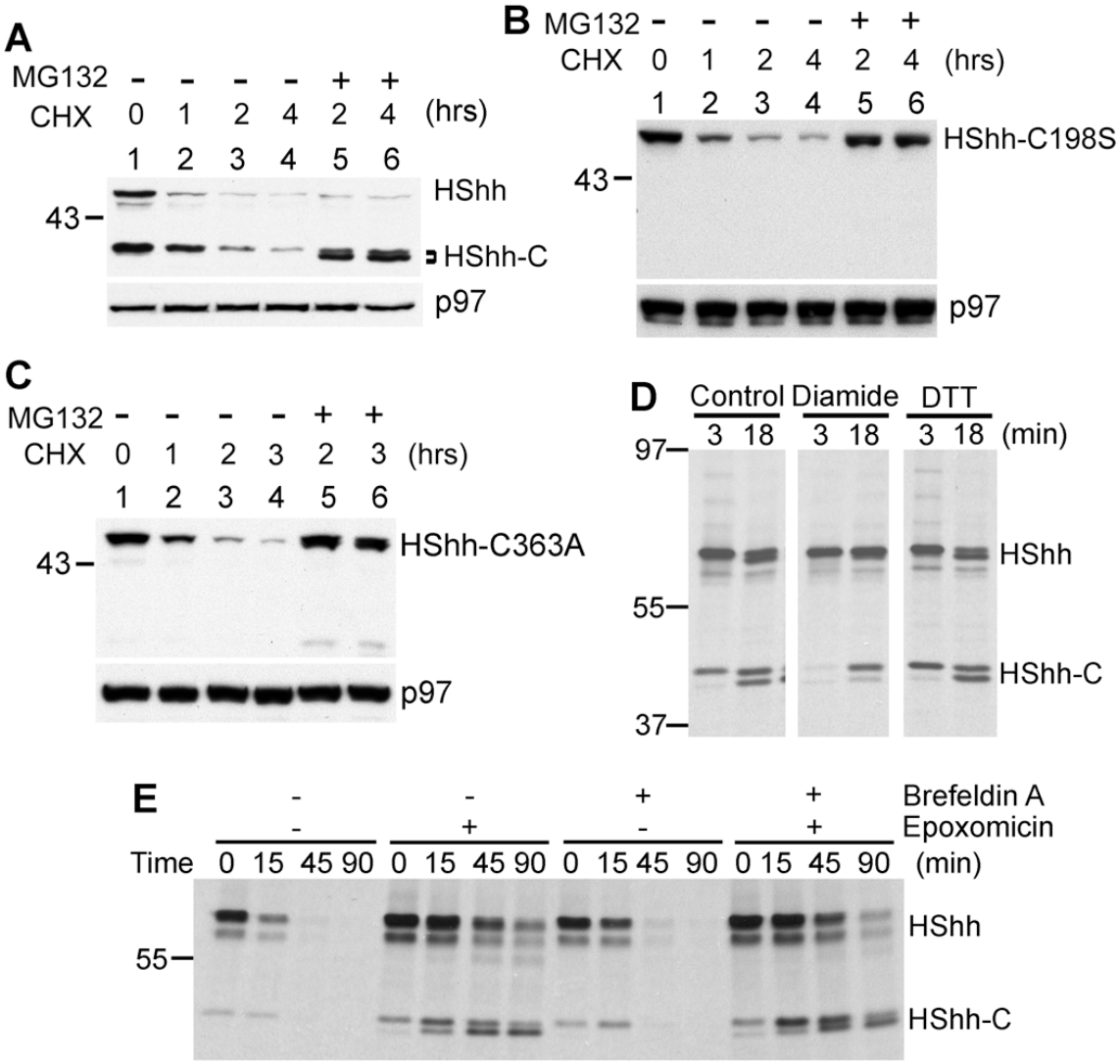

Figure 2.3 Processing of HShh is dependent on disulfide bridge formation and reduction.
(A) HShh-HA was stably expressed in 293T cells. Protein synthesis was inhibited with cycloheximide (CHX), and the fate of the protein followed by SDS-PAGE and immunoblotting with anti-HA antibodies. Immunoblotting for p97 was used as a loading control.
(B) As in (A), but with HShh-HA containing a mutation in the catalytic cysteine (C198S).
(C) As in (A), but with HShh-HA containing a mutation in the conserved non-catalytic cysteine (C363A).
(D) HA-tagged HShh was stably expressed in 293T cells. The cells were pulsed with ^{35}S-methionine for 3 min and chase-incubated with unlabeled methionine for the indicated times. Diamide (200 uM) or DTT (0.5 mM) were added 10 minutes before the pulse, and were present during the pulse and chase. The proteasome inhibitor epoxomicin (1 uM) was present, added 1 hour before the pulse. The samples were analyzed by immunoprecipitation with HA-antibodies followed by reducing SDS-PAGE and fluorography. Equal number of cells were processed for each condition.
(E) As in (D), except that, where indicated, 10 uM brefeldin A and 1 uM epoxomicin were present, added 1 hr before the pulse. The samples were analyzed as in (D).

The Hh protein is a substrate for PDI

It seemed likely that the remodeling of the conserved disulfide bridge in Hh is catalyzed by a member of the ER-localized thioredoxin (Trx)-like oxidoreductases, a class of enzymes generally responsible for such reactions. These enzymes contain at least one CXXC motif, the first cysteine of which forms a transient mixed disulfide bridge with the substrate; this mixed disulfide intermediate can be trapped by mutating the second cysteine in the CXXC motif (CXXA mutants). We therefore screened CXXA-mutants of ER-localized human Trx-like proteins for the formation of a mixed disulfide bridge with Hh. We co-expressed in 293T cells FLAG-tagged CXXA-mutants of 9 different Trx-like ER proteins together with HShh-HA. Because some of the proteins contain more than one CXXC motif, we tested a total of 17 different constructs (Schulman et al., 2010). In each case, the formation of a mixed disulfide bridge was assayed by immunoprecipitation with HA- or FLAG- antibodies, followed by non-reducing SDS-PAGE and immunoblotting.

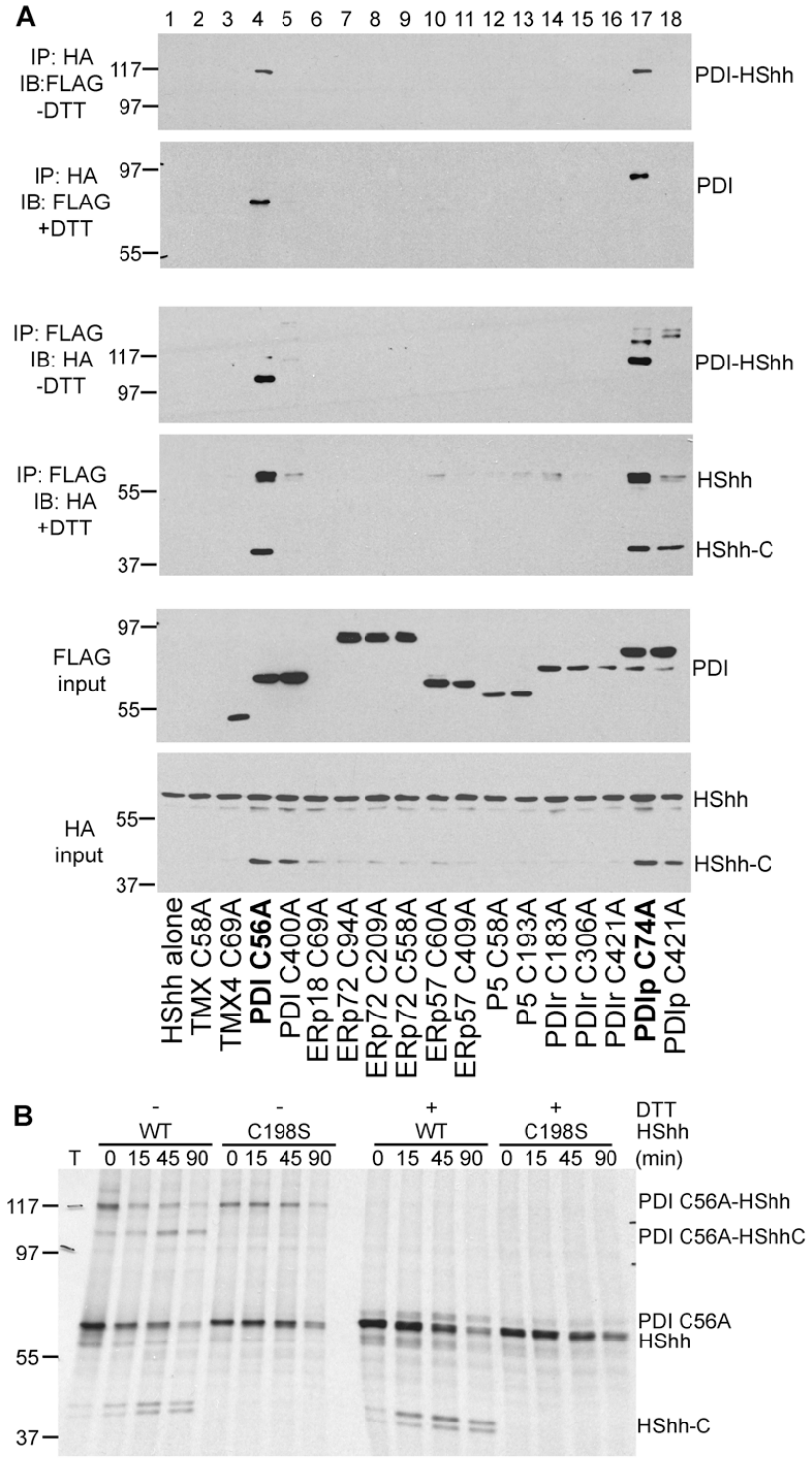

Figure 2.4 PDI and PDIp are involved in remodeling of the conserved disulfide bridge in HShh
(A) HShh-HA and FLAG-tagged thioredoxin-like ER proteins, in which one their CXXC motifs was changed to CXXA, were co-expressed in 293T cells. Cell extracts were subjected to immunoprecipitation with HA- or FLAG-antibodies, followed by SDS-PAGE and immunoblotting with FLAG- and HA- antibodies. Where indicated, the immunoprecipitated samples were reduced with DTT prior to electrophoresis.

Figure 2.4 (Continued)
(B) Wild type (WT) HShh-HA or the processing-defective C198A mutant were co-expressed with a FLAG-tagged CXXA mutant of PDI (C56A) in 293T cells. The cells were pulse-labeled with ^{35}S-methionine for 3 min and chase-incubated for different time periods. The proteasome inhibitor epoxomicin (1 uM) was added 1 hr before the pulse. All samples were subjected to immunoprecipitation with HA-antibodies followed by SDS-PAGE and fluorography. Where indicated, the samples were reduced with DTT before electrophoresis.

The strongest interactions were observed for PDI and the closely related PDIp protein (Figure 2.4A, first and third panel). As expected, both mixed disulfide adducts were sensitive to DTT treatment (second and fourth panels), and no adducts were seen when one of the two components was omitted (Supplemental Figure 2.S4). PDI and PDIp contain two CXXC motifs, but the reaction with Hh occurred overwhelmingly with the N-terminal motif. This data implies that the first CXXC motif of PDI is dedicated to substrate interaction, whereas the second CXXC motif interacts with the oxidase Ero1p (Tsai and Rapoport, 2002).

PDI and PDIp reacted with both the Hh precursor and HShh-C (Figure 2.4A, fourth panel), as expected from the fact that both contain the two conserved cysteines. Pulse-chase experiments in the presence of proteasome inhibitor demonstrated that the formation of the mixed disulfide between the Hh precursor and the CXXA-mutant of PDI occurs rapidly and precedes Hh processing, including the appearance of the mixed disulfide adduct between HShh-C and the PDI mutant (Figure 2.4B). Interestingly, the mixed disulfide species can undergo the intein reaction with about the same kinetics as the Hh precursor itself. This also suggests that the non-catalytic cysteine of Hh is linked to PDI. Furthermore, when Hh processing was blocked by mutation of the catalytic cysteine, the Hh precursor formed a mixed disulfide bond with the PDI mutant.

These data are consistent with a model in which PDI function is linked and required for Hh processing. Finally, it should be noted that overexpression of the PDI and PDIp mutants

caused the accumulation of HShh-C (Figure 2.4A, bottom panel), likely because a mixed disulfide adduct with PDI is not susceptible to degradation.

HShh-C is degraded in the ER

To study the fate of HShh-C, we first considered the possibility that it might be secreted together with the N-terminal fragment (HShh-N). HShh-HA was stably expressed in 293T cells, and HShh-N and HShh-C were analyzed by immunoblotting with Hh- and HA-antibodies, respectively, both in cells and in equivalent amounts of culture medium. Whereas HShh-N partitioned equally between cells and medium, HShh-C was present only in cells (Figure 2.5A, left panel). Even when HShh-C accumulated in cells after treatment with a proteasome inhibitor, only very small amounts of HShh-C were found in the medium (Figure 2.5A, right panel). These results show that HShh-C is not secreted, in contrast to HShh-N, the Hh ligand. Rather, the instability of HShh-C and its stabilization by proteasome inhibitors, even under conditions where vesicular transport out of the ER is blocked, suggests that HShh-C is degraded in the ER. Previous reports on the secretion of HShh-C can be explained by its massive overexpression and by the lack of quantification (Bumcrot et al., 1995).

To confirm that HShh-C is degraded in the ER, we tagged HShh with mCherry at its C-terminus and visualized the protein by fluorescence microscopy. The protein showed the typical ER staining, co-localizing with calnexin (Figure 2.5B), in both 293T and in 3T3 cells stably expressing HShh-Cherry. When 3T3 cells stably expressing HShh-HA were treated with the proteasome inhibitor epoxomicin, the intensity of the staining increased significantly,

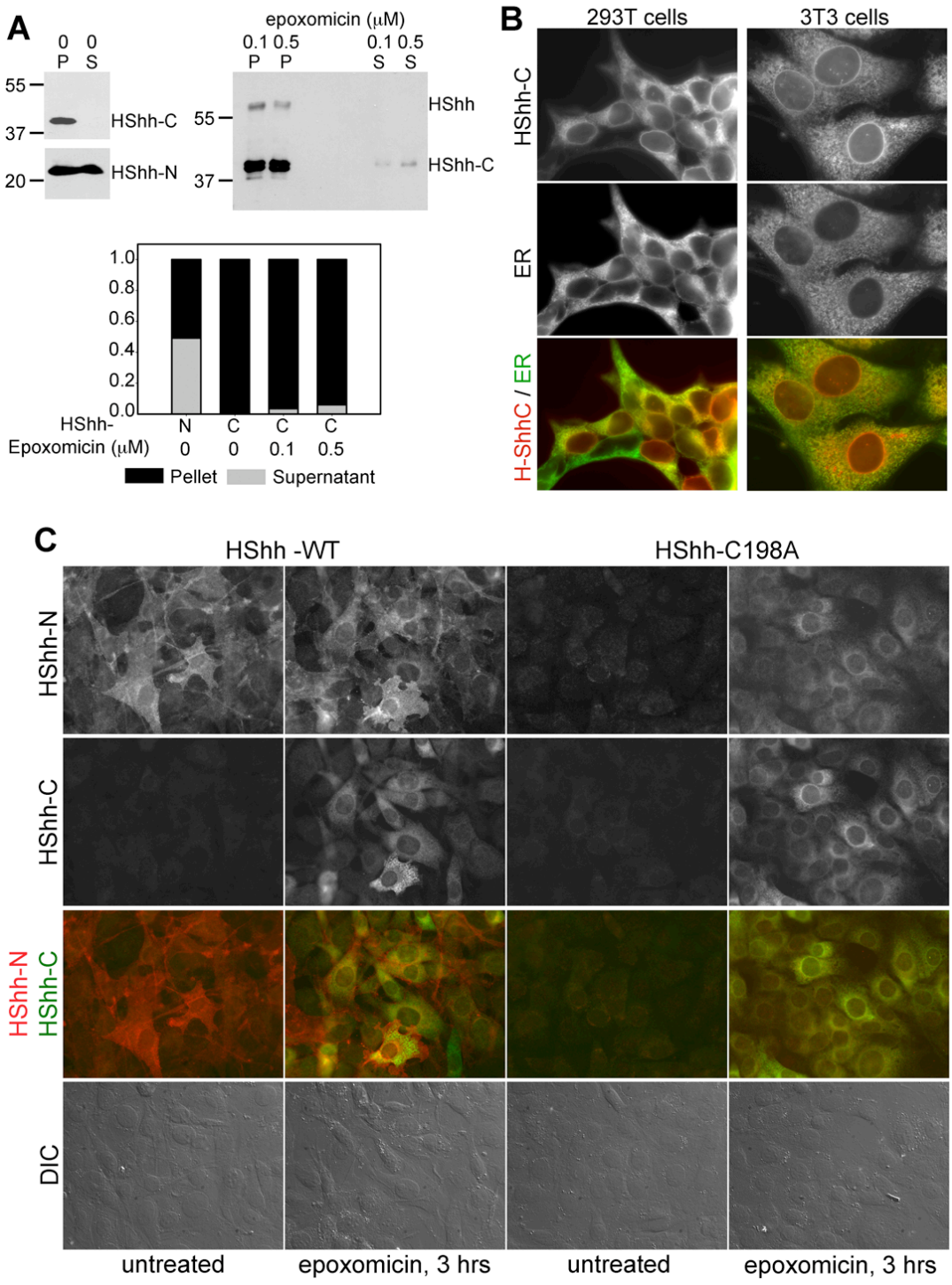

Figure 2.5 HShh-C is not secreted and is degraded in the ER.
(A) HShh-HA was stably expressed in 293T cells. The cells were washed and incubated for 12 hrs with DMEM containing 0.5% fetal bovine serum. The cell pellets and equivalent amounts of culture medium were analyzed for the presence of HShh-N and HShh-C by immunoblotting with HShh-N antibodies and HA-antibodies. Where indicated, the proteasome inhibitor epoxomicin was present during the last 3 hrs of incubation. The graph shows the distribution of HShh-N and HShh-C between cells and medium.

Figure 2.5 (Continued)
(B) HShh was tagged with mCherry at its C-terminus and stably expressed in 293T or in 3T3 cells. Its localization was determined by fluorescence microscopy. The ER was revealed by immunostaining with rabbit antibodies against calnexin. The bottom panels show merged images.
(C) Wild type HShh-HA or the processing-defective mutant HShh-C198A-HA were stably expressed in 3T3 cells. Cells were immunostained with rat HA-and rabbit HShh-N- antibodies, followed by goat anti-rat Alexa488 (green) and goat anti-rabbit Alexa594 (red) secondary antibodies. The cells were incubated for 3 hrs with or without the proteasome inhibitor epoxomicin (1 uM). The third row shows merged images of the green and red channels. The bottom row shows DIC images.

consistent with HShh-C being degraded in the ER (Figure 2.5C; second row; also Supplemental Figure 2.S5). Identical results were obtained with the proteasome inhibitors MG132 and bortezomib (not shown), and in 293T cells (Supplemental Figure 2.S5). The immunofluorescent staining observed under these conditions corresponds mostly to HShh-C (see immunoblot in Figure 2.5A). In contrast to HShh-C, HShh-N was not degraded, as demonstrated by staining with antibodies directed against the N-terminus of HShh (Figure 2.5C, first row). The subcellular localization of HShh-N was also different from that of HShh-C, with much of HShh-N localizing to the plasma membrane (see overlay in the third row of Figure 2.5C). The processing-defective HShh precursor mutant (HShh-C198A) was as unstable as HShh-C when analyzed by antibodies against either the N- or C-terminus, and it localized to the ER when stabilized by proteasome inhibitors (Figure 2.5C; the two right most panels). These data demonstrate that failure of processing results in rapid degradation of the full-length HShh precursor in the ER.

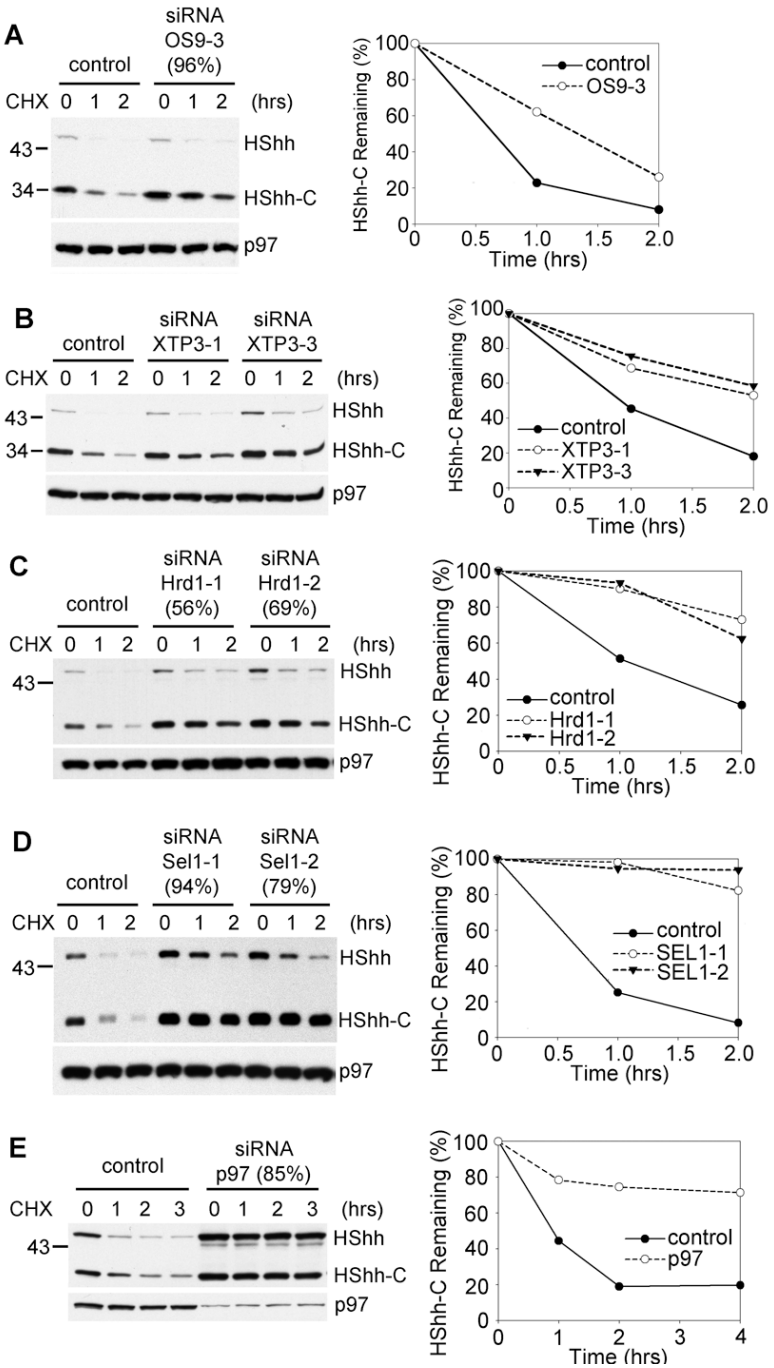

Figure 2.6 ERAD components required for the degradation of HShh-C.
(A) Cells were depleted of the ER-luminal lectin OS9 by siRNA and the fate of stably expressed HShh-HA was followed after cycloheximide (CHX) addition. The extent of OS9 depletion (in brackets) was determined by quantitative RT-PCR. Controls were treated with an unrelated siRNA. All samples were analyzed by SDS-PAGE and immunoblotting with HA-antibodies. The right panel shows quantification of HShh-C in the experiment. All samples were also analyzed by immunoblotting for p97 (loading control).
(B) As in (A), but with depletion of the ER-luminal lectin XTP3 by two different siRNAs.
(C) As in (A), but with depletion of the ubiquitin ligase Hrd1 by two different siRNAs
(D) As in (A), but with depletion of the Hrd1-interacting protein Sel1 by two different siRNAs.
(E) As in (A), but with depletion of the ATPase p97 by siRNA.

Hh is degraded by ERAD

Next we examined if HShh-C generated in the ER lumen is degraded by the "ER-associated degradation" (ERAD) pathway. Luminal, glycosylated ERAD substrates are generally processed by glycosidases in their carbohydrate moiety, which is subsequently recognized by lectins. The substrates are then translocated into the cytosol, poly-ubiquitinated by the ubiquitin ligase Hrd1, moved into the cytosol by the p97 ATPase, and finally degraded by the proteasome. Proteolysis is often preceded by deglycosylation (Wiertz et al., 1996). We tested which aspects of the ERAD pathway apply to the degradation of HShh-C.

We used RNAi to identify ERAD components required for the degradation of HShh-C. Depletion of the lectins implicated in recognizing glycosylated ERAD substrates, OS9 or XTP3 (Bernasconi et al., 2010; Christianson et al., 2008; Hosokawa et al., 2009; Hosokawa et al., 2008), caused a significant inhibition of degradation (Figures 2.6A, B; quantification in the right panels). No further inhibition was seen when both lectin were depleted at the same time (Supplemental Figure 2.S6). Depletion of the ubiquitin ligase Hrd1 (Bays et al., 2001a) and of its interacting partner Sel1, strongly stabilized HShh-C (Figures 2.6C, D). Finally, depletion of the ATPase p97 (Ye et al., 2001) also had a drastic inhibitory effect (Figure 2.6E); both the HShh precursor and HShh-C accumulated, indicating that they both undergo ERAD. The depletion by RNAi of other ERAD components (the Ring-finger ubiquitin ligases gp78 (Fang et al., 2001), TRC8 (Stagg et al., 2009), TEB4 (Hassink et al., 2005), as well as Derlin-1 (Lilley and Ploegh, 2004; Ye et al., 2004), Herp (Carvalho et al., 2006; Kokame et al., 2000; Schulze et al., 2005), BiP (Denic et al., 2006), and ERdj5 (Ushioda et al., 2008) had no effect on HShh-C degradation (Supplemental Figure 2.S5). Addition of kifunensine or 1-deoxymannojirimycin (DMJ) (Elbein,

1991) had no significant effect on the degradation of HShh-C (Supplemental Figure 2.S6), indicating that mannosidase I is not required for processing of the glycan on HShh-C.

The role of various ERAD components in the degradation of HShh was also tested by expression of dominant-negative constructs. A catalytically inactive mutant of the ubiquitin ligase Hrd1p, in which a cysteine in the Ring-finger domain is altered, strongly inhibited HShh-C degradation (Figure 2.7A). While overexpression of the wild type p97 ATPase only slightly delayed degradation of HShh-C, the catalytically inactive p97-QQ mutant was strongly inhibitory (Figure 2.7B). ERAD was similarly inhibited by overexpression of catalytically inactive Ubc6e (Ubc6e-C91S), or by overexpression of a GFP fusion of the SEL1L-interacting protein, UbxD8 (UbxD8-GFP (Lilley and Ploegh, 2004; Mueller et al., 2008)) (Figure 2.7C).

As with other ERAD substrates that are deglycosylated when arriving in the cytosol, we found that the major species of HShh-C accumulating in the presence of MG132 migrated slightly faster in SDS-gels than the glycosylated fragment (Figures 2.3A, 2.3E, 2.8A). This band is indeed deglycosylated as treatment of the glycosylated fragment with protein N-glycanase F generated a species of the same size (Figure 2.8A). As expected, depletion of ERAD components that block dislocation from the ER, led to the accumulation of glycosylated HShh-C (see, for example, Figure 2.6).

To test whether HShh-C was poly-ubiquitinated, we subjected cell extracts expressing HShh-HA to immunoprecipitation with HA-antibodies, followed by SDS-PAGE and immunoblotting with ubiquitin antibodies (Figure 2.8B). Poly-ubiquitinated

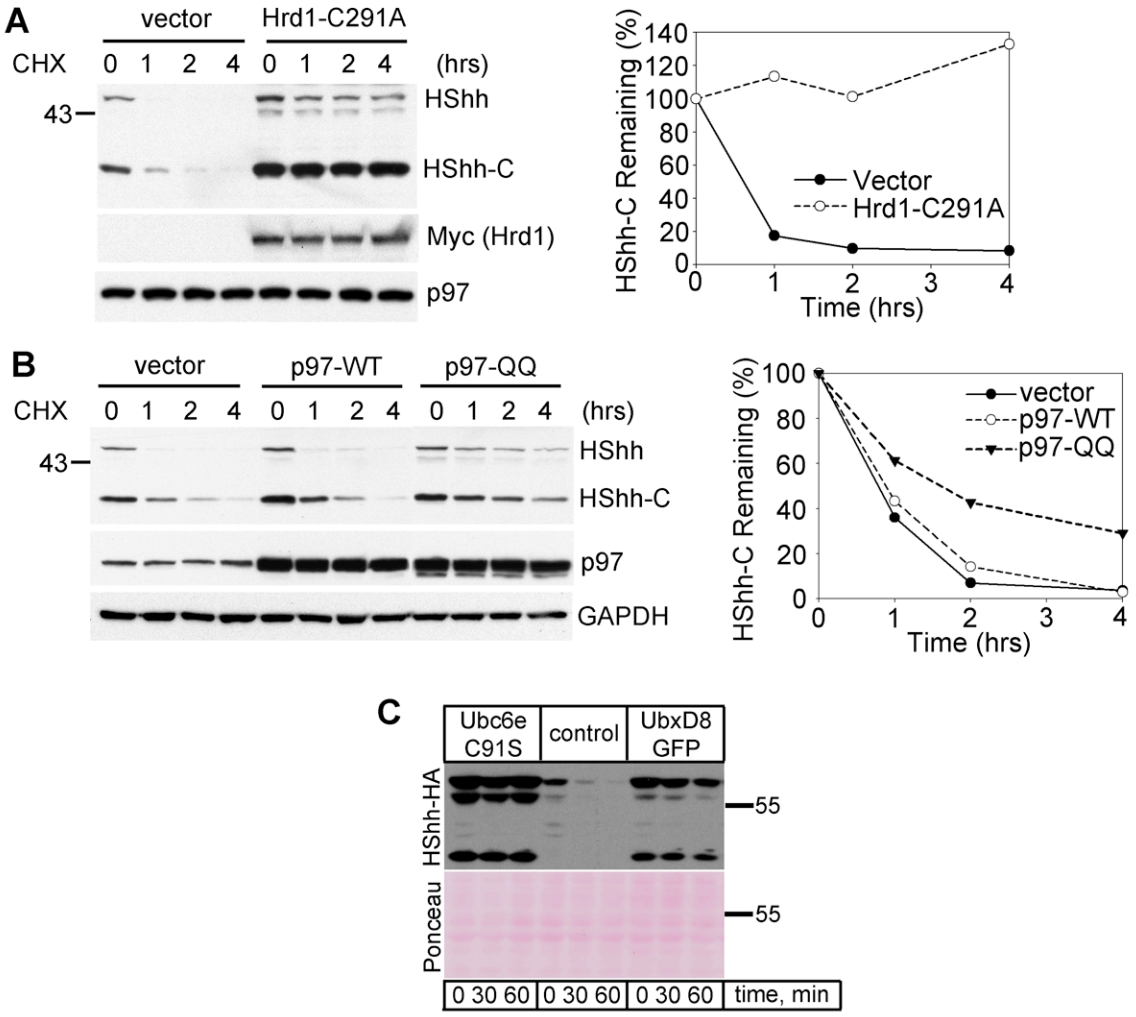

Figure 2.7 Dominant-negative ERAD components inhibit HShh-C degradation.
(A) Cells stably expressing HShh-HA precursor were transfected with a catalytically inactive Myc-tagged Hrd1 (Hrd1-C291A) or with empty vector. The fate of HShh-HA was followed after addition of cycloheximide (CHX) by SDS-PAGE and immunoblotting with HA-antibodies. The right panel shows quantification of the HShh-C in the experiment. All samples were also analyzed by immunoblotting for p97 (loading control) and myc (Hrd1-C291A).
(B) As in (A), but with transfection of either wild type p97, a catalytically inactive p97 mutant (p97-QQ), or with empty vector. Immunoblotting for GAPDH served as loading control.
(C) HShh-HA was transiently expressed in 293T cells, together with dominant-negative Ubc6e (Ubc6e-C91S), control vector, or UbxD8-GFP. Greater than 90% of the cells showed strong GFP signal, by live cell fluorescence microscopy (not shown). Protein synthesis was inhibited with CHX, and the fate of HShh-HA was followed by SDS-PAGE and immunoblotting with HA-antibodies. Ponceau S staining of the blot is shown to demonstrate loading of equal amounts of protein.

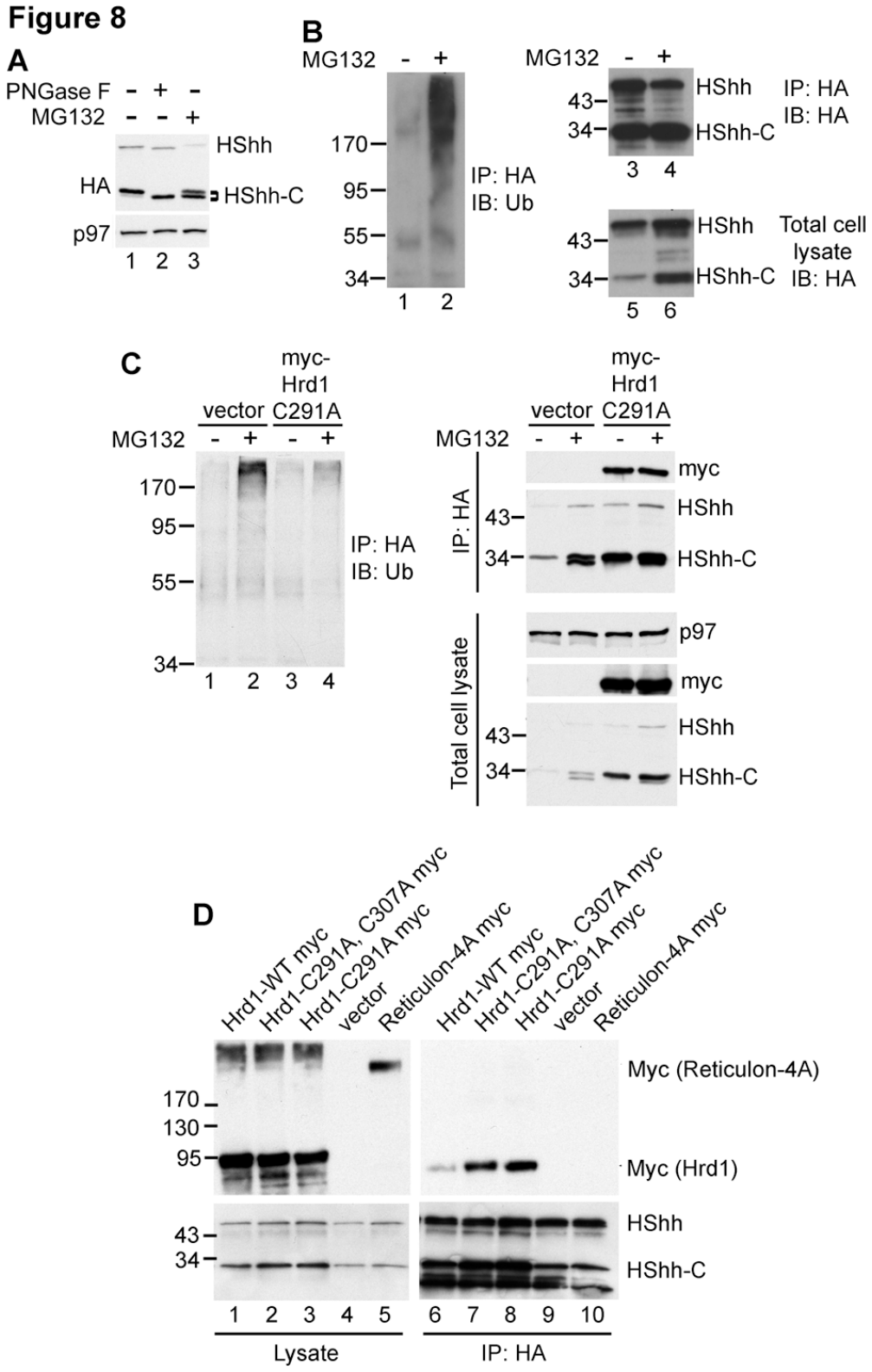

Figure 2.8 Cytoplasmic events preceding HShh-C proteolysis.

Figure 2.8 (Continued)
(A) To test for deglycosylation of HShh-C, HShh-HA was stably expressed in 293T cells. A cycloheximide chase was performed for 2 hrs in the presence or absence of the proteasome inhibitor MG132. Cell lysates were incubated in the absence or presence of the glycanase PNGase F, as indicated. Samples were analyzed by SDS-PAGE and immunoblotting with HA- antibodies. Immunoblotting with p97 antibodies served as loading control.
(B) To test for poly-ubiquitination of HShh, cells stably expressing HShh-HA were incubated in the absence or presence of MG132 for 2 hrs. Extracts were subjected to immunoprecipitation (IP) with HA-antibodies and the proteins were analyzed by SDS-PAGE and immunoblotting (IB) with HA-antibodies (lanes 3,4) or ubiquitin (Ub)-antibodies (lanes 1,2). Lanes 5 and 6 show blots of the extract before IP.
(C) To test if Hrd1 poly-ubiquitinates HShh, an experiment as in (B) was performed, except that, where indicated, cells were transfected with a myc-tagged dominant-negative Hrd1 mutant (myc-Hrd1-291A). To test for the presence of the Hrd1 mutant, the samples were also analyzed by blotting with myc antibodies. Immunoblotting for p97 served as loading control.
(D) Cells stably expressing HShh-HA were transfected with Myc-tagged wild type Hrd1 or catalytically inactive Hrd1 mutants (Hrd1 C291A or Hrd1 C291A-C307A). As a control, a myc-tagged version of reticulon 4A was used. Cell extracts were either analyzed directly (lanes 1-4) or subjected to immunoprecipitation with HA-antibodies (lanes 5-8). All samples were analyzed by SDS-PAGE and immunoblotting with HA- or myc- antibodies.

HShh-HA was detected in cells treated with the proteasome inhibitor MG132 (lane 2), but not in untreated cells, even though equal amounts of HA-tagged protein were precipitated (lanes 3 and 4). The specificity of the immunoprecipitation was demonstrated by a control IgG pull-down (Supplemental Figure 2.S7). Poly-ubiquitination of HShh was dependent on Hrd1, as it was inhibited by the expression of a dominant-negative Hrd1 mutant (Figure 2.8C).

To further confirm the role of Hrd1, we tested whether it interacts with its HShh substrate. Myc-tagged, wild type or dominant-negative Hrd1p were introduced into cells stably expressing HShh-HA. Cell extracts were subjected to immunoprecipitation with HA antibodies and precipitated proteins were analyzed by SDS-PAGE and immunoblotting with Myc antibodies. These experiments showed that HShh-HA precipitated all versions of Hrd1p-Myc (Figure 2.8D, lanes 6-8); less precipitation was seen with wild type Hrd1-Myc (lane 6). An unrelated ER protein, Myc-tagged reticulon, did not interact with HShh-HA (lane 5). Together, these experiments indicate that the ubiquitin ligase Hrd1p interacts with HShh substrates undergoing ERAD.

Finally, because the full-length Hh precursor is also degraded by ERAD (see Figures 2.3B, 2.3C, 2.6E), we tested whether it requires the same components as HShh-C. Indeed, ERAD of the processing-defective HShh C198S mutant stably expressed in 293T cells was inhibited by depleting the same components, i.e. OS9, Hrd1, Sel1, and p97 (Supplemental Figure 2.S8). These results show that the Hh precursor undergoes two competing reactions in the ER, cholesterol-dependent processing and degradation by an ERAD pathway identical to that employed by HShh-C.

DISCUSSION

The main result of the present study is that processing of the Hh precursor takes place in the ER. This conclusion is based on several observations: (1) the insensitivity of Hh processing to inhibition of vesicular transport out of the ER, (2) the requirement for disulfide bridge formation and reduction for Hh processing, (3) the involvement of the ER luminal PDI in disulfide remodeling of Hh, (4) the degradation of Hh precursor and its C-terminal fragment by ERAD, and (5) microscopic visualization of Hh degradation in the ER. Processing of the Hh precursor in the ER is somewhat unexpected given the relatively low concentration of cholesterol in the ER membrane. In fact, it was previously speculated that Hh processing might occur in another, cholesterol-rich compartment of the secretory pathway (Maity et al., 2005). How cholesterol modification can occur at the low cholesterol concentrations of the ER remains unclear, but one possibility is that an additional factor in the ER facilitates the reaction.

We show that a disulfide bond needs to form between the catalytic cysteine and the only other cysteine in the C-terminal domain, a disulfide bond that is conserved among all Hh proteins. Again, this is a surprising result, because in the next step of Hh processing, the catalytic

cysteine needs to be reduced in order to initiate cleavage of the polypeptide backbone. Why then form a disulfide bridge in the first place? We speculate that the Hh precursor requires a disulfide bridge for proper folding, which in turn is required for the autocatalytic activity of the C-terminal domain. Both the formation and reduction of the essential disulfide bridge require the activity of a member of the PDI family. While the oxidation of cysteines to form disulfide bridges is a common protein modification in the ER, net disulfide bond reduction is less common. One example is provided by the reduction of a disulfide bond that links the A1 and A2 chains of cholera toxin by PDI itself; the A1 chain thus freed from the rest of the toxin is retro-translocated into the cytosol (Tsai et al., 2001).

Our results show that PDI and the closely related PDIp protein are involved in remodeling of the conserved disulfide bridge in Hh. The specificity of these enzymes is indicated by the fact that seven other tested ER-localized family members do not interact and that only one of the two catalytic CXXC motifs of PDI and PDIp forms a mixed disulfide intermediate with Hh. Whether these enzymes are involved in the formation of the disulfide bridge, its reduction, or both, is unclear. However, our observation that a mixed disulfide adduct between Hh and PDI forms rapidly and undergoes the intein reaction, suggests that PDI reduces the disulfide bridge in Hh and remains bound to the non-catalytic cysteine while the Hh precursor is processed. Thus, disulfide bridge reduction by PDI might be mechanistically coupled to Hh processing and attachment of cholesterol.

Consistent with our conclusion that Hh processing takes place in the ER, we find that the resulting C-terminal fragment is degraded by ERAD. The degradation of the C-terminal fragment generated in the ER lumen requires several of the previously identified ERAD components. Our data suggest the following series of events in the degradation of the C-terminal

fragment. The process probably begins with recognition of the single carbohydrate chain in the C-terminal fragment, as suggested by the requirement for either of the two lectins implicated in ERAD, OS9 and XTP-3B. The C-terminal fragment is also likely recognized by Sel1, similarly to substrate recognition by the yeast homolog Hrd3p (Denic et al., 2006; Gauss et al., 2006). The next step in the process involves the ubiquitin ligase Hrd1, which forms a complex with Sel1. Once the substrate is poly-ubiquitinated on the cytosolic side of the ER membrane, the p97 ATPase complex moves the C-terminal fragment from the membrane into the cytosol. The protein is also deglycosylated, likely by the cytoplasmic glycanase (Hirsch et al., 2003). Finally, the protein is degraded by the proteasome. As a result of ERAD, the C-terminal fragment never leaves the ER and is not secreted, in contrast to the N-terminal fragment, the Hh ligand. Given that the C-terminal fragment is not secreted even when stabilized by proteasome inhibitors, it appears that it is actively retained in the ER, possibly by its association with PDI.

ERAD is normally used to degrade misfolded ER proteins. In addition, there are several native proteins, such as HMG CoA reductase (Chin et al., 1985; Gil et al., 1985; Hampton and Rine, 1994), that are degraded in a regulated manner by ERAD. However, to our knowledge, there is only one native protein, Ubc6p, that is a constitutive ERAD substrate (Walter et al., 2001). This yeast membrane protein is exposed to the cytosol and is continuously ubiquitinated by the Doa10p ubiquitin ligase (Swanson et al., 2001). The C-terminal fragment of Hh is the first example of a native luminal ER protein that is constitutively degraded by ERAD. Whereas it is conceivable that HMG CoA reductase is induced to unfold by binding of cholesterol and that Ubc6p is not properly folded, the C-terminal fragment of Hh must be properly folded to allow the self-cleavage reaction to happen. This hypothesis is supported by the fact that non-cleavable versions of the full-length Hh precursor are degraded by ERAD at least as fast as the C-terminal

fragment, and by the same ERAD components. Apparently, the rapid degradation of the full-length Hh precursor by ERAD is competing with its proper processing. This can explain why human Shh mutants that are defective in precursor processing are causing holoprosencephaly, a frequent congenital brain malformation; these mutant proteins would be quickly degraded in the ER and no active ligand would be secreted. Thus, our results suggest that ERAD plays a critical role in birth defects caused by Hh precursor mutations. Even for the wild type Hh precursor, ERAD might play a role in determining how much active ligand is generated; perhaps the concentration of cholesterol in the ER determines the balance between degradation and processing of the full-length precursor. Interestingly, the C-terminal fragment expressed by itself is also degraded, but more slowly than the C-terminal fragment generated through processing. Perhaps, when the fragment is generated close to the ER membrane, there is a more efficient handover to the ERAD machinery. The signal that targets Hh to the ERAD pathway remains unclear, but it could be related to the hydrophobic properties of the C-terminus.

Why is the post-translational processing of Hh proteins so complicated? Much of the complexity of the processing mechanism seems to originate from the requirement for cholesterol modification of the Hh ligand. Cholesterol attachment necessitates the autocatalytic intein-like reaction, which in turn requires the C-terminal domain to be properly folded. The formation of a critical disulfide bond involving the catalytic cysteine ensures that proper folding precedes catalysis. Once the C-terminus has done its job, however, it becomes dispensable, explaining why it is cleared by ERAD. Despite the progress, it remains to be clarified why the Hh ligand is modified by cholesterol, how cholesterol attachment changes its membrane association, and how the cholesterol-modified Hh ligand is ultimately released from cells.

MATERIALS AND METHODS

Materials

The following materials were used in this study: MG132 (Biomol), bortezomib (gift from Dr Alfred Goldberg), epoxomicin (Enzo Life Sciences), diamide (TCI), rat anti-HA antibody (3F10, Roche), mouse anti-Myc antibody (9E10, Roche), rabbit anti-ubiquitin antibody (Biomol), rabbit anti-calnexin antibody (Abcam), rabbit anti-gigantin antibody (Abcam), rabbit anti-Shh (Cell Signaling), protein G-agarose (GE Bioscience), mouse anti-FLAG M2 agarose (Sigma). Stealth siRNA duplexes were custom-synthesized by Invitrogen.

Protein purification and in vitro Drosophila Hedgehog processing assays

A fragment of Drosophila Hedgehog comprising amino acids 244-471 was expressed in bacteria as a maltose-binding protein (MBP) fusion (MBP-DHh). The soluble MBP-DHh was purified on amylose beads (New England Biolabs), according to the manufacturer's instructions. Point mutations in DHh were generated using the QuickChange kit (Stratagene), were confirmed by DNA sequencing, and expressed and purified as MBP fusions, as for the wild type protein. The purified proteins were concentrated to 2.5 mg/mL and were stored at –80C.

Processing reactions contained 0.2-0.5 mg/mL MBP-DHh in incubation buffer (20 mM Hepes, pH 7.5, 50 mM NaCl, 0.1% Triton-X100), with or without reducing agent (DTT or glutathione), and with or without cholesterol (250 microM final, added from a stock solution in DMSO). The reactions were incubated at room temperature and were stopped at the indicated times by addition of SDS-PAGE sample buffer (with or without DTT). The samples were boiled, separated by SDS-PAGE and the proteins were visualized by staining with GelCode Blue reagent (Pierce).

To assay cysteine modification by maleimide-polyethyleneglycol (MalPEG), ^{35}S-labeled MBP-DHh proteins (wild type and mutants) were generated by in vitro translation in reticulocyte lysates, and were dialyzed overnight against PBS, to remove small molecule thiols. The proteins were incubated with or without 5 mM tris(2-carboxyethyl)phosphine (TCEP) for 10 min, followed by incubation with 7 mM Mal-PEG 5kDa (Laysan Bio. Inc) for 30 min, at room temperature. The reaction was terminated with 100 mM DTT, and the samples were separated by SDS-PAGE, followed by autoradiography.

To determine if MBP-DHh is modified with cholesterol, processing reactions were performed in the presence of 0.5 uCi/microL radioactive cholesterol (1,2,3,6,7-3H-cholesterol, 100 mCi/mmol, American Radiolabeled Chemicals). The samples were separated by SDS-PAGE and radioactive proteins were visualized by fluorography (Bonner and Laskey, 1974).

Hh processing in Xenopus egg extracts

Xenopus Sonic Hedgehog (XShh) was cloned into the pCS2+ vector (Rupp et al., 1994), and radioactive XShh was generated by in vitro translation (TNT SP6 Coupled Reticulocyte Lysate System, Promega), in the presence of ^{35}S-methionine (New England Nuclear). Xenopus egg extracts were prepared as described (Salic et al., 2000). A typical XShh processing reaction contained 1 uL of in vitro translated protein in 14 uL of Xenopus egg extract, supplemented with cycloheximide (100 ug/mL). The processing reactions were incubated at room temperature, and aliquots were removed at the indicated times, and mixed with SDS-PAGE sample buffer. The samples were boiled, separated by SDS-PAGE, and radioactive proteins were visualized by autoradiography. Triton-X114 partitioning experiments were performed as described (Bordier, 1981), using radioactive proteins incubated with or without Xenopus egg extract for 1 hr at room

temperature. Point mutants of XShh were generated using the QuickChange kit (Stratagene), and were confirmed by DNA sequencing.

Cell culture and generation of stable cell lines

Human 293T cells were grown in DMEM supplemented with 10% fetal bovine serum, penicillin and streptomycin. NIH-3T3 cells were grown in DMEM with 10% bovine calf serum, penicillin and streptomycin. To generate stable cell lines, constructs encoding full-length human Sonic Hedgehog (HShh), C-terminally tagged with an HA epitope (HShh-HA) or fused with mCherry (HShh-Cherry) were cloned into the retroviral vector pLHCX (Clontech), and retroviruses were produced in 293T cells. The retroviruses were used to infect NIH-3T3 or 293T cells, and cells stably expressing HShh-HA or HShh-Cherry were generated by hygromycin selection. Expression of HShh-HA or HShh-Cherry was confirmed by Western blotting and by immunofluorescence.

Immunofluorescence

Cultured cells were fixed in PBS with 4% formaldehyde, and were permeabilized with TBST (10 mM Tris pH 7.5, 150 mM NaCl, 0.2% Triton X-100). Antibodies against HA (3F10, rat monoclonal, Roche), calnexin (rabbit polyclonal, Abcam) and gigantin (rabbit polyclonal, Abcam) were used at a final concentration of 0.25 and 0.5 ug/mL, respectively. Alexa-594- and Alexa-488-conjugated secondary antibodies (Invitrogen) were used at a final concentration of 1 ug/mL. The immunostained cells were imaged by epi-fluorescence microscopy on an inverted Nikon TE2000U microscope equipped with an OrcaER digital camera (Hammamatsu) and a

100x PlanApo 1.4NA oil objective (Nikon). Images were collected using Metamorph image acquisition software (Applied Precision).

293T and 3T3 cells stably expressing HShh-HA were incubated for 3 hrs in the presence of control media or the proteasome inhibitors MG132 (10 uM), bortezomib (1 uM) or epoxomicin (1 uM). The cells were fixed and processed for immunofluorescence, to detect the HA epitope and calnexin.

DNA constructs for mammalian cell transfection

Full-length HShh, tagged at the C-terminus with one copy of the HA epitope (HShh-HA), was cloned into pIRES2-eGFP (Clontech). The C-terminal fragment of HShh (HShh-C, amino acids 198-462, HA-tagged at the C-terminus) was cloned into pIRES2-eGFP, behind a sequence encoding the signal sequence of CD5. Site-directed mutagenesis of HShh was carried out using the Quickchange kit (Stratagene). Wild type and catalytically inactive p97 (p97-WT and p97-QQ) were provided by Dr. Yihong Ye; myc-tagged wild type and the two dominant negative mutants of Hrd1 (Hrd1-WT, Hrd1-C291A and Hrd1-C291A-C307A) were provided by Dr. Emmanuel Wiertz; myc-tagged reticulon 4A was from Dr. Stephan M. Strittmatter. The Ubc6e-C91S and UbxD8-GFP expression constructs were described previously (Lilley and Ploegh, 2004; Mueller et al., 2008). The expression constructs for the mutant ER-localized thioredoxin-like proteins were described previously (Schulman et al., 2010).

Transfection of plasmids and siRNAs into cultured cells

Plasmids were transfected using Lipofectamine 2000 (Invitrogen), according to the manufacturer's instructions. SiRNA duplexes were transfected using the TransIT-SiQuest

transfection reagent (Mirus), at a final concentration of 50 nM siRNA, according to the manufacturer's instructions. SiRNA transfection was performed twice, on days 1 and 3 of the experiment. On day 5, the cells were treated with cycloheximide (CHX, 50 uM) or CHX plus MG132 (50 uM) for the indicated period of time, after which cells were harvested, and proteins were analyzed by SDS-PAGE and immunoblotting. SiRNA sequences are shown in Table 2.S1.

Quantitative RT-PCR analysis

Total RNA was extracted with TRIzol reagent, and cDNA was synthesized with ImProm-IITM reverse transcriptase (Promega). Quantitative PCR was performed on an ABI Prism 7900 cycler, using SYBR Green PCR Master Mix (ABI). The degree of siRNA knockdown was calculated relative to HPRT1 mRNA levels. The primers used to quantify mRNA knockdown are shown in Table S2.

Immunoblotting

Cells were lysed on ice for 20 min, in TBS (10 mM Tris, pH 7.5, 150 mM NaCl), supplemented with protease inhibitors and 1% Triton X-100. The lysate was centrifuged for 30 min at 4C and 20,000g. The supernatant was collected, mixed with SDS-PAGE sample buffer with DTT (50 mM final), and separated by SDS-PAGE, followed by immunoblotting.

Immunoprecipitation and ubiquitination of HShh-HA

293T cells expressing HShh-HA were treated with either DMSO or MG132 (50 uM) for 2 hrs, and immunoprecipitation with anti-HA (3F10) antibody was carried out as described

(Mueller et al., 2008). The precipitated proteins were separated by SDS-PAGE and ubiquitin conjugates were detected by immunoblotting with anti-ubiquitin antibodies (Biomol).

Pulse-chase assays

Pulse-chase experiments were performed as described (Mueller et al., 2006). 293T cells were detached from plates and were incubated in suspension in methionine- and cysteine-free DMEM for 1 hour at 37C. The cells were then labeled for 3 min at 37C with 300 uCi/mL ^{35}S-methionine and -cysteine (^{35}S-Protein Express Labeling Mix, New England Nuclear). Cellular density during labeling was $1x10^7$ cells/mL. The chase was started by adding cold methionine and cysteine, at a final concentration of 5 mM and 1 mM, respectively. Aliquots of the cell suspension were removed at different time points, and cellular pellets were frozen. Cellular lysates were subjected to denaturing immunoprecipitation with HA antibodies. The precipitated proteins were separated on SDS-PAGE, and were visualized by autoradiography.

Cycloheximide chase assays

293T cells stably expressing HShh-HA were incubated with cycloheximide (50 ug/mL) in OptiMEM (Invitrogen), in agitated suspension, at 37C. At the indicated times, aliquots were removed, the cells were harvested and HShh-HA was detected by immunoblotting.

To determine the effect of various dominant-negative constructs on HShh processing, 293T cells expressing HShh-HA were transfected with expression constructs for Derlin1-GFP, UbxD8-GFP or dominant-negative Ubc6e, as described (Mueller et al., 2008; Mueller et al., 2006), followed by cycloheximide chase, 24 hours after transfection.

Screening for thioredoxin-like enzymes involved in Hh processing

We used a collection of FLAG-tagged CXXA mutants representing 9 different human ER-localized thioredoxin-like proteins (Schulman et al., 2010). Each construct was co-expressed in 293T cells with HShh-HA, either wild type of the processing-defective C198A mutant. Twenty-four hours later the cells were harvested, lysed, and the lysate was subjected to denaturing immunoprecipitation with HA- and FLAG-antibodies, as described (Schulman et al., 2010). The precipitated proteins were separated by SDS-PAGE, under either reducing or non-reducing conditions, followed by immunoblotting with FLAG or HA antibodies.

Analyzing Hh secretion

293T cells stably expressing HShh-HA were incubated for 12 hrs in DMEM containing 0.5% fetal bovine serum, with or without epoxomicin added for the last 3 hrs of the incubation. The cells were harvested and lyzed, while the protein in the culture medium was precipitated with trichloracetic acid. HShh-N and HShh-C were analyzed by SDS-PAGE, followed by immunoblotting with Shh antibodies (Cell Signaling) and HA antibodies (Roche).

ACKNOWLEDGMENTS

We thank Y. Ye, E. Wiertz, S. Strittmatter, and K. Nagata for providing reagents. H.T. and C. J. are supported by predoctoral fellowships from the American Heart Association and from the NSF, respectively. T.A.R. is supported by NIH grant GM052586 and is a Howard Hughes Medical Institute Investigator. XC is supported by funds from NRPGM, National Science Council and NHRI (Taiwan). A.S. acknowledges the support from the Rita Allen Foundation and the Beckman Foundation. We thank Pedro Carvalho for reading the manuscript.

REFERENCES

Bays, N.W., R.G. Gardner, L.P. Seelig, C.A. Joazeiro, and R.Y. Hampton. 2001a. Hrd1p/Der3p is a membrane-anchored ubiquitin ligase required for ER-associated degradation. *Nat Cell Biol*. 3:24-9.

Bays, N.W., S.K. Wilhovsky, A. Goradia, K. Hodgkiss-Harlow, and R.Y. Hampton. 2001b. HRD4/NPL4 Is Required for the Proteasomal Processing of Ubiquitinated ER Proteins. *Mol Biol Cell*. 12:4114-4128.

Bernasconi, R., C. Galli, V. Calanca, T. Nakajima, and M. Molinari. 2010. Stringent requirement for HRD1, SEL1L, and OS-9/XTP3-B for disposal of ERAD-LS substrates. *J Cell Biol*. 188:223-35.

Bonner, W.M., and R.A. Laskey. 1974. A film detection method for tritium-labelled proteins and nucleic acids in polyacrylamide gels. *Eur J Biochem*. 46:83-8.

Bordallo, J., R.K. Plemper, A. Finger, and D.H. Wolf. 1998. Der3p/Hrd1p is required for endoplasmic reticulum-associated degradation of misfolded lumenal and integral membrane proteins. *Mol Biol Cell*. 9:209-22.

Bordier, C. 1981. Phase separation of integral membrane proteins in Triton X-114 solution. *J Biol Chem*. 256:1604-7.

Bumcrot, D.A., R. Takada, and A.P. McMahon. 1995. Proteolytic processing yields two secreted forms of sonic hedgehog. *Mol Cell Biol*. 15:2294-303.

Carvalho, P., V. Goder, and T.A. Rapoport. 2006. Distinct ubiquitin-ligase complexes define convergent pathways for the degradation of ER proteins. *Cell*. 126:361-73.

Chamoun, Z., R.K. Mann, D. Nellen, D.P. von Kessler, M. Bellotto, P.A. Beachy, and K. Basler. 2001. Skinny hedgehog, an acyltransferase required for palmitoylation and activity of the hedgehog signal. *Science*. 293:2080-4.

Chin, D.J., G. Gil, J.R. Faust, J.L. Goldstein, M.S. Brown, and K.L. Luskey. 1985. Sterols accelerate degradation of hamster 3-hydroxy-3-methylglutaryl coenzyme A reductase encoded by a constitutively expressed cDNA. *Mol Cell Biol*. 5:634-41.

Christianson, J.C., T.A. Shaler, R.E. Tyler, and R.R. Kopito. 2008. OS-9 and GRP94 deliver mutant alpha1-antitrypsin to the Hrd1-SEL1L ubiquitin ligase complex for ERAD. *Nat Cell Biol*. 10:272-82.

Denic, V., E.M. Quan, and J.S. Weissman. 2006. A luminal surveillance complex that selects misfolded glycoproteins for ER-associated degradation. *Cell*. 126:349-59.

Elbein, A.D. 1991. Glycosidase inhibitors: inhibitors of N-linked oligosaccharide processing. *FASEB J*. 5:3055-63.

Fang, S., M. Ferrone, C. Yang, J.P. Jensen, S. Tiwari, and A.M. Weissman. 2001. The tumor autocrine motility factor receptor, gp78, is a ubiquitin protein ligase implicated in degradation from the endoplasmic reticulum. *Proc Natl Acad Sci U S A*. 98:14422-7.

Gardner, R.G., G.M. Swarbrick, N.W. Bays, S.R. Cronin, S. Wilhovsky, L. Seelig, C. Kim, and R.Y. Hampton. 2000. Endoplasmic reticulum degradation requires lumen to cytosol signaling. Transmembrane control of Hrd1p by Hrd3p. *J Cell Biol*. 151:69-82.

Gauss, R., E. Jarosch, T. Sommer, and C. Hirsch. 2006. A complex of Yos9p and the HRD ligase integrates endoplasmic reticulum quality control into the degradation machinery. *Nat Cell Biol*. 8:849-54.

Gil, G., J.R. Faust, D.J. Chin, J.L. Goldstein, and M.S. Brown. 1985. Membrane-bound domain of HMG CoA reductase is required for sterol-enhanced degradation of the enzyme. *Cell*. 41:249-58.

Hall, T.M., J.A. Porter, K.E. Young, E.V. Koonin, P.A. Beachy, and D.J. Leahy. 1997. Crystal structure of a Hedgehog autoprocessing domain: homology between Hedgehog and self-splicing proteins. *Cell*. 91:85-97.

Hampton, R.Y., and J. Rine. 1994. Regulated degradation of HMG-CoA reductase, an integral membrane protein of the endoplasmic reticulum, in yeast. *J Cell Biol*. 125:299-312.

Hassink, G., M. Kikkert, S. van Voorden, S.J. Lee, R. Spaapen, T. van Laar, C.S. Coleman, E. Bartee, K. Fruh, V. Chau, and E. Wiertz. 2005. TEB4 is a C4HC3 RING finger-containing ubiquitin ligase of the endoplasmic reticulum. *Biochem J*. 388:647-55.

Hirsch, C., D. Blom, and H.L. Ploegh. 2003. A role for N-glycanase in the cytosolic turnover of glycoproteins. *EMBO J*. 22:1036-46.

Hirsch, C., R. Gauss, S.C. Horn, O. Neuber, and T. Sommer. 2009. The ubiquitylation machinery of the endoplasmic reticulum. *Nature*. 458:453-60.

Hosokawa, N., Y. Kamiya, D. Kamiya, K. Kato, and K. Nagata. 2009. Human OS-9, a lectin required for glycoprotein endoplasmic reticulum-associated degradation, recognizes mannose-trimmed N-glycans. *J Biol Chem*. 284:17061-8.

Hosokawa, N., I. Wada, K. Nagasawa, T. Moriyama, K. Okawa, and K. Nagata. 2008. Human XTP3-B forms an endoplasmic reticulum quality control scaffold with the HRD1-SEL1L ubiquitin ligase complex and BiP. *J Biol Chem*. 283:20914-24.

Jarosch, E., C. Taxis, C. Volkwein, J. Bordallo, D. Finley, D.H. Wolf, and T. Sommer. 2002. Protein dislocation from the ER requires polyubiquitination and the AAA-ATPase Cdc48. *Nat Cell Biol*. 4:134-9.

Kalderon, D. 2005. The mechanism of hedgehog signal transduction. *Biochem Soc Trans*. 33:1509-12.

Kokame, K., K.L. Agarwala, H. Kato, and T. Miyata. 2000. Herp, a new ubiquitin-like membrane protein induced by endoplasmic reticulum stress. *J Biol Chem*. 275:32846-53.

Lai, C.J., S.C. Ekker, P.A. Beachy, and R.T. Moon. 1995. Patterning of the neural ectoderm of Xenopus laevis by the amino-terminal product of hedgehog autoproteolytic cleavage. *Development*. 121:2349-60.

Lee, J.J., S.C. Ekker, D.P. von Kessler, J.A. Porter, B.I. Sun, and P.A. Beachy. 1994. Autoproteolysis in hedgehog protein biogenesis. *Science*. 266:1528-37.

Lilley, B.N., and H.L. Ploegh. 2004. A membrane protein required for dislocation of misfolded proteins from the ER. *Nature*. 429:834-40.

Lum, L., and P.A. Beachy. 2004. The Hedgehog response network: sensors, switches, and routers. *Science*. 304:1755-9.

Maity, T., N. Fuse, and P.A. Beachy. 2005. Molecular mechanisms of Sonic hedgehog mutant effects in holoprosencephaly. *Proc Natl Acad Sci U S A*. 102:17026-31.

Marigo, V., R.A. Davey, Y. Zuo, J.M. Cunningham, and C.J. Tabin. 1996. Biochemical evidence that patched is the Hedgehog receptor. *Nature*. 384:176-9.

Mueller, B., E.J. Klemm, E. Spooner, J.H. Claessen, and H.L. Ploegh. 2008. SEL1L nucleates a protein complex required for dislocation of misfolded glycoproteins. *Proc Natl Acad Sci U S A*. 105:12325-30.

Mueller, B., B.N. Lilley, and H.L. Ploegh. 2006. SEL1L, the homologue of yeast Hrd3p, is involved in protein dislocation from the mammalian ER. *J Cell Biol*. 175:261-70.

Ogden, S.K., M. Ascano, Jr., M.A. Stegman, and D.J. Robbins. 2004. Regulation of Hedgehog signaling: a complex story. *Biochem Pharmacol*. 67:805-14.

Porter, J.A., S.C. Ekker, W.J. Park, D.P. von Kessler, K.E. Young, C.H. Chen, Y. Ma, A.S. Woods, R.J. Cotter, E.V. Koonin, and P.A. Beachy. 1996a. Hedgehog patterning activity: role of a lipophilic modification mediated by the carboxy-terminal autoprocessing domain. *Cell*. 86:21-34.

Porter, J.A., D.P. von Kessler, S.C. Ekker, K.E. Young, J.J. Lee, K. Moses, and P.A. Beachy. 1995. The product of hedgehog autoproteolytic cleavage active in local and long-range signalling. *Nature*. 374:363-6.

Porter, J.A., K.E. Young, and P.A. Beachy. 1996b. Cholesterol modification of hedgehog signaling proteins in animal development. *Science*. 274:255-9.

Rabinovich, E., A. Kerem, K.U. Frohlich, N. Diamant, and S. Bar-Nun. 2002. AAA-ATPase p97/Cdc48p, a Cytosolic Chaperone Required for Endoplasmic Reticulum-Associated Protein Degradation. *Mol Cell Biol*. 22:626-34.

Roessler, E., K.B. El-Jaick, C. Dubourg, J.I. Velez, B.D. Solomon, D.E. Pineda-Alvarez, F. Lacbawan, N. Zhou, M. Ouspenskaia, A. Paulussen, H.J. Smeets, U. Hehr, C. Bendavid, S. Bale, S. Odent, V. David, and M. Muenke. 2009. The mutational spectrum of holoprosencephaly-associated changes within the SHH gene in humans predicts loss-of-function through either key structural alterations of the ligand or its altered synthesis. *Hum Mutat*. 30:E921-35.

Rupp, R.A., L. Snider, and H. Weintraub. 1994. Xenopus embryos regulate the nuclear localization of XMyoD. *Genes Dev*. 8:1311-23.

Salic, A., E. Lee, L. Mayer, and M.W. Kirschner. 2000. Control of beta-catenin stability: reconstitution of the cytoplasmic steps of the wnt pathway in Xenopus egg extracts. *Mol Cell*. 5:523-32.

Schulman, S., B. Wang, W. Li, and T.A. Rapoport. 2010. Vitamin K epoxide reductase prefers ER membrane-anchored thioredoxin-like redox partners. *Proc Natl Acad Sci U S A*. 107:15027-32.

Schulze, A., S. Standera, E. Buerger, M. Kikkert, S. van Voorden, E. Wiertz, F. Koning, P.M. Kloetzel, and M. Seeger. 2005. The ubiquitin-domain protein HERP forms a complex with components of the endoplasmic reticulum associated degradation pathway. *J Mol Biol*. 354:1021-7.

Stagg, H.R., M. Thomas, D. van den Boomen, E.J. Wiertz, H.A. Drabkin, R.M. Gemmill, and P.J. Lehner. 2009. The TRC8 E3 ligase ubiquitinates MHC class I molecules before dislocation from the ER. *J Cell Biol*. 186:685-92.

Stone, D.M., M. Hynes, M. Armanini, T.A. Swanson, Q. Gu, R.L. Johnson, M.P. Scott, D. Pennica, A. Goddard, H. Phillips, M. Noll, J.E. Hooper, F. de Sauvage, and A. Rosenthal. 1996. The tumour-suppressor gene patched encodes a candidate receptor for Sonic hedgehog. *Nature*. 384:129-34.

Swanson, R., M. Locher, and M. Hochstrasser. 2001. A conserved ubiquitin ligase of the nuclear envelope/endoplasmic reticulum that functions in both ER-associated and Matalpha2 repressor degradation. *Genes Dev*. 15:2660-74.

Traiffort, E., C. Dubourg, H. Faure, D. Rognan, S. Odent, M.R. Durou, V. David, and M. Ruat. 2004. Functional characterization of sonic hedgehog mutations associated with holoprosencephaly. *J Biol Chem*. 279:42889-97.

Tsai, B., and T.A. Rapoport. 2002. Unfolded cholera toxin is transferred to the ER membrane and released from protein disulfide isomerase upon oxidation by Ero1. *J Cell Biol*. 159:207-16.

Tsai, B., C. Rodighiero, W.I. Lencer, and T.A. Rapoport. 2001. Protein disulfide isomerase acts as a redox-dependent chaperone to unfold cholera toxin. *Cell*. 104:937-48.

Ushioda, R., J. Hoseki, K. Araki, G. Jansen, D.Y. Thomas, and K. Nagata. 2008. ERdj5 is required as a disulfide reductase for degradation of misfolded proteins in the ER. *Science*. 321:569-72.

Walter, J., J. Urban, C. Volkwein, and T. Sommer. 2001. Sec61p-independent degradation of the tail-anchored ER membrane protein Ubc6p. *Embo J*. 20:3124-31.

Wiertz, E.J.H.J., T.R. Jones, L. Sun, M. Bogyo, H.J. Geuze, and H.L. Ploegh. 1996. The human cytomegalovirus US11 gene product dislocates MHC class I heavy chains from the endoplasmic reticulum to the cytosol. *Cell*. 84:769-779.

Xie, W., and D.T. Ng. ERAD substrate recognition in budding yeast. *Semin Cell Dev Biol*.

Ye, Y., H.H. Meyer, and T.A. Rapoport. 2001. The AAA ATPase Cdc48/p97 and its partners transport proteins from the ER into the cytosol. *Nature*. 414:652-6.

Ye, Y., Y. Shibata, C. Yun, D. Ron, and T.A. Rapoport. 2004. A membrane protein complex mediates retro-translocation from the ER lumen into the cytosol. *Nature*. 429:841-7.

CHAPTER THREE:

SECRETION OF THE LIPIDATED HEDGEHOG LIGAND

The following section contains previously published material from:

Tukachinsky H, Kuzmickas RP, Jao CY, Liu J, Salic A. Dispatched and Scube Mediate the Efficient Secretion of the Cholesterol-Modified Hedgehog Ligand. *Cell Reports*. (2012) **2(2):**308-20.

Author contributions:

I performed most of the experiments in this chapter. CY Jao and J Liu synthesized 25-aza cholesterol and RP Kuzmickas performed the experiments using photocholesterol analogs.

SUMMARY

The Hedgehog signaling pathway plays critical roles in metazoan development and in cancer. How the Hedgehog ligand is secreted and spreads to distant cells is unclear, given its covalent modification with a hydrophobic cholesterol molecule, which makes it stick to membranes. We demonstrate that Hedgehog ligand secretion from vertebrate cells is accomplished via two distinct and synergistic cholesterol-dependent binding events, mediated by two proteins essential for vertebrate Hedgehog signaling: the membrane protein Dispatched and a member of the Scube family of secreted proteins. Cholesterol modification is sufficient for a heterologous protein to interact with Scube, and to be secreted in a Scube-dependent manner. Dispatched and Scube recognize different structural aspects of cholesterol, similar to how Niemann-Pick disease proteins 1 and 2 interact with cholesterol, suggesting a hand-off mechanism for transferring Hedgehog from Dispatched to Scube. Thus, Dispatched and Scube cooperate to dramatically enhance secretion and solubility of the cholesterol-modified Hedgehog ligand.

INTRODUCTION

The Hedgehog (Hh) signaling pathway has fundamental roles in embryonic development, adult stem cell maintenance and carcinogenesis (Lum and Beachy, 2004). Hh signaling is triggered by binding of the secreted Hh ligand to its membrane receptor, Patched (Ptch), setting in motion signal transduction events that ultimately lead to the specific transcriptional output of the Hh pathway. The Hh ligand is generated from a precursor protein, which is translocated into the endoplasmic reticulum (ER), undergoes signal sequence cleavage and then is modified covalently with two lipids: 1) a palmityl residue is attached at the N-terminus by the palmityl

transferase Skinny hedgehog (Chamoun et al., 2001); and 2) a cholesteryl residue is attached at the C-terminus by autocatalytic modification (Porter et al., 1996). The cholesterol modification reaction relies on the intein activity of the C-terminal domain of the Hh precursor, and generates an N-terminal fragment (the cholesterol-modified Hh ligand) and a C-terminal fragment that is disposed of by ER-associated degradation (Chen et al., 2011). The two lipid modifications of the Hh ligand occur independently (Chamoun et al., 2001) and are both essential for normal Hh signaling (Chamoun et al., 2001; Traiffort et al., 2004).

The Hh ligand is strongly hydrophobic and hence membrane-associated, which raises the critical question of how it is secreted and how it reaches cells located at a distance from the signaling cell. Genetic analysis identified Dispatched (Disp) and the Scube family of proteins as essential for long-range Hh signaling. Disp is a multi-spanning membrane protein required for long-range Hh signaling in Drosophila (Burke et al., 1999), mouse (Ma et al., 2002) and zebrafish (Nakano et al., 2004). Disp belongs to the RND family of transporters (Tseng et al., 1999) and contains a sterol-sensing domain (SSD), a sequence of 5 consecutive membrane-spanning helices found in several membrane proteins involved in cholesterol homeostasis (Kuwabara and Labouesse, 2002). Disp is specifically required for secretion of cholesterol-modified Hh, as the N-terminal fragment of Hh without the cholesterol modification can be released in the absence of Disp. The Scube family (Grimmond et al., 2000) consists of the secreted proteins Scube 1, 2 and 3, and is required for long-range Hh signaling in zebrafish (Johnson et al., 2012). Scube2 was first identified in zebrafish (Hollway et al., 2006; Kawakami et al., 2005; Woods and Talbot, 2005) as playing a non-cell autonomous role in long-range Hh signaling. Epistatic analysis led to the proposal that Scube2 is involved in the transport or

stability of Hh ligand in the extracellular space (Hollway et al., 2006; Kawakami et al., 2005; Woods and Talbot, 2005).

For both Disp and Scube proteins, the mechanism by which they promote long-range Hh signaling is unknown. Although Disp is required for Hh secretion, there is no direct evidence that Disp participates in Hh release from cells. Additionally, it is unclear how the Hh ligand is kept soluble in the extracellular space, and how it is delivered to responding cells. Regarding Scube proteins, it is unclear if they are involved in Hh biosynthesis, secretion or in another aspect of Hh function outside the producing cell.

Here we dissect the mechanism of Hh secretion in vertebrate cells. We show that the vertebrate homologue, Dispatched-A (DispA) interacts with human Sonic hedgehog (hShh) via its cholesterol anchor, and that this interaction is necessary for hShh secretion. Interestingly, an inactive DispA mutant binds hShh more strongly than wild-type DispA, suggesting that dissociation of hShh from DispA is important for efficient secretion. However, DispA alone is not sufficient to release hShh from cells, indicating that additional factors are required to overcome the insolubility conferred by cholesterol modification. We demonstrate that a Scube family member, Scube2, synergizes with DispA to cause a dramatic increase in hShh secretion. Scube2 binds the cholesterol anchor of hShh and this interaction is required for promoting hShh secretion. Cholesterol modification is sufficient for a heterologous protein to bind Scube2 and to be secreted in a Scube2-dependent manner. Importantly, DispA and Scube2 recognize different aspects of the cholesterol anchor of hShh. Our results support a model in which membrane-associated hShh is secreted by being handed off from DispA to Scube2, in a manner reminiscent of the transport of free cholesterol by the Niemann-Pick disease proteins NPC1 and NPC2

(Infante et al., 2008b). Thus a relay mechanism involving DispA and Scube2 promotes the release of cholesterol-modified hShh from the plasma membrane of producing cells.

RESULTS

Dispatched-A interacts with hShh in a cholesterol-dependent manner

It was suggested that Dispatched (Disp) might bind cholesterol-modified Hh (Burke et al., 1999); however, such an interaction has not been demonstrated. We first tested if mouse Dispatched-A (DispA) binds cholesterol-modified human Sonic Hedgehog (hShh) by co-immunoprecipitation. DispA and hShh were stably co-expressed in 293T cells, followed by detergent solubilization and immunoprecipitation. Under these conditions wild-type DispA showed modest but reproducible binding to cholesterol-modified hShh (Figure 1A), consistent with the expectation of a transient DispA-hShh interaction. To probe the cholesterol dependence of the interaction, we expressed a construct that encodes the N-terminal fragment of hShh (hShhN, amino acids 1-198), which generates a protein lacking cholesterol but which is still palmitylated (Chamoun et al., 2001; Chen et al., 2004). DispA did not bind hShhN (Figure 1A), indicating that binding to hShh is cholesterol-dependent. Interestingly, the inactive DispA mutant, DispA-NNN (Ma et al., 2002) showed significantly stronger hShh binding compared to wild-type DispA (Figure 3.1A); the same result was obtained with the inactive DispA-AAA mutant. DispA-NNN and DispA-AAA are triple point mutants in which 3 aspartate residues located in transmembrane helices 4 and 10 are mutated to asparagines or alanines; one of these aspartates is conserved in RND family proteins and is required for their transporter function. Our results suggest that DispA-NNN and DispA-AAA are defective in hShh secretion perhaps because they bind hShh too tightly, thus interfering with its release from cells.

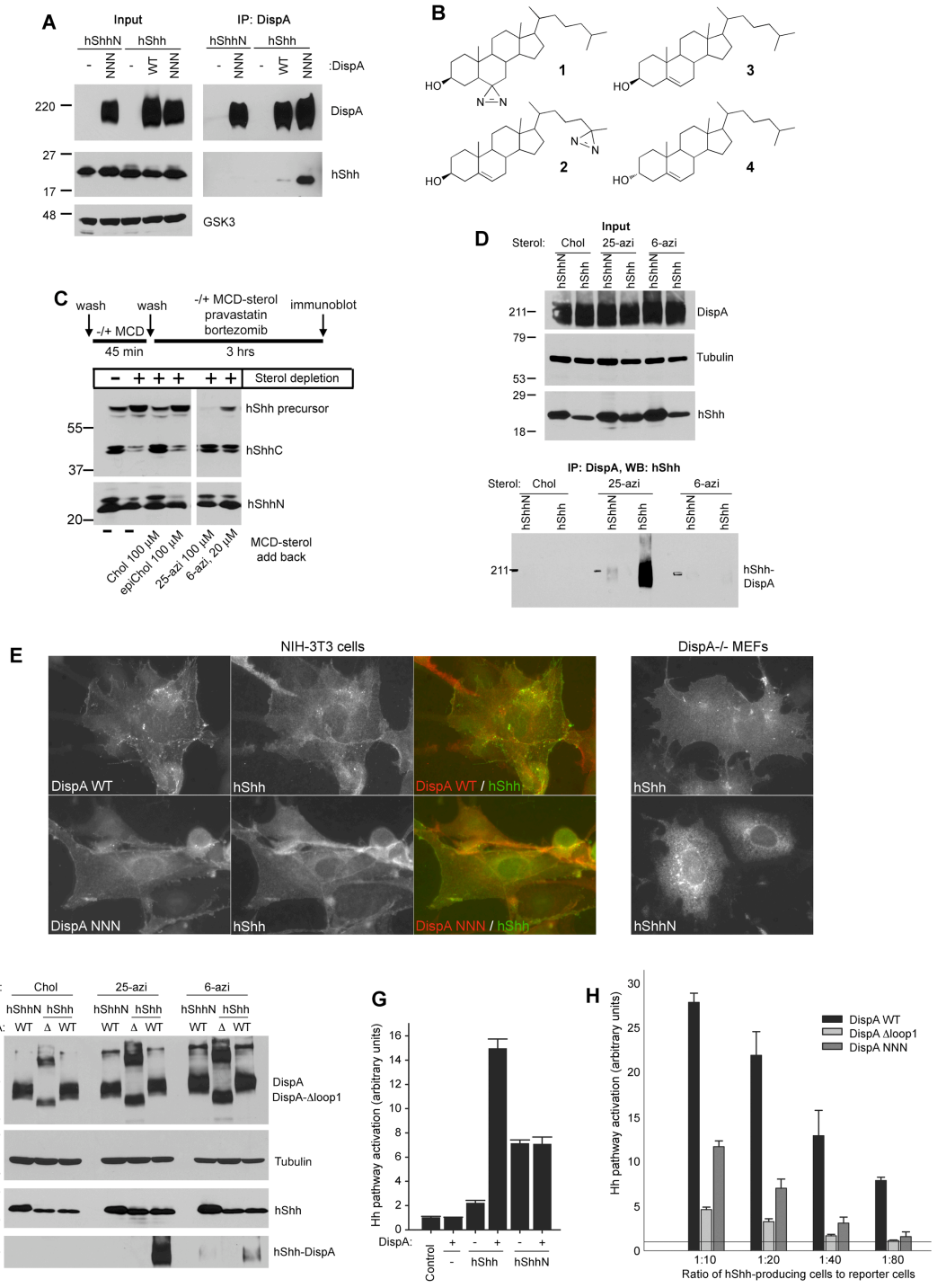

Figure 3.1 Cholesterol-dependent binding of hShh to DispA is required for hShh secretion
(A) 293T cells stably co-expressing hShh or hShhN, and myc-tagged wild-type DispA (WT) or DispA-NNN (NNN) were lysed with detergent and analyzed by immunoprecipitation with anti-myc antibodies, followed by SDS-PAGE and immunoblotting with anti-hShh antibodies.
(B) Structures of the photoreactive sterols, 6-azicholestanol (1) and 25-azicholesterol (2). Also shown are the structures of cholesterol (3) and the inactive diastereomer, epicholesterol (4).

Figure 3.1 (Continued)
(C) HShh, HA-tagged at the C-terminus (hShh-HA) was stably expressed in 293T cells. The cells were sterol-depleted with methyl-β-cyclodextrin (MCD), after which cholesterol (Chol), epicholesterol (epiChol), 6-azicholestanol (6-azi) or 25-azicholesterol (25-azi) were added back as soluble MCD complexes, for 3 hours. Lysates were analyzed by SDS-PAGE and immunoblotting with HA antibodies (to detect the hShh precursor and the C-terminal fragment, hShhC) and hShh antibodies (to detect the hShh ligand).
(D) 293T cells stably co-expressing myc-tagged DispA-WT and hShh or hShhN were labeled with the indicated sterols, as in (B). After incubation for 6 hours, the cells were UV-irradiated and DispA-hShh photocrosslinking was analyzed by denaturing immunoprecipitation with myc antibodies, followed by SDS-PAGE and immunoblotting for hShh. Immunoblotting for tubulin served as loading control.
(E) Left panels: immunofluorescence microscopy of hShh stably co-expressed with myc-tagged DispA-WT or DispA-NNN in NIH-3T3 cells. Cells were stained with rabbit anti-hShh and mouse anti-myc antibodies, followed by goat anti-rabbit Alexa488 and goat anti-mouse Alexa594 secondary antibodies. Right panels: localization by immunofluorescence microscopy of hShh and hShhN expressed in DispA-/- MEFs.
(F) As in (C) but with 293T cells stably co-expressing myc-tagged DispA or the mutant missing the first extracellular loop, DispA-Δloop1 (Δ), together with hShh or hShhN.
(G) DispA-/- MEFs stably expressing hShh or hShhN, rescued by lentiviral expression of mCherry-tagged DispA or not, were co-cultured with Hh-responsive Shh Light II cells at a 1:20 ratio. Luciferase measurements were normalized to reporter cells grown alone (control). All experiments were performed in triplicate. Error bars represent the standard deviation of the mean.
(H) DispA-/- MEFs stably expressing hShh, transduced with lentiviruses expressing mCherry-tagged DispA-WT, DispA-Δloop1 or DispA-NNN were analyzed as in (G), at four different ratios of hShh-producing cells to reporter cells.

A potential problem with our binding assay is that detergent solubilization could have a negative effect on the native conformation of DispA and/or might disrupt the DispA-hShh interaction. We thus developed a strategy to examine the DispA-hShh interaction in intact cells, using two different photoreactive cholesterol derivatives: 1) 6-azicholestanol (compound 1 in Figure 3.1B), a photoreactive sterol that carries a diazirine group on the B ring of the molecule (Thiele et al., 2000), and 2) 25-azicholesterol (compound 2 in Figure 3.1B), a novel photoreactive sterol that we synthesized, which carries a diazirine group at the end of the isooctyl tail. We reasoned that having the photoreactive group in two locations of the sterol molecule would increase the chance of detecting a potential interaction with DispA. We first asked if the two photoreactive sterols modify hShh in cells. When cells stably expressing hShh (Chen et al., 2011) were depleted of sterols by acute treatment with methyl-β-cyclodextrin (MCD), hShh processing was strongly inhibited, causing the accumulation of the unprocessed hShh precursor (Figure 3.1C). Processing was rescued by adding back cholesterol (compound 3 in Figure 3.1B)

but not the diastereomer epicholesterol (compound 4 in Figure 3.1B), which is inactive in modifying Hh proteins (Mann and Beachy, 2004). Adding back either of the two photoreactive sterols fully rescued hShh processing (Figure 3.1C). We next used this strategy to generate hShh modified with photoreactive sterols by labeling cells that stably express DispA and hShh. The cells were then UV-irradiated, and formation of a covalent DispA-hShh bond was tested by denaturing immunoprecipitation of DispA followed by immunoblotting for hShh. DispA showed crosslinking to hShh modified with photoreactive sterol (Figure 3.1D), but not to hShhN, demonstrating that DispA binds hShh in a cholesterol-dependent manner in intact cells. Interestingly, DispA was photocrosslinked much more efficiently when hShh was modified with 25-azicholesterol than with 6-azicholestanol (Figure 3.1D and 3.1F), suggesting that the isooctyl tail of cholesterol is a feature recognized by DispA during its interaction with hShh. Consistent with a DispA-hShh interaction in cells, DispA (wild-type and the NNN mutant) and hShh are both present at the plasma membrane by immunofluorescence microscopy (Figure 3.1E). Importantly, not all hShh puncta co-localize with DispA at the membrane, as expected from a transient interaction between the two proteins. In contrast to hShh, hShhN is found predominantly in intracellular vesicles and not at the plasma membrane (Figure 3.1E), consistent with the efficient release of hShhN from the cell surface.

We next asked if binding of DispA to hShh is important for hShh secretion. To generate a DispA mutant that cannot bind hShh, we deleted the first extracellular loop of DispA. This choice was based on the role that the first extracellular loop plays in two Disp-related proteins: it is required in the SREBP cleavage-activating protein (SCAP) for binding cholesterol (Motamed et al., 2011), and in Ptch for binding hShh (Marigo et al., 1996). Indeed, DispA-Δloop1 did not bind hShh in our in vivo photocrosslinking assay (Figure 3.1F). We turned to a cellular assay that

relies on the function of DispA in hShh secretion and long-range signaling. DispA-/- mouse embryonic fibroblasts (MEFs) (Ma et al., 2002) were co-cultured with the Hh reporter cells, Shh Light II (Taipale et al., 2000). Stable expression of hShh in DispA-/- MEFs caused a slight activation of the Hh pathway in reporter cells (Figure 3.1G) because short-range Hh signaling does not require DispA. Co-expression of mCherry-tagged DispA in DispA-/- MEFs strongly increased the response of reporter cells, indicating that DispA rescued hShh secretion (Figure 3.1G). As expected, DispA did not affect signaling by DispA-/- MEFs expressing hShhN (Figure 3.1G), because DispA is only required for secretion of cholesterol-modified hShh. Similar results were obtained by overexpressing DispA in NIH 3T3 cells (Supplemental Figure 3.S1). In contrast to wild-type DispA, mCherry-tagged DispA-Δloop1 or DispA-NNN did not rescue signaling by DispA-/- MEFs expressing hShh, a result more obvious at a lower ratio of signaling cells to reporter cells (Figure 3.1H). The fact that DispA-Δloop1 is inactive suggests that cholesterol-dependent binding of hShh to DispA is required for hShh secretion.

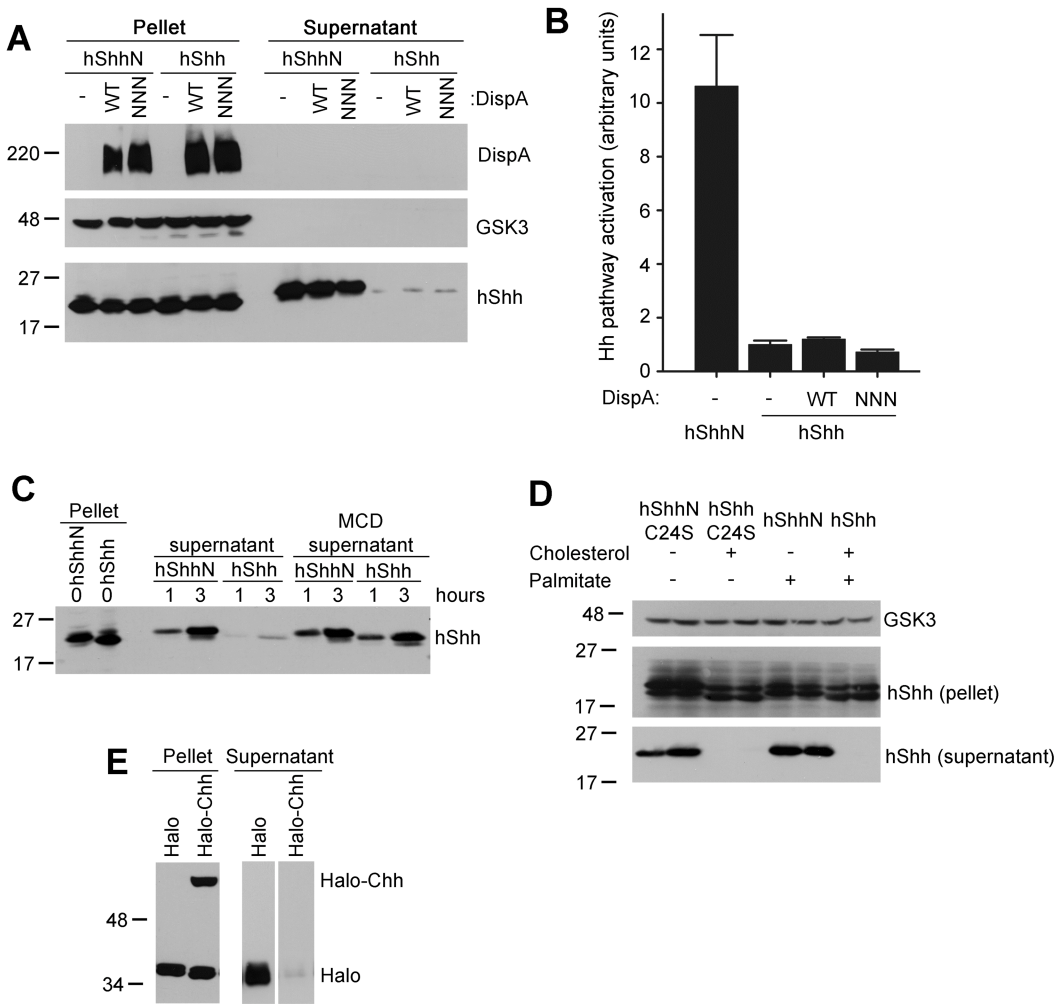

Figure 3.2 DispA is not sufficient for release of cholesterol-modified hShh

(A) 293T cells stably expressing hShh and myc-tagged DispA constructs were washed of serum and were incubated with serum-free media for 6 hours. Secreted proteins were precipitated with trichloroacetic acid (TCA). Pellet and supernatant fractions were analyzed by SDS-PAGE and immunoblotting with anti-myc and anti-hShh antibodies. Blotting for GSK3 served as loading control.

(B) Supernatants collected as in (A) were diluted 1:2 with serum-free media and hShh activity was assayed using Shh Light II reporter cells. Measurements were performed in triplicate and error bars represent standard deviation of the mean.

(C) 293T cells expressing hShhN or hShh were incubated with serum-free media, with or without methyl-β-cyclodextrin (MCD, 100 μM), and supernatants were harvested after 1 or 3 hours. Secretion of hShh and hShhN was analyzed as in (A).

(D) 293T cells transiently expressing hShh, hShhN, hShh with a palmitylation site mutation (hShhC24S), or hShhN with a palmitylation site mutation (hShhN-C24S) were incubated in serum-free media for 4 hours, and secreted proteins were TCA-precipitated. Pellet and supernatant fractions were analyzed as in (A). The samples in this panel were loaded in duplicate.

(E) A secreted HA-tagged Halotag protein was fused to amino acids 190-462 of hShh (Halo-Chh); autocatalytic processing of Halo-Chh generates Halotag fused to amino acids 190-198 of hShh, modified with cholesterol. Secreted HA-Halotag fused to amino acids 190-198 of hShh (Halo) is not cholesterol-modified and serves as negative control. The Halotag constructs were expressed in 293T cells, and secreted proteins were collected into serum free media for 4 hours. Pellet and supernatant fractions were analyzed by SDS-PAGE and immunoblotting with anti-HA antibodies.

DispA is not sufficient to release cholesterol-modified hShh from cells

Although the co-culture system provides a good functional assay for DispA, it measures hShh secretion only indirectly. We next tested directly if DispA is sufficient for hShh release from membranes, by examining secretion of hShh from 293T cells that stably over-express DispA. Since we observed that serum releases hShh in a non-specific, DispA-independent manner, we took care to remove residual serum from the cells by repeated washes with serum-free medium. Under serum-free conditions, no hShh was released into the medium, in the absence or presence of overexpressed DispA, as assayed by Western blotting (Figure 3.2A) or by Hh activity assays (Figure 3.2B). These cells expressed large amounts of hShh, which was properly processed (Figure 3.2A) and strongly localized to plasma membrane, as determined by immunofluorescence microscopy. In contrast, stably expressed hShhN was efficiently secreted into serum-free medium and was active; as expected, DispA had no effect on hShhN secretion (Figure 3.2A and B). These results indicate that DispA alone is not sufficient to release hShh, perhaps because another factor is required to solubilize it in the media; in the absence of such a factor, hShh remains membrane-associated.

Cholesterol is the main determinant of hShh membrane association

Given that hShhN is efficiently secreted, we tested if the cholesterol anchor is responsible for the strong association of hShh with membranes. HShh was quickly released from cells when media were supplemented with methyl-β-cyclodextrin (MCD) (Figure 3.2C), which can be explained by MCD binding the cholesterol anchor and promoting hShh solubilization. In contrast to hShh, secretion of hShhN was not further enhanced by MCD (Figure 3.2C).

We next asked if the other hydrophobic modification of hShh, palmitylation, plays a role in hShh association with membranes. Like wild-type hShh, hShh-C24S, a mutant of hShh that cannot be palmitylated but is still modified with cholesterol (Chamoun et al., 2001)) was membrane-associated and was not secreted into serum-free medium (Figure 3.2D). As expected, hShhN and a mutant that lacks both the cholesteryl and palmityl moieties (hShhN-C24S) were efficiently secreted (Figure 3.2D).

Finally, we asked if cholesterol modification of an unrelated soluble protein is sufficient to recapitulate the strong membrane attachment of hShh. We used a construct encoding a secreted version of the Halotag protein fused to the C-terminal domain of hShh (Halotag-Chh); in cells, this fusion undergoes autocatalytic processing to generate cholesterol-modified Halotag. HA-tagged Halotag-Chh was expressed in 293T cells and secretion into serum-free medium was measured by immunoblotting with HA antibodies. Under these conditions, cholesterol-modified Halotag was not secreted and remained membrane-associated (Figure 3.2E); in contrast, Halotag without the cholesterol modification was soluble (Figure 3.2E).

Together, these results indicate that the cholesterol anchor is necessary and sufficient for hShh membrane attachment, while the palmityl moiety plays a less important role, if any. Thus in order to secrete hShh, cells must find a way to solubilize its cholesterol anchor.

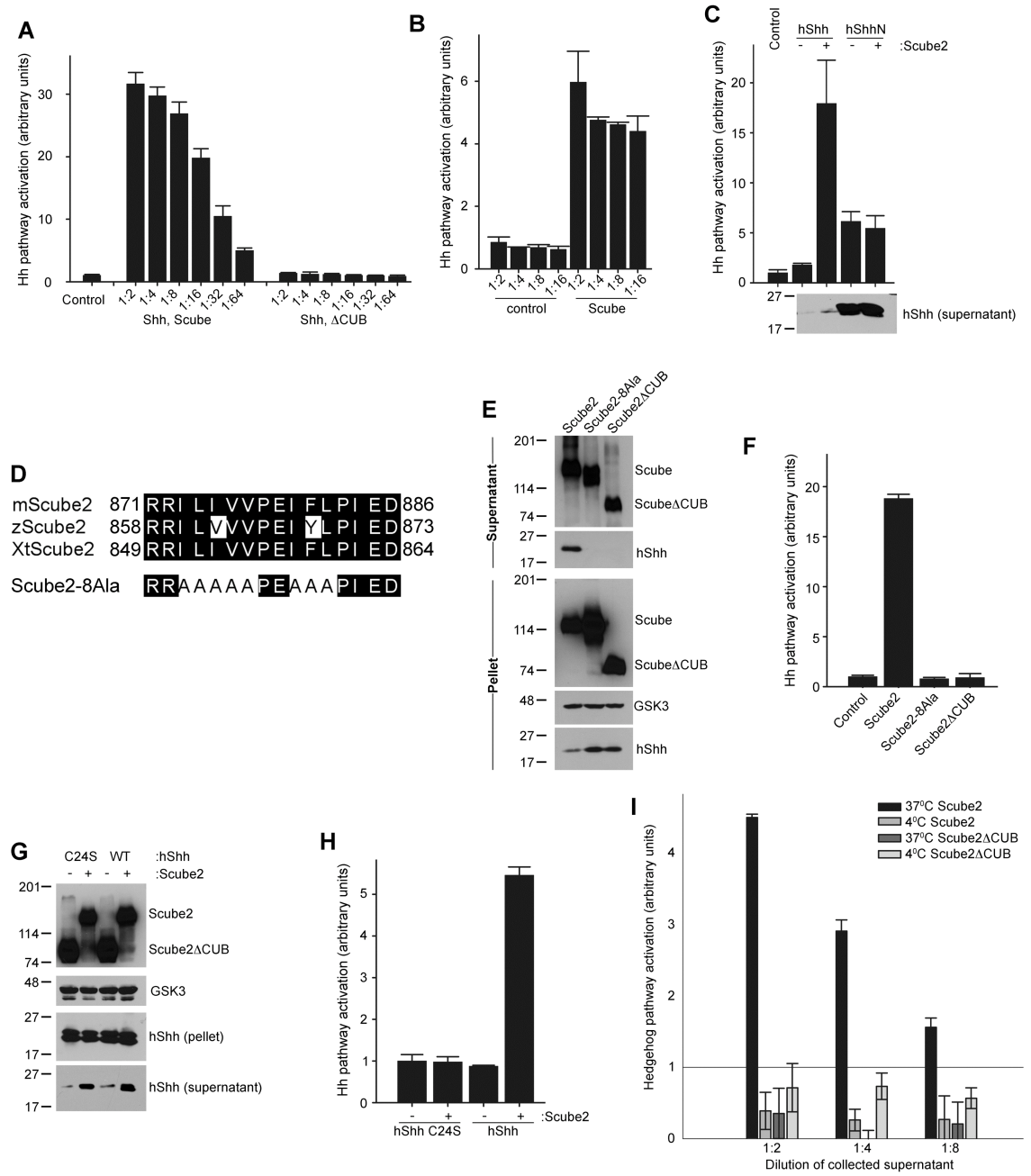

Figure 3.3 The extracellular protein Scube2 stimulates secretion of cholesterol-modified hShh
(A) Scube2 or Scube2ΔCUB was transfected into 293T cells stably expressing hShh, and 24 hours later secreted proteins were collected into serum-free media for 4 hours. HShh activity in serial dilutions of the supernatant was measured by luciferase assay in Shh Light II reporter cells. All experiments were performed in triplicate. Error bars represent the standard deviation of the mean.
(B) Scube2 or Scube2ΔCUB was added in serum-free media to 293T cells stably expressing hShh, for 4 hours. Activity of secreted hShh was measured as in (A).
(C) As in (A) but with 293T cells stably expressing hShh or hShhN. Secreted hShh and hShhN were collected for 6 hours, and were analyzed by reporter assay in Shh Light II cells and by immunoblotting with anti-hShh antibodies. Note the much higher amount of secreted hShhN compared to hShh.
(D) Sequence of the conserved hydrophobic patch in the CUB domain of vertebrate Scube2 orthologs. Also shown is the sequence of the Scube2-8Ala mutant, in which 8 hydrophobic residues are mutated to alanines.

Figure 3.3 (Continued)
(E) HA-tagged Scube2, Scube2-8Ala, or Scube2ΔCUB were transfected into 293T cells stably expressing hShh. Secreted proteins were collected 24 hours later, for 6 hours into serum-free media. Aliquots of the cell pellet and supernatants were analyzed by SDS-PAGE and immunoblotting for HA and hShh.
(F) HShh activity in the supernatants collected in (E) was measured as in (A).
(G) HShh or the palmitylation-defective mutant hShhC24S were co-expressed in 293T cells with HA-tagged Scube2 or Scube2ΔCUB. HShh and hShhC24S secretion was analyzed as in (E).
(H) HShh and hShhC24S activity in the supernatants collected in (G) was measured as in (A).
(I) Scube2 or Scube2ΔCUB was added in serum-free medium to 293T cells stably expressing hShh, for 1 hour at 37^0C or 4^0C. HShh activity in the supernatants was measured as in (A).

Scube2 dramatically increases secretion of cholesterol-modified hShh

The experiments above suggest the existence of an extracellular protein that helps the secretion of hShh by overcoming its cholesterol-dependent insolubility. The Scube family of secreted proteins is required for long-range Hh signaling in zebrafish (Johnson et al., 2012), but its mechanism is unknown. We examined if the first Scube protein implicated in Hh signaling, Scube2 (Hollway et al., 2006; Kawakami et al., 2005; Woods and Talbot, 2005), is involved in releasing hShh from cells. When Scube2 was expressed in 293T cells stably expressing hShh, it caused a dramatic increase in secretion of active hShh (Figure 3.3A). As negative control we used Scube2ΔCUB, a truncation mutant of Scube2 that lacks a C-terminal portion of the protein, including a cysteine-rich domain and a CUB domain; this loss-of-function mutation was identified in the initial cloning of zebrafish Scube2 (Woods and Talbot, 2005). Scube2ΔCUB was efficiently secreted but failed to stimulate hShh secretion (Figure 3.3A). Scube2 supplied exogenously also released hShh into serum-free media, indicating that Scube2 and hShh do not have to be co-expressed (Figure 3.3B). Scube2 had no effect on the secretion of hShhN, indicating that it acts specifically to release cholesterol-modified hShh (Figure 3.3C). Interestingly, although the amount of released hShh was significantly smaller than that of hShhN, the signaling activity of hShh was much higher than that of hShhN (Figure 3.3C), suggesting that cholesterol modification greatly enhances the potency of the hShh ligand.

It is known that hShh can be released from cells by serum (Chen et al., 2011) and by high levels of heparin. HShh released with either serum or heparin was inactive in signaling assays, in contrast to hShh released by Scube2 (Supplemental Figure 3.S2). Thus, unlike other factors that can release hShh, release by Scube2 is physiological.

All Scube2 orthologs contain a conserved hydrophobic stretch in the middle of the CUB domain (Figure 3.3D), while the rest of the protein shows little clustering of hydrophobic amino acids outside the signal sequence. We reasoned that this hydrophobic stretch might be important for release of hShh. Indeed, a Scube2 mutant in which 8 amino acid residues in the hydrophobic stretch are mutated to alanines (Scube2-8Ala) is secreted (Figure 3.3E) but is completely inactive in releasing hShh (Figure 3.3E, F). This indicates that the conserved hydrophobic sequence in the CUB domain is necessary for Scube2 activity.

We next asked if palmitylation of hShh is required for release by Scube2. Like wild-type hShh, the non-palmitylated mutant hShhC24S was released by Scube2 but not by Scube2ΔCUB (Figure 3.3G), indicating that the palmitylation is not required for Scube-mediated hShh secretion. The Scube2-released hShhC24S was inactive in Hh signaling assays (Figure 3.3H), consistent with the requirement of the palmityl modification for Hh activity (Chamoun et al., 2001).

We also performed an experiment to determine the effect of temperature on the release of hShh from cells by Scube2. While added Scube2 released a significant amount of hShh during 1 hour at 37^0C, no hShh was released at 4^0C (Figure 3.3I). This is consistent with Scube2 having to overcome the hydrophobic interaction between the cholesterol anchor of hShh and the membrane, an interaction of increased strength at lower temperature.

Scube2 does not affect hShh processing in producing cells or signaling in responding cells

One possible explanation for the enhanced secretion of hShh is that Scube2 stimulates hShh processing in producing cells. Radioactive pulse-chase analysis of hShh processing showed that it proceeded with the same kinetics in the presence of co-expressed Scube2 or the inactive Scube2ΔCUB mutant (Figure 3.4A). This result indicates that Scube2 does not affect hShh processing.

To determine if Scube2 has an effect on Hh signal transduction, we performed two experiments. First, we asked if Scube2 affects signaling by hShhN. Increasing concentrations of Scube2 added to a fixed concentration of hShhN had no effect on Hh pathway stimulation (Figure 3.4B, left side of the graph). In a second experiment, we asked if excess Scube2 affects signaling by hShh. When increasing amounts of Scube2 were added to hShh released into Scube2-containing media, there was no effect on Hh pathway stimulation (Figure 3.4B, right side of the graph); furthermore, Scube2 had no effect on Hh signaling on its own. Although it was proposed that Scube2 promotes Hh signaling at the level of the responding cell, possibly via its interaction with Ptch (Tsai et al., 2009), our Scube2 titration experiment argues against such a model. Our data, however, cannot exclude the possibility that the hShh-Scube2 complex (see below) is the active species in long-range Hh signaling.

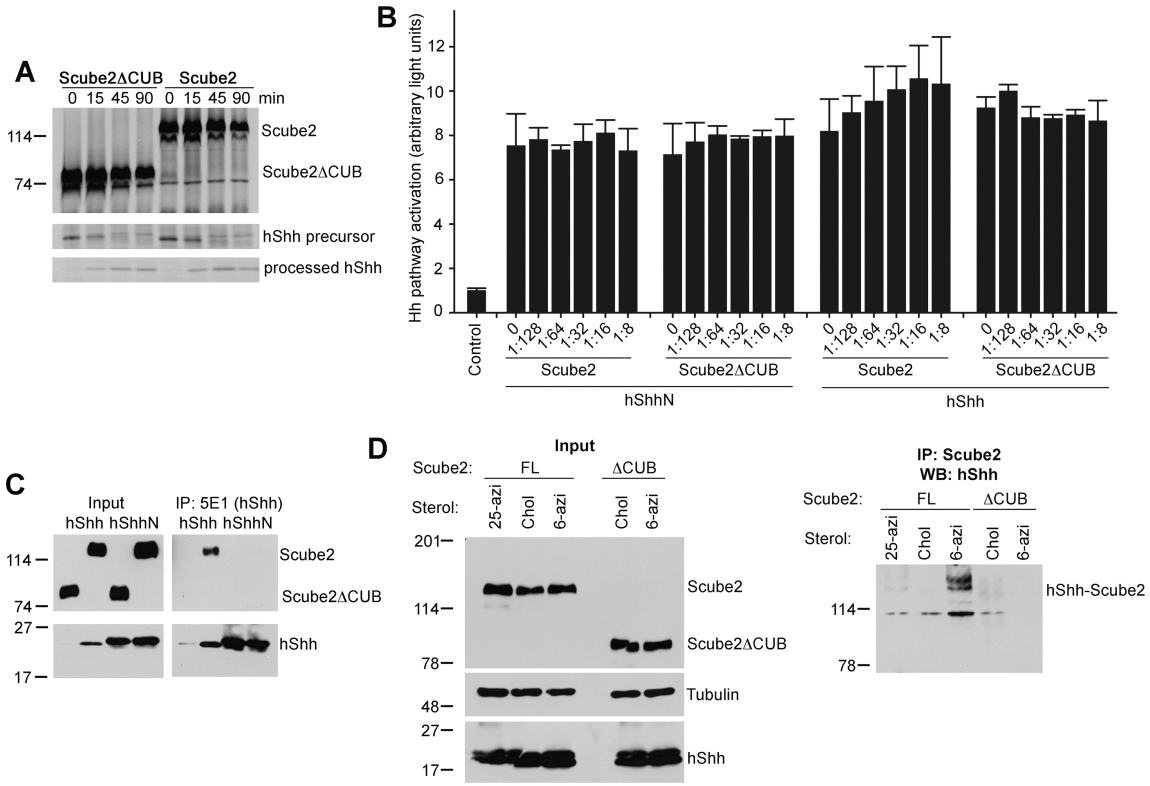

Figure 3.4 Cholesterol-dependent binding of Scube2 to hShh is required for hShh secretion
(A) HA-tagged Scube2 or Scube2ΔCUB was expressed in 293T cells stably expressing hShh. The cells were pulsed with ^{35}S-methionine for 3 min and were chased with media containing unlabeled methionine for the indicated times. HShh processing was analyzed by immunoprecipitation with the 5E1 antibody, which recognizes full-length and processed hShh. Scube2 and Scube2ΔCUB were immunoprecipitated with anti-HA antibodies. The precipitated protein was analyzed by SDS-PAGE and fluorography. The same number of cells was processed for each condition.
(B) The two graphs on the left show that Scube2 does not affect hShhN activity. HShhN was mixed with HA-tagged Scube2 or Scube2ΔCUB, in the indicated ratios, and its activity was measured in Shh Light II reporter cells. The two graphs on the right show Scube2 does not affect the activity of hShh pre-released with Scube2. 293T cells co-expressing hShh and HA-tagged Scube2 were used to generate serum-free hShh-Scube2 conditioned media. This media was mixed with HA-tagged Scube2 or Scube2ΔCUB, in the indicated ratios, and its activity was measured in Shh Light II reporter cells. All experiments were performed in triplicate. Error bars represent the standard deviation of the mean.
(C) 293T cells co-expressing hShh or hShhN, and HA-tagged Scube2 or Scube2ΔCUB were incubated in serum-free media for 4 hours. HShh and hShhN were immunoprecipitated from the supernatant with 5E1 antibodies. A portion of the supernatant was TCA-precipitated to serve as input. All samples were analyzed by SDS-PAGE and immunoblotting with anti-HA and anti-hShh antibodies.
(D) HShh or hShhN was stably co-expressed with HA-tagged Scube2 or Scube2ΔCUB in 293T cells. The cells were labeled with the indicated sterols, followed by UV irradiation. Photocrosslinked Scube2-hShh was analyzed by denaturing immunoprecipitation with HA antibodies, followed by SDS-PAGE and immunoblotting for hShh.

Scube2 binds hShh in a cholesterol-dependent manner

It seemed likely that Scube2 might stimulate hShh secretion by direct binding. We first tested this hypothesis by immunoprecipitation of hShh secreted into serum-free medium by cells co-expressing hShh and HA-tagged Scube2, followed by immunoblotting for HA. Under these conditions we detected binding of Scube2 to hShh (Figure 3.4C). Scube2 did not bind hShhN, indicating that Scube2 binds hShh in a cholesterol-dependent manner (Figure 3.4C). As expected, the inactive mutant Scube2ΔCUB did not release or bind hShh, suggesting that binding to Scube2 is required for hShh secretion.

In the experiment above, hShh was immunoprecipitated with the 5E1 monoclonal antibody, which blocks binding of hShh to Ptch and to the antagonist Hedgehog-interacting protein (HIP), due to the very similar binding interfaces between hShh and 5E1, HIP, and Ptch (Maun et al., 2010). In contrast, the 5E1 antibody did not block binding of hShh to Scube2, indicating that the hShh-Scube2 interface is distinct and thus hShh binding to Scube2 might allow hShh interaction with the downstream components Ptch and HIP.

Finally, we examined the interaction between Scube2 and hShh in cells by photocrosslinking. Cells stably expressing HA-tagged Scube2 and hShh were labeled with photoreactive sterols, and were then UV-irradiated. Lysates were subjected to denaturing immunoprecipitation with HA antibodies followed by immunoblotting for hShh. We detected crosslinking between hShh modified with 6-azicholestanol and Scube2; as expected, Scube2ΔCUB was not crosslinked to Scube2 (Figure 3.4D). Interestingly, hShh modified with 25-azicholesterol showed much less crosslinking to Scube2 (Figure 3.4D), in contrast to DispA-hShh crosslinking, which occurred preferentially with 25-azicholesterol. This differential crosslinking suggests that Scube2 and DispA recognize different structural aspects of the

cholesterol molecule, in a manner that might facilitate the hand-off of hShh from DispA to Scube2.

DispA synergizes with Scube2 to promote hShh secretion

We next tested if DispA and Scube2 act synergistically to promote hShh secretion, first in the co-culture system of DispA-/- MEFs and Hh reporter cells. DispA-/- MEFs expressing hShh and DispA were plated at different ratios with Hh reporter cells, and the co-cultures were incubated with Scube2 in serum-free media, followed by Hh activity assays. Under these conditions, Scube2 strongly synergized with wild-type DispA to cause hShh secretion and Hh pathway activation (Figure 3.5A). As expected, Scube2 did not synergize with DispA-NNN and had no effect on signaling by hShhN; also, Scube2ΔCUB had no effect on hShh (Figure 3.5A). Interestingly, at a higher ratio of hShh-producing cells to reporter cells, Scube2 was able to release some hShh even in the absence of DispA (Figure 3.5A); this is consistent with a model in which hShh partitions between the membrane and Scube2 in the media.

Similar results were obtained when we measured hShh secretion in 293T cells, in the absence or presence of co-expressed myc-tagged DispA. Addition of Scube2 to the cells synergized with wild-type DispA to release hShh into the supernatant, as assayed by immunoblotting (Figure 3.5B). As expected, Scube2 did not synergize with DispA-NNN, and Scube2ΔCUB had no effect on hShh secretion, irrespective of the presence of DispA (Figure 3.5B). Similarly, Scube2 added to 293T cells synergized with DispA but not with DispA-Δloop1, to cause secretion of hShh, as measured by Hh reporter assays (Figure 3.5C). Together, these data show that DispA and Scube2 act synergistically to promote hShh secretion.

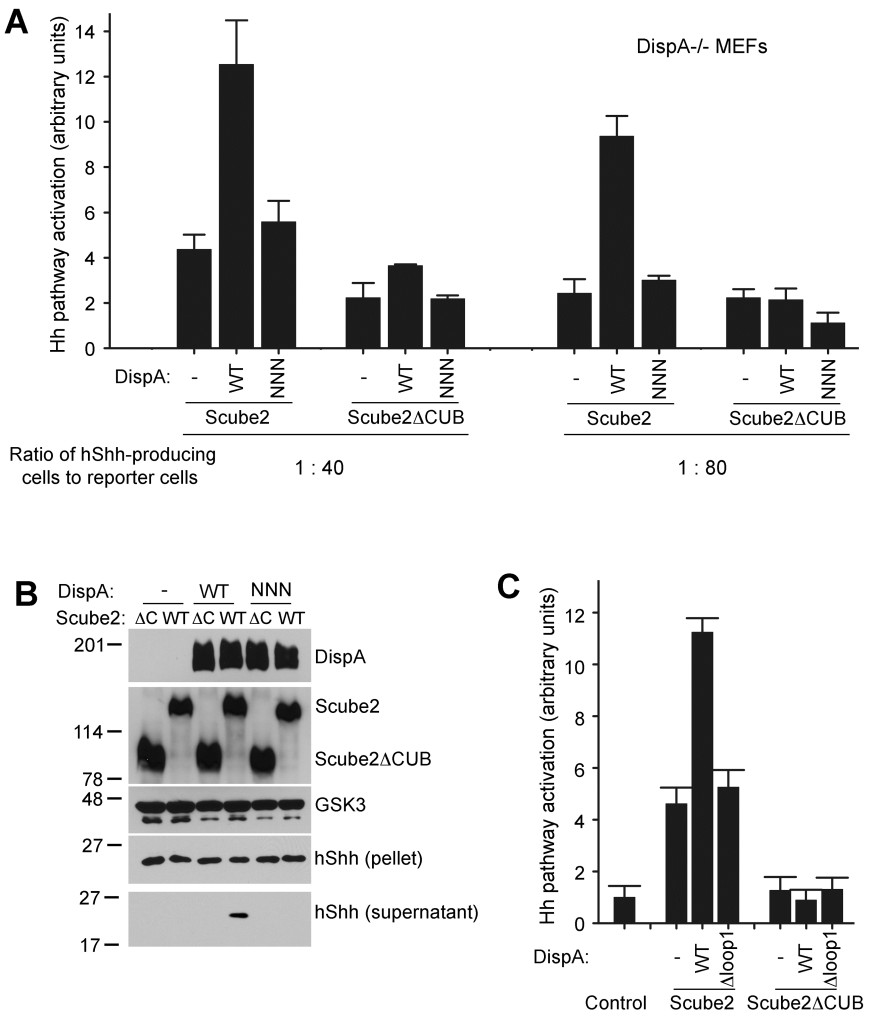

Figure 3.5 Scube2 synergizes with DispA to stimulate secretion of cholesterol-modified hShh
(A) DispA-/- MEFs stably expressing hShh, transduced with lentiviruses expressing mCherry-tagged wild-type DispA or DispNNN, were plated with Shh Light II reporter cells at 1:40 and 1:80 ratios. After 12 hours, Scube2 or Scube2ΔCUB was added in serum-free media. Luciferase measurements were performed 30 hours later and were normalized to untreated reporter cells. All experiments were done in triplicate. Error bars represent the standard deviation of the mean.
(B) HA-tagged Scube2 or Scube2ΔCUB was transfected into 293T cells that stably express hShh, hShh and myc-tagged DispA-WT, or hShh and myc-tagged DispA-NNN. Secreted proteins were collected into serum-free media 24 hours later, for 4 hours. Aliquots of the cellular pellets and supernatants were analyzed by SDS-PAGE and immunoblotting with HA, myc and hShh antibodies. Blotting for GSK3 served as loading control.
(C) As in (B), but with 293T cells expressing DispA-Δloop1 instead of DispA-NNN. Activity of secreted hShh was measured as in (A).

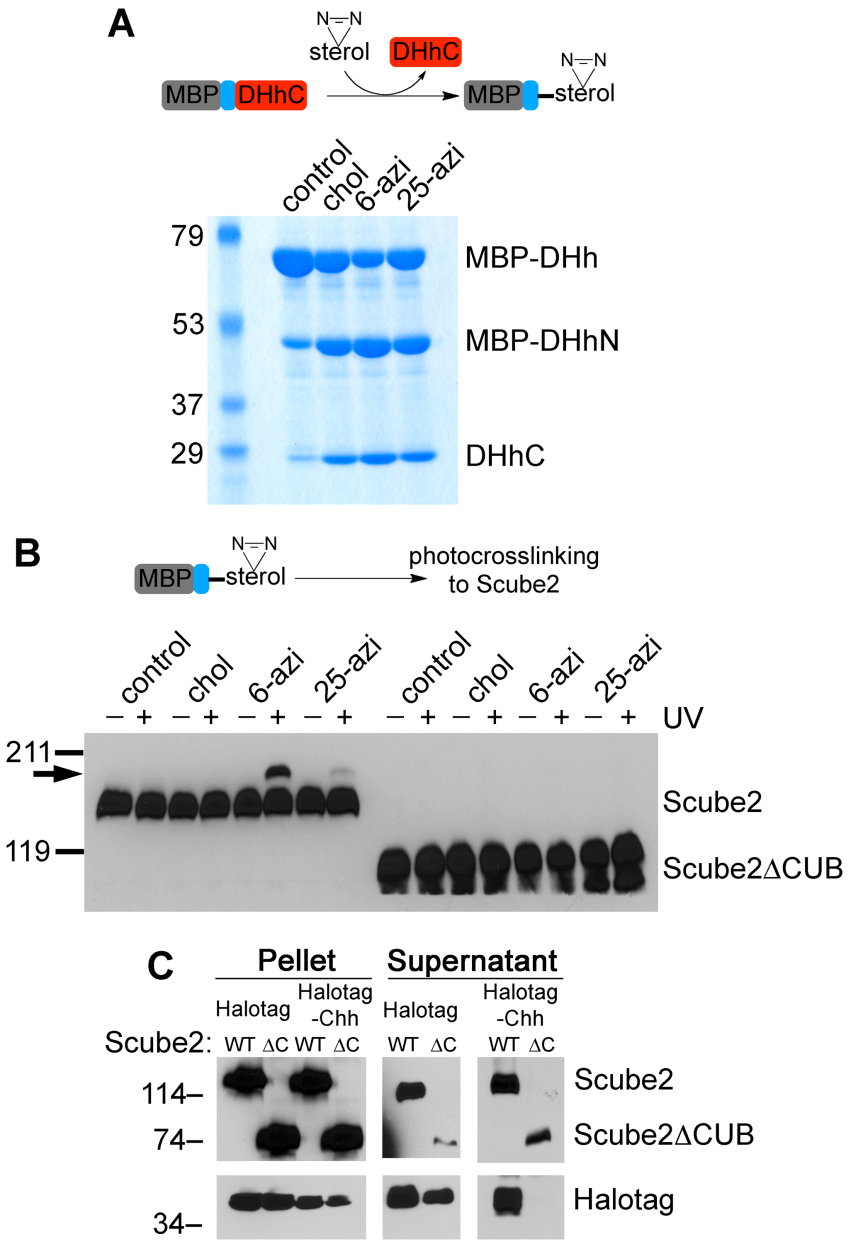

Figure 3.6 Cholesterol modification is sufficient for interaction with and secretion by Scube2
(A) Purified maltose-binding protein (MBP) fused to amino acids 244-471 of Drosophila Hedgehog (MBP-DHh) was used in *in vitro* processing reactions to generate MBP modified with either cholesterol (control), 6-azicholestanol or 25-azicholesterol. The samples were analyzed by SDS-PAGE and Coomassie staining. MBP-DHhN and DHh-C are the two fragments generated by *in vitro* processing.
(B) The processing reactions in (A) were incubated with HA-tagged Scube2 or Scube2ΔCUB, followed by UV irradiation to induce photocrosslinking. The samples were analyzed by reducing SDS-PAGE and immunoblotting with HA antibodies. The arrow indicates the position of the photocrosslinked Scube2-MBP species.
(C) Constructs that generate Halotag protein modified with cholesterol (Halotag-Chh) or not (Halotag) were co-expressed in 293T cells with myc-tagged Scube or Scube2ΔCUB. Secreted proteins were collected in serum-free media for 6 hours, followed by TCA precipitation and immunoblotting with HA and myc antibodies.

Cholesterol modification is sufficient for interaction with Scube2 and Scube2-dependent secretion

We asked if cholesterol modification is sufficient for interaction with Scube2, by photocrosslinking in vitro. To this end, we used an unrelated protein, maltose-binding protein (MBP) that we modified with photoreactive sterols by in vitro processing (Chen et al., 2011) (Figure 3.6A). Sterol-modified MBP fusions were then incubated with HA-tagged Scube2, followed by UV irradiation and immunoblotting with HA antibodies, to detect an increase in Scube2 size due to photocrosslinking. Under these conditions, Scube2 was crosslinked to MBP modified with 6-azicholestanol (Figure 3.6B), and much less efficiently to MBP modified with 25-azicholesterol. This is the same preference for 6-azicholestanol over 25-azicholesterol that we observed for hShh-Scube2 photocrosslinking in cells (Figure 3.4D). The size of the electrophoretic mobility shift in Scube2 crosslinked to MBP (Figure 3.6B) is consistent with the addition of one molecule of MBP (40 kDa), indicating a 1:1 binding ratio between Scube2 and sterol-modified MBP. As expected, Scube2ΔCUB was not crosslinked to any of the sterol-modified MBP proteins. These results suggest that cholesterol modification is sufficient for binding to Scube2.

Finally, we asked if cholesterol modification is sufficient for Scube2-dependent secretion. For this purpose we used cholesterol-modified Halotag, which is membrane-associated (Figure 3.2E). HA-tagged Halotag-Chh was co-expressed in 293T cells with myc-tagged Scube2, and secretion into serum-free medium was measured by immunoblotting. As shown in figure 3.6C, cholesterol-modified Halotag was secreted only in the presence of Scube2, while Halotag without a cholesterol anchor was secreted independently of Scube2. As expected, Scube2ΔCUB did not release cholesterol-modified Halotag. These data demonstrate that a cholesterol anchor is

sufficient for an unrelated soluble protein to become membrane-associated, to bind Scube2, and to be secreted in a Scube2-dependent manner.

DISCUSSION

The present study suggests a mechanism for how hShh is released from cells, in spite of its strong association with membranes. HShh has two lipid modifications, a palmityl residue at the N-terminus and a cholesteryl residue at the C-terminus. The cholesteryl moiety is mainly responsible for the insolubility of hShh, which has to be overcome to allow hShh mobilization and long-range Hh signaling. We now show that the multi-spanning membrane protein Dispatched-A (DispA), and the secreted protein Scube2 cooperate to accomplish hShh secretion. We demonstrate that during secretion hShh uses its unique cholesterol modification to interact with DispA and Scube2 via two distinct and synergistic binding events, and that these two interactions are required for hShh secretion. Interestingly, DispA and Scube2 recognize different structural aspects of the cholesterol molecule (Figure 3.7A), suggesting a hand-off mechanism for transferring hShh from DispA to Scube2. The advantage of such a mechanism is that it ensures hShh is never free in the aqueous environment, thus preventing its precipitation. According to this model, DispA would act in the hShh-synthesizing cell, whereas Scube2 could be provided either by the producing cell or by another cell.

Our results are in agreement with previous genetic evidence that showed that long-range Hh signaling absolutely requires Disp in vertebrates (Ma et al., 2002; Nakano et al., 2004) and in insects (Burke et al., 1999), and the Scube family of secreted proteins in zebrafish (Hollway et al., 2006; Johnson et al., 2012; Kawakami et al., 2005; Woods and Talbot, 2005). Both Disp and Scube are not required for short-range Hh signaling, consistent with their demonstrated role in

hShh secretion, rather than signal transduction. In addition, consistent with our results, genetic analysis shows that Scube2 acts non-cell autonomously, in contrast to Disp. So far, an essential role for Scube proteins in Hh signaling has only been demonstrated in zebrafish (Johnson et al., 2012), but sequence conservation suggests that the function of Scube is conserved in mammalian Hh signaling.

While this manuscript was under review, another study (Creanga et al., 2012) was published, showing that Scube2 mediates release of cholesterol- and palmityl-modified hShh. Both this study and ours agree that cholesterol but not palmitate is strictly required for hShh release by Scube2; however Creanga et al. show that palmitylation enhances release of hShh by Scube2, which we did not observe in our experiments. The reason for this discrepancy remains to be elucidated. It should be pointed out that Scube-released hShh that lacks the palmitate modification is completely inactive in signaling assays (Creanga et al., 2012, and this study).

Our data support the following sequence of events in hShh biosynthesis (Figure 7B). Following autocatalytic cholesterol modification in the endoplasmic reticulum and palmitylation, hShh reaches the plasma membrane, to which it remains strongly attached via its cholesterol anchor. HShh then binds DispA, a cholesterol-dependent interaction that lowers the activation energy required for hShh extraction from the bilayer. Alternatively, hShh could associate with DispA earlier in the secretory pathway, and the two proteins might travel together to the plasma membrane. Binding to DispA is necessary but not sufficient for hShh secretion, because an extracellular binding partner is needed for hShh solubility. Additionally, if DispA binding is too strong, hShh secretion is impaired, as seen with some inactive DispA mutants. In the next step, hShh is transferred from DispA to the secreted protein Scube2, which is required for long-range Hh signaling in zebrafish. Scube2 interacts with the cholesterol anchor of hShh and dramatically

enhances hShh secretion by promoting its solubility. Cholesterol modification is sufficient, as demonstrated by the fact that an unrelated protein can be secreted in a Scube2-dependent manner. Although it is possible that Scube and Shh associate before reaching the plasma membrane when synthesized in the same cell, it is clear that this is not required for hShh secretion, as exogenous Scube2 can release hShh displayed on the cell surface.

It should be emphasized that the steps in hShh secretion outlined above represent partitioning equilibria of cholesterol-modified hShh, so that high concentrations of Scube2 solubilize hShh from membranes even without DispA (the equilibrium on the left of Figure 3.7B). HShh secretion however is greatly enhanced by DispA, as demonstrated by the strong synergy we observed between DispA and Scube2. How DispA synergizes with Scube2 remains to be elucidated. One possibility is that the orientation of the cholesterol anchor of hShh in the membrane favors its transfer to DispA, and is less favorable for a direct transfer to Scube2. Alternatively, Scube2 might bind DispA, which could facilitate the transfer of hShh between the two proteins. Based on homology to RND transporters, it was postulated that DispA acts as a pump (Ma et al., 2002). We speculate that the pumping activity of DispA might be involved in the transfer of hShh to Scube2. It will be important to elucidate the source of energy that DispA uses to pump hShh.

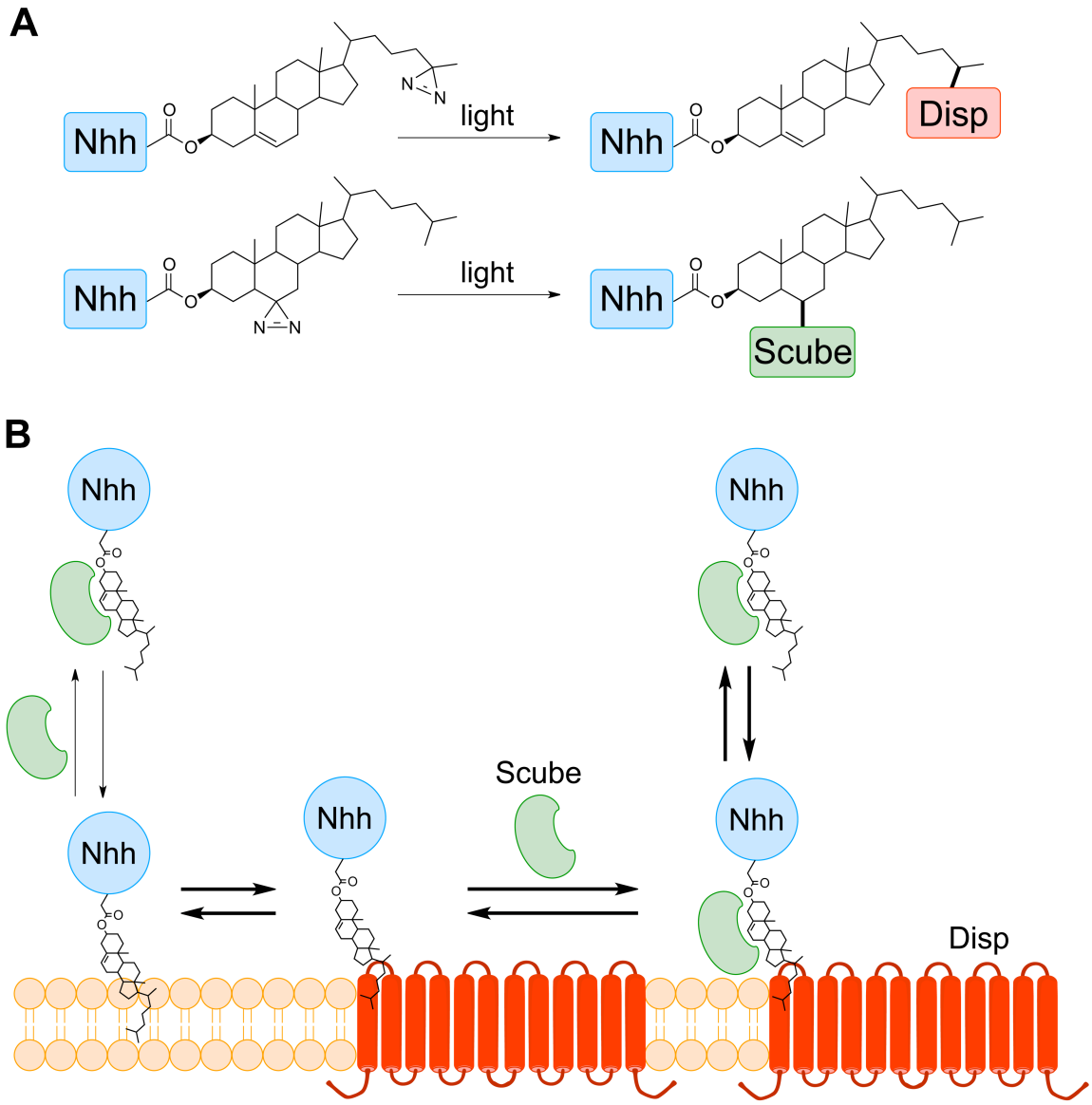

Figure 3.7. Mechanism of hShh secretion by the DispA and Scube2
(A) Summary of the results for photocrosslinking of hShh to DispA and to Scube2 in cells. DispA is crosslinked to hShh modified with 25-azicholesterol and Scube2 is crosslinked to hShh modified with 6-azicholestanol, suggesting that DispA and Scube2 recognize different aspects of the cholesterol molecule.
(B) The hShh ligand associates with membranes due to its hydrophobic cholesterol anchor. HShh binds DispA in a cholesterol-dependent manner, and this interaction is required for hShh secretion, perhaps by lowering the activation energy for hShh extraction from the lipid bilayer. From DispA, hShh is transferred to the secreted protein Scube2. The fact that DispA and Scube2 recognize different features of the cholesterol molecule suggests a hand-off mechanism for this transfer, such that the cholesterol anchor of hShh never contacts directly the aqueous environment, and is thus kept soluble. This mechanism is reminiscent of the transfer of free cholesterol between the Niemann-Pick disease proteins NPC1 and NPC2 during cholesterol egress from late endosomes/lysosomes.

The interaction between Scube2 and hShh is expected to be dynamic, to allow hShh release. Such a transient interaction raises the question of how Scube2 keeps hShh soluble. One model is that hShh is kept soluble by an excess of Scube2, similar to sterol solubilization by complexation with methyl-β-cyclodextrin (MCD), in which sterol-MCD binding is dynamic and a several-fold molar excess of MCD is usually required for keeping the sterol soluble in aqueous solution. In a more complicated model, Scube2 might chaperone hShh and help it form a soluble multimeric species in which the cholesterol anchors are shielded from the aqueous environment by interactions between hShh monomers. A more detailed biochemical and structural analysis of the hShh-Scube interaction will be needed to answer these questions.

Our results suggest that Scube2 is not simply a solubilizing factor. HShh can be released by other agents, such as heparin and serum, but this requires very high concentrations and the released hShh is inactive in signaling assays. Thus, Scube2 interacts with hShh in a specific and efficient manner that maintains hShh activity. This raises the possibility that the hShh-Scube complex is the active species that signals to responding cells. For example, Scube2 might interact with Ptch, a possibility suggested by our finding that the 5E1 antibody, which blocks hShh binding to Ptch does not block hShh binding to Scube2. Alternatively, Scube2 might interact with one of the hShh co-receptors Gas1, Cdo and Boc. Any such interaction could facilitate the delivery of hShh to responding cells.

While cholesterol modification of Hh and the role of Disp are conserved between invertebrates and vertebrates, Scube proteins are only present in vertebrates. How then do invertebrates secrete Hh? A likely possibility is that the role of Scube is fulfilled in invertebrates by another secreted protein or by lipoprotein particles. Lipoproteins have been implicated in systemic transport of Hh in Drosophila (Panakova et al., 2005). It is unclear, however, if

lipoproteins are present in the extracellular space of early embryonic tissues, and thus if they play a role in Hh signaling at that stage. A biochemical approach will be required to determine if a secreted protein and/or lipoproteins function in invertebrates in a manner similar to Scube in vertebrates.

The proposed mechanism of hShh secretion is reminiscent of cholesterol trafficking by the Niemann-Pick disease proteins NPC1 and NPC2 (Infante et al., 2008b), which are involved in the egress of cholesterol from late endosomes/lysosomes. Cholesteryl esters are hydrolyzed in the lumen of the lysosome, releasing free cholesterol that binds NPC2, a soluble luminal cholesterol-binding protein. NPC2 transfers cholesterol to NPC1, a multispanning membrane protein in the limiting membrane of the lysosome. Cholesterol is then released from NPC1 into the lysosomal membrane, followed by its transport to other cellular membranes, perhaps through the cytosolic face of the membrane.

A comparison of hShh secretion to cholesterol egress from lysosomes reveals similarities as well as some important differences. DispA and NPC1 are both members of the RND family of transporters, and DispA binds the cholesterol anchor of hShh as NPC1 binds cholesterol (Infante et al., 2008a). While there is no homology between Scube2 and NPC2, they localize to topologically equivalent spaces (the extracellular space for Scube2 and the lumen of the late endosome/lysosome for NPC2), and Scube2 binds the cholesterol anchor of hShh as NPC2 binds cholesterol (Infante et al., 2008b). Importantly, DispA and Scube2 recognize different aspects of the cholesterol molecule (Figure 3.7A), which parallels the two distinct binding modes of NPC1 and NPC2 to cholesterol (Kwon et al., 2009). However, while DispA appears to recognize the isooctyl tail of cholesterol, NPC1 binds cholesterol with the 3β-hydroxy buried and the isooctyl tail exposed (Kwon et al., 2009). Also, Scube2 appears to not bind the isooctyl tail of cholesterol,

while NPC2 binds the isooctyl tail (Kwon et al., 2009). Finally, one important difference is the direction of transport: DispA and Scube2 move hShh from the membrane to the extracellular space, while NPC1 and NPC2 transport cholesterol in reverse, from the lumen of the lysosome into the limiting membrane.

In summary, our results demonstrate a mechanism for hShh secretion that is reminiscent of the egress of free cholesterol from late endosomes/lysosomes. Both processes rely on the recognition of unique aspects of the cholesterol molecule and in both cases a similar mechanism is used to achieve solubility of the hydrophobic ligand. As mutations in NPC proteins cause disease, it seems possible that Disp and Scube could be involved in the pathogenesis of Hh signaling defects, such as those causing holoprosencephaly.

EXPERIMENTAL PROCEDURES

Chemicals

Synthesis of the two photoreactive sterols used in this study is described in the Supplemental Information.

Cell culture

Details of cell culture conditions, DNA constructs, immunofluorescence microscopy, pulse-chase assays, immunoprecipitation, and production of Scube2-conditioned media are provided in Supplemental Information. To determine if photoreactive sterols modify hShh in vivo, 293T cells stably expressing hShh-HA (Chen et al., 2011) were sterol-depleted with 1% methyl-β-cyclodextrin (MCD) in Dulbecco's Modified Eagle's Medium (DMEM) for 45

minutes. Sterols were then added back as soluble MCD complexes. After 3 hours, the cells were harvested and hShh processing was assayed by immunoblotting.

Photocrosslinking in cells

Human 293T cells stably expressing myc-tagged DispA and hShh constructs were sterol-depleted, followed by incubation with sterol-MCD complexes (75 μM for cholesterol and 25-azicholesterol, and 25 μM for 6-azicholestanol) in OptiMEM (Invitrogen), for 2 hours. After washing with OptiMEM, cells were incubated for 6 hours, followed by UV irradiation for 10 minutes on ice. The cells were harvested and DispA constructs were subjected to denaturing immunoprecipitation with anti-myc antibodies (9E10) followed by SDS-PAGE and immunoblotting with rabbit anti-hShhN antibodies (Cell Signaling). A similar protocol was used to detect interaction of hShh to HA-tagged Scube2 in cells.

Photocrosslinking in vitro

A fragment of Drosophila Hedgehog comprising amino acids 244-471 was expressed and purified from bacteria as a soluble maltose-binding protein (MBP) fusion (Chen et al., 2011), and was used to generate photoreactive sterol-modified MBP by in vitro processing. Sterol-modified MBP was incubated for 1 hour with HA-tagged Scube2 or Scube2ΔCUB, followed by UV irradiation for 10 minutes on ice. The samples were analyzed by SDS-PAGE and immunoblotting with HA antibodies.

Secretion assays

293T cells stably expressing hShh were washed several times with DMEM to remove serum, and were incubated in DMEM, with or without the indicated factors. At the indicated time, the culture medium was harvested and secreted protein was analyzed by either precipitation with trichloroacetic acid followed by SDS-PAGE and immunoblotting, or by Hh reporter assays.

Reporter assays

Hh activity was assayed in Shh Light II cells (Taipale et al., 2000). After incubation for 30 hours, firefly luciferase (expressed under control of a Hh-responsive promoter) and Renilla luciferase (expressed under control of a constitutive promoter) were measured using the Dual-Glo kit (Promega). Hh pathway activity was calculated as the firefly/Renilla ratio, normalized to 1 for unstimulated cells. Each experiment was performed in triplicate, and error bars represent standard deviation of the mean. For co-culture assays, 293T cells or DispA-/- MEFs expressing various hShh, DispA and Scube2 constructs were plated together with Shh Light II cells. After 12 hours, serum was washed off and the cells were incubated for 30 hours in serum-free media, followed by luciferase reporter assays.

ACKNOWLEDGEMENTS

We thank P. Beachy for DispA-/- mouse embryonic fibroblasts and T. Rapoport for critical reading of the manuscript. A.S. is supported in part by NIH grant RO1 GM092924. The authors declare no competing financial interests.

REFERENCES

Burke, R., D. Nellen, M. Bellotto, E. Hafen, K.A. Senti, B.J. Dickson, and K. Basler. 1999. Dispatched, a novel sterol-sensing domain protein dedicated to the release of cholesterol-modified hedgehog from signaling cells. *Cell*. 99:803-815.

Chamoun, Z., R.K. Mann, D. Nellen, D.P. von Kessler, M. Bellotto, P.A. Beachy, and K. Basler. 2001. Skinny hedgehog, an acyltransferase required for palmitoylation and activity of the hedgehog signal. *Science*. 293:2080-2084.

Chen, M.H., Y.J. Li, T. Kawakami, S.M. Xu, and P.T. Chuang. 2004. Palmitoylation is required for the production of a soluble multimeric Hedgehog protein complex and long-range signaling in vertebrates. *Genes Dev*. 18:641-659.

Chen, X., H. Tukachinsky, C.H. Huang, C. Jao, Y.R. Chu, H.Y. Tang, B. Mueller, S. Schulman, T.A. Rapoport, and A. Salic. 2011. Processing and turnover of the Hedgehog protein in the endoplasmic reticulum. *J Cell Biol*. 192:825-838.

Creanga, A., T.D. Glenn, R.K. Mann, A.M. Saunders, W.S. Talbot, and P.A. Beachy. 2012. Scube/You activity mediates release of dually lipid-modified Hedgehog signal in soluble form. *Genes Dev*. 26:1312-1325.

Grimmond, S., R. Larder, N. Van Hateren, P. Siggers, T.J. Hulsebos, R. Arkell, and A. Greenfield. 2000. Cloning, mapping, and expression analysis of a gene encoding a novel mammalian EGF-related protein (SCUBE1). *Genomics*. 70:74-81.

Hollway, G.E., J. Maule, P. Gautier, T.M. Evans, D.G. Keenan, C. Lohs, D. Fischer, C. Wicking, and P.D. Currie. 2006. Scube2 mediates Hedgehog signalling in the zebrafish embryo. *Dev Biol*. 294:104-118.

Infante, R.E., L. Abi-Mosleh, A. Radhakrishnan, J.D. Dale, M.S. Brown, and J.L. Goldstein. 2008a. Purified NPC1 protein. I. Binding of cholesterol and oxysterols to a 1278-amino acid membrane protein. *J Biol Chem*. 283:1052-1063.

Infante, R.E., M.L. Wang, A. Radhakrishnan, H.J. Kwon, M.S. Brown, and J.L. Goldstein. 2008b. NPC2 facilitates bidirectional transfer of cholesterol between NPC1 and lipid bilayers, a step in cholesterol egress from lysosomes. *Proc Natl Acad Sci U S A*. 105:15287-15292.

Johnson, J.L., T. Hall, J. Dyson, C. Sonntag, K. Ayers, S. Berger, P. Gautier, C. Mitchell, G.E. Hollway, and P.D. Currie. 2012. Scube activity is necessary for Hedgehog signal transduction in vivo. *Dev Biol*.

Kawakami, A., Y. Nojima, A. Toyoda, M. Takahoko, M. Satoh, H. Tanaka, H. Wada, I. Masai, H. Terasaki, Y. Sakaki, H. Takeda, and H. Okamoto. 2005. The zebrafish-secreted matrix

protein you/scube2 is implicated in long-range regulation of hedgehog signaling. *Curr Biol*. 15:480-488.

Kuwabara, P.E., and M. Labouesse. 2002. The sterol-sensing domain: multiple families, a unique role? *Trends Genet*. 18:193-201.

Kwon, H.J., L. Abi-Mosleh, M.L. Wang, J. Deisenhofer, J.L. Goldstein, M.S. Brown, and R.E. Infante. 2009. Structure of N-terminal domain of NPC1 reveals distinct subdomains for binding and transfer of cholesterol. *Cell*. 137:1213-1224.

Lum, L., and P.A. Beachy. 2004. The Hedgehog response network: sensors, switches, and routers. *Science*. 304:1755-1759.

Ma, Y., A. Erkner, R. Gong, S. Yao, J. Taipale, K. Basler, and P.A. Beachy. 2002. Hedgehog-mediated patterning of the mammalian embryo requires transporter-like function of dispatched. *Cell*. 111:63-75.

Mann, R.K., and P.A. Beachy. 2004. Novel lipid modifications of secreted protein signals. *Annu Rev Biochem*. 73:891-923.

Marigo, V., R.A. Davey, Y. Zuo, J.M. Cunningham, and C.J. Tabin. 1996. Biochemical evidence that patched is the Hedgehog receptor. *Nature*. 384:176-179.

Maun, H.R., X. Wen, A. Lingel, F.J. de Sauvage, R.A. Lazarus, S.J. Scales, and S.G. Hymowitz. 2010. Hedgehog pathway antagonist 5E1 binds hedgehog at the pseudo-active site. *J Biol Chem*. 285:26570-26580.

Motamed, M., Y. Zhang, M.L. Wang, J. Seemann, H.J. Kwon, J.L. Goldstein, and M.S. Brown. 2011. Identification of luminal Loop 1 of Scap protein as the sterol sensor that maintains cholesterol homeostasis. *J Biol Chem*. 286:18002-18012.

Nakano, Y., H.R. Kim, A. Kawakami, S. Roy, A.F. Schier, and P.W. Ingham. 2004. Inactivation of dispatched 1 by the chameleon mutation disrupts Hedgehog signalling in the zebrafish embryo. *Dev Biol*. 269:381-392.

Panakova, D., H. Sprong, E. Marois, C. Thiele, and S. Eaton. 2005. Lipoprotein particles are required for Hedgehog and Wingless signalling. *Nature*. 435:58-65.

Porter, J.A., K.E. Young, and P.A. Beachy. 1996. Cholesterol modification of hedgehog signaling proteins in animal development. *Science*. 274:255-259.

Taipale, J., J.K. Chen, M.K. Cooper, B. Wang, R.K. Mann, L. Milenkovic, M.P. Scott, and P.A. Beachy. 2000. Effects of oncogenic mutations in Smoothened and Patched can be reversed by cyclopamine. *Nature*. 406:1005-1009.

Thiele, C., M.J. Hannah, F. Fahrenholz, and W.B. Huttner. 2000. Cholesterol binds to synaptophysin and is required for biogenesis of synaptic vesicles. *Nat Cell Biol*. 2:42-49.

Traiffort, E., C. Dubourg, H. Faure, D. Rognan, S. Odent, M.R. Durou, V. David, and M. Ruat. 2004. Functional characterization of sonic hedgehog mutations associated with holoprosencephaly. *J Biol Chem*. 279:42889-42897.

Tsai, M.T., C.J. Cheng, Y.C. Lin, C.C. Chen, A.R. Wu, M.T. Wu, C.C. Hsu, and R.B. Yang. 2009. Isolation and characterization of a secreted, cell-surface glycoprotein SCUBE2 from humans. *Biochem J*. 422:119-128.

Tseng, T.T., K.S. Gratwick, J. Kollman, D. Park, D.H. Nies, A. Goffeau, and M.H. Saier, Jr. 1999. The RND permease superfamily: an ancient, ubiquitous and diverse family that includes human disease and development proteins. *Journal of molecular microbiology and biotechnology*. 1:107-125.

Woods, I.G., and W.S. Talbot. 2005. The you gene encodes an EGF-CUB protein essential for Hedgehog signaling in zebrafish. *PLoS biology*. 3:e66.

CHAPTER FOUR:

TRANSDUCTION OF THE HEDGEHOG SIGNAL

INSIDE THE PRIMARY CILIUM

The following section contains previously published material from:

Tukachinsky H, Lopez LV, Salic A. A mechanism for vertebrate Hedgehog signaling: recruitment to cilia and dissociation of SuFu-Gli protein complexes. *Journal of Cell Biology*. **191**(2):415-28 (2010).

Author contributions:
LV Lopez and I contributed to the manuscript equally. We performed the immunofluorescence experiments studying SuFu and Gli recruitment together. LV Lopez performed the RT-PCR experiments studying effects on downstream signaling. I carried out the biochemical experiments showing complex dissociation upon signal activation.

ABSTRACT

In vertebrates, Hedgehog (Hh) signaling initiated in primary cilia activates the membrane protein Smoothened (Smo) and leads to activation of Gli proteins, the transcriptional effectors of the pathway. In the absence of signaling, Gli proteins are inhibited by the cytoplasmic protein Suppressor of Fused (SuFu). It is unclear how Hh activates Gli and whether it directly regulates SuFu. We find that Hh stimulation quickly recruits endogenous SuFu-Gli complexes to cilia, suggesting a model in which Smo activates Gli by relieving inhibition by SuFu. In support of this model, we find that Hh causes rapid dissociation of the SuFu-Gli complex, thus allowing Gli to enter the nucleus and activate transcription. Activation of protein kinase A (PKA), an inhibitor of Hh signaling, blocks ciliary localization of SuFu-Gli complexes, which in turn prevents their dissociation by signaling. Our results support a simple mechanism in which Hh signals at vertebrate cilia cause dissociation of inactive SuFu-Gli complexes, a process inhibited by PKA.

INTRODUCTION

The Hedgehog (Hh) cell-cell signaling pathway is conserved in animals and has critical roles in embryonic development, in the maintenance of adult stem cells and in cancer (Huangfu and Anderson, 2006; Kalderon, 2005; Lum and Beachy, 2004; Rohatgi and Scott, 2007). In the resting state of Hh signaling, the transcriptional output of the pathway is kept off by the membrane protein Patched (Ptc), which inhibits the seven-spanner Smoothened (Smo) (Alcedo et al., 1996). The Hh pathway is activated when the secreted protein Hh binds and inactivates Ptc (Marigo et al., 1996; Stone et al., 1996),

thus relieving the inhibition exerted on Smo, which becomes active. Active Smo signals to the cytoplasm, leading to the activation of the zinc finger transcription factors that control the output of the Hh pathway, Cubitus interruptus (Ci) in Drosophila (Aza-Blanc et al., 1997; Ohlmeyer and Kalderon, 1998) and the Gli proteins (Gli1, 2, and 3) in vertebrates.

A unique feature of vertebrate Hh pathway is that primary cilia are essential for signal transduction (Huangfu and Anderson, 2005), and the initial membrane events occur at cilia. Ptc is located at the base of the primary cilium (Rohatgi et al., 2007), and binding of Hh to Ptc leads to activation and recruitment of Smo to the cilium (Corbit et al., 2005; Rohatgi et al., 2007). Through an unknown mechanism, active Smo at the cilium relays Hh signals to the cytoplasm, resulting in the activation of Gli2 and Gli3 (Lipinski et al., 2006; Ohlmeyer and Kalderon, 1998; Wang et al., 2000), which control transcription of Hh target genes (Alexandre et al., 1996; Dai et al., 1999; Ruiz i Altaba, 1998). Since the discovery that Ptc and Smo function at the vertebrate primary cilium, an important question has been to understand how signaling through these upstream components of the Hh pathway couples to activation of the downstream Gli proteins.

An early study showed that Gli proteins localize to cilia in vertebrate limb bud cells (Haycraft et al., 2005); however, the relationship between ciliary localization and the state of Hh signaling was not investigated. Recently, Gli2 and Gli3 were shown to be recruited to the tip of primary cilia upon Hh stimulation (Chen et al., 2009; Kim et al., 2009; Wen et al., 2010), consistent with the idea that activation of Gli2 and Gli3 by Hh signaling occurs at cilia; however, the mechanism by which Gli proteins are activated at cilia has not been clarified.

In the cytoplasm of unstimulated cells, two major negative regulators ensure that the vertebrate Hh pathway is kept off. The first negative regulator is the Gli-binding protein Suppressor of Fused (SuFu), which in vertebrates is essential for repressing Hh signaling: in cells lacking SuFu, the Hh pathway is maximally activated in a ligand-independent manner (Cooper et al., 2005; Svard et al., 2006). SuFu is thought to inhibit Gli proteins by preventing their nuclear translocation (Ding et al., 1999; Kogerman et al., 1999; Methot and Basler, 2000). Interestingly, constitutive activation of the Hh pathway in the absence of SuFu is independent of cilia (Jia et al., 2009), suggesting that Hh signaling at cilia may activate Gli proteins by inhibiting SuFu.

The second major negative regulator of Hh signaling is protein kinase A (PKA). In Drosophila, PKA phosphorylates Ci and loss of PKA leads to Hh pathway activation (Jiang and Struhl, 1995; Lepage et al., 1995; Li et al., 1995; Price and Kalderon, 1999), while overexpression of PKA inhibits Hh signaling (Li et al., 1995). The inhibitory effect of PKA is conserved in vertebrate Hh signaling (Concordet et al., 1996; Epstein et al., 1996) and, interestingly, depends on SuFu (Chen et al., 2009; Svard et al., 2006), suggesting that PKA might inhibit Gli proteins by modulating their interaction with SuFu.

Although SuFu is essential for inhibiting Gli in unstimulated cells, it is unclear if Hh signaling regulates SuFu. In one model, SuFu is a simple buffer for Gli, and is not regulated by Hh signaling. This model is consistent with a recent study (Chen et al., 2009), which found that Hh stimulation does not affect the interaction between overexpressed Gli2 and Gli3, and SuFu; however, the relevance of this result for normal Hh signaling is unclear, given the non-physiological levels of Gli and SuFu proteins

produced by transient transfection. In another model, Hh signaling at cilia activates Gli proteins by relieving SuFu inhibition, resulting in Gli nuclear translocation and transcriptional activation. This simple model is consistent with at least two findings: 1) the Hh pathway is constitutively active in SuFu-/- cells independent of cilia (Chen et al., 2009; Jia et al., 2009), suggesting that active Smo at cilia might signal by inhibiting SuFu; and 2) activation of PKA by forskolin inhibits signaling by active Smo in cells that have SuFu (Wu et al., 2004), but cannot block constitutive signaling caused by loss of SuFu (Chen et al., 2009; Svard et al., 2006), suggesting that Smo and PKA might exert their opposing effects on Hh signaling through SuFu.

To begin deciphering how active Smo at the cilium activates Gli proteins, we examined the behavior of endogenous SuFu, Gli2, and full-length Gli3 (Gli3-FL) in Hh-responsive mammalian cultured cells. Focusing on endogenous proteins avoided problems associated with misregulation of overexpressed proteins. Furthermore, we analyzed biochemically the effect of Hh signaling on endogenous SuFu-Gli protein complexes, after brief Hh pathway stimulation, to avoid any confounding secondary effects due to prolonged pathway stimulation. Our results complement and extend the findings of a recent study (Humke et al., 2010) that described how Hh signaling leads to the dissociation of SuFu from Gli. Specifically, our study demonstrates that Hh stimulation through active Smo leads to the recruitment of endogenous SuFu-Gli complexes to cilia, and causes the rapid dissociation of a defined SuFu-Gli complex. Activation of PKA blocks localization of SuFu-Gli complexes to cilia and inhibits their dissociation by Smo, providing an explanation for how PKA inhibits Hh signaling: by uncoupling Smo activation from dissociation of SuFu-Gli complexes. We propose that

vertebrate Hh signals are transduced by active Smo at the primary cilium by dissociating inhibitory SuFu from Gli, and that a protein complex that likely contains only SuFu and Gli forms the core of vertebrate Hh signal transduction downstream of Smo.

RESULTS

Hedgehog stimulation quickly recruits endogenous SuFu and Gli proteins to the cilium

Tagged SuFu and Gli proteins localize to primary cilia in vertebrate cells (Haycraft et al., 2005). To study the subcellular dynamics of SuFu and Gli during Hh signaling and to avoid expressing proteins at non-physiological levels, we raised polyclonal antibodies that specifically detect endogenous mouse SuFu, Gli2, and Gli3 in Hh-responsive cells (Supplemental Figure 4.S1). We first used these antibodies to examine how Sonic hedgehog (Shh) stimulation affects subcellular localization of endogenous SuFu, Gli2 and Gli3-FL (Figure 4.1A). Without Shh stimulation, low levels of SuFu, Gli2, and Gli3-FL were detected at cilia in NIH-3T3 cells and in MEFs; in contrast, Smo was absent from cilia in the absence of Shh stimulation (Figure 4.1A, B; see also Supplementary Table 4.1 for SuFu, Gli, and Smo behavior in all cell lines used in this study). Hh stimulation led to the dramatic increase in the localization of SuFu, Gli2, and Gli3-FL to cilia (Figure 4.1A), similar to that recently reported for endogenous or overexpressed Gli2 and Gli3 (Chen et al., 2009; Kim et al., 2009; Wen et al., 2010) and paralleling the recruitment of Smo to cilia (Rohatgi et al., 2007). Previous studies (Chen et al., 2009) failed to detect a signal-dependent recruitment of SuFu to cilia; one reason for this discrepancy might be that our antibodies are more sensitive than the

commercial antibodies used for SuFu detection. Our other findings (that SuFu and Gli form a complex and that SuFu localization to cilia is strictly dependent on Gli – see below) are consistent with the Hh-stimulated recruitment of SuFu to cilia that we observed.

Recruitment of SuFu, Gli2, Gli3-FL and Smo was very rapid: strong ciliary localization of all these proteins was seen in as little as 30 minutes after addition of Shh to cells. The number of cilia positive for SuFu, Gli2, Gli3-FL and Smo continued to increase with time (Figure 4.1B). We conclude that, although low amounts of SuFu and Gli proteins are present at cilia in unstimulated cells, the ciliary levels of these proteins quickly rise upon Hh stimulation.

SuFu, Gli2, and Gli3-FL show very similar "comet tail" patterns at the cilium, with the highest accumulation at the distal tip (Figure 4.1C). This pattern is different from that of Smo, which localizes along the entire length of the cilium, often at higher level towards its base (Figure 4.1A, C). Identical results were obtained when the Hh pathway was activated by the oxysterols 20-hydroxycholesterol (20-OHC) and 25-hydroxycholesterol (25-OHC) (Corcoran and Scott, 2006; Dwyer et al., 2007) (Supplemental Figure 4.S2A), as well as by the synthetic Smo activator, SAG (Chen et al., 2002; Frank-Kamenetsky et al., 2002) (Figure 4.1D).

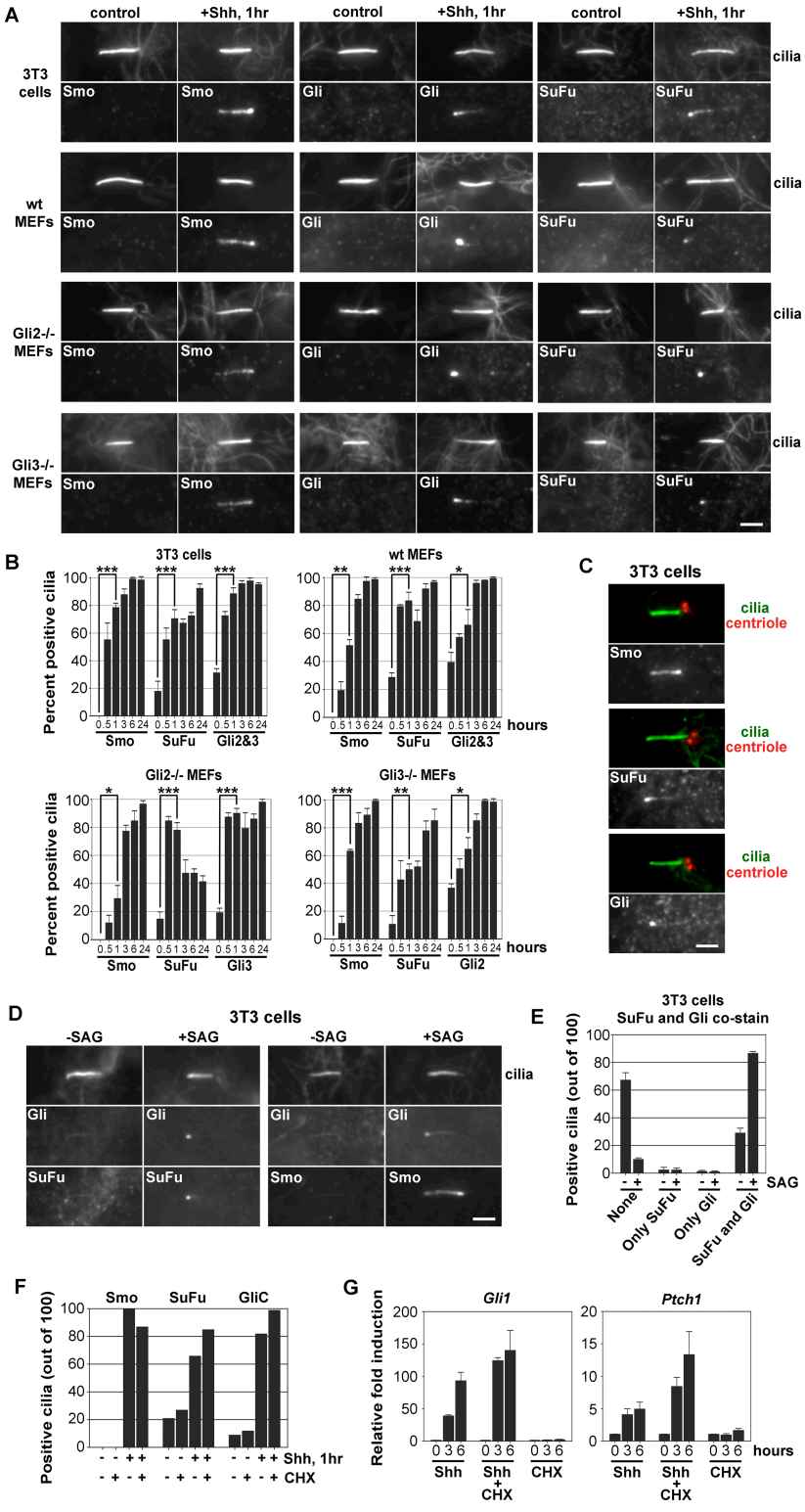

Figure 4.1 Endogenous SuFu is rapidly recruited to primary cilia by Hh signaling, paralleling recruitment of endogenous Smo, Gli2 and full-length Gli3 (Gli3-FL).

Figure 4.1 (Continued)
A) Fluorescence micrographs of cilia from untreated cells or cells treated with Shh. Cilia were detected by staining against acetylated tubulin. Since the anti-GliC antibody detects both Gli2 and Gli3-FL, Gli2-/- and Gli3-/- mouse embryonic fibroblasts (MEFs) are shown to demonstrate ciliary recruitment of Gli2 and Gli3-FL separately. In all panels, the tip of the cilium points to the left. Scale bar is 2 μm.
B) Cells were treated with Shh for varying amounts of time, and ciliary recruitment of SuFu, Smo, Gli2 and Gli3-FL was determined. Data shown are mean ± SD for three independent counts. Asterisks indicate P value for ciliary recruitment at one hour, compared to t=0 (one asterisk $P<0.05$, two asterisks $P<0.01$, three asterisks $P<0.001$). $P<0.05$ for all later time points.
C) In NIH-3T3 cells stimulated with Shh for 1 hr, SuFu and Gli proteins localize at the tip, while Smo localizes along the length of cilia. Cilia were stained as in (A) and centrioles were stained with anti-γ-tubulin.
D) Endogenous SuFu and Gli proteins co-localize at the tips of primary cilia in SAG-treated NIH-3T3 cells. Left panels: cilia co-stained for endogenous SuFu (rabbit antibody) and Gli (goat antibody). Right panels: cilia co-stained for Smo (rabbit antibody) and Gli (goat antibody).
E) Cilia counts for the experiment in (D), left panels. Endogenous SuFu and Gli co-localize, both in the resting and the stimulated states of the Hh pathway.
F) Recruitment of SuFu, Smo, and Gli to cilia in response to Hh stimulation does not require new protein synthesis. Ciliary localization was determined in NIH-3T3 cells treated or not with Shh, in the presence or absence of cycloheximide (CHX).
G) Inhibition of protein synthesis does not block the transcriptional output of the Hh pathway. Transcription of the direct transcriptional targets, Gli1 and Ptch1 was assayed by Q-PCR after 3 and 6 hours of stimulation with Shh, in the presence or absence of CHX.

The similar localization pattern of SuFu and Gli at the tips of cilia, and the fact that SuFu binds Gli proteins (Pearse et al., 1999) suggests that SuFu and Gli likely localize to the cilium as a complex. Co-staining for endogenous SuFu and Gli (using a goat anti-Gli antibody, Supplemental figure 4.S1E) shows identical patterns at cilia (Figure 4.1D); furthermore, SuFu and Gli always appear together in cilia, both in the unstimulated and stimulated states of Hh signaling (Figure 4.1E). We thus propose that Hh stimulation quickly recruits SuFu-Gli complexes to cilia, suggesting that the molecular species to which the signal from active Smo is relayed might be the SuFu-Gli complex.

Recruitment of endogenous SuFu and Gli proteins to the cilium does not require new protein synthesis

Although the rapid recruitment of SuFu, Gli and Smo suggests that it represents an immediate response to Hh activation, results from Drosophila cultured cells showed that protein synthesis is required for certain aspects of Hh signal transduction (Lum et al., 2003). In contrast to Drosophila cells, we find that in Shh-stimulated NIH-3T3 cells, inhibiting protein synthesis does not block the recruitment of endogenous SuFu, Gli, and Smo to cilia (Figure 4.1F and Supplemental Figure 4.S2B, C) or the transcriptional activation of Hh target genes (Figure 4.1G). Also in contrast to Drosophila cells, we did not observe any change in the electrophoretic mobility of SuFu or SuFu levels upon stimulation of the Hh pathway in NIH-3T3 cells or in MEFs (Supplemental Figure 4.S4A, B). Recruitment of SuFu and Gli protein to cilia is thus an immediate response to Hh stimulation.

Uncoupling ciliary recruitment of SuFu and Gli from the transcriptional response to Hh signaling: the role of dynamic microtubules

Recruitment of SuFu, Gli and Smo to cilia upon Shh stimulation is not affected when microtubules (MTs) are depolymerized with nocodazole (Noc, Supplemental Figure 4.S2D, E), suggesting that these proteins do not need dynamic MTs to arrive at the ciliary base. Noc does not disrupt the stable MTs of primary cilia (Supplemental Figure 4.S2F), suggesting that in the presence of Noc, motors such as Kif3a (Kovacs et al., 2008) and Kif7 (Cheung et al., 2009; Endoh-Yamagami et al., 2009; Liem et al., 2009), which were implicated in Hh signaling, can still move along ciliary MTs, explaining the

proper SuFu, Gli and Smo localization to cilia. Interestingly, Noc inhibits Hh transcriptional responses in a dose-dependent manner (Supplemental Figure 4.S2G). Thus dynamic MTs are not required for recruitment of SuFu, Gli and Smo to cilia, but are required for the transcriptional output of the pathway. We speculate that dynamic MTs are required downstream of ciliary events, such as the transport of Gli from cilia to the nucleus (Humke et al., 2010; Kim et al., 2009).

Active Smo is required for the recruitment and continued maintenance of SuFu and Gli to cilia

Low levels of SuFu and Gli localize to cilia even in unstimulated cells, and do not require Smo, as seen in Smo-/- MEFs (Supplemental Figure 3-S3A). Shh stimulation of Smo-/- MEFs does not increase ciliary SuFu and Gli, indicating that signal-dependent recruitment of SuFu and Gli requires Smo.

Active Smo translocates to cilia during normal Hh signaling, but inactive Smo can be pharmacologically forced to localize to cilia with the Smo inhibitor cyclopamine (Cyc) (Rohatgi et al., 2009; Wang et al., 2009; Wilson et al., 2009). Thus Smo might recruit SuFu and Gli to cilia irrespective of its activation state; alternatively, only active Smo recruits SuFu and Gli. To distinguish between these two alternatives, we compared SuFu, Gli and Smo localization in cells treated with SAG (Chen et al., 2002; Frank-Kamenetsky et al., 2002) or Cyc (Taipale et al., 2000). While both SAG and Cyc recruited Smo to cilia, SuFu and Gli were recruited only by SAG but not by Cyc (Figure 4.2A-C), demonstrating that only active Smo recruits SuFu and Gli to cilia.

We next asked if maintaining high levels of SuFu and Gli in cilia is continuously dependent on active Smo. We first activated Hh signaling by addition of Shh, followed by Smo inhibition with Cyc; in this manner, Smo is inactivated without changing its ciliary localization. When Smo, SuFu, and Gli were recruited to cilia by Shh stimulation, addition of Cyc caused the levels of SuFu and Gli at the cilium to drop, while levels of Smo continued to rise (Figure 4.2D). Similar kinetics for the exit of SuFu and Gli from cilia were seen when cells were first stimulated with Shh, followed by Smo inhibition with the small molecule inhibitor, SANT-1 (Figure 4.2E). Smo inhibited by SANT-1 exited cilia more rapidly than SuFu and Gli proteins. Taken together, these experiments demonstrate that active Smo at cilia is required for maintaining high levels of SuFu and Gli at cilia during Hh signaling.

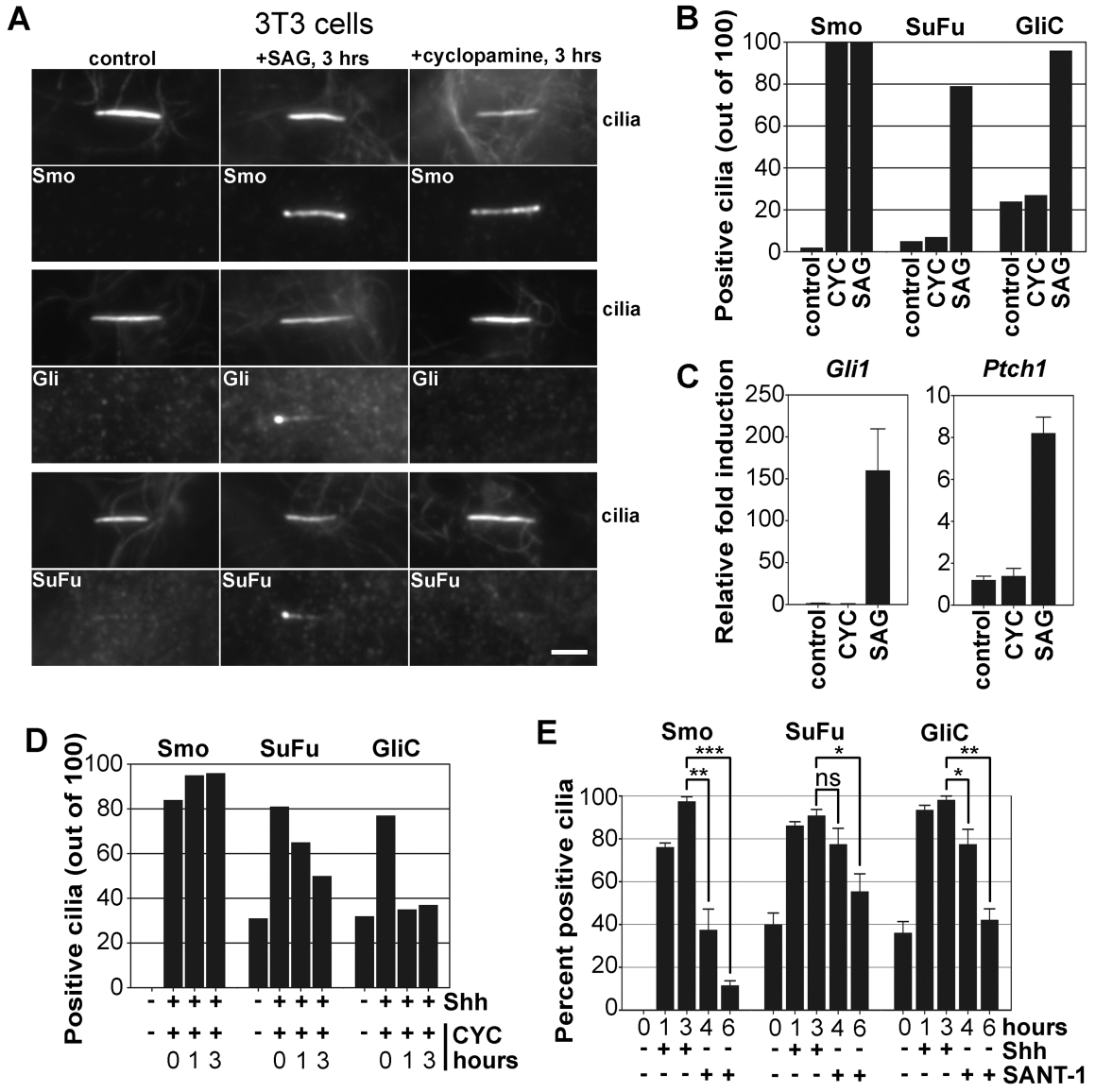

Figure 4.2 Hh-dependent recruitment of SuFu and Gli proteins to cilia requires active Smo.
A) NIH-3T3 cells were treated with the Smo agonist, SAG, or with the antagonist cyclopamine (Cyc). SuFu and Gli are recruited to cilia by SAG but not by Cyc, although both SAG and Cyc recruit Smo to cilia. In all panels, the tips of cilia point to the left. Scale bar is 2 μm.
B) Cilia counts for the experiment in (A).
C) Q-PCR assay of Hh pathway target genes for the experiment in (A).
D) Maintaining increased levels of SuFu and Gli at cilia is continuously dependent on active Smo. Cyc was added in the presence of Shh to NIH-3T3 cells, pre-stimulated with Shh for 3 hours. Ciliary localization was determined before and after 3 hours of Shh stimulation, and after 1 and 3 hours following Cyc addition.
E) NIH-3T3 cells were stimulated with Shh for 3 hrs, followed by incubation with the Smo antagonist, SANT-1 for 3 hrs. Ciliary localization of SuFu, Gli and Smo was measured at the indicated times. P values were all less than 0.002 for the recruitment of Smo, SuFu and Gli by Shh stimulation. P values for exit from the cilium were calculated relative to ciliary localization after 3 hrs of Hh stimulation. Asterisks indicate the P value for ciliary exit (one asterisk $P<0.05$, two asterisks $P<0.01$, three asterisks $P<0.001$, ns – not significant).

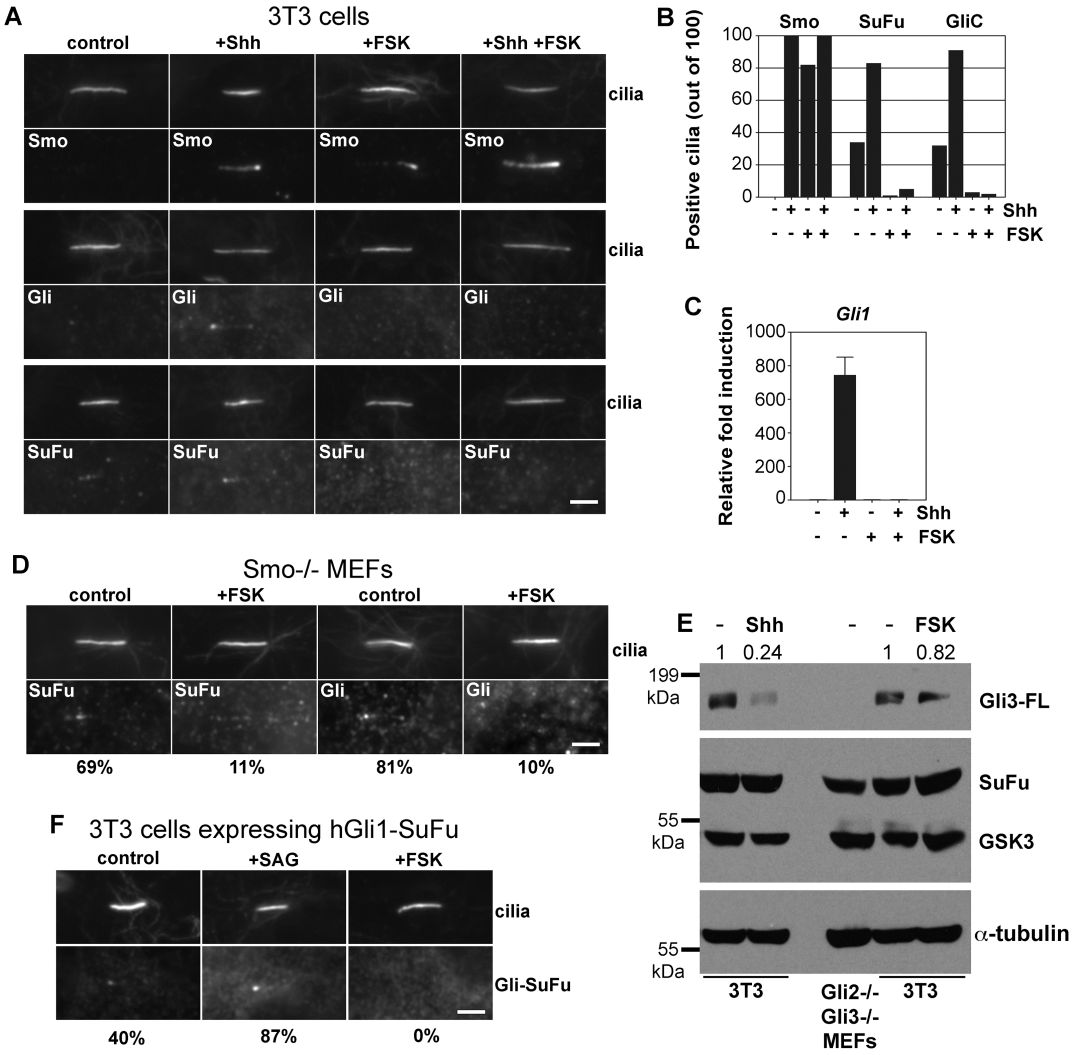

Figure 4.3 Localization of endogenous SuFu and Gli to cilia is antagonized by protein kinase A (PKA).

A) Activation of PKA by forskolin (FSK) blocks localization of endogenous SuFu and Gli proteins to cilia. NIH-3T3 cells were treated with or without Shh and FSK. Shh, FSK, or Shh and FSK recruit Smo to the cilium; in contrast, endogenous SuFu and Gli are removed from cilia by FSK, both in the presence and absence of Shh stimulation. Scale bar is 2 μm.

B) Cilia counts for the experiment in (A).

C) Q-PCR analysis of the experiment in (A). Inhibition of SuFu and Gli ciliary localization by FSK correlates with complete inhibition of the transcriptional output of the Hh pathway.

D) FSK inhibits localization of SuFu and Gli to primary cilia in Smo-/- MEFs. The percentages under the bottom panels indicate corresponding ciliary counts.

E) NIH-3T3 cells were incubated with or without Shh (the two left-most lanes), or with or without FSK (the two right-most lanes), followed by immunoblotting for SuFu, Gli3-FL, GSK3 and α-tubulin. The numbers above the top panel indicate levels of Gli3-FL in each lane, relative to α-tubulin. FSK treatment causes only a slight reduction in Gli3-FL, much smaller than the decrease caused by Shh.

F) NIH-3T3 cells stably expressing a Gli1-SuFu fusion were incubated with control media, SAG, or FSK. The Gli1-SuFu fusion localizes to cilia in unstimulated cells and its localization is increased by SAG. FSK treatment completely blocks ciliary localization of the Gli1-SuFu fusion. Percentages below the lower panels indicate ciliary localization of the fusion.

Activation of protein kinase A (PKA) blocks ciliary trafficking of endogenous SuFu and Gli

PKA is a negative regulator of the Hh pathway and forskolin (FSK), which activates PKA, is a potent inhibitor of Hh signaling. Recently, FSK was shown to recruit Smo to the cilium without activation of Hh signaling (Wilson et al., 2009). Interestingly, FSK treatment abolishes the ciliary localization of SuFu and Gli in both unstimulated and Shh-stimulated cells (Figure 4.3A and B), correlating with a complete inhibition of the transcriptional response to Hh stimulation (Figure 4.3C). We next asked if the effect of FSK on SuFu and Gli localization to cilia depends on Smo. SuFu and Gli localize to the tips of cilia in Smo-/- MEFs (Supplemental Figure 4.S3A), and FSK causes a strong decrease in ciliary SuFu and Gli (Figure 4.3D), demonstrating that FSK prevents SuFu-Gli ciliary localization independently of Smo.

One possible explanation for the dramatic inhibition of SuFu-Gli localization to cilia by FSK is an increased degradation of Gli proteins; indeed, FSK promotes partial proteolysis of overexpressed Gli2 and Gli3-FL (Pan et al., 2006; Wang and Li, 2006). In cells treated with FSK, endogenous SuFu levels do not change, and Gli3-FL levels decrease only modestly (much less than the decrease caused by Shh stimulation, figure 3E), demonstrating that absence of SuFu-Gli from cilia in the presence of FSK is not due to degradation of SuFu or Gli proteins. Another explanation is that FSK blocks ciliary localization of the SuFu-Gli complex by promoting its dissociation. We excluded this possibility using 3T3 cells stably expressing a direct fusion between Gli1 and SuFu, in which FSK completely abolishes ciliary localization of the fusion (Figure 4.3F), without significantly affecting its expression level (Supplemental Figure 4.S3B). This effect of

FSK is mediated by PKA, as it is reversed by the small molecule inhibitor of PKA, H-89 (Supplemental Figure 4.S3C). Furthermore, in FSK-treated cells, binding between endogenous SuFu and Gli3-FL is unaffected (Figure 4.5I). We conclude that activation of PKA by FSK blocks ciliary trafficking of the SuFu-Gli complex, providing a pharmacological means for uncoupling recruitment of Smo to cilia from that of the SuFu-Gli complex.

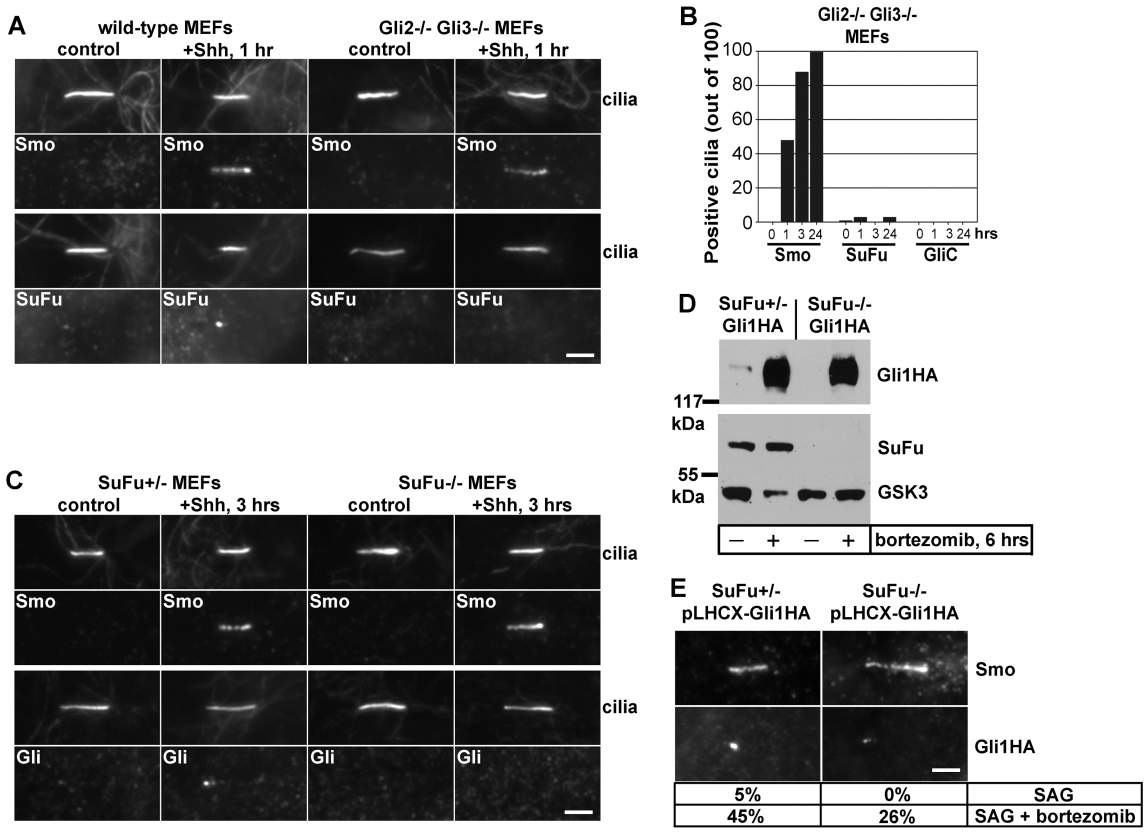

Figure 4.4 Gli proteins are required to localize SuFu to cilia but Gli proteins can localize to cilia in the absence of SuFu

A) Wild-type and Gli2-/- Gli3-/- MEFs were incubated with or without Shh. SuFu does not localize to cilia, with or without Shh stimulation in Gli2-/- Gli3-/- MEFs, while Smo recruitment is normal. Scale bar is 2 μm.

B) Cilia counts for a time course of ciliary recruitment of Smo, SuFu, and Gli in Gli2-/- Gli3-/- MEFs stimulated with Shh.

C) SuFu+/- and SuFu-/- MEFs were stimulated or not with Shh. Endogenous Gli proteins do not localize to cilia, with or without Shh stimulation, in the absence of SuFu. Recruitment of Smo is normal.

Figure 4.4 (Continued)
D) Immunoblot of SuFu-/- and SuFu+/- MEFs, stably expressing HA-tagged Gli1 (Gli1HA) and treated with the proteasome inhibitor bortezomib. Proteasome inhibition allows SuFu-/- cells to accumulate Gli1HA to levels similar to those in the control SuFu+/- cells.
E) Stably expressed Gli1HA localizes to ciliary tips in SuFu-/- MEFs stimulated with SAG, in the presence of bortezomib. Percentages below the lower panels indicate corresponding ciliary counts.

Gli proteins are required to recruit SuFu to cilia but Gli proteins can localize to cilia in the absence of SuFu

Since SuFu and Gli interact, we asked if they require each other for ciliary localization, by examining localization of Gli and SuFu in MEFs lacking SuFu and Gli proteins, respectively. Gli proteins are necessary for SuFu localization to cilia: in Gli2-/- Gli3-/- MEFs (Lipinski et al., 2006), SuFu is completely absent from cilia, with or without Shh stimulation (Figure 4.4A and B), although SuFu levels are normal (Supplemental Figure 4.S4A); this excludes SuFu degradation as causing its absence from cilia in cells without Gli2 and 3. Importantly, Smo recruitment to cilia was normal in Gli2-/- Gli3-/- MEFs (Figure 4.4A and B), showing that ciliary transport and upstream Hh signaling were intact in these cells, and that localization of Smo to cilia does not depend on SuFu and Gli proteins. Either Gli2 or Gli3 is sufficient to localize SuFu to cilia, as seen in Gli2-/- and Gli3-/- MEFs (Figure 4.1A and B). Taken together, these findings argue in favor of the recruitment of SuFu-Gli2 and SuFu-Gli3 complexes to cilia.

We next asked if, conversely, SuFu is required for localizing Gli proteins to cilia. In SuFu-/- MEFs, Gli proteins do not localize to cilia, with or without Shh stimulation, although Smo recruitment is normal (Figure 4.4C and Supplemental Figure 4.S3D). Localization of Gli to cilia was restored by stable expression of SuFu in SuFu-/- MEFs (Supplemental Figure 4.S3E). One explanation for the absence of Gli proteins from cilia

in SuFu-/- cells is the dramatically reduced Gli levels in the absence of SuFu (Chen et al., 2009; Ohlmeyer and Kalderon, 1998). Indeed, in SuFu-/- MEFs, Gli3-FL is dramatically decreased compared to SuFu+/- MEFs (Supplemental Figure 4.S3F), and pharmacological inhibition of the proteasome only partially rescues Gli3-FL levels. To overcome the instability of Gli proteins, we generated SuFu-/- cells stably overexpressing HA-tagged Gli1 (Gli1HA), which we stabilized by proteasomal inhibition with bortezomib. This treatment allowed Gli1HA to accumulate in SuFu-/- MEFs to levels similar to those in the SuFu+/- MEFs (Figure 4.4D). Under these conditions, some Gli1HA can be detected in cilia of SuFu-/- MEFs (Figure 4.4E), demonstrating that at least Gli1 can localize to cilia in the absence of SuFu, as demonstrated for transiently transfected Gli proteins (Chen et al., 2009). In SuFu-/- cells, Gli1HA was concentrated in the nucleus, while in SuFu+/- cells it was excluded from the nucleus (Supplemental Figure 4.S3G), consistent with the proposed mechanism of SuFu inhibition by sequestering Gli proteins in the cytoplasm (Ding et al., 1999; Kogerman et al., 1999; Methot and Basler, 2000). Nuclear accumulation of Gli1 in the absence of SuFu might also explain why ciliary levels of Gli1HA in SuFu-/- cells were lower than in SuFu+/- cells expressing comparable amounts of Gli1HA (Figure 4.4E).

Hh stimulation causes the rapid disappearance of a defined SuFu-Gli complex

Our cellular studies of endogenous SuFu and Gli proteins suggested that active Smo at cilia relays the signal to cytoplasmic SuFu-Gli complexes. As SuFu blocks nuclear import of Gli proteins, the major mechanistic question is how active Smo at the cilium modifies the SuFu-Gli complex to allow Gli activation and nuclear entry. Since

Hh signaling can occur in the absence of new protein synthesis (Figure 4.1F, G), we hypothesized that signaling must regulate SuFu-Gli complexes posttranslationally. To identify possible changes in endogenous SuFu-Gli complexes caused by Hh stimulation, we turned to measuring the size of native protein complexes by sucrose gradient centrifugation (Martin and Ames, 1961) of cellular lysates. Since prolonged Hh signaling causes a decrease in the level of Gli proteins (Supplemental Figure 4.S4A-C), we examined the effect of brief Hh stimulation (1-1.5 hours). Given that SuFu and Gli proteins are recruited to cilia within 30 minutes or less, we reasoned that such a brief period of pathway activation should be sufficient to observe changes in SuFu-Gli complexes.

NIH-3T3 cells were stimulated or not with Shh for 1 hour, after which they were lysed and SuFu was analyzed by sucrose gradient centrifugation. The majority of endogenous SuFu (MW=54 kDa) migrates as a small molecular weight peak (Figure 5A), similar in size and shape to the peak of glycogen synthase kinase 3 (GSK3, MW=47 kDa). This hydrodynamic behavior indicates that most SuFu in cells is present as a monomer. In untreated cells, a small fraction of SuFu appears in fractions of higher Stokes radius (Figure 4.5A, top panel), consistent with SuFu associating with other proteins. Stimulating cells with Shh for 1 hour causes the dramatic decrease of the higher molecular weight SuFu (Figure 4.5A, middle panel), an effect that is completely reversed by the small molecule Smo inhibitor, SANT1 (Figure 4.5A, bottom panel). In another experiment, a 1.5-hour stimulation of NIH-3T3 cells with the Smo agonist, SAG, causes the complete disappearance of the high molecular weight SuFu complex (Figure 4.5E, F).

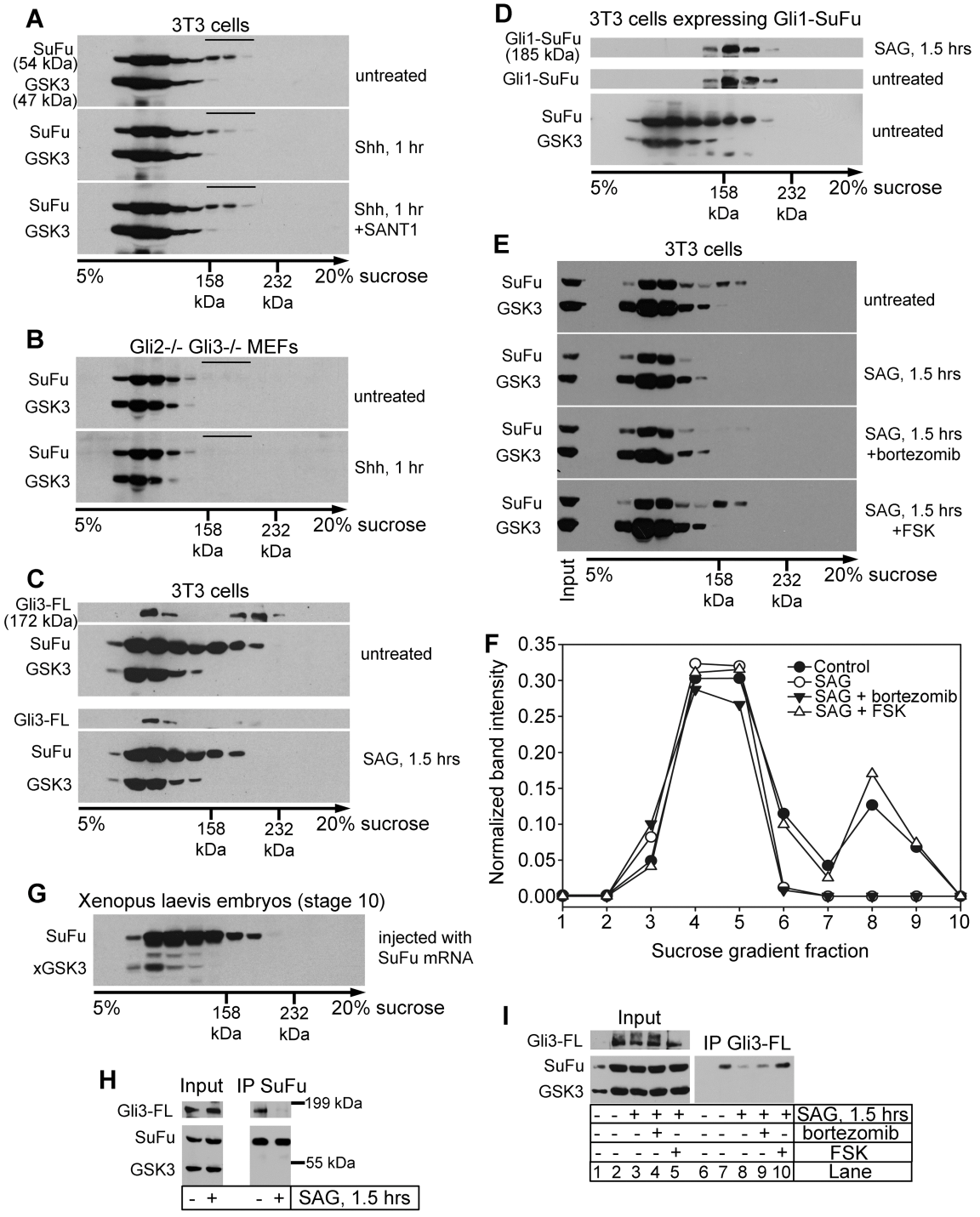

Figure 4.5 Biochemical evidence that Hh pathway activation causes rapid dissociation of endogenous SuFu-Gli complexes.
Endogenous SuFu-Gli complexes were analyzed by sucrose gradient centrifugation (A-G) and by immunoprecipitation (H, I).

Figure 4.5 (Continued)
A) In untreated NIH-3T3 cells, the majority of endogenous SuFu (MW=54 kDa) exists as a monomer, of similar size as the kinase GSK3β (MW=47 kDa). A small fraction of SuFu from untreated cells forms a higher molecular weight complex (top panel, overlined in black), the level of which quickly drops in cells treated with Shh for 1 hour (middle panel), an effect completely blocked if Smo is inhibited with SANT-1 (200 nM, bottom panel). The position in the gradient of two size markers run in parallel is shown below the Western blots: aldolase, MW= 158 kDa, Stokes radius=48.1 Angstrom; and catalase, MW=232 kDa, Stokes radius=52.2 Angstrom.
B) In Gli2-/- Gli3-/- MEFs, only the monomeric SuFu peak is seen by sucrose gradient centrifugation. Hh stimulation of Gli2-/- Gli3-/- MEFs does not change the size of the SuFu peak, although Smo is recruited to the cilia normally in these cells.
C) As in (A) but cells were stimulated or not with SAG and sucrose gradient fractions were immunoblotted for endogenous SuFu, GSK3, and Gli3-FL. The higher molecular weight SuFu peak overlaps with endogenous Gli3-FL in unstimulated cells. Acute Hh pathway stimulation causes the simultaneous disappearance of the overlapping, higher molecular weight SuFu and Gli3-FL peaks.
D) To prevent dissociation of SuFu from Gli, a direct fusion of Gli1 to SuFu was generated. NIH-3T3 cells stably expressing this Gli1-SuFu fusion were stimulated or not with SAG. The apparent size of the Gli1-SuFu fusion peak does not change upon Hh pathway activation.
E) Treatment of NIH-3T3 cells with SAG causes complete disappearance of the SuFu-Gli complex, which is not reversed by inhibition of the proteasome with bortezomib. In contrast, activation of PKA with forskolin (FSK) completely blocks SuFu-Gli dissociation induced by SAG stimulation.
F) Quantification of the experiment in (E). The amount of SuFu in each fraction was measured relative to the amount of SuFu in the input lane. The first fraction represents the top of the sucrose gradient.
G) Mouse SuFu expressed in Xenopus embryos shows the same size distribution as endogenous SuFu in mammalian cultured cells, suggesting that SuFu forms a similar complex with endogenous Gli proteins in Xenopus embryos.
H) NIH-3T3 cells were incubated with or without SAG, followed by immunoprecipitation with anti-SuFu antibodies. The level of Gli3-FL is similar in SAG-treated and in untreated cells (left panels). Gli3-FL co-immunoprecipitates with SuFu only in untreated cells but not in SAG-stimulated cells (right panels), indicating that acute Hh pathway activation dissociates endogenous Gli3-FL from SuFu.
I) NIH-3T3 cells were incubated with control media, SAG, SAG and bortezomib, and SAG and FSK, followed by immunoprecipitation with anti-Gli3-FL antibodies. Gli2-/-Gli3-/- MEFs were used as negative control (lanes 1 and 6). Endogenous SuFu does not co-immunoprecipitate with Gli3-FL in cells stimulated with SAG, although levels of Gli3-FL decrease only slightly. Proteasome inhibition by bortezomib (sufficient to abolish any decrease in the level of Gli3-FL) does not block dissociation of endogenous SuFu from Gli3-FL. In contrast, SAG-induced dissociation of SuFu from Gli3-FL is completely blocked by FSK.

Two lines of evidence demonstrate that the high molecular weight SuFu species is a SuFu-Gli complex: 1) The SuFu complex is absent from Gli2-/- Gli3-/- MEFs (Lipinski et al., 2006), in which only monomeric SuFu is seen on sucrose gradients (Figure 5B, top panel). This also indicates that SuFu is dedicated to binding Gli proteins and, in their absence, SuFu does not stably associate with other proteins. Additionally, the size of endogenous SuFu in Gli2-/- Gli3-/- cells does not change upon Hh pathway stimulation (Figure 4.5B, bottom panel), indicating that signaling specifically couples to SuFu-Gli complexes and not to monomeric SuFu. 2) The high molecular weight SuFu complex

overlaps with a Gli3-FL peak (Figure 5C, top panel), and Hh stimulation causes the simultaneous disappearance of the high molecular weight SuFu and Gli3-FL peaks (Figure 4.5C, bottom panel). Taken together, these data demonstrate that Hh stimulation causes the quick disappearance of the SuFu-Gli complex.

Although we do not know the shape of the SuFu-Gli complex and thus cannot determine its exact size, its migration on sucrose gradients is consistent with the calculated size of a 1:1 complex (54+172=226 kDa for a mouse SuFu-Gli3-FL complex), suggesting that the complex might contain only one molecule of SuFu and Gli3-FL. To examine if SuFu behavior is conserved in other vertebrate systems, we determined the sucrose gradient profile of SuFu expressed in Xenopus embryos (Figure 4.5G), and found it very similar to that in NIH-3T3 cells, suggesting that SuFu forms complexes of a similar size with endogenous Gli proteins in Xenopus embryos.

The SuFu-Gli complex dissociates in response to Hh signaling

We considered two possibilities for the mechanism underlying the disappearance of the SuFu-Gli complex in response to Hh stimulation: 1) the SuFu-Gli complex disappears through proteolysis, either of SuFu or Gli; and 2) the SuFu-Gli complex disappears due to dissociation. Our results support the idea that Hh stimulation causes the dissociation of the SuFu-Gli complex.

A recent study suggested that Hh signaling triggers the proteasomal degradation of SuFu in certain cancer cells (Yue et al., 2009). We find that in NIH-3T3 cells, neither the steady-state level nor the half-life of SuFu changes upon Shh stimulation (Supplemental Figure 4.S4A-E), suggesting that Hh signaling does not affect bulk SuFu

levels or stability. It is, however conceivable that Hh signaling might stimulate degradation of the small fraction of SuFu in SuFu-Gli complexes, but that the size of this pool is too small to detect. We excluded this possibility by blocking proteasomal degradation with the small molecule, bortezomib (see below).

The levels of both Gli3-FL and Gli3-R (Supplemental Figure 4.S4A-C), and the half-life of Gli3-FL (Supplemental Figure 4.S4D, E) decrease following Hh pathway activation; it is thus possible that the disappearance of the SuFu-Gli complex reflects the increased turnover of Gli caused by Hh signaling. The following results show that SuFu-Gli dissociation and not Gli degradation is responsible for the disappearance of the SuFu-Gli complex: 1) the SuFu-Gli complex disappears after as little as 1.5 hours of SAG stimulation, which has little or no effect on Gli3-FL levels (Figure 4.5H and I); 2) the SuFu-Gli complex disappears even when the proteasome is blocked with high levels of bortezomib (Figure 4.5E, F and I), which are sufficient to completely block Gli3-FL degradation (see also Supplemental Figure 4.S4B); and 3) if dissociation is prevented by fusing SuFu and Gli1, the size of the stably expressed covalent SuFu-Gli1 complex no longer changes in response to Hh stimulation (Figure 4.5D).

Finally, we used immunoprecipitation of endogenous SuFu and Gli3-FL from 3T3 cells to demonstrate dissociation of SuFu-Gli3-FL by Hh stimulation. The amount of Gli3-FL immunoprecipitated with SuFu from stimulated cells is dramatically reduced compared to untreated cells, although total Gli3-FL levels do not change appreciably during the 1.5 hour stimulation time (Figure 4.5H). Conversely, the amount of SuFu immunoprecipitated with Gli3-FL is greatly decreased following acute Hh stimulation, an

effect that is not reversed if Gli3-FL levels are stabilized by inhibition of the proteasome (Figure 4.5I).

In summary, Hh signaling causes the rapid dissociation of SuFu from Gli, suggesting a simple mechanism for relieving the inhibition of Gli by SuFu. We also conclude that Gli3-FL degradation during Hh signaling is not a cause but a consequence of dissociation from SuFu, consistent with the pronounced instability of Gli in cells lacking SuFu, in spite of maximal activation of Gli target genes.

PKA inhibits SuFu-Gli complex dissociation: evidence that dissociation occurs at cilia

Activation of PKA by FSK potently inhibits Hh signaling, and we found that FSK completely blocks the localization of the SuFu-Gli complex to cilia. Since FSK does not prevent recruitment of Smo to cilia by Hh stimulation, we used FSK to uncouple activation and recruitment of Smo to cilia, from ciliary recruitment of SuFu-Gli. We then asked if FSK affects dissociation of the SuFu-Gli complex caused by Hh stimulation. In cells treated with FSK, dissociation of endogenous SuFu-Gli3-FL by acute Hh stimulation is completely blocked (Figure 4.5E, F and I). This result is consistent with a model in which dissociation of SuFu-Gli complexes by active Smo occurs at cilia; alternatively, FSK might independently inhibit both SuFu-Gli ciliary localization and dissociation. We favor the first model because it is consistent with inhibition of SuFu-Gli dissociation in Kif3a-/- cells, in which ciliary localization of Smo is inhibited (Humke et al., 2010). Our findings also provide a new mechanism explaining the inhibition of Hh

signaling by FSK, and its strict dependence on SuFu (Chen et al., 2009; Svard et al., 2006).

DISCUSSION

A unique feature of the vertebrate Hh pathway is that primary cilia are critical for signal transduction (Huangfu and Anderson, 2005). The Hh ligand binds its receptor, Patched (Ptc), localized at the primary cilium (Rohatgi et al., 2007), leading to activation and recruitment of the seven-spanner Smo to the cilium (Corbit et al., 2005; Rohatgi et al., 2007), from where it signals to the cytoplasm to activate Gli proteins. In unstimulated cells, Gli proteins are kept inactive by the cytoplasmic protein SuFu. In vertebrate cells lacking SuFu, the Hh pathway is maximally active, independent of Smo (Cooper et al., 2005; Svard et al., 2006) and independent of cilia (Jia et al., 2009). A simple model for vertebrate Hh signaling is that active Smo at the cilium inhibits SuFu, to allow Gli activation; however, a major unanswered question has been if and how SuFu is regulated by Hh signaling.

We found that the endogenous complex formed by SuFu and Gli proteins localizes to cilia, and that this ciliary localization is strongly increased by Hh signaling through active Smo. This suggested that the Hh signal is transmitted from active Smo to the SuFu-Gli complex, leading to Gli activation. To determine the mechanism that activates Gli, we searched for biochemical changes of SuFu-Gli complexes caused by acute Hh stimulation. SuFu is an abundant protein (we estimated its concentration in 3T3 cells at about 100 nM) and a small fraction of SuFu forms a complex with Gli in unstimulated cells, while most SuFu is monomeric. Hh stimulation leads to the rapid

dissociation of the SuFu-Gli complex (Humke et al., 2010), suggesting a simple mechanism in which Gli activation is the consequence of relieving its inhibition by SuFu, which allows Gli to enter the nucleus (Figure 4.6). We do not yet know if SuFu dissociation from Gli is sufficient to activate Gli or if posttranslational changes are also required (Ohlmeyer and Kalderon, 1998), such as Gli phosphorylation (Humke et al., 2010). We also do not know if all dissociation of the SuFu-Gli complex takes place at cilia or if it also occurs in other parts of the cell. We propose that SuFu-Gli dissociation is the first step in a series of molecular events through which Gli proteins are activated by Hh signaling. This mechanism of vertebrate Hh signaling is reminiscent of Hh signal transduction in Drosophila, in which Hh stimulation causes the release of Ci complexes by decreasing the affinity of the atypical kinesin Costal-2 for microtubules (Robbins et al., 1997).

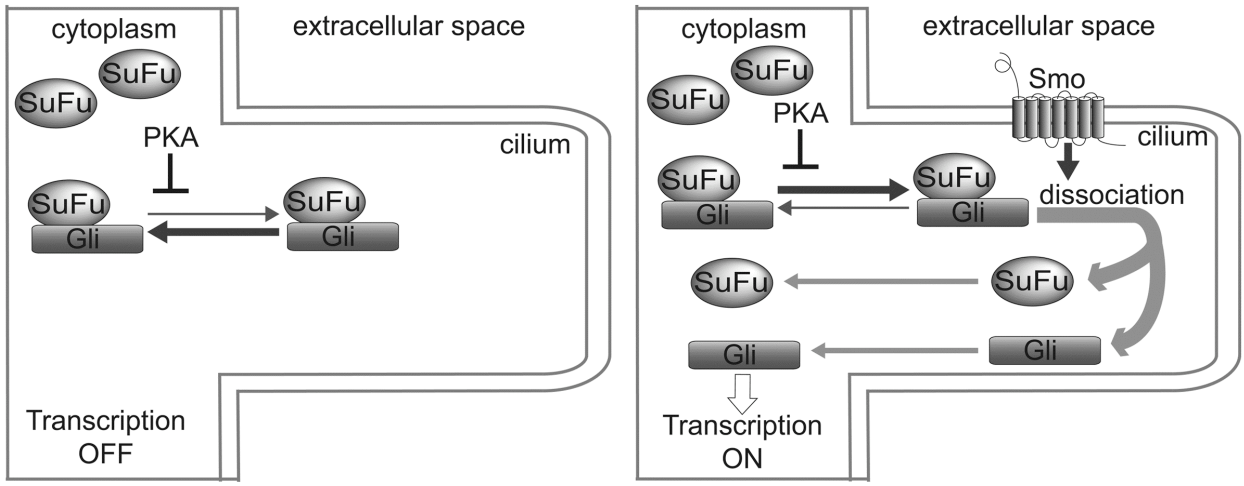

Figure 4.6 A model for activation of Gli proteins during vertebrate Hh signaling.
In the resting state of the Hh pathway (left panel), SuFu forms inactive complexes with Gli2 and Gli3-FL, which are sequestered in the cytoplasm. Without Hh stimulation, SuFu-Gli complexes traffic to the primary cilium at low level, independently of Smo; this basal ciliary trafficking is antagonized by PKA. Hh pathway stimulation (right panel) leads to the translocation of active Smo to the cilium, which, in turn, recruits SuFu-Gli complexes. Active Smo at cilia causes the dissociation of SuFu from Gli. Monomeric SuFu and Gli leave the cilium, followed by Gli nuclear translocation and activation of the transcriptional program of the Hh pathway. PKA antagonizes Hh signaling by blocking ciliary localization of SuFu-Gli complexes, thus preventing coupling between active Smo and dissociation of SuFu-Gli complexes.

Whether "active" Gli moves to the nucleus by itself or in complex with SuFu has been a matter of debate. We favor a model in which Gli enters the nucleus without SuFu, for the following reasons: 1) SuFu blocks nuclear localization of overexpressed Gli (Barnfield et al., 2005), while Gli proteins are nuclear in the absence of SuFu ((Humke et al., 2010) and the present study); 2) Hh stimulation causes the rapid dissociation of SuFu-Gli complexes, indicating that a critical step in generating active Gli is the removal of bound SuFu; and 3) SuFu is not required in the nucleus, as the transcriptional output of the Hh pathway is maximal in SuFu-/- cells (Svard et al., 2006).

Recently, the BTB domain protein SPOP was suggested to antagonize the interaction between SuFu and Gli (Chen et al., 2009). However, SPOP does not localize to cilia (Chen et al., 2009), and loss of SPOP causes only a modest increase in the unstimulated transcription of Hh target genes (Wen et al., 2010), suggesting that while SPOP might play a role in Gli turnover, it likely does not regulate the SuFu-Gli complex during the initial Hh signaling events at the ciliary membrane.

The compartmentalization of vertebrate Hh signaling in primary cilia is accomplished through at least three, largely independent ciliary localization events: 1) localization of Ptc, which is independent of Smo (Rohatgi et al., 2007); 2) localization of Smo, which can be uncoupled from upstream components (Ptc and Hh), is independent of downstream components (SuFu and Gli), and is stimulated by PKA; and 3) localization of SuFu-Gli complexes, which is inhibited by PKA. We speculate that recruitment of SuFu-Gli complexes to cilia ensures that the signal from active Smo is channeled to Gli molecules inhibited by SuFu. If SuFu were recruited to cilia alone, it would compete with

SuFu-Gli complexes and inhibit signaling because monomeric SuFu is present in a large excess over SuFu-Gli. Gli-SuFu complexes thus serve not only to keep Gli proteins inactive and stable but also to make them activatable by Hh signaling at the cilium.

Based on the size of the endogenous SuFu-Gli complex, we estimate it might consist of only these two proteins. Thus an unexpectedly simple protein complex lies at the core of vertebrate Hh signal transduction downstream of Smo. It will be important to understand how the integrity of the SuFu-Gli complex is maintained, how signaling stimulates its dissociation, and whether the posttranslational control of SuFu-Gli dissociation occurs at the levels of SuFu, Gli, or both. Additionally, it will be important to determine how SuFu-Gli complexes localize to cilia, and how active Smo increases their ciliary localization.

The PKA activator, forskolin (FSK), blocks the transcriptional output of the Hh pathway, although only in the presence of SuFu. We found that FSK abolishes the localization of the SuFu-Gli complex to cilia, and its dissociation by Hh stimulation. We interpret these findings as follows: 1) dissociation of SuFu-Gli occurs at cilia during Hh signaling, and is inhibited if SuFu-Gli cannot travel to the cilium, similar to inhibition of SuFu-Gli dissociation observed in Kif3a-/- cells (Humke et al., 2010); and 2) PKA controls trafficking of SuFu-Gli complexes to cilia, independent of Smo, suggesting a novel mechanism for Hh inhibition by PKA. Although PKA localizes to the base of cilia (Barzi et al., 2010), whether Hh signaling regulates PKA remains unclear; one possibility is that local inhibition of PKA might allow coupling between active Smo and SuFu-Gli complexes at cilia. It is likely, however, that additional events are required to transmit the

signal from active Smo to the SuFu-Gli complex, since pharmacological inhibition of PKA blocks, rather than activates, Hh signaling (not shown).

Of the three members of the Gli family of transcription factors, our study focused only on Gli2 and Gli3, which mediate the initial response to Hh stimulation. Gli1 is synthesized in response to Hh signaling (Dai et al., 1999; Ruiz i Altaba, 1998) and is part of a positive feedback loop that amplifies the output of the pathway. Gli1 binds to and is inhibited by SuFu (Chen et al., 2009; Merchant et al., 2004). We envision that another role of SuFu is to inhibit newly synthesized Gli1, and that the SuFu-Gli1 complex has to pass through the cilium in the presence of active Smo in order for Gli1 to become active. This would ensure that the Hh pathway remains signal-dependent even after prolonged stimulation and accumulation of Gli1 protein, avoiding runaway transcriptional activation.

MATERIALS AND METHODS

Cell culture and Hh pathway assays

NIH-3T3 cells were grown in DMEM supplemented with 10% bovine calf serum, penicillin and streptomycin. Mouse embryonic fibroblasts (MEFs) were grown in DMEM supplemented with 10% fetal bovine serum, sodium pyruvate, non-essential amino acids, penicillin and streptomycin. To assay Hh signaling, confluent cell cultures were starved for 24-48 hours in starvation media (DMEM without serum for NIH-3T3 cells or with 0.2% fetal bovine serum for MEFs). The media was then replaced with starvation media

supplemented with the appropriate Hh pathway agonist, antagonist or control vehicle. After incubation for the desired amount of time, the cultures were processed for immunofluorescence or were harvested for real-time PCR, Western blotting, immunoprecipitation or sucrose gradient centrifugation.

Antibodies

Polyclonal antibodies against mouse Smo, SuFu and Gli were generated in rabbits or goats (Cocalico Biologicals, Reamstown, PA), and were affinity-purified. The antibodies were tested for specificity by immunoblot (on either overexpressed or endogenous proteins) and by immunofluorescence on cells (against endogenous proteins) – see Supplemental Figure 4.S1.

For the anti-Smo antibody, a fragment of the intracellular C-terminal domain of mouse Smo (amino acids 683-794) was expressed in bacteria as a soluble fusion with the maltose-binding protein (MBP). Serum from rabbits immunized with this recombinant protein was depleted of anti-MBP antibodies, after which anti-Smo antibodies were affinity purified against the antigen immobilized on Affigel 15 beads (BioRad). To generate anti-SuFu antibodies, full-length mouse SuFu (mSuFu) was expressed and purified from bacteria as an MBP fusion. The serum was affinity purified against a 6His-tagged eGFP fusion of mSuFu covalently attached to Affigel 15. To generate anti-Gli antibodies, two fragments of the human Gli3 protein (an N-terminal fragment consisting of amino acids 1-799 and a C-terminal fragment consisting of amino acids 1061-1599) were expressed in bacteria as insoluble 6His-MBP-tagged fusions. Inclusion bodies were isolated, separated by SDS-PAGE and gel slices were used to immunize rabbits or goats

(Cocalico Biologicals, Reamstown, PA). The serum from rabbits immunized with the mixed recombinant Gli3 fragments was affinity purified successively against 6His-hGli3(1-799) and 6His-hGli3(1061-1599), to generate the anti-GliN and anti-GliC antibodies. On immunoblots, anti-GliN detects both full-length and processed Gli3, while anti-GliC only detects full-length Gli3. By immunofluorescence, anti-GliC detects strongly both Gli2 and full-length Gli3, while anti-GliN detects Gli3 strongly and Gli2 only weakly (Supplemental Figure 4.S1 and data not shown). Anti-GliN and anti-GliC do not detect human or mouse Gli1 by either immunoblotting or immunofluorescence.

Real-time PCR assays of Hh pathway activity

Total cellular RNA was treated with DNase (Promega), purified, and cDNA was generated from 1 microgram of total RNA using Transcriptor reverse transcriptase (Roche) and random hexamers. *Gli1* and *Ptch1* gene expression was assayed by Quantitative Real Time PCR using FastStart SYBR Green (Roche) on a Rotor-Gene 6000 (Corbett Robotics). Relative gene expression was calculated using a Two Standard Curve method in which each gene-of-interest was normalized to the *Ribosomal Protein L27* gene. The sequences for gene-specific primers are: *L27*: 5'-GTCGAGATGGGCAAGTTCAT-3' and 5'-GCTTGGCGATCTTCTTCTTG-3', *Gli1*: 5'-GGCCAATCACAAGTCAAGGT-3' and 5'-TTCAGGAGGAGGGTACAACG -3', *Ptch1*: 5'-ACTGTCCAGCTACCCCAATG-3' and 5'-CATCATGCCAAAGAGCTCAA-3'. Error bars represent standard error of the mean for 3 independent experiments.

Effect of protein synthesis inhibition on Hh signaling in NIH-3T3 cells

To determine if ciliary recruitment and transcription activation by the Hh pathway require new protein synthesis, NIH-3T3 cells were starved overnight and then were incubated for 30 minutes in starvation media supplemented or not with cycloheximide (CHX, 50 microgram/mL final). CHX-treated cells or controls were then incubated with Shh, in the presence or absence of CHX, respectively. Recruitment of Smo, SuFu and Gli to cilia was assayed by immunofluorescence following 3 hours of Shh stimulation. Expression of Gli1 and Ptch genes was assayed by Q-PCR after 0, 3 and 6 hours of stimulation. To determine the degree of protein synthesis inhibition by CHX, cell cultures were starved for methionine by incubation for 2 hours in Met-starvation media (DMEM without methionine). The cells were then incubated for 30 minutes in Met-starvation media with or without 50 microgram/mL CHX, followed by incubation with or without CHX for 3 hours in Met-starvation media supplemented with 35S-methionine (50 microCi/mL final). The cells were harvested and 35S-labeled proteins were detected by SDS-PAGE and autoradiography. Protein synthesis was also measured by scintillation counting of 35S incorporated into TCA-insoluble material during the 3-hour incubation period.

Requirement of active Smo for ciliary recruitment of SuFu and Gli proteins

Starved, confluent NIH-3T3 cells were incubated with or without 200 nM SAG or 10 microM cyclopamine. After 3 hours, parallel cell cultures were either processed for immunofluorescence (to assay Smo, SuFu and Gli recruitment to cilia) or for Q-PCR (to assay Gli1 and Ptch1 transcription). To determine if continued localization of SuFu and Gli proteins to cilia requires active Smo, confluent NIH-3T3 cells were first incubated in

the absence or presence of Shh for 3 hours, to recruit Smo, SuFu and Gli to cilia. Cyclopamine (10 microM) was then added to Shh-stimulated cells, and ciliary localization of Smo, SuFu and Gli was determined, after the desired incubation time. To determine the effects of forskolin (FSK), starved, confluent NIH-3T3 cells were treated overnight with control vehicle, Shh, FSK (10 microM, from Sigma) or FSK (10microM) and Shh. Parallel cell cultures were processed for immunofluorescence or analyzed by Q-PCR. To reverse the effects of FSK, the small molecule PKA inhibitor, H-89 (Calbiochem), was used at 10 microM.

Immunoprecipitation

Affinity-purified anti-Gli3 and anti-SuFu antibodies were covalently attached to AffiPrep Protein A beads (Bio-Rad), by crosslinking with dimethyl-pimelimidate (Pierce). Confluent cell cultures were starved for 48 hours, followed by treatment for 1.5 hours with or without SAG (100 nM), bortezomib (2 microM) or FSK (20 microM). The cells were lysed on ice in lysis buffer (20 mM HEPES pH 7.5, 50 mM potassium chloride, 1 mM magnesium chloride) with 0.5% digitonin, in the presence of protease inhibitors (Complete, Roche). The lysate was clarified by centrifugation at 20,000g and the supernatant was incubated with antibody beads for 1.5 hours at 4C. The beads were washed in lysis buffer with 0.1% digitonin before elution in SDS-PAGE sample buffer and analysis by SDS-PAGE followed by immunoblotting.

Sucrose gradient centrifugation

Linear sucrose gradients (5-20% sucrose, 12.8 mLs) in XB buffer (10 mM HEPES pH 7.5, 100 mM potassium chloride, 1 mM magnesium chloride, 100 microM calcium chloride, supplemented with protease inhibitors) were prepared using a gradient maker (BioComp), and were cooled to 4C. Cells were treated and lysed as described for immunoprecipitation experiments and a volume of 150 microL of clarified lysate was layered on the top of the gradient. Gradients were centrifuged for 20 hours at 4 C at 38,000 RPM in a SW-40 rotor (Beckman). The sucrose gradients were fractionated and each fraction was precipitated with trichloracetic acid (TCA). The TCA-precipitated proteins were analyzed by SDS-PAGE followed by immunobloting for endogenous SuFu, Gli3 and GSK3. The sucrose gradients were calibrated using the molecular weight markers ovalbumin (MW=44 kDa, Stokes radius=30.5A), aldolase (MW=158 kDa, Stokes radius=48.1A), catalase (MW=232 kDa, Stokes radius=52.2A), ferritin (MW=440 kDa, Stokes radius=61A) and thyroglobulin (MW=669 kDa, Stokes radius=85A).

Immunofluorescence

Cells grown on glass coverslips were fixed for 30 minutes at room temperature in PBS with 4% formaldehyde. The coverslips were rinsed with TBST (10 mM Tris pH 7.5, 150 mM NaCl, 0.2% Triton X-100) and then non-specific binding sites were blocked by incubation in TBST supplemented with 25 mg/mL bovine serum albumin (TBST-BSA). The coverslips were incubated with primary antibodies diluted in TBST-BSA, for one hour at room temperature. Coverslips were then washed with TBST, blocked again with TBST-BSA and incubated with the appropriate secondary antibodies in TBST-BSA. After washing, the coverslips were mounted on glass slides in mounting media (0.5% p-phenylenediamine, 20 mM Tris pH 8.8, 90% glycerol). Affinity-purified primary

antibodies against Smo, Gli3 and SuFu were used at a final concentration of 1-2 microgram/mL. Mouse anti-acetylated tubulin, mouse anti-gamma-tubulin, and mouse anti-FLAG antibodies were purchased from Sigma. Alexa dye-conjugated secondary antibodies (Invitrogen) were used at a final concentration of 1 microgram/mL. The immunostained cells were imaged by epi-fluorescence microscopy on an inverted Nikon TE2000U microscope equipped with an OrcaER digital camera (Hammamatsu) and a 100x PlanApo 1.4NA oil objective (Nikon). Images were collected using Metamorph image acquisition software (Applied Precision). To measure ciliary localization of SuFu, Smo, and Gli, 150 cilia for each coverslip were identified by anti-acetylated tubulin staining and were scored visually for the presence or absence of SuFu, Smo, or Gli at the cilium. Error bars represent the standard deviation for groups of 50 cilia counted on different visual fields, on the same coverslip. P values for cilia counts were calculated using an unpaired two-tailed T test, comparing each time point to t=0.

All experiments showing ciliary counts were repeated independently at least twice. Quantification of a representative experiment is shown in the panels where error bars are not provided.

Immunoblotting

Cells were resuspended in TBS with protease inhibitors, and were lysed with 1% Triton X-100 on ice for 20-30 minutes. The cell lysate was clarified by centrifugation for 30 minutes in a refrigerated microfuge at 20,000g. The supernatant was collected, mixed with DTT (50 mM final) and 5x SDS-PAGE sample buffer, and separated by SDS-PAGE on 5-15% polyacrylamide gradient gels, followed by transfer to nitrocellulose

membranes. For immunoblotting, antibodies were used at a final concentration of 1 microgram/mL in TBST with 5% non-fat dry milk.

Measurement of the half-life of endogenous SuFu by CHX chase

To determine if activation of Hh signaling affects the half-life of endogenous SuFu, confluent, starved NIH-3T3 cells were pre-treated for 15 minutes in DMEM with CHX (50 microgram/mL). Parallel cultures were then incubated with CHX, in the presence or absence of 200 nM SAG in DMEM. At the indicated times, the cells were harvested and endogenous SuFu protein was detected by immunoblotting.

Nocodazole treatment

To test if microtubules (MTs) are required for recruitment of Smo, SuFu and Gli to cilia and for the transcriptional responses of Hh signaling, confluent, starved NIH-3T3 cells were pre-incubated for 1 hour with 0.25-5 microM nocodazole (Noc) or with control vehicle. The cells were then stimulated or not with Shh or with 200 nM SAG, in the presence of the same Noc concentration as during pre-incubation. After 1 hour, the cells were processed for immunofluorescence against Smo, SuFu and Gli. Cilia were stained with the mouse anti-acetylated tubulin monoclonal antibody. To determine MT depolymerization, cells treated in parallel were stained with a mouse anti-α-tubulin antibody (DM1α, Sigma). For Q-PCR analysis, cells were harvested after 2 hours of incubation with or without Shh (or SAG), and in the absence or presence of the indicated concentration of Noc.

Shh, chemical agonists and antagonists of the Hh pathway

Shh was produced in 293T cells by transient transfection of an expression plasmid encoding amino acids 1-198 of human Sonic Hedgehog. Shh-conditioned media was harvested after 48 hours, pooled, filter sterilized and used in cellular assays, usually diluted 1:4 in starvation media. Media conditioned by mock-transfected 293T cells was used as control; it had no effect on ciliary recruitment of Smo, Gli or SuFu. The Smo agonist SAG was from Axxora, the Smo antagonists SANT-1 was from Calbiochem, cyclopamine was from LC Laboratories, 20-hydroxycholesterol (20-OHC) and 25-hydroxycholesterol (25-OHC) were from Steraloids Inc.

Pharmacological inhibition of the proteasome

To block ubiquitin-dependent proteolysis, confluent cells were starved for 24-48 hours and were then pretreated with or without 2 microM bortezomib for 0.5-3 hours. The cells were then incubated with or without Hh pathway agonist, in the presence or absence of 2 microM bortezomib for the desired amount of time. Parallel cultures were processed for immunofluorescent detection, Western blotting, Q-PCR or sucrose gradient centrifugation.

Generation of stable cell lines

Constructs were generated in the retroviral vector pLHCX (Clontech), and retroviruses produced in 293T cells were used to infect NIH-3T3 cells or MEFs. Stably transduced lines were generated by hygromycin selection. Expression of the desired protein was confirmed by Western blotting and immunofluorescence. The retroviral

constructs used in this study were: 1) full-length mouse SuFu tagged at the C-terminus with 3 copies of the FLAG epitope; 2) full-length human Gli1 tagged at the C-terminus with one copy of the HA epitope; 3) a fusion between N-terminally Myc-tagged human Gli1 and mouse SuFu, which incorporates a flexible, 24 amino acid linker between Gli1 and SuFu.

Quantitation of endogenous SuFu levels in NIH-3T3 cells

The concentration of endogenous SuFu protein in NIH-3T3 cells was estimated by immunoblotting, against serial dilutions of recombinant mouse SuFu expressed and purified from baculovirus-infected Sf9 cells.

Xenopus embryo injections

Capped messenger RNA for mouse SuFu was generated in vitro using the Message Machine kit (Ambion). One hundred picograms of SuFu mRNA in 10 nL of water were injected per blastomere, into both blastomeres of a two cell stage Xenopus embryo. Twenty-five injected embryos were harvested at stage 10-11 (staged according to Nieuwkoop and Faber) and were homogenized on ice in 150 microliters of XB buffer supplemented with 10 micrograms/mL cytochalasin B and protease inhibitors. The homogenate was clarified by centrifugation for 15 minutes at 20,000g, at 4 Celsius. The supernatant was harvested and subjected to sucrose gradient centrifugation, as described above for lysates from cultured cells.

ACKNOWLEDGMENTS

We thank Robert Lipinski, Wade Bushman, Rajat Rohatgi, Matt Scott, Rune Toftgard, Stefan Englund, Philip Beachy and Andy McMahon for sharing reagents. HT is the recipient of a predoctoral fellowship from the American Heart Association. This work was supported by the Sontag Foundation, the Beckman Foundation and the Rita Allen Foundation.

ABBREVIATIONS USED IN THIS PAPER

CHX (cycloheximide), Cyc (cyclopamine), FSK (forskolin), Gli1HA (HA-tagged Gli1), Gli3-FL (full-length Gli3), GSK3 (glycogen synthase kinase 3), Hh (Hedgehog), Shh (Sonic hedgehog), MT (microtubules), Noc (Nocodazole), MEF (mouse embryonic fibroblast), PKA (protein kinase A), Ptc (Patched), Smo (Smoothened), SuFu (Suppressor of Fused).

REFERENCES

Alcedo, J., M. Ayzenzon, T. Von Ohlen, M. Noll, and J.E. Hooper. 1996. The Drosophila smoothened gene encodes a seven-pass membrane protein, a putative receptor for the hedgehog signal. *Cell*. 86:221-32.

Alexandre, C., A. Jacinto, and P.W. Ingham. 1996. Transcriptional activation of hedgehog target genes in Drosophila is mediated directly by the cubitus interruptus protein, a member of the GLI family of zinc finger DNA-binding proteins. *Genes Dev*. 10:2003-13.

Aza-Blanc, P., F.A. Ramirez-Weber, M.P. Laget, C. Schwartz, and T.B. Kornberg. 1997. Proteolysis that is inhibited by hedgehog targets Cubitus interruptus protein to the nucleus and converts it to a repressor. *Cell*. 89:1043-53.

Barnfield, P.C., X. Zhang, V. Thanabalasingham, M. Yoshida, and C.C. Hui. 2005. Negative regulation of Gli1 and Gli2 activator function by Suppressor of fused through multiple mechanisms. *Differentiation*. 73:397-405.

Barzi, M., J. Berenguer, A. Menendez, R. Alvarez-Rodriguez, and S. Pons. 2010. Sonic-hedgehog-mediated proliferation requires the localization of PKA to the cilium base. *J Cell Sci*. 123:62-9.

Chen, J.K., J. Taipale, K.E. Young, T. Maiti, and P.A. Beachy. 2002. Small molecule modulation of Smoothened activity. *Proc Natl Acad Sci U S A*. 99:14071-6.

Chen, M.H., C.W. Wilson, Y.J. Li, K.K. Law, C.S. Lu, R. Gacayan, X. Zhang, C.C. Hui, and P.T. Chuang. 2009. Cilium-independent regulation of Gli protein function by Sufu in Hedgehog signaling is evolutionarily conserved. *Genes Dev*. 23:1910-28.

Cheung, H.O., X. Zhang, A. Ribeiro, R. Mo, S. Makino, V. Puviindran, K.K. Law, J. Briscoe, and C.C. Hui. 2009. The kinesin protein Kif7 is a critical regulator of Gli transcription factors in mammalian hedgehog signaling. *Sci Signal*. 2:ra29.

Concordet, J.P., K.E. Lewis, J.W. Moore, L.V. Goodrich, R.L. Johnson, M.P. Scott, and P.W. Ingham. 1996. Spatial regulation of a zebrafish patched homologue reflects the roles of sonic hedgehog and protein kinase A in neural tube and somite patterning. *Development*. 122:2835-46.

Cooper, A.F., K.P. Yu, M. Brueckner, L.L. Brailey, L. Johnson, J.M. McGrath, and A.E. Bale. 2005. Cardiac and CNS defects in a mouse with targeted disruption of suppressor of fused. *Development*. 132:4407-17.

Corbit, K.C., P. Aanstad, V. Singla, A.R. Norman, D.Y. Stainier, and J.F. Reiter. 2005. Vertebrate Smoothened functions at the primary cilium. *Nature*. 437:1018-21.

Corcoran, R.B., and M.P. Scott. 2006. Oxysterols stimulate Sonic hedgehog signal transduction and proliferation of medulloblastoma cells. *Proc Natl Acad Sci U S A*. 103:8408-13.

Dai, P., H. Akimaru, Y. Tanaka, T. Maekawa, M. Nakafuku, and S. Ishii. 1999. Sonic Hedgehog-induced activation of the Gli1 promoter is mediated by GLI3. *J Biol Chem*. 274:8143-52.

Ding, Q., S. Fukami, X. Meng, Y. Nishizaki, X. Zhang, H. Sasaki, A. Dlugosz, M. Nakafuku, and C. Hui. 1999. Mouse suppressor of fused is a negative regulator of sonic hedgehog signaling and alters the subcellular distribution of Gli1. *Curr Biol*. 9:1119-22.

Dwyer, J.R., N. Sever, M. Carlson, S.F. Nelson, P.A. Beachy, and F. Parhami. 2007. Oxysterols are novel activators of the hedgehog signaling pathway in pluripotent mesenchymal cells. *J Biol Chem*. 282:8959-68.

Endoh-Yamagami, S., M. Evangelista, D. Wilson, X. Wen, J.W. Theunissen, K. Phamluong, M. Davis, S.J. Scales, M.J. Solloway, F.J. de Sauvage, and A.S. Peterson. 2009. The mammalian Cos2 homolog Kif7 plays an essential role in modulating Hh signal transduction during development. *Curr Biol*. 19:1320-6.

Epstein, D.J., E. Marti, M.P. Scott, and A.P. McMahon. 1996. Antagonizing cAMP-dependent protein kinase A in the dorsal CNS activates a conserved Sonic hedgehog signaling pathway. *Development*. 122:2885-94.

Frank-Kamenetsky, M., X.M. Zhang, S. Bottega, O. Guicherit, H. Wichterle, H. Dudek, D. Bumcrot, F.Y. Wang, S. Jones, J. Shulok, L.L. Rubin, and J.A. Porter. 2002. Small-molecule modulators of Hedgehog signaling: identification and characterization of Smoothened agonists and antagonists. *J Biol*. 1:10.

Haycraft, C.J., B. Banizs, Y. Aydin-Son, Q. Zhang, E.J. Michaud, and B.K. Yoder. 2005. Gli2 and Gli3 localize to cilia and require the intraflagellar transport protein polaris for processing and function. *PLoS Genet*. 1:e53.

Huangfu, D., and K.V. Anderson. 2005. Cilia and Hedgehog responsiveness in the mouse. *Proc Natl Acad Sci U S A*. 102:11325-30.

Huangfu, D., and K.V. Anderson. 2006. Signaling from Smo to Ci/Gli: conservation and divergence of Hedgehog pathways from Drosophila to vertebrates. *Development*. 133:3-14.

Humke, E.W., K.V. Dorn, L. Milenkovic, M.P. Scott, and R. Rohatgi. 2010. The output of Hedgehog signaling is controlled by the dynamic association between Suppressor of Fused and the Gli proteins. *Genes Dev*. 24:670-82.

Jia, J., A. Kolterud, H. Zeng, A. Hoover, S. Teglund, R. Toftgard, and A. Liu. 2009. Suppressor of Fused inhibits mammalian Hedgehog signaling in the absence of cilia. *Dev Biol*. 330:452-60.

Jiang, J., and G. Struhl. 1995. Protein kinase A and hedgehog signaling in Drosophila limb development. *Cell*. 80:563-72.

Kalderon, D. 2005. The mechanism of hedgehog signal transduction. *Biochem Soc Trans*. 33:1509-12.

Kim, J., M. Kato, and P.A. Beachy. 2009. Gli2 trafficking links Hedgehog-dependent activation of Smoothened in the primary cilium to transcriptional activation in the nucleus. *Proc Natl Acad Sci U S A*. 106:21666-71.

Kogerman, P., T. Grimm, L. Kogerman, D. Krause, A.B. Unden, B. Sandstedt, R. Toftgard, and P.G. Zaphiropoulos. 1999. Mammalian suppressor-of-fused modulates nuclear-cytoplasmic shuttling of Gli-1. *Nat Cell Biol*. 1:312-9.

Kovacs, J.J., E.J. Whalen, R. Liu, K. Xiao, J. Kim, M. Chen, J. Wang, W. Chen, and R.J. Lefkowitz. 2008. Beta-arrestin-mediated localization of smoothened to the primary cilium. *Science*. 320:1777-81.

Lepage, T., S.M. Cohen, F.J. Diaz-Benjumea, and S.M. Parkhurst. 1995. Signal transduction by cAMP-dependent protein kinase A in Drosophila limb patterning. *Nature*. 373:711-5.

Li, W., J.T. Ohlmeyer, M.E. Lane, and D. Kalderon. 1995. Function of protein kinase A in hedgehog signal transduction and Drosophila imaginal disc development. *Cell*. 80:553-62.

Liem, K.F., Jr., M. He, P.J. Ocbina, and K.V. Anderson. 2009. Mouse Kif7/Costal2 is a cilia-associated protein that regulates Sonic hedgehog signaling. *Proc Natl Acad Sci U S A*. 106:13377-82.

Lipinski, R.J., J.J. Gipp, J. Zhang, J.D. Doles, and W. Bushman. 2006. Unique and complimentary activities of the Gli transcription factors in Hedgehog signaling. *Exp Cell Res*. 312:1925-38.

Lum, L., and P.A. Beachy. 2004. The Hedgehog response network: sensors, switches, and routers. *Science*. 304:1755-9.

Lum, L., C. Zhang, S. Oh, R.K. Mann, D.P. von Kessler, J. Taipale, F. Weis-Garcia, R. Gong, B. Wang, and P.A. Beachy. 2003. Hedgehog signal transduction via Smoothened association with a cytoplasmic complex scaffolded by the atypical kinesin, Costal-2. *Mol Cell*. 12:1261-74.

Marigo, V., R.A. Davey, Y. Zuo, J.M. Cunningham, and C.J. Tabin. 1996. Biochemical evidence that patched is the Hedgehog receptor. *Nature*. 384:176-9.

Martin, R.G., and B.N. Ames. 1961. A method for determining the sedimentation behavior of enzymes: application to protein mixtures. *J Biol Chem*. 236:1372-9.

Merchant, M., F.F. Vajdos, M. Ultsch, H.R. Maun, U. Wendt, J. Cannon, W. Desmarais, R.A. Lazarus, A.M. de Vos, and F.J. de Sauvage. 2004. Suppressor of fused regulates Gli activity through a dual binding mechanism. *Mol Cell Biol*. 24:8627-41.

Methot, N., and K. Basler. 2000. Suppressor of fused opposes hedgehog signal transduction by impeding nuclear accumulation of the activator form of Cubitus interruptus. *Development*. 127:4001-10.

Ohlmeyer, J.T., and D. Kalderon. 1998. Hedgehog stimulates maturation of Cubitus interruptus into a labile transcriptional activator. *Nature*. 396:749-53.

Pan, Y., C.B. Bai, A.L. Joyner, and B. Wang. 2006. Sonic hedgehog signaling regulates Gli2 transcriptional activity by suppressing its processing and degradation. *Mol Cell Biol*. 26:3365-77.

Pearse, R.V., 2nd, L.S. Collier, M.P. Scott, and C.J. Tabin. 1999. Vertebrate homologs of Drosophila suppressor of fused interact with the gli family of transcriptional regulators. *Dev Biol*. 212:323-36.

Price, M.A., and D. Kalderon. 1999. Proteolysis of cubitus interruptus in Drosophila requires phosphorylation by protein kinase A. *Development*. 126:4331-9.

Robbins, D.J., K.E. Nybakken, R. Kobayashi, J.C. Sisson, J.M. Bishop, and P.P. Therond. 1997. Hedgehog elicits signal transduction by means of a large complex containing the kinesin-related protein costal2. *Cell*. 90:225-34.

Rohatgi, R., L. Milenkovic, R.B. Corcoran, and M.P. Scott. 2009. Hedgehog signal transduction by Smoothened: pharmacologic evidence for a 2-step activation process. *Proc Natl Acad Sci U S A*. 106:3196-201.

Rohatgi, R., L. Milenkovic, and M.P. Scott. 2007. Patched1 regulates hedgehog signaling at the primary cilium. *Science*. 317:372-6.

Rohatgi, R., and M.P. Scott. 2007. Patching the gaps in Hedgehog signalling. *Nat Cell Biol*. 9:1005-9.

Ruiz i Altaba, A. 1998. Combinatorial Gli gene function in floor plate and neuronal inductions by Sonic hedgehog. *Development*. 125:2203-12.

Stone, D.M., M. Hynes, M. Armanini, T.A. Swanson, Q. Gu, R.L. Johnson, M.P. Scott, D. Pennica, A. Goddard, H. Phillips, M. Noll, J.E. Hooper, F. de Sauvage, and A. Rosenthal. 1996. The tumour-suppressor gene patched encodes a candidate receptor for Sonic hedgehog. *Nature*. 384:129-34.

Svard, J., K. Heby-Henricson, M. Persson-Lek, B. Rozell, M. Lauth, A. Bergstrom, J. Ericson, R. Toftgard, and S. Teglund. 2006. Genetic elimination of Suppressor of fused reveals an essential repressor function in the mammalian Hedgehog signaling pathway. *Dev Cell*. 10:187-97.

Taipale, J., J.K. Chen, M.K. Cooper, B. Wang, R.K. Mann, L. Milenkovic, M.P. Scott, and P.A. Beachy. 2000. Effects of oncogenic mutations in Smoothened and Patched can be reversed by cyclopamine. *Nature*. 406:1005-9.

Wang, B., J.F. Fallon, and P.A. Beachy. 2000. Hedgehog-regulated processing of Gli3 produces an anterior/posterior repressor gradient in the developing vertebrate limb. *Cell*. 100:423-34.

Wang, B., and Y. Li. 2006. Evidence for the direct involvement of {beta}TrCP in Gli3 protein processing. *Proc Natl Acad Sci U S A*. 103:33-8.

Wang, Y., Z. Zhou, C.T. Walsh, and A.P. McMahon. 2009. Selective translocation of intracellular Smoothened to the primary cilium in response to Hedgehog pathway modulation. *Proc Natl Acad Sci U S A*. 106:2623-8.

Wen, X., C.K. Lai, M. Evangelista, J.A. Hongo, F.J. de Sauvage, and S.J. Scales. 2010. Kinetics of hedgehog-dependent full-length Gli3 accumulation in primary cilia and subsequent degradation. *Mol Cell Biol*. 30:1910-22.

Wilson, C.W., M.H. Chen, and P.T. Chuang. 2009. Smoothened adopts multiple active and inactive conformations capable of trafficking to the primary cilium. *PLoS One*. 4:e5182.

Wu, X., J. Walker, J. Zhang, S. Ding, and P.G. Schultz. 2004. Purmorphamine induces osteogenesis by activation of the hedgehog signaling pathway. *Chem Biol*. 11:1229-38.

Yue, S., Y. Chen, and S.Y. Cheng. 2009. Hedgehog signaling promotes the degradation of tumor suppressor Sufu through the ubiquitin-proteasome pathway. *Oncogene*. 28:492-9.

CHAPTER FIVE:

CONCLUSIONS AND PERSPECTIVES

Hedgehog ligand production and secretion

In chapter 2, I presented work that placed the cellular location of Hedgehog processing in the endoplasmic reticulum. This result was surprising because the endoplasmic reticulum membrane is cholesterol-poor compared to the plasma membrane. The location of Hedgehog processing also led to an understanding of how the Hedgehog tail forms an essential disulfide bridge during folding that involves the catalytic cysteine. I showed that after folding, the disulfide bond is undone by protein disulfide isomerases to free the thiol group and allow the auto-proteolysis reaction to take place. This represents the first identification of a cellular factor that participates in the Hedgehog processing reaction. I also demonstrated that the cleaved C-terminal tail is degraded prior to reaching the Golgi, and a colleague's work showed that the tail is retrotranslocated back into the cytoplasm to be destroyed by the proteasome by ER-associated degradation machinery (ERAD) usually dedicated to destruction of misfolded proteins. The Hedgehog tail represents the first constitutive ERAD substrate identified in multicellular organisms. Finally, we demonstrated that Hedgehog mutants that do not process themselves efficiently are degraded by ERAD in their entirety, suggesting that degradation and auto-proteolysis are competing events.

The work on Hedgehog secretion in chapter 3 started as a question raised by a final experiment I was attempting for the manuscript in chapter 2. When I tried to demonstrate that wild type Hedgehog protein was secreted while processing mutants were not, I realized that detecting active, cholesterol-modified Hedgehog ligand in aqueous media was difficult. I began working on Dispatched in hopes of being able to study Hedgehog secretion biochemically. While I showed that Dispatched bound Hedgehog in a cholesterol dependent manner, it was still almost impossible to measure Hedgehog secretion. I devised a system where cells secreting Hedgehog were cocultured with responsive reporter cells, and in this way began to study

Dispatched functionally. In a parallel endeavor, we tested the function of Scube2, a protein identified in a zebrafish screen as a Hedgehog component that acts at or upstream of Patched. When I coexpressed Scube2 and Hedgehog, I saw a dramatic increase of Hedgehog in the medium. Although there were other proteins that increased Hedgehog solubility as observed by us and others, including heparin, suramin, and anything containing lipoproteins such as bovine serum, none of them resulted in an aqueous fraction with potent signaling. In contrast, the Scube2-liberated Hedgehog was very active.

I demonstrated that Scube2 acts non-cell autonomously and binds Hedgehog directly to stabilize it in aqueous solution. Scube2 binding depended on the cholesterol adduct, and I went on to show that Scube2 was capable of binding and solubilizing a sterolated chimeric protein bearing almost no resemblance to Hedgehog. I then demonstrated that Dispatched synergizes with Scube2 to release Hedgehog into the medium. Finally, we managed to incorporate photocrosslinkable cholesterol analogs into Hedgehog to confirm cholesterol-specific binding to both Dispatched and Scube2. Using two different analogs we demonstrated that Dispatched and Scube2 bind the cholesterol adduct on different faces, suggesting that they might synergize by a handoff mechanism. This work represents a big step forward in understanding how cholesterol-modified Hedgehog manages to diffuse long distances, and puts into question some of the models proposing Hedgehog multimerization or lipoprotein having a significant role in Hedgehog transport.

One of the questions raised by the dramatic effect of Scube2 in vitro is whether it participates in Hedgehog signaling in every physiological setting, especially since mutation of Scube2 results in a less severe phenotype than mutations of Hedgehog or Smoothened. One possibility is that Scube2 is required for long-range but not short-range Hedgehog signaling. In

support of this, the *you* mutation was identified in a screen for altered myotome morphology, but the notochord was still able to induce the floor plate in these mutants (van Eeden et al., 1996). Floor plate induction is known to be contact-dependent, whereas signaling to somites requires Hedgehog to diffuse a much longer distance (Placzek et al., 1990; Placzek et al., 1993; Fan and Tessier-Lavigne, 1994; Johnson et al., 1994).

Another possibility is that there is some functional redundancy of Scube2. Scube2 is part of a family of three related proteins, all sharing the domain topology they are named after: signal sequence-EGF repeats- spacer- cysteine rich repeats-CUB domain. Scube1 and Scube2 were first identified as embryonically expressed genes in mouse embryos (Grimmond et al., 2000; Grimmond et al., 2001) and also found as genes expressed by human vascular endothelium (Yang JBC 2002). Scube3 bears 60% homology to the other two genes (Wu et al., 2004). The most obvious question is whether the two other Scube proteins can also function to mobilize Hedgehog from the membrane. The Scube proteins are expressed in somewhat different regions of the embryo that are known to be patterned using Hedgehog signaling, with Scube2 concentrated along the neuroectoderm (Grimmond et al., 2001), Scube1 expressed more broadly in surface ectoderm, limb buds, and the gonads (Grimmond et al., 2000), and Scube3 expressed along the neural tube, branchial arches and fronto-nasal region, limb buds, and developing tooth and hair follicles (Haworth et al., 2007). It is conceivable that Scube proteins might all participate in the Hedgehog pathway, but differentially expressed according to tissue type. A recently published study examined the effects of morpholino knockdown of all three Scube proteins and found that although Scube2 was the major contributor to the phenotype, that all three genes overlapped in expression in some tissue and knockdown of Scube1 and Scube3 enhanced the phenotype (Johnson et al., 2012).

As a protein necessary for Hedgehog secretion, Scube2 might provide a point of spatial and temporal regulation for the pathway. It is not yet clear if Scube2 is secreted only by the cells that synthesize Hedgehog, by the cells expressing Patched and primed to receive the signal, or by some other population. Evidence that Scube transcription might be regulated by other signaling pathways comes from the ordered patterns of expression and timing during embryogenesis in the mouse (Grimmond et al., 2000; Grimmond et al., 2001; Haworth et al., 2007), as well as some evidence that Scube proteins expression is downregulated by cytokine inflammatory signaling (Yang et al., 2002) and upregulated by insulin-mimetic compound vanadate (Tiago et al., 2011).

The potency of the Hedgehog/Scube2 supernatant raises the question of whether Scube2 plays any additional role besides stabilizing the hydrophobic adduct of Hedgehog in aqueous solution. In the simplest scenario, Scube2 binds Hedgehog and diffuses through media or interstitial fluid before dropping it off on Patched or other coreceptors in Hedgehog responsive cells. Another alternative is that Scube2 remains bound to Hedgehog and is endocytosed along with Patched. This is possible because of the ability to immunoprecipitate a complex of Scube2 and Hedgehog using 5E1, a monoclonal antibody raised against Hedgehog that binds the face that interacts with Patched and acts as an inhibitor of the Hedgehog ligand (Ericson et al., 1996; Pepinsky et al., 2000; Maun et al., 2010). A third possibility is that Scube2 plays an active, positive role in targeting Hedgehog to its receptors. Indeed, when the role of Scube2 in Hedgehog signaling was first reported, it was speculated that Scube2 might be acting as a peripheral protein coreceptor on the signal receiving cell, mediating Hedgehog ligand endocytosis (Hollway et al., 2006). There is precedent for proteins containing CUB domains to act as endocytic receptors for cells, most notably the multipurpose cubilin receptor which is named after its 27 CUB domains, which was discovered as a receptor for intrinsic

factor/cobalamin complex, and later found to mediate endocytosis of many other molecules, such as hemoglobin, transferrin, vitamin D receptor, and apolipoproteins (reviewed in (Christensen and Birn, 2002)). The N-terminal half of the Scube2 protein contains EGF repeats which might participate in a secondary targeting function separate from the CUB domain, given other examples of receptor/ligand interactions that depend on the EGF motif. However, mutant analysis in a recent study showed little difference between Hedgehog activity after release by full length Scube2 versus Scube2 with the EGF repeats deleted (Creanga et al., 2012). It remains to be determined if Scube2 binds Patched or any of the Hedgehog coreceptors.

Drosophila do not have a clear homolog to Scube proteins, and the most closely related protein Tolloid is a BMP-1 homolog that binds Decapentaplegic, a member of the TGF-beta family (Finelli et al., 1994). Tolloid has no known role in Hedgehog signaling, however. A more likely candidate is Shifted, the Drosophila homolog of Wnt inhibitory factor-1 (WIF). Shifted is a secreted protein that promotes long range diffusion of cholesterol-modified Hedgehog, and does not act through the Wingless pathway to do so, suggesting there might be a direct interaction (Glise et al., 2005; Gorfinkiel et al., 2005). It is possible that since the actual range of Hedgehog action in Drosophila is much smaller than in vertebrates, and there is no requirement for a soluble transporting protein like Scube2. Hedgehog in flies might rely on other means, such as interactions with the extracellular matrix, to travel from cell to cell once it is secreted by the actions of Dispatched.

Scube2 demonstrates some degree of flexibility in binding a cholesterol modified protein, as it can liberate not only Hedgehog but a chimera of HaloTag protein fused to the Hedgehog C-terminus that shares only a few amino acids with the processed Hedgehog ligand. It is possible that Scube proteins function to release other cholesterol modified proteins, if they exist. The

existence of other sterolated proteins has been postulated by an experiment in which COS-7 cells were metabolically labeled with [3H]cholesterol and several bands were visible after SDS-PAGE, but none of these have been identified to date (Porter et al., 1996). Scube proteins could be used as a tool to fish out these proteins if, like Hedgehog, they are lumenal and peripheral.

The ability of Hedgehog to covalently incorporate photocholesterol analogs opens up the possibility of identifying Hedgehog interactors in both secreting and receiving cells by photocrosslinking and Hedgehog immunoprecipitation. My finding that protein disulfide isomerases participate in the reaction suggests there might be other ER factors involved in optimal Hedgehog processing (chapter 2). Although the processing reaction carries out robustly in vitro, using purified protein, there is some evidence that Hedgehog processing in the ER of cells proceeds more efficiently than processing of chimeras that use the Hedgehog self-proteolysis domain as a module (unpublished data). Photocholesterol might be used to identify these factors, if they exist. In the receptive cell, there is a growing list of Hedgehog interactors that exert positive and negative effects on Hedgehog signaling, and photocholesterol might be used to identify others, particularly coreceptors that might be interacting specifically with the cholesterol adduct.

Photocholesterol can also potentially be used to map the regions of Dispatched that directly interact with the cholesterol adduct. This can either be done by expressing pieces of the Dispatched protein, expressing Dispatched that is missing certain domains, or by using strategically inserted protease sites that can be cleaved after crosslinking. Given the much stronger and more stable binding of Hedgehog to the Dispatched-NNN mutant, it can be exploited to identify the binding site.

The cell culture system I developed to quantitatively measure Dispatched activity can now be used for testing various Dispatched mutants and narrowing down the domains essential for Dispatched function. It can also be used to quantitate Dispatched synergy with other proteins, as I have demonstrated for Scube2. One of the drawbacks of the system as presented in this dissertation is the inability to distinguish strong short range signaling from weaker but broader signaling, and the addition of Dispatched-independent noise from activation of Hedgehog signaling in immediately adjacent cells (Burke et al., 1999; Caspary et al., 2002). This was circumvented by using low ratios of Hedgehog secreting cells to Hedgehog responsive cells, but the system could be adapted into one that better recapitulates physiological signaling. A more sophisticated plating scheme where Hedgehog secreting cells are plated together and subsequently inserted as a block into a lawn of Hedgehog responsive cells would reduce adjacent cell contact and emphasize the long range Hedgehog signal. It might also allow for direct quantitation of Hedgehog activation at varying distances. This system would combine the genetic and biochemical tractability of the tissue culture system with a better recapitulation of Hedgehog secretion and spreading in whole organisms.

My discovery that mutation of the SSD aspartates in Dispatched results in stronger binding to Hedgehog is interesting, because it speaks to the existence of two distinct events in Dispatched-mediated Hedgehog secretion: binding, followed by a separate action that mediates the actual release. It remains to be determined whether Dispatched function is an energy-driven process, or depends on any kind of gradient across the plasma membrane. This result also brings up the possibility that the corresponding aspartate mutant of Patched might be locked tightly with its substrate. Dispatched-NNN robustly immunoprecipitates with cholesterol-modified

Hedgehog still bound, so it might be possible to exploit the Patched-NNN mutant and use it to try to copurify its elusive lipid substrate—one of the holy grails of the Hedgehog field.

Signal transduction at the cilium

In chapter 4 of this dissertation, I presented evidence that SuFu and Gli localize to cilia in a manner that depends on activated Smoothened. We showed that the proteins accumulate in cilia tips within minutes and this change did not depend on de novo protein synthesis. We also showed that mere presence of Smoothened at the cilium was not sufficient for SuFu and Gli recruitment by using cyclopamine, which is a pathway inhibitor that paradoxically also prompts Smoothened to localize to the cilium. We found that another pathway inhibitor, PKA activator forskolin, weakly recruited Smoothened to the cilium but completely abolished even basal levels of SuFu and Gli at the ciliary tip.

We showed that in the absence of Gli, SuFu does not localize to cilia, hinting that it is the nuclear localization sequence of Gli that might be targeting the complex to the cilium. In the absence of SuFu, Gli does not appreciably localize to cilia unless massively overexpressed. Bypassing the cilium, Gli readily enters the nucleus to drive transcription of target genes. This result argues that the main function of the primary cilium is to relieve the inhibition of Gli by SuFu.

I proceeded to examine the nature of Hedgehog signal activation in terms of biochemical changes of the Gli and SuFu complex, and demonstrated that the complex dissociates upon signal activation. I exploited our finding that forskolin blocks ciliary transport of SuFu and Gli but not Smoothened to show that SuFu/Gli dissociation in response to pathway activation does not occur unless the two proteins enter the cilium. This conclusion was also supported by work

from another group showing that IFT protein Kif3a was required for SuFu/Gli dissociation (Humke et al., 2010).

The work presented in chapter 4 provided the first evidence that the signal is transduced from Smoothened to Gli at the primary cilium, and provided a mechanism for Gli activation, although how Smoothened triggers this mechanism remains unresolved.

Study of the signal transduction events that occur inside the primary cilium is greatly hampered by the lack of a protocol to purify cilia away from the rest of the cell. Although Hedgehog components concentrate at cilia, it is unlikely that a significant fraction of abundant cytoplasmic proteins like SuFu and Gli is inside the organelle at any one time. Thus, it has been difficult to determine what Smoothened activation entails in physical terms, and how it might promote the dissociation of the SuFu-Gli complex.

For example, it has been difficult to test whether all full length Gli species that enter the nucleus have traveled through the primary cilium first. SuFu appears to be in significant excess of Gli2 and Gli3 in the cell, and appears to bind both efficiently before they can enter the nucleus. SuFu is also capable of binding Gli1, and might be providing regulation to what would otherwise be a runaway positive feedback loop of Hedgehog driving transcription of Gli1, which then drives its own transcription in addition to other target genes. Furthermore, despite a few reports of detecting SuFu in the nucleus (Kogerman et al., 1999; Stone et al., 1999), it has no evident nuclear localization sequence and most of the literature now agrees that SuFu sequesters Gli before its entry into the nucleus, rather than shuttling it out. It is interesting to consider the differences between the nuclear pore and putative ciliary pore complex, and what might allow SuFu/Gli to shuttle in and out of the cilium while being kept out of the nucleus. It also remains

possible that SuFu/Gli do shuttle in and out of the nucleus, but are simply much easier to detect in a small primary cilium than a cell nucleus.

Another rather simple question that has been difficult to address is where in the cell Gli is degraded, and whether partial degradation versus full degradation occur in different locations. One of the first mechanistic explanations offered for the requirement of cilia for *negative* regulation of the Hedgehog signaling is that mutation of IFT components like Ift88, Ift172, Kif3a, and Dnchc2 decreases the processing of Gli3 into a repressor form (Huangfu and Anderson, 2005). This suggests that partial degradation is either triggered or carried out by Gli passage through the primary cilium. Although there has been no proteasomal machinery detected inside the ciliary shaft, there is a significant clustering of proteasomes around the basal body (Wigley et al., 1999). Thus, it is possible that Gli3 passes through the cilium in complex with SuFu, obtains a posttranslational modification of some sort, is recognized and partially degraded by proteasomes at the cilium's base, and, free of SuFu binding, translocates to the nucleus to carry out repressor functions. Evidence of such a cilium-dependent posttranslational modification remains elusive. Furthermore, although IFT and SuFu affect the ratio of full length and repressor forms of Gli3, they are not essential for Gli3 processing (unpublished data).

One of the more interesting aspects of Gli proteins is that their activation is not synonymous with stabilization of a full-length form. SuFu in fact functions to increase levels of full length Gli, while also keeping its activity in check. This is most easily explained by a model in which SuFu binds the activator domain of Gli—borne out by a lack of binding between SuFu and Gli repressor forms—and directly blocks access by the proteasome or the kinases that mark Gli for degradation. When the SuFu/Gli complex dissociates, Gli becomes destabilized, and it is far more difficult to detect its presence in the nucleus than the transcriptional consequences of its

entry. The quick clearance of Gli3 is likely to occur inside the nucleus, and may represent a way for the cell to tightly control the length of transcriptional response to a pulse of Hedgehog pathway activation. Thus, stabilization and activity of Gli3 are almost diametrically opposed. In flies, Ci-155 does appear to get stabilized in response to Hedgehog activation. This does not represent a contradiction, because vertebrates produce increased levels of Gli1 and Gli2 in response to Hedgehog signaling.

Another question is where the dissociation of SuFu and Gli occurs in the cell. The accumulation of the two proteins at the tip might be indicative of a delay in retrograde movement caused by dissociation inside the cilium. We attempted to compare entry and exit rates of SuFu and Gli, to see if there was a difference between them in one direction but not the other, but these experiments did not yield statistically significant results. This is a question for which a definitive answer can only be obtained by obtaining a purified ciliary fraction.

The most interesting question about the events at the primary cilium is what activated Smoothened does to trigger Gli dissociation from SuFu. The most obvious hypothesis is triggering a phosphorylation event on one or the other. Gli has an enormous number of phosphorylation sites, at least some of which are important for partial degradation, but have no documented effect on its ability to activate genes. I mapped three phosphorylation sites on SuFu in collaboration with Wilhelm Haas of the Gygi laboratory, and used stable isotope labeling by amino acids (SILAC) to see if Hedgehog activation triggers phosphorylation or dephosphorylation of any of these, but there was no significant difference. Once again, the ability to purify cilia away from the rest of the cytoplasm would greatly help in identifying the biochemical changes that occur to SuFu or Gli to trigger their dissociation.

An understanding of Hedgehog signal transduction events downstream of Smoothened is especially important given the role Hedgehog plays in driving certain types of aggressive tumors. The emergence of Smoothened antagonists as chemotherapeutic agents for Hedgehog-reliant cancers is promising, and vismodegib was FDA-approved for treatment of basal cell carcinomas to great fanfare. There are ongoing trials to test vismodegib's ability to treat other cancers, including tamoxifen-resistant breast cancer, pancreatic cancers, and medulloblastoma caused by mutations in *PTCH*. However, in one of the early trials there was a report of a patient with metastatic medulloblastoma that initially responded well to vismodegib treatment, but the cancer rapidly became resistant to the drug via a point mutation in Smoothened (Rudin et al., 2009). Thus, multiple targeted therapies are probably needed to decrease a tumor's chances to evolve resistance. Furthermore, tumors driven by inactivating mutations in tumor suppressors *SUFU* and *GLI3,* activating mutations in oncogenes *GLI2* or *GLI1*, and those which acquire mechanisms to turn on Gli transcription in non-canonical ways are still therapeutically intractable.

References

Burke, R., Nellen, D., Bellotto, M., Hafen, E., Senti, K.A., Dickson, B.J., and Basler, K. (1999). Dispatched, a novel sterol-sensing domain protein dedicated to the release of cholesterol-modified hedgehog from signaling cells. *Cell* 99, 803-815.

Caspary, T., Garcia-Garcia, M.J., Huangfu, D., Eggenschwiler, J.T., Wyler, M.R., Rakeman, A.S., Alcorn, H.L., and Anderson, K.V. (2002). Mouse Dispatched homolog1 is required for long-range, but not juxtacrine, Hh signaling. *Curr Biol* 12, 1628-1632.

Christensen, E.I., and Birn, H. (2002). Megalin and cubilin: multifunctional endocytic receptors. *Nat Rev Mol Cell Biol* 3, 256-266.

Creanga, A., Glenn, T.D., Mann, R.K., Saunders, A.M., Talbot, W.S., and Beachy, P.A. (2012). Scube/You activity mediates release of dually lipid-modified Hedgehog signal in soluble form. *Genes Dev* 26, 1312-1325.

Ericson, J., Morton, S., Kawakami, A., Roelink, H., and Jessell, T.M. (1996). Two critical periods of Sonic Hedgehog signaling required for the specification of motor neuron identity. *Cell* 87, 661-673.

Fan, C.M., and Tessier-Lavigne, M. (1994). Patterning of mammalian somites by surface ectoderm and notochord: evidence for sclerotome induction by a hedgehog homolog. *Cell* 79, 1175-1186.

Finelli, A.L., Bossie, C.A., Xie, T., and Padgett, R.W. (1994). Mutational analysis of the Drosophila tolloid gene, a human BMP-1 homolog. *Development* 120, 861-870.

Glise, B., Miller, C.A., Crozatier, M., Halbisen, M.A., Wise, S., Olson, D.J., Vincent, A., and Blair, S.S. (2005). Shifted, the Drosophila ortholog of Wnt inhibitory factor-1, controls the distribution and movement of Hedgehog. *Dev Cell* 8, 255-266.

Gorfinkiel, N., Sierra, J., Callejo, A., Ibanez, C., and Guerrero, I. (2005). The Drosophila ortholog of the human Wnt inhibitor factor Shifted controls the diffusion of lipid-modified Hedgehog. *Dev Cell* 8, 241-253.

Grimmond, S., Larder, R., Van Hateren, N., Siggers, P., Hulsebos, T.J., Arkell, R., and Greenfield, A. (2000). Cloning, mapping, and expression analysis of a gene encoding a novel mammalian EGF-related protein (SCUBE1). *Genomics* 70, 74-81.

Grimmond, S., Larder, R., Van Hateren, N., Siggers, P., Morse, S., Hacker, T., Arkell, R., and Greenfield, A. (2001). Expression of a novel mammalian epidermal growth factor-related gene during mouse neural development. *Mech Dev* 102, 209-211.

Haworth, K., Smith, F., Zoupa, M., Seppala, M., Sharpe, P.T., and Cobourne, M.T. (2007). Expression of the Scube3 epidermal growth factor-related gene during early embryonic development in the mouse. *Gene Expr Patterns* 7, 630-634.

Hollway, G.E., Maule, J., Gautier, P., Evans, T.M., Keenan, D.G., Lohs, C., Fischer, D., Wicking, C., and Currie, P.D. (2006). Scube2 mediates Hedgehog signalling in the zebrafish embryo. *Dev Biol* 294, 104-118.

Huangfu, D., and Anderson, K.V. (2005). Cilia and Hedgehog responsiveness in the mouse. *Proc Natl Acad Sci U S A* 102, 11325-11330.

Humke, E.W., Dorn, K.V., Milenkovic, L., Scott, M.P., and Rohatgi, R. (2010). The output of Hedgehog signaling is controlled by the dynamic association between Suppressor of Fused and the Gli proteins. *Genes Dev* 24, 670-682.

Johnson, J.L., Hall, T.E., Dyson, J.M., Sonntag, C., Ayers, K., Berger, S., Gautier, P., Mitchell, C., Hollway, G.E., and Currie, P.D. (2012). Scube activity is necessary for Hedgehog signal transduction in vivo. *Dev Biol* 368, 193-202.

Johnson, R.L., Laufer, E., Riddle, R.D., and Tabin, C. (1994). Ectopic expression of Sonic hedgehog alters dorsal-ventral patterning of somites. *Cell* 79, 1165-1173.

Kogerman, P., Grimm, T., Kogerman, L., Krause, D., Unden, A.B., Sandstedt, B., Toftgard, R., and Zaphiropoulos, P.G. (1999). Mammalian suppressor-of-fused modulates nuclear-cytoplasmic shuttling of Gli-1. *Nat Cell Biol* 1, 312-319.

Maun, H.R., Wen, X., Lingel, A., de Sauvage, F.J., Lazarus, R.A., Scales, S.J., and Hymowitz, S.G. (2010). Hedgehog pathway antagonist 5E1 binds hedgehog at the pseudo-active site. *J Biol Chem* 285, 26570-26580.

Pepinsky, R.B., Rayhorn, P., Day, E.S., Dergay, A., Williams, K.P., Galdes, A., Taylor, F.R., Boriack-Sjodin, P.A., and Garber, E.A. (2000). Mapping sonic hedgehog-receptor interactions by steric interference. *J Biol Chem* 275, 10995-11001.

Placzek, M., Jessell, T.M., and Dodd, J. (1993). Induction of floor plate differentiation by contact-dependent, homeogenetic signals. *Development* 117, 205-218.

Placzek, M., Tessier-Lavigne, M., Yamada, T., Jessell, T., and Dodd, J. (1990). Mesodermal control of neural cell identity: floor plate induction by the notochord. *Science* 250, 985-988.

Porter, J.A., Young, K.E., and Beachy, P.A. (1996). Cholesterol modification of hedgehog signaling proteins in animal development. *Science* 274, 255-259.

Rudin C.M., Hann C.L., Laterra J., Yauch R.L. , Callahan C.A., Fu L., Holcomb T., Stinson J., Gould S.E., Coleman B., *et al.* (2009). Treatment of medulloblastoma with hedgehog pathway inhibitor GDC-0449. *N Engl J Med.* 361(12), 1173-1178.

Stone, D.M., Murone, M., Luoh, S., Ye, W., Armanini, M.P., Gurney, A., Phillips, H., Brush, J., Goddard, A., de Sauvage, F.J*., et al.* (1999). Characterization of the human suppressor of fused, a negative regulator of the zinc-finger transcription factor Gli. *J Cell Sci* 112 (Pt 23), 4437-4448.

Tiago, D.M., Laize, V., Bargelloni, L., Ferraresso, S., Romualdi, C., and Cancela, M.L. (2011). Global analysis of gene expression in mineralizing fish vertebra-derived cell lines: new insights into anti-mineralogenic effect of vanadate. *BMC Genomics* 12, 310.

van Eeden, F.J., Granato, M., Schach, U., Brand, M., Furutani-Seiki, M., Haffter, P., Hammerschmidt, M., Heisenberg, C.P., Jiang, Y.J., Kane, D.A*., et al.* (1996). Mutations affecting somite formation and patterning in the zebrafish, Danio rerio. *Development* 123, 153-164.

Wigley, W.C., Fabunmi, R.P., Lee, M.G., Marino, C.R., Muallem, S., DeMartino, G.N., and Thomas, P.J. (1999). Dynamic association of proteasomal machinery with the centrosome. *J Cell Biol* 145, 481-490.

Wu, B.T., Su, Y.H., Tsai, M.T., Wasserman, S.M., Topper, J.N., and Yang, R.B. (2004). A novel secreted, cell-surface glycoprotein containing multiple epidermal growth factor-like repeats and one CUB domain is highly expressed in primary osteoblasts and bones. *J Biol Chem* 279, 37485-37490.

Yang, R.B., Ng, C.K., Wasserman, S.M., Colman, S.D., Shenoy, S., Mehraban, F., Komuves, L.G., Tomlinson, J.E., and Topper, J.N. (2002). Identification of a novel family of cell-surface proteins expressed in human vascular endothelium. *J Biol Chem* 277, 46364-46373.

APPENDIX

SUPPLEMENTARY MATERIAL (CHAPTER 2)

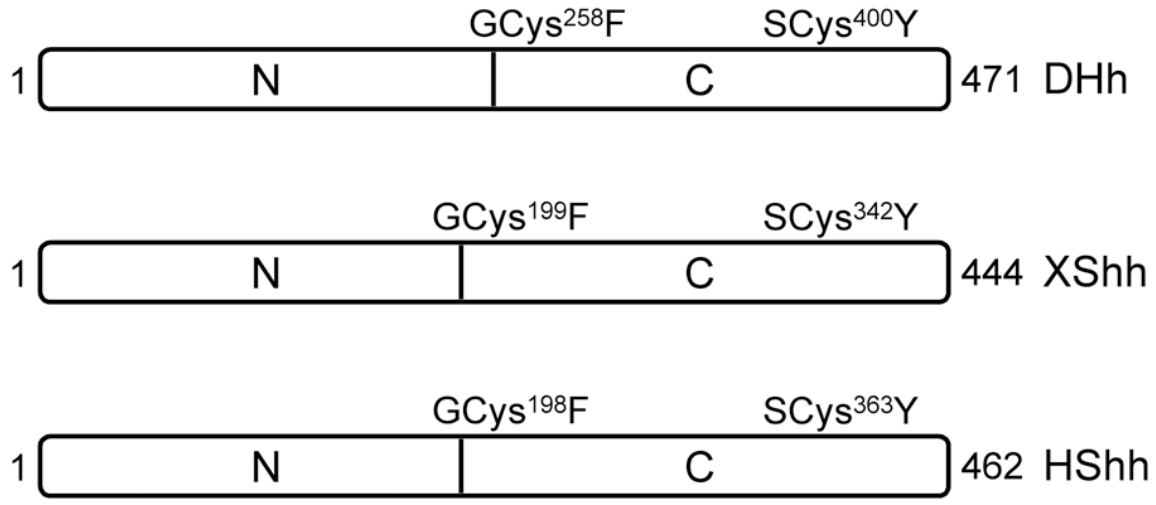

Supplemental Figure 2.S1 Schematic of the Hh proteins used in this study
The domain structure of Drosophila Hedgehog (DHh), Xenopus Sonic Hedgehog (XShh) and human Sonic Hedgehog (HShh) is shown. The catalytic cysteine is part of a conserved GCF sequence, while the non-catalytic cysteine is part of a conserved SCY sequence. Auto-proteolytic cleavage of the Hh precursor is driven by the intein-like C-terminal part of the molecule (C), and generates the N-terminal signaling fragment (N), attached to cholesterol via the carboxyl group of the glycine residue preceding the catalytic cysteine.

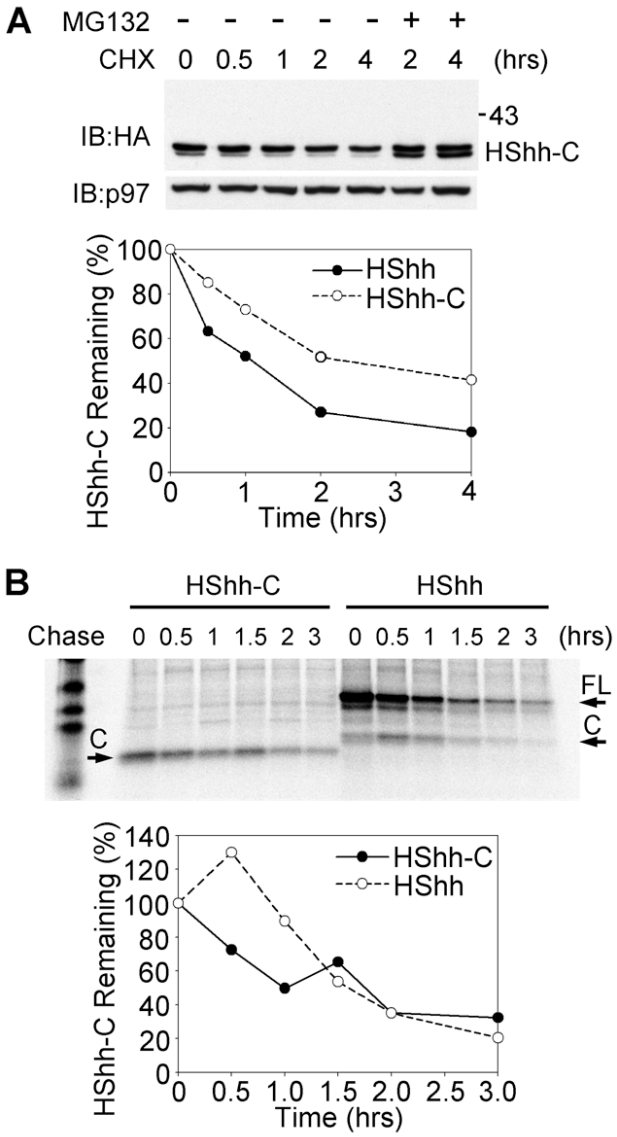

Supplemental Figure 2.S2 ERAD of HShh-C expressed in isolation.
(A) HShh-C with a C-terminal HA tag was expressed directly in 293T cells. Protein synthesis was inhibited with cycloheximide (CHX), and the fate of the protein followed by SDS-PAGE and immunoblotting (IB) with HA-antibodies. Where indicated, cells were incubated in the presence of the proteasome inhibitor MG132. The lower panel shows the quantification of the experiment in comparison with the degradation of HShh-C generated from the HShh precursor.
(B) As in (A), but cells expressing either HShh-C or HShh precursor were labeled with ^{35}S-methionine and -cysteine, and chase- incubated with unlabeled amino acids for the indicated time periods. The samples were analyzed by SDS-PAGE and autoradiography. Arrows indicate the position of the C-terminal fragment (C) and that of the full length HShh (FL). The C-terminal fragment generated by HShh processing is larger than the one expressed directly because of a linker sequence placed between the end of the HShh protein and the HA tag.

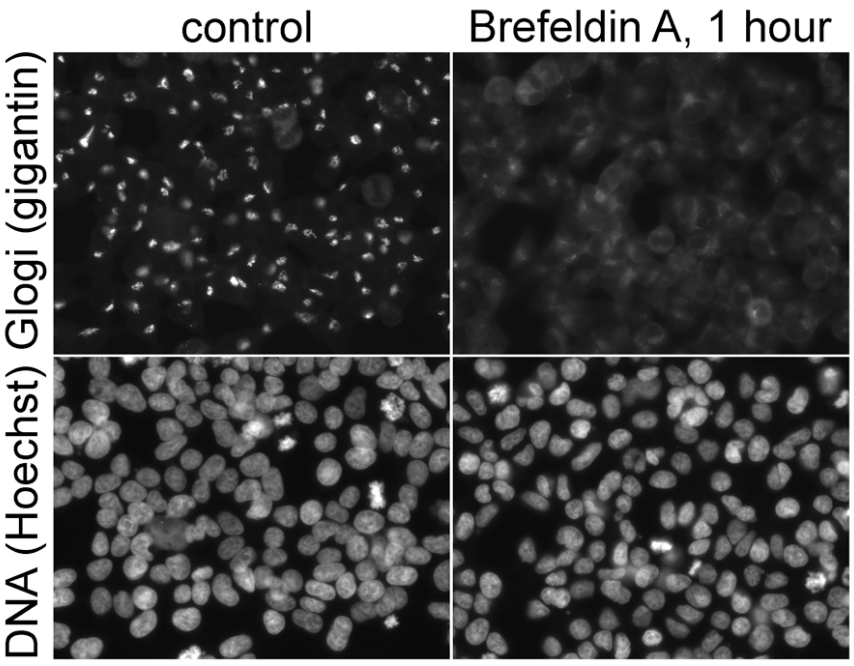

Supplemental Figure 2.S3 Control showing dispersion of the Golgi by brefeldin A.
Cells stably expressing HShh-HA were incubated in the absence or presence of 10 uM brefeldin A for 1 hr, in parallel to the experiment shown in Figure 3E. The cells were fixed and processed for immunofluorescence with gigantin antibodies to reveal the Golgi. The cells were counter-stained with Hoechst dye to visualize nuclei.

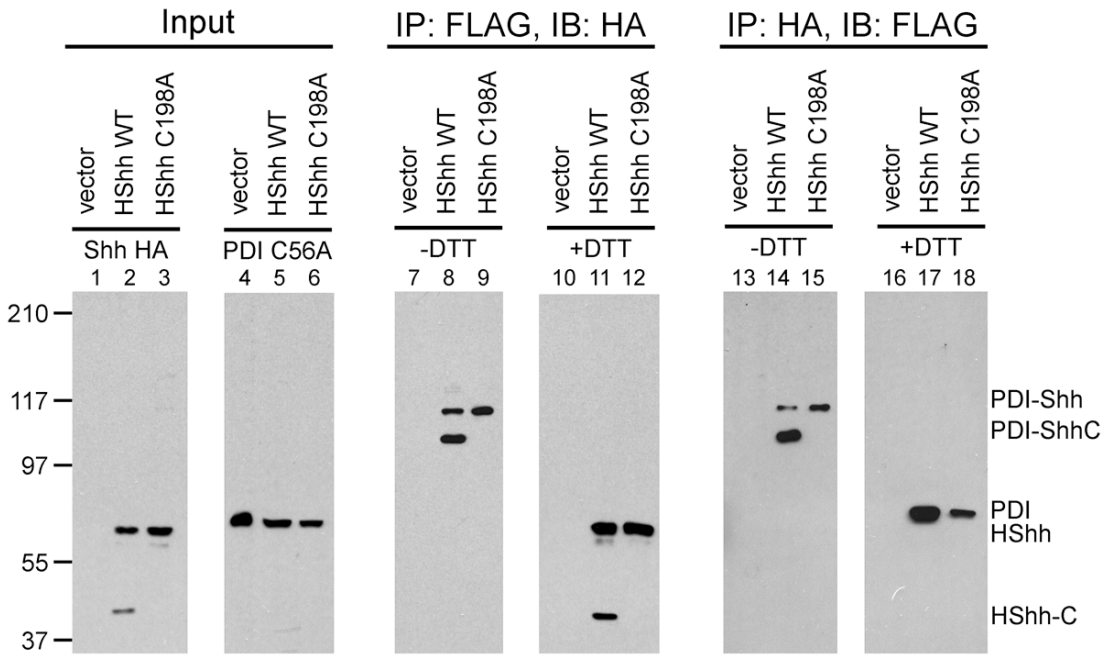

Supplemental Figure 2.S4 Control showing specificity of the HShh-PDI mixed disulfide detection.
Wild type (WT) HShh-HA, the processing-defective C198A mutant, or empty vector were co-transfected with a FLAG-tagged CXXA mutant of PDI (C56A) in 293T cells. Cell extracts were subjected to immunoprecipitation with HA- or FLAG- antibodies, followed by SDS-PAGE and immunoblotting with FLAG- and HA- antibodies. Where indicated, the immunoprecipitated samples were reduced with DTT prior to electrophoresis.

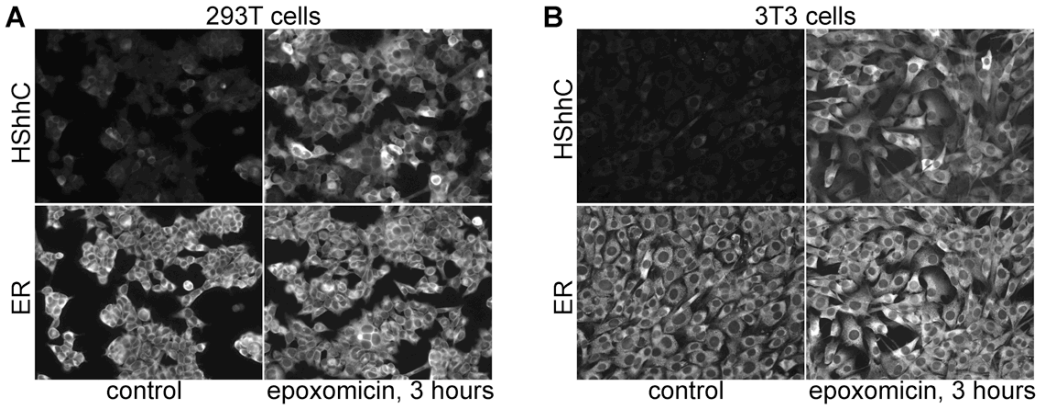

Supplemental Figure 2.S5 HShh-C is degraded by the proteasome
(A) HShh-HA was stably expressed in 293T cells. Cells were immunostained with rat HA antibodies, following a 3-hr treatment with or without the proteasome inhibitor epoxomicin (1 uM). The ER was stained with rabbit calnexin antibodies.
(B) As in (C), but with HShh-HA stably expressed in 3T3 cells.

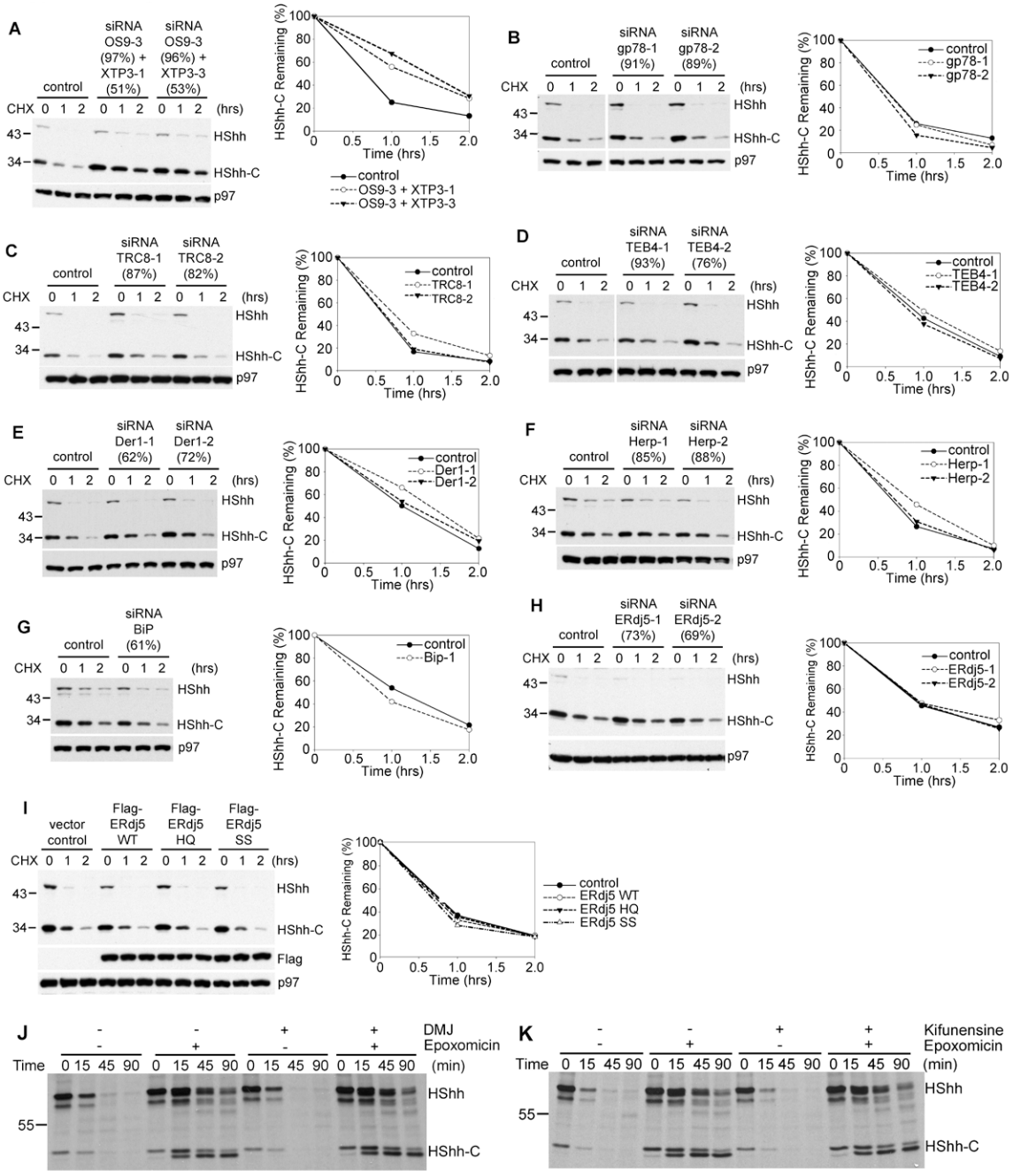

Supplemental Figure 2.S6 Testing various factor for their effects on HShh-C ERAD.
(A) Cells were simultaneously depleted of the ER-luminal lectins OS9 and XTP3 and the fate of stably expressed HShh-HA precursor was followed after cycloheximide (CHX) addition by SDS-PAGE and immunoblotting with HA-antibodies. The extent of depletion (in brackets) was determined by quantitative RT-PCR. Controls were treated with an unrelated siRNA. The right panel shows quantification of HShh-C in the experiment. All samples were also analyzed by immunoblotting for p97 (loading control).
(B) As in (A), but cells were depleted of the ubiquitin ligase gp78 using two siRNAs.
(C) As in (A), but cells were depleted of the ubiquitin ligase TRC8 using two siRNAs.
(D) As in (A), but cells were depleted of the ubiquitin ligase TEB4 using two siRNAs.
(E) As in (A), but cells were depleted of the ER membrane protein Derlin-1 (Der1) using two siRNAs.
(F) As in (A), but cells were depleted of the human Usa1 homologue Herp using two siRNAs.
(G) As in (A), but cells were depleted of the ER luminal chaperone BiP.

Supplemental Figure 2.S6 (Continued)
(H) As in (A), but cells were depleted of the ER-localized oxidoreductase ERdj5 using two siRNAs.
(I) Cells stably expressing HShh-HA were transiently transfected with FLAG-tagged ERdj5 (wild type) or with dominant-negative constructs (HQ and SS) (Ushioda et al., 2008). An empty vector served as control. A cycloheximide chase was performed as in (A).
(J) Cells stably expressing HShh-HA were pulsed with ^{35}S-methionine for 3 min and chase-incubated with unlabeled methionine for the indicated time periods. Both the pulse and the chase were performed in the presence or absence of 100 ug/mL 1-deoxymannojirimycin (DMJ) and 1 uM of the proteasome inhibitor epoxomicin. The samples were analyzed by immunoprecipitation with HA-antibodies followed by reducing SDS-PAGE and fluorography. Equal number of cells were processed for each condition.
(K) As in (J), but cells were incubated in the absence or presence of 50 uM kifunensine instead of DMJ.

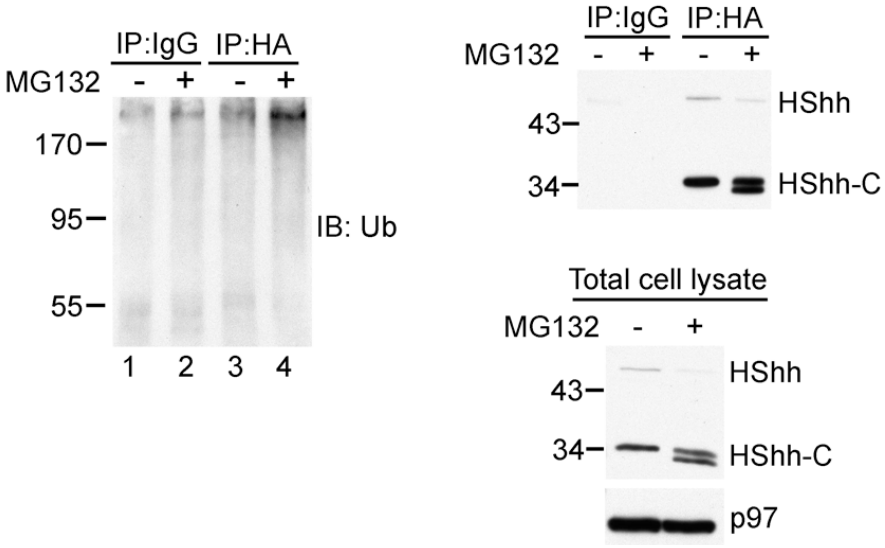

Supplemental Figure 2.S7 Control showing specificity of the immunoprecipitation of poly-ubiquitinated HShh.
This experiment serves as a control for those shown in Figures 8B and C. Cells stably expressing HShh-HA were incubated in the absence or presence of MG132 for 2 hrs. Extracts were subjected to immunoprecipitation (IP) with HA-antibodies or with control IgG, and the proteins were analyzed by SDS-PAGE and immunoblotting (IB) with HA-antibodies or ubiquitin (Ub)- antibodies. Immunoblotting for p97 served as loading control.

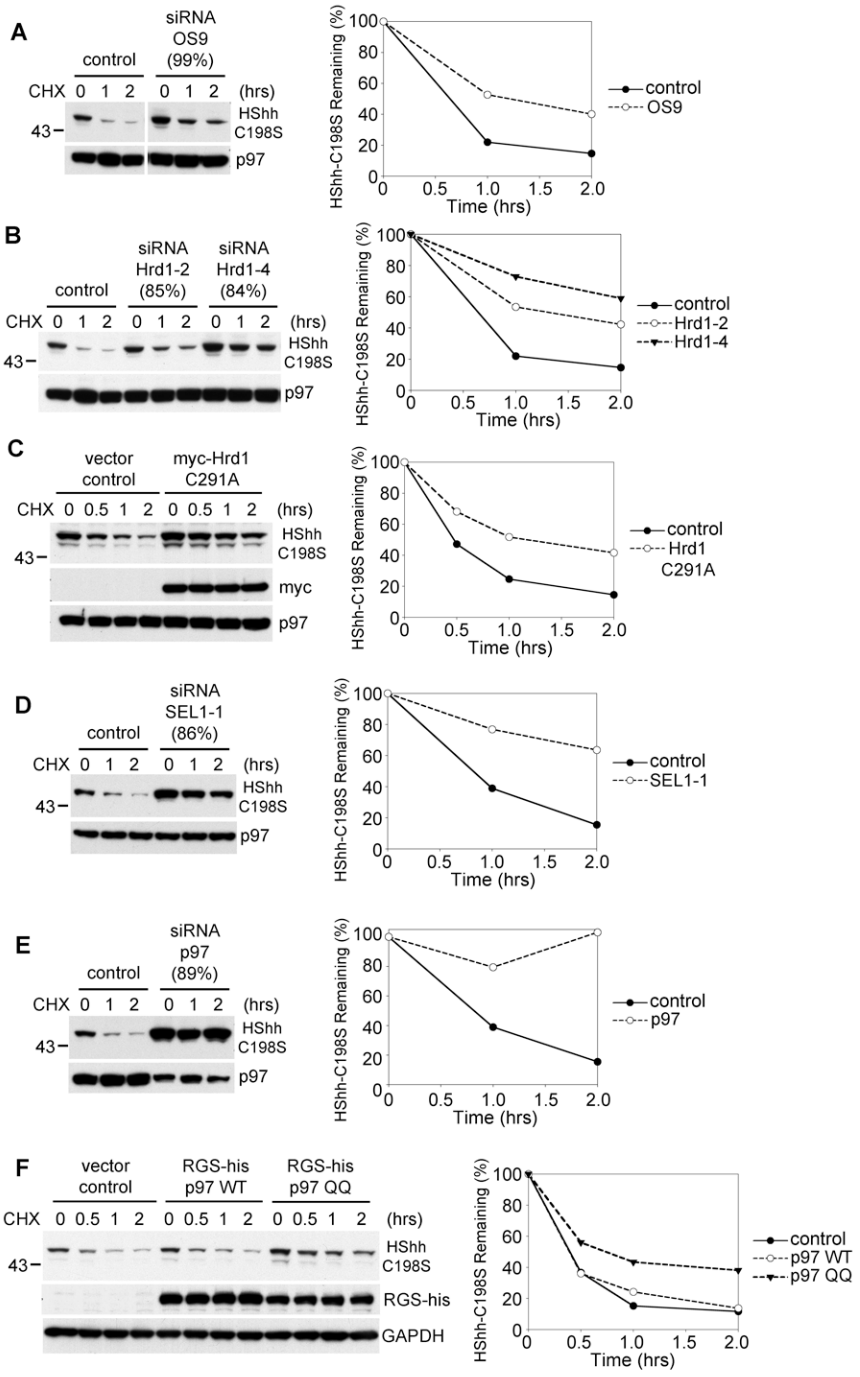

Supplemental Figure 2.S8 ERAD components required for the degradation of HShh precursor.
(A) The processing defective mutant of HShh-HA with mutation of the catalytic cysteine (C198S) was stably expressed in 293T cells. Cells were depleted of the ER-luminal lectin OS9 by siRNA and the fate of HShh-HA precursor was followed after cycloheximide (CHX) addition. The extent of OS9 depletion (in brackets) was determined by quantitative RT-PCR. Controls were treated with an unrelated siRNA. All samples were analyzed by SDS-PAGE and immunoblotting with HA-antibodies. The right panel shows quantification of HShh-C298S in the experiment. All samples were also analyzed by immunoblotting for p97 (loading control).
(B) As in (A), but with depletion of the ubiquitin ligase Hrd1 by two different siRNAs.

Supplemental Figure 2.S8 (Continued)
(C) Cells stably expressing HShh-C198S-HA were transfected with a catalytically inactive Myc-tagged Hrd1 (Hrd1-C291A) or with empty vector. The fate of HShh-HA was followed as in (A). All samples were also analyzed by immunoblotting for p97 (loading control) and myc (Hrd1-C291A).
(D) As in (A), but with depletion of the Hrd1-interacting protein Sel1 by siRNAs.
(E) As in (A), but with depletion of the ATPase p97 by siRNA.
(F) As in (C), but with transfection of RGS-his-tagged wild type p97, a catalytically inactive p97 mutant (p97-QQ), or with empty vector. All samples were also analyzed by immunoblotting for GAPDH (loading control) and RGS-his.

Supplemental Table 2.S1: Sequences of SiRNA duplexes used in this study.

Gene	Nucleotides	Primers (forward and reverse)
Control	390-414	UGGAGUAGUUGAGUCAAUCAAGCUG
(NM_005065)		CAGCUUGAUUGACUCAACUACUCCA
p97(VCP)-1	1272-1292	GAUGAUGGCAGGAGCAUUCUU
(NM_007126)		AAGAAUGCUCCUGCCAUCAUC
Hrd1-1	530-554	CAGCUGGUGUUUGGCUUUGAGUAUG
(BC141662)		CAUACUCAAAGCCAAACACCAGCUG
Hrd1-2	264-288	UGGGCAAGGUGAUGGGCAAGGUGUU
(BC141662)		AACACCUUGCCCAUCACCUUGCCCA
gp78-1	453-477	UUUACUAGAACCCACACGAAGAGGC
(BC069197)		GCCUCUUCGUGUGGGUUCUAGUAAA
gp78-2	517-541	AAGAGGGCCAAACACAAUACACUGG
(BC069197)		CCAGUGUAUUGUGUUUGGCCCUCUU
TRC8-1	1361-1379	UAAUCGUCAAGCUUUUCCCdTdT
(NM_007218)		GGGAAAAGCUUGACGAUUAdTdT
TRC8-2	517-541	GCUCUUUGGUGUAUUUGCAUCCAGU
(NM_007218)		ACUGGAUGCAAAUACACCAAAGAGC
TEB4-1	240-264	UACACAAGGAUGAUAAAGCGGUUUC
(NM_005885)		GAAACCGCUUUAUCAUCCUUGUGUA
TEB4-2	383-407	CAGAUAUGCCUUCACGGCUUCCAAU
(NM_005885)		AUUGGAAGCCGUGAAGGCAUAUCUG
SEL1-1	390-414	CAGCUUUCUAGAGUCUCCAAAUCCA
(NM_005065)		UGGAUUUGGAGACUCUAGAAAGCUG

Supplemental Table 2.S1 (Continued)

SEL1-2	450-474	GAAACCAGCUUUGACCGCCAUUGAA
(NM_005065)		UUCAAUGGCGGUCAAAGCUGGUUUC
HERpUD1(Herp1)-1	560 -584	CCAGAGGACCAGAGGUUAAUUUAUU
(NM_001010989)		AAUAAAUUAACCUCUGGUCCUCUGG
HERpUD1(Herp1)-2	609-633	AAUGUCUCAGGGACUUGCUUCCAAA
(NM_001010989)		UUUGGAAGCAAGUCCCUGAGACAUU
OS9	465-489	GGAGGAGGAAACACCUGCUUACCAA
(NM_001017956)		UUGGUAAGCAGGUGUUUCCUCCUCC
Bip(HSPA5)	819-843	GAACUAUUGCUGGCCUAAAUGUUAU
(NM_005347)		AUAACAUUUAGGCCAGCAAUAGUUC
XTP-3(ERLEC1)-1	823-847	CGAAGGUCAGAUGACACCAUACUAU
(NM_015701)		AUAGUAUGGUGUCAUCUGACCUUCG
XTP-3(ERLEC1)-2	999-1023	CACCACUCUUGUGCAGUCAUCCUAA
(NM_015701)		UUAGGAUGACUGCACAAGAGUGGUG
ERdj5-1	728-752	CAUACUGGCCACCUUGAUUAUCCUC
(NM_018981)		GAGGAUAAUCAAGGUGGCCAGUAUG
ERdj5-2	1153-1177	CAACUCCAUACAAACUGCCUUUGCU
(NM_018981)		AGCAAAGGCAGUUUGUAUGGAGUUG

Supplemental Table 2.S2: Primers for quantitative RT-PCR.

Homo sapiens gene	Nucleotides	Primers (forward and reverse)
P97	658-853	GTGGAACTGCCCCTGAGACATC
(VCP)		TGCTCTCAGACTCACCAGCCAA
Hrd1	860-945	TGGACAATGTCTGCATCATCTG
		CAGCTGGTATGGAAAATGTGGTT
Gp78	1570-1640	GACCAGGAAGAGGGAGAAACTTC
		CCTCCAGGCGAGGACTGA
Trc8	579-828	CCTGGCAGTGAAACTGAAGTGG
(RNF139)		GAGGTCCCAAAAATCATCCCAA
TEB4	779-953	GGAATGCTTTAGAATGGGACCG
(MARCH6)		CCAACAAGGGAGAAATGACCAA
SEL1L	1750-1931	CAGGGCTATGAAGTGGCACAAA
		TCGGTGCCAAACCCATAGAAAT
HERPUD1	794-907	TGGATTGGACCTATTCAGCAGC
(Herp)		GCAGGTACATAACAACGGTGGC
OS9	247-396	CAGCGTGAAAGGGAGGAGGAAA
		GTGGTATTGCTGGATGTGGCGT
HSPA5	820-1037	ACGGGCAAAGATGTCAGGAAAG
(Bip)		AACACTTTCTGGACGGGCTTCA
DERL1	524-650	TTGGAAATCTGGTTGGACATCTTT
(Derlin-1)		ACTCCTCCTCTCCTACTGGGCA
XTP-3	254-406	CAAGTGGGGATGAGGAAGAAGA
(ERLEC1)		CATGGTACTGCCGAATGTGTTT
ERdj5	1683-1877	TACACCCACCACCTTCAACGA
		TCCTGGGCACAAAAAGAATGAT

SUPPLEMENTARY MATERIAL (CHAPTER THREE)

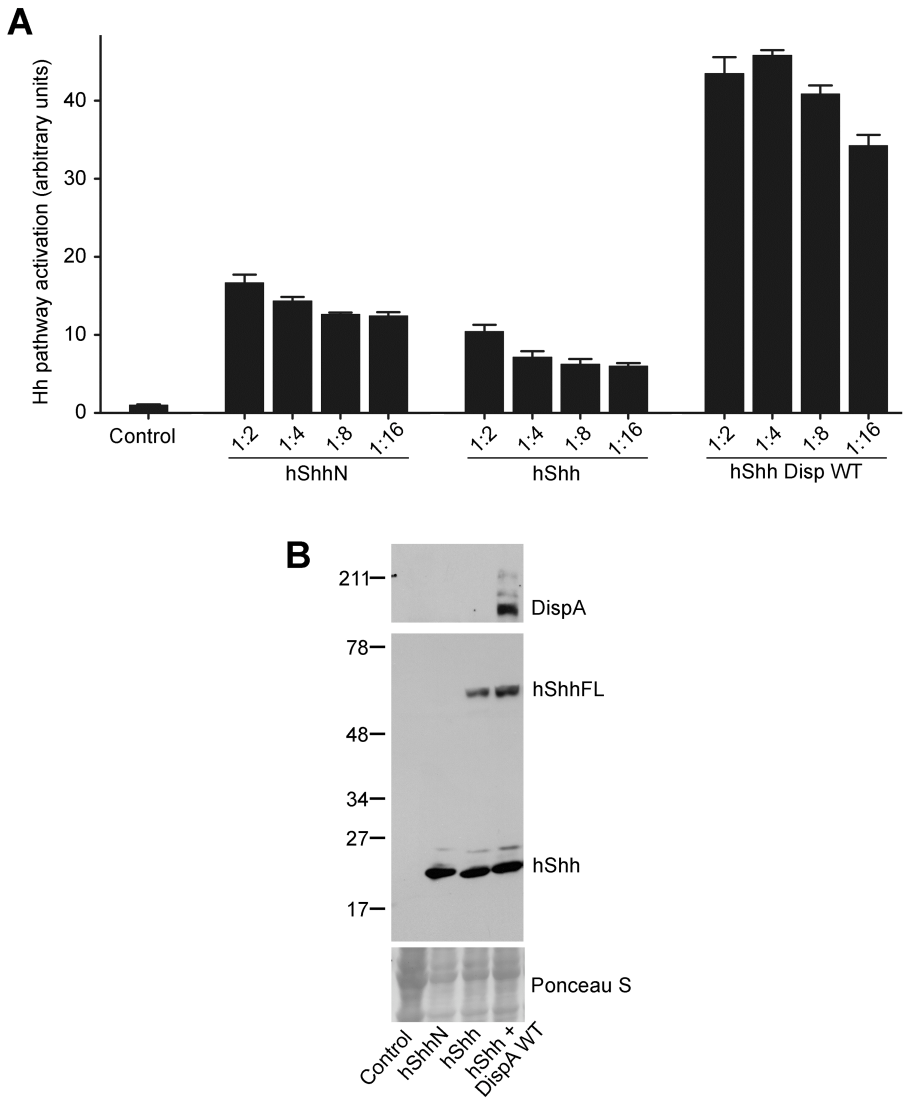

Supplemental Figure 3.S1 DispA Activity Measured in NIH 3T3 Cells, Related to Figure 3.1
(A) NIH 3T3 cells stably expressing hShh or hShhN, transduced with a lentivirus expressing myc-tagged DispA-WT or not, were cocultured at the indicated dilution ratios with Hh-responsive Shh Light II cells. Twelve hours after plating, serum was washed off and the cells were incubated for 30 hr in serum-free media, followed by luciferase reporter assays. Luciferase measurements were normalized to Shh Light II cells grown alone (control). All experiments were performed in triplicate. Error bars represent SD of the mean. DispA expression increased the response of reporter cells to hShh but not to hShhN.
(B) The cells used in (A) were analyzed by SDS-PAGE followed by immunblotting with anti-hShh and anti-myc antibodies. Shh Light II cells were used as negative control. HShhFL denotes the full-length hShh precursor. Ponceau S staining of the blotting membrane is shown for loading control.

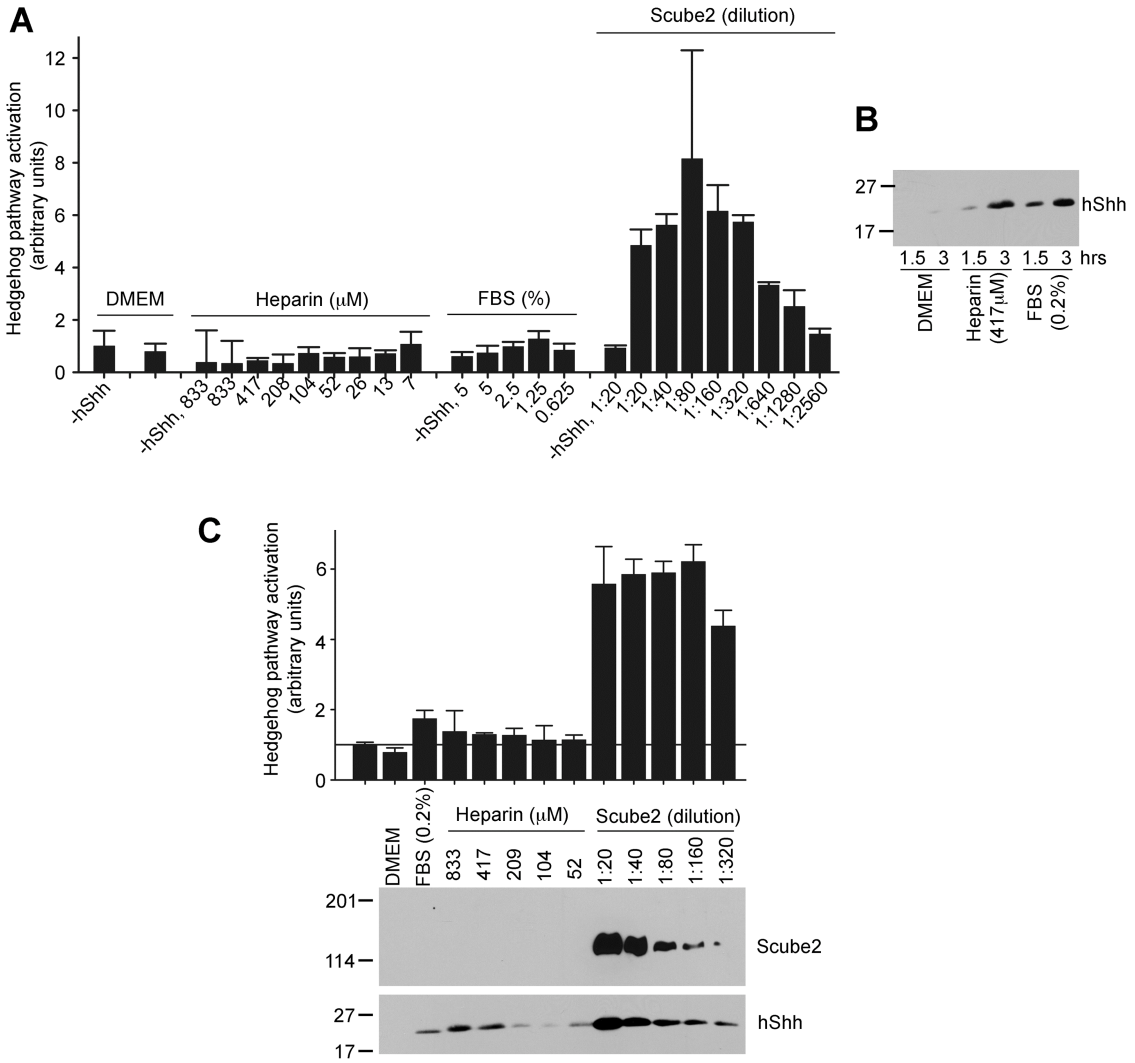

Supplemental Figure 3.S2 HShh Released by Serum or Heparin Is Inactive, in Contrast to hShh Released by Scube2, Related to Figure 3.3

(A) 293T cells stably expressing hShh were incubated with heparin, fetal bovine serum (FBS), or HA-tagged Scube2 added at the indicated concentrations in serum-free media (DMEM). Secreted hShh was collected for 3 hr and then analyzed by luciferase assay in Shh Light II reporter cells. As negative controls (−hShh), reporter cells were incubated with DMEM alone, DMEM with heparin (883 μM), DMEM with serum (5%), or DMEM with Scube2 (1:20 dilution)

(B) 293T cells stably expressing hShh were incubated with serum-free media, heparin, or FBS for 1.5 or 3 hr. Supernatants were precipitated with TCA, and were analyzed by SDS-PAGE and immunoblotting with anti-hShh antibodies.

(C) Collection of supernatants and analysis by luciferase reporter assays was performed as in (A). Aliquots of the supernatants were precipitated and analyzed as in (B), with additional immunoblotting for Scube2 with anti-HA antibodies.

SUPPLEMENTARY MATERIAL (CHAPTER FOUR)

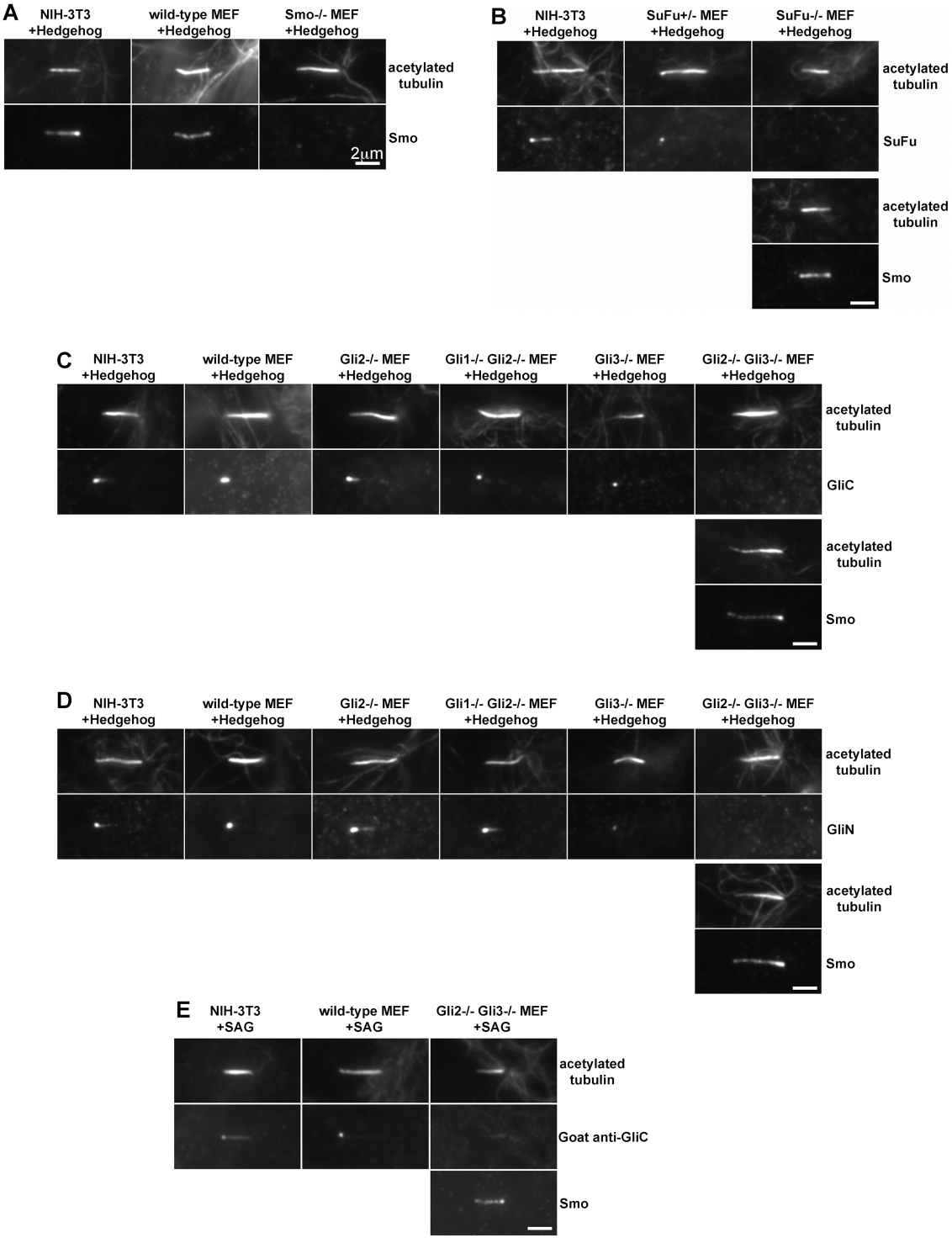

Supplemental Figure 4.S1 Specificity of the novel polyclonal antibodies used for immunofluorescence staining in this study

Supplemental Figure 4.S1 (Continued)

A) Specificity of the rabbit anti-mSmo antibody in immunofluorescence staining
NIH-3T3 cells, wild-type mouse embryonic fibroblasts (MEFs) and Smo-/- MEFs were grown to confluence, starved and stimulated with Shh for 6 hours. The cells were stained with mouse anti-acetylated tubulin antibody (to reveal primary cilia) and affinity-purified rabbit anti-mSmo antibody. Strong staining of cilia is seen in NIH-3T3 cells, wild-type MEFs but not in Smo-/- MEFs. Scale bar is 2 μm.

B) Specificity of the rabbit anti-mSuFu antibody in immunofluorescence staining
NIH-3T3 cells, SuFu+/- MEFs and SuFu-/- MEFs were treated as in A). The cells were stained with mouse anti-acetylated tubulin antibody and affinity-purified rabbit anti-mSuFu antibody. Specific staining of cilia is seen in NIH-3T3 cells and SuFu+/- MEFs, while staining is absent in SuFu-/- MEFs. SuFu-/- MEFs respond to Hh stimulation as shown by Smo recruitment to cilia (bottom panels), demonstrating that the lack of SuFu staining is not due to a defect in signaling at the level of Smo. Scale bar is 2 μm.

C) Specificity of the rabbit anti-GliC antibody in immunofluorescence staining
NIH-3T3 cells, wild-type MEFs, Gli2-/- MEFs, Gli1-/- Gli2-/- MEFs, Gli3-/- MEFs and Gli2-/- Gli3-/- MEFs were treated as in A). The cells were stained with mouse anti-acetylated tubulin antibody and rabbit anti-Gli antibody affinity purified against a C-terminal fragment of human Gli3 (amino acids 1061-1599). Specific staining of cilia is seen in NIH-3T3 cells, wild-type MEFs, Gli2-/- MEFs, Gli1-/- Gli2-/- MEFs and Gli3-/- MEFs. Gli staining is absent in Gli2-/- Gli3-/- MEFs, although Smo is recruited to cilia normally upon Shh stimulation of Gli2-/- Gli3-/- MEFs (bottom panels), demonstrating that the lack of Gli staining is not due to a defect in signaling at the level of Smo. Data in this figure demonstrate that the rabbit anti-GliC antibody recognizes both mouse Gli2 and Gli3 proteins. Scale bar is 2 μm.

D) Specificity of the rabbit anti-GliN antibody in immunofluorescence staining
NIH-3T3 cells, wild-type MEFs, Gli2-/- MEFs, Gli1-/- Gli2-/- MEFs, Gli3-/- MEFs and Gli2-/- Gli3-/- MEFs were treated as in A). The cells were stained with mouse anti-acetylated tubulin antibody and rabbit anti-Gli antibody affinity purified against an N-terminal fragment of human Gli3 (amino acids 1-799). Strong specific staining of cilia is seen in NIH-3T3 cells, wild-type MEFs, Gli2-/- MEFs and Gli1-/- Gli2-/- MEFs. Weak but specific staining is seen in Gli3-/- MEFs. The anti-GliN antibody does not stain Gli2-/- Gli3-/- MEFs, although Smo is recruited to cilia normally upon Hh stimulation of Gli2-/- Gli3-/- MEFs (bottom panels), demonstrating that the lack of Gli staining is not due to a defect in signaling at the level of Smo. These data demonstrate that the anti-GliN antibody recognizes endogenous mouse Gli2 only poorly and most of the signal corresponds to endogenous mouse Gli3 protein, consistent with the staining of overexpressed Gli proteins (not shown). Scale bar is 2 μm.

E) Specificity of the goat anti-GliC antiserum in immunofluorescence staining
NIH-3T3 cells, wild-type MEFs, and Gli2-/- Gli3-/- MEFs were treated as in A). The cells were stained with mouse anti-acetylated tubulin, rabbit anti-Smo, and goat anti-human Gli3C antibodies. Strong specific staining of cilia tips is seen in NIH-3T3 cells and wild-type MEFs, as well as a faint non-specific staining of the cilium shaft. The goat anti-GliC antibody does not stain Gli2-/- Gli3-/- MEFs, although Smo is recruited to cilia normally upon Shh stimulation of Gli2-/- Gli3-/- MEFs (bottom panel). Scale bar is 2 μm.

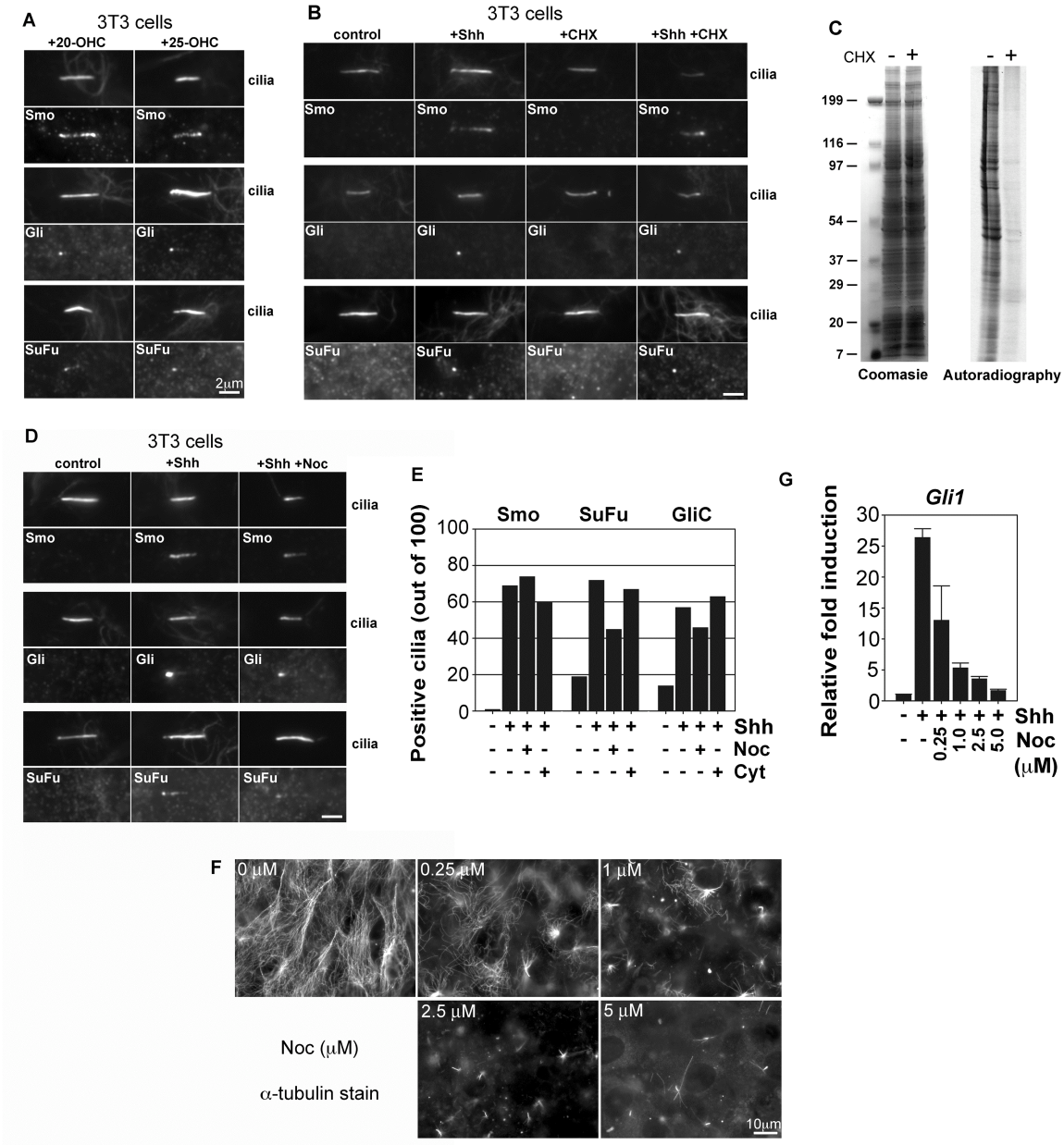

Supplemental Figure 4.S2 The effects of oxysterols, protein synthesis inhibition, and microtubule depolymerization

A) NIH-3T3 cells were treated with 10 microM of either 20-hydroxycholesterol or 25-hydroxycholesterol, for 3 hours. Immunofluorescence micrographs show recruitment of SuFu and Gli to cilia. The oxysterol 7-hydroxycholesterol, which does not activate the Hh pathway, does not recruit SuFu and Gli to cilia above basal levels (not shown). Scale bar is 2 μm.

B) Inhibition of protein synthesis by cycloheximide (CHX) does not block recruitment of Smo, Gli and SuFu to cilia. NIH-3T3 cells were treated or not with Shh for 1 hour, in the presence or absence of CHX (50 micrograms/mL). Scale bar is 2 μm.

C) Inhibition of proteins synthesis by CHX in the experiment in B). NIH-3T3 cells were incubated with or without CHX (50 micrograms/mL), in the presence of 35S-methionine. Total cell lysates were separated by SDS-PAGE and either stained by Coomassie for total protein or autoradiographed to reveal new protein synthesis.

Supplemental Figure 4.S2 (Continued)
D) Microtubule (MT) depolymerization does not affect recruitment of SuFu, Gli and Smo to cilia. NIH-3T3 cells were pre-treated or not with nocodazole (Noc, 2.5 microM) for 1 hour, then stimulated or not with Shh for 3 hours, in the continued presence or absence of Noc. Recruitment of Smo, SuFu and Gli is not affected by MT depolymerization. Scale bar is 2 μm.
E) Cilia counts for the experiment in (D).
F) MT depolymerization by Noc in the experiment in D). NIH-3T3 cells were treated with various concentrations of Noc for 4 hours, and were immunostained for α-tubulin. Even the highest concentration of Noc does not affect the stable MTs in cilia, which are visible against the diffuse cytoplasmic staining due to depolymerized tubulin. Disappearance of cytoplasmic MTs in the presence of increased Noc concentration correlates with the degree of inhibition of Hh signaling by Noc. Scale bar is 10 μm.
G) MT depolymerization by Noc inhibits the transcriptional output of the Hh pathway in a dose-dependent manner. NIH-3T3 cells pre-incubated for 1 hour with the indicated Noc concentrations, were then treated for 3 hours with Shh, in the continued presence of Noc. Transcription of the Gli1 gene was measured by Q-PCR relative to the RPL27 transcript. Error bars represent standard error of three independent experiments.

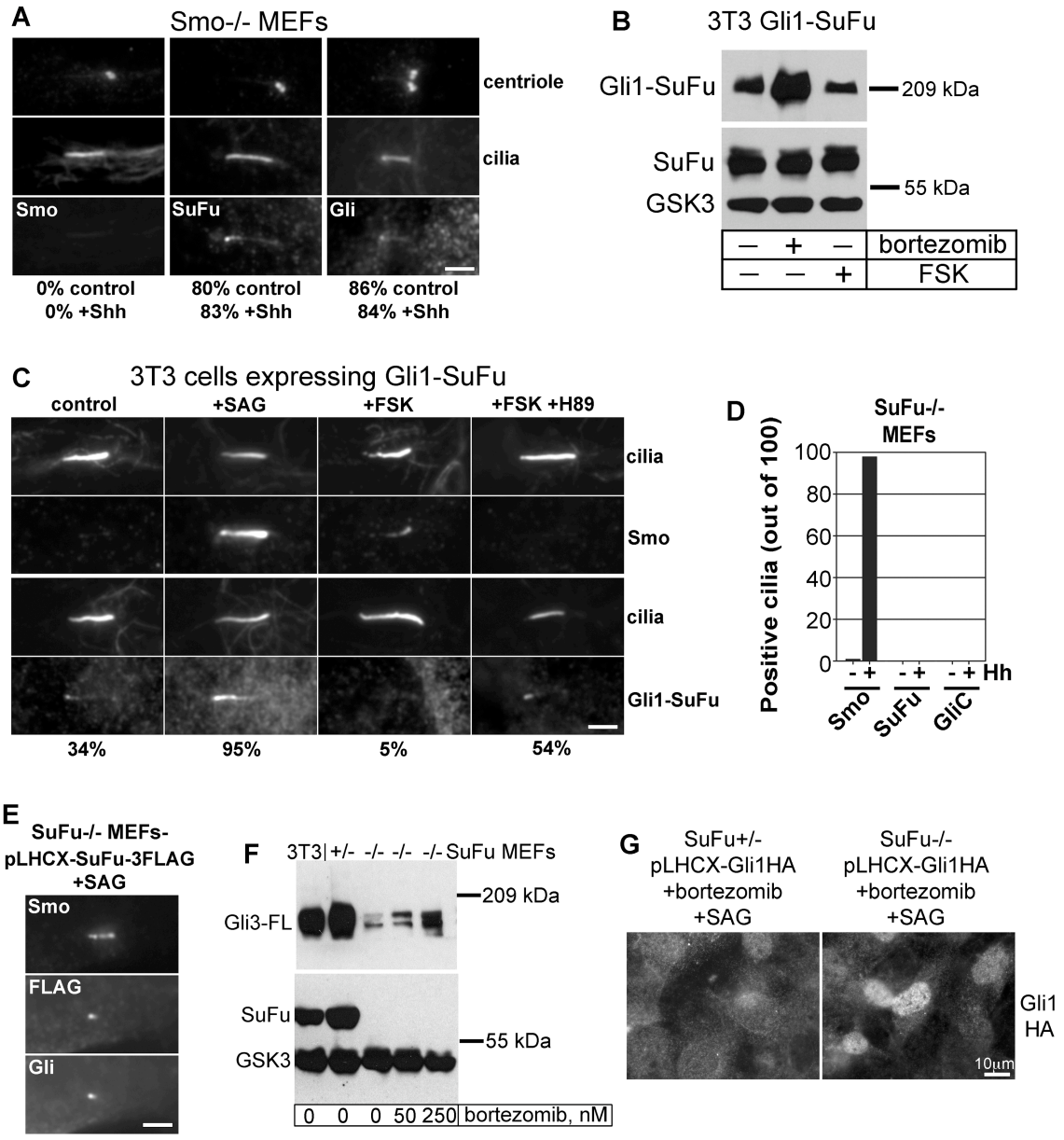

Supplemental Figure 4.S3 Experiments characterizing Smo-/- MEFs, SuFu-/- MEFs, and 3T3 cells expressing Gli1-SuFu fusion

A) SuFu and Gli localize to the tips of cilia in Smo-/- MEFs. Cilia were stained with anti-acetylated tubulin and basal bodies were stained with anti-gamma tubulin. Percentages shown under the bottom panels indicate ciliary localization of Smo, SuFu and Gli, in untreated cells and in cells stimulated overnight with Shh. SuFu and Gli are not recruited to cilia above basal levels following Shh stimulation of Smo-/- MEFs. Scale bar is 2 μm.

B) The effect of forskolin (FSK) on the levels of Gli1-SuFu fusion. NIH-3T3 cells stably expressing Gli1 directly fused to SuFu, were treated overnight with control vehicle, the proteasome inhibitor bortezomib (100 nM), or FSK (10 microM). Expression levels of Gli1-SuFu fusion, endogenous SuFu and GSK3 (loading control) were determined by immunoblotting.

Supplemental Figure 4.S3 (Continued)
C) The effect of FSK on localization of Smo and Gli1-SuFu fusion to cilia is reversed by the small molecule PKA inhibitor, H-89. NIH-3T3 cells stably expressing Gli1-SuFu fusion were treated overnight with control vehicle, SAG (200 nM), FSK (5 microM), or FSK and H-89 (5 and 10 microM, respectively). Recruitment of endogenous Smo to cilia by FSK is reversed by H-89. Ciliary localization of Gli1-SuFu, which is abolished by FSK, is rescued by H-89. Percentages shown under the bottom panels show ciliary localization of the Gli1-SuFu fusion for the various treatments. Scale bar is 2 μm.
D) No Gli signal is present at cilia in SuFu-/- MEFs, while recruitment of Smo to cilia by Shh is normal in SuFu-/- MEFs. The graph shows cilia counts for the experiment shown in figure 4C.
E) Expression of FLAG-tagged SuFu in SuFu-/- MEFs rescues ciliary localization of Gli. SuFu-/- MEFs stably expressing mouse SuFu tagged with 3 FLAG epitopes were stimulated with 100 nM SAG for 6 hours. Endogenous Smo was detected with a rabbit antibody, SuFu-3FLAG was detected with a mouse anti-FLAG antibody and endogenous Gli was detected with a goat antibody. Scale bar is 2 μm.
F) Gli3-FL levels are greatly decreased in SuFu-/- MEFs, compared to SuFu+/- MEFs and to NIH-3T3 cells. Gli3-FL levels are partially rescued by inhibition of the proteasome with bortezomib. Cell cultures were incubated for 6 hours in the absence or presence of bortezomib, and probed with antibodies against GliC, SuFu and GSK3. Lane 1: NIH-3T3 cells, lane 2: SuFu+/- MEFs, lanes 3-5: SuFu-/- MEFs treated with 0, 50, or 250 nM bortezomib, respectively.
G) Overexpressed Gli1 accumulates in the nucleus in SuFu-/- MEFs, but not in SuFu+/- MEFs. The cells shown are from the same experiment as the one in figure 4E. Gli1-HA was overexpressed in both SuFu+/- and SuFu-/- MEFs by stable retroviral transduction, followed by treatment with 2 microM bortezomib for 6 hours. Scale bar is 10 μm.

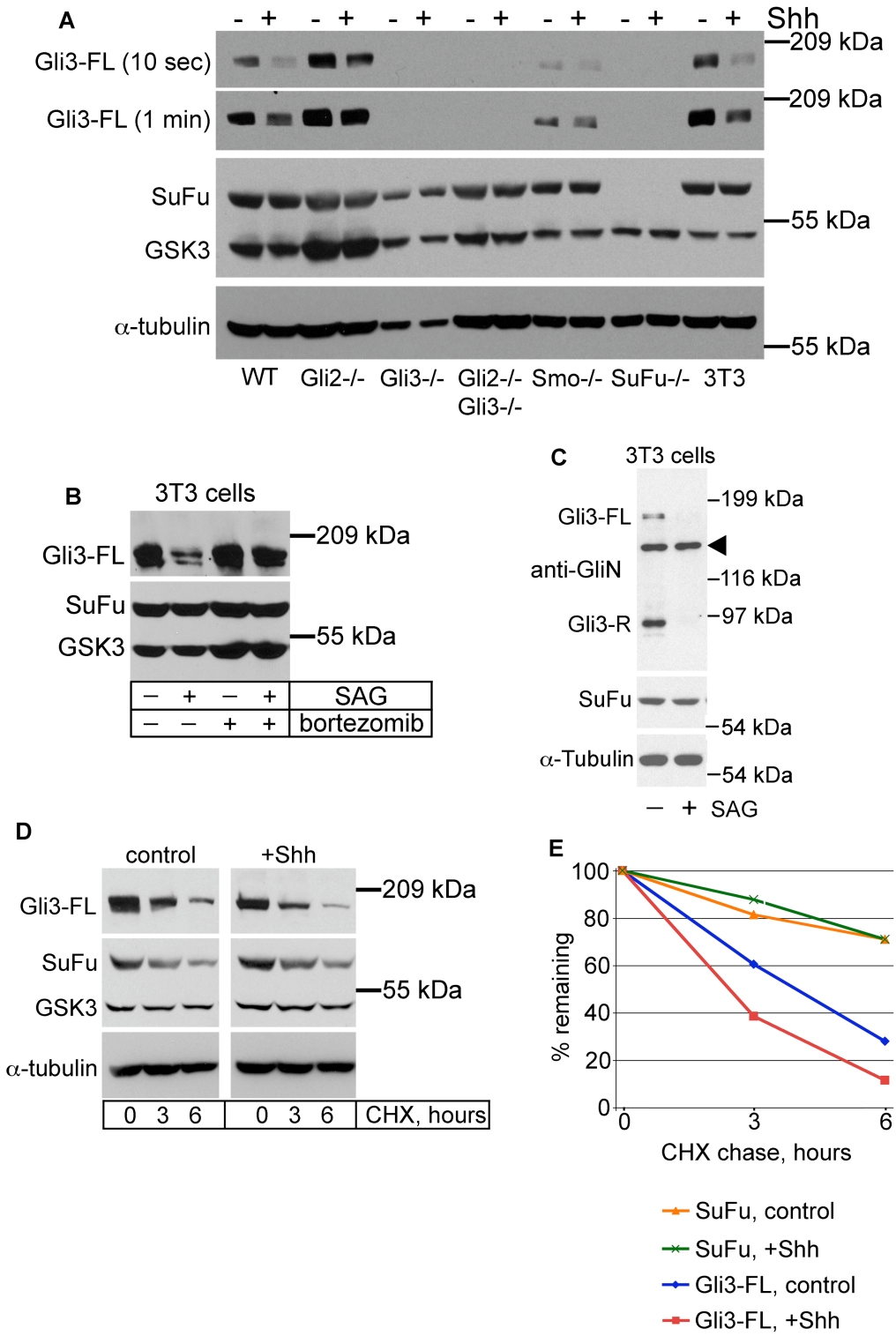

Supplemental Figure 4.S4 Levels of SuFu and Gli3 in the cell lines used in this study

Supplemental Figure 4.S4 (Continued)
A) Effect of Shh stimulation on SuFu and Gli3-FL levels in various cell lines used in this study. Starved, confluent cultures of wild-type MEFs, Gli2-/- MEFs, Gli3-/- MEFs, Gli2-/-Gli3-/- MEFs, Smo-/- MEFs, SuFu-/- MEFs, and NIH-3T3 cells were incubated overnight in the absence or presence of Shh. SuFu, Gli3-FL and the loading controls GSK3 and α-tubulin, were detected by immunoblotting. Two different exposures of the immunoblot for Gli3-FL are shown. Gli3-FL levels decrease during prolonged Shh stimulation in wild-type MEFs, Gli2-/- MEFs, and in 3T3 cells. Gli3-FL levels are not affected by Shh stimulation in Smo-/- MEFs. Gli3-FL is not detectable in MEFs that lack Gli3, as well as in SuFu-/- MEFs, in which Gli proteins are very unstable. SuFu levels and its electrophoretic mobility are not affected by Shh stimulation in any of the cell lines in this panel. Blotting against GSK3 and α-tubulin was used to control for loading.
B) Endogenous Gli3-FL levels are decreased following stimulation of 3T3 cells with 100 nM SAG for 6 hours. Gli3-FL was detected by immunoblotting with anti-GliC antibodies. The decrease in Gli3-FL levels can be reversed by incubation with 2 microM of the proteasome inhibitor bortezomib.
C) The levels of both Gli3-FL and Gli3 repressor (Gli3-R) are decreased following prolonged Hh pathway stimulation. Serum-starved, confluent cultures of 3T3 cells were incubated for 12 hours in starvation media in the absence or presence of 100 nM SAG. Arrowhead indicates a non-specific band.
D) Hh pathway stimulation does not change the half-life of endogenous SuFu but reduces the half-life of Gli3-FL. Confluent, starved 3T3 cells were pre-incubated for 10 minutes with CHX (100 micrograms/mL), followed by incubation with CHX in the absence or presence of Shh, for the indicated amount of time. Endogenous levels of SuFu and Gli3-FL were determined by immunoblotting. Immunoblotting against GSK3 and α-tubulin was used to control loading.
E) Quantification of the experiment in D). The plot shows the percentage of endogenous SuFu and Gli3-FL remaining during the CHX chase, measured relative to the level of α-tubulin.

Supplementary Table 4.S1

Recruitment of Smo, SuFu, Gli2 and Gli3 to primary cilia in NIH-3T3 cells and in various mouse embryonic fibroblast lines

	Smo	**SuFu**	**Gli2 & 3**
Cell Line			
WT 3T3	-, I	+, I	+, I
WT 3T3 + cyclopamine	+	-, N	-, N
WT 3T3 + SANT-1	-, N	-, N	-, N
WT 3T3 + forskolin	+, I	-, N	-, N
WT MEFs	-, I	+, I	+, I
SuFu-/-	-, I	-	-, N
SuFu+/-	-, I	+, I	+, I
Smo-/-	-	+, N	+, N
Smo-/- + forskolin	-	-, N	-, N
Gli2-/-	-, I	+, I	+, I
Gli3-/-	-, I	+, I	+, I
Gli1-/- Gli2-/-	-, I	+, I	+, I
Gli2-/- Gli3-/-	-, I	-, N	-

- = not detectable at cilia without Shh treatment
+ = detectable at cilia without Shh treatment
N = not inducible by Shh
I = inducible by Shh

Mass Spectrometry Results

Peptides of endogenous Gli2 identified in Sufu pulldown

In collaboration with Wilhelm Haas

IPI:IPI00284476.2 Mus musculus (Mouse) PREDICTED: GLI-KRUPPEL FAMILY MEMBER GLI2 ISOFORM 1. [MASS=165031]

METSAPAPAL EKKEAKSGLL EDSSFPDPGK KACPLAVAAA VAAHGVPQQL LPAFHAPLPI DMRHQEGRYH
YDPHSVHSVH GPPTLSGSPV ISDISLIRLS PHPAGPGESP FSAHHPYVNP HMEHYLRSVH SSPTLSMISA
ARGLSPADVA HEHLKERGLF SLAAPGTNPS DYYHQMTLMA SHPTPYGDLL MQSGGAASAP HLHDYLNPVD
ASRFSSPRVT PRLSRKRALS ISPLSDASLD LQRMIRTSPN SLVAYINNSR SSSAASGSYG HLSAGALSPA
FTFPHPINPV AYQQILSQQR GLGSAFGHTP PLIQPSPTFL AQQPMTLTSI STMPTQLSSS SSNCLNDANQ
NKQNSESAVS STVNPITIHK RSKVKTEAEG LRPASPLGLT QEQLADLKED LDRDDCKQEA EVVIYETNCH
WADCTKEYDT QEQLVHHINN EHIHGEKKEF VCRWQACTRE QKPFKAQYML VVHMRRHTGE KPHKCTFEGC
SKAYSRLENL KTHLRSHTGE KPYVCEHEGC NKAFSNASDR AKHQNRTHSN EKPYICKIPG CTKRYTDPSS
LRKHVKTVHG PDAHVTKKQR NDVHVRAPLL KENGDNEASA EPGGRGPEES VEASSTSHTV EDCLHIKAIK
TESSGLCQSS PGAQSSCSSE PSPLGSAPNN DSGMEMPGTG PGSLGDLTAL ADTCPGADTS ALAAPSTGGL
QLRKHMSTVH RFEQLKREKL KSLKDSCSWA GPAPHTRNTK LPPLPVNGSV LENFNNTGGG GPAGLLPSQR
LPELTEVTML SQLQERRDSS TSTMSSAYTV SRRSSGISPY FSSRRSSEAS PLGGLRPHNA SSADSYDPIS
TDASRRSSEA SQCSGGGPGL LNLTPAQQYN LRAKYAAATG GPPPTPLPGL DRVSLRTRLA LLDAPERALP
GACPHPLGPR RGSDGPTYSH GHGHGYAGAA PAFPHEGPNS STRRASDPVR RPDPLILPRV QRFHSTHNMN
PGSLPPCADR RGLHVQSHPS VDSNLTRNAY SPRPPSINEN VVMEAVAAGV DGPGLECDLG LVEDELVLPD
DVVQYIKAHT GGTLDDGIRQ GYPTEGTGFP ENSKLPSPGL QGHRRLAAAD SNMGPSAPGL GGCQLSYSPS
SNLNKSNMPV QWNEVSSGTV DALPTQVKPP PFPHSNLAVV QQKPAFGQYP GYNPQSVQSS SGGLDSTQPH
LQLRGAPSAS RGSYTQQPRQ PAAGSQCLGM SAAMSPQASY SQAHPQLSPN IVSGSLNQFS PSCSNMAAKP
SHLGLPQQME VVPNATIMNG HQREHGVPNS SLAAVSQPHP VLSYPQQDSY QQGSNLLSSH QPGFMESQQN
AGFGLMQPRP PLEPNTASRH RGVRSGQQQL YARTTGQAMV TSANQETAEA MPKGPAGTMV SLAPQPSQDT
GRAQDQNTLY YYGQIHMYEQ NGGCPAVQPQ PPQPQACSDS IQPEPLPSPG VNQVSSTVDS QLLEPPQIDF
DAIMDDGDHS SLFSGALSPT LLHNLSQNSS RLTTPRNSLT LPSIPAGISN MAVGDMSSML TSLAEESKFL
NMMT

ScanF	z	XCorr	ΔCorr	# Ions	*Gene ↓	Redun	-	Peptide
3732	2	3.102	0.298	13/26	IPI00284476	2		K.SGLLEDSSFPDPGK.K
1497	2	2.257	0.373	15/28	IPI00284476	4		R.SVHSSPTLSM*ISAAR.G
6226	2	3.680	0.485	18/30	IPI00284476	3		R.ALSISPLSDASLDLQR.M
6153	2	3.504	0.457	17/30	IPI00284476	3		R.ALSISPLSDASLDLQR.M
4121	2	2.635	0.377	13/26	IPI00284476	3		R.TSPNSLVAYINNSR.S
6390	2	4.274	0.554	25/30	IPI00284476	4		R.LPELTEVTM*LSQLQER.R
2520	2	2.201	0.154	16/20	IPI00284476	4		R.SSGISPYFSSR.R
3260	2	4.237	0.424	21/34	IPI00284476	3		K.YAAATGGPPPTPLPGLDR.V
1384	2	4.365	0.675	21/36	IPI00284476	2		K.GPAGTM*VSLAPQPSQDTGR.A
1590	2	5.337	0.560	23/36	IPI00284476	2		K.GPAGTM*VSLAPQPSQDTGR.A

Mass Spectrometry Results

Peptides of endogenous Gli3 identified in Sufu pulldown

In collaboration with Wilhelm Haas

IPI:IPI00123429.1 Mus musculus (Mouse) ZINC FINGER PROTEIN GLI3. [MASS=173512]

MEAQAHSSTA TERKKAENSI GKCPTRTDVS EKAVASSTTS NEDESPGQIY HRERRNAITM QPQSVQGLNK
ISEEPSTSSD ERASLIKKEI HGSLPHLAEP SLPYRGTVFA MDPRNGYMEP HYHPPHLFPA FHPPVPIDAR
HHEGRYHYDP SPIPPLHVPS ALSSSPTYPD LPFIRISPHR NPTAASESPF SPPHPYINPY MDYIRSLHCS
PSLSMISAAR GLSPTDAPHA GVSPAEYYHQ MALLTGQRSP YADILPSAAT AGAGAIHMEY LHAMDSTRFP
SPRLSARPSR KRTLSISPLS DHSFDLQTMI RTSPNSLVTI LNNSRSSSSA SGSYGHLSAS AISPALSFTY
PSAPVSLHMH QQILSRQQSL GSAFGHSPPL IHPAPTFPTQ RPIPGIPTVL NPVQVSSGPS ESSQSKPTSE
SAVSSTGGPM HNKRSKIKPD EDLPSPGSRG QQEQPEGTTL VKEEADKDES KQEPEVIYET NCHWEGCTRE
FDTQDQLVHH INNDHIHGEK KEFVCRWLDC SREQKPFKAQ YMLVVHMRRH TGEKPHKCTF EGCTKAYSRL
ENLKTHLRSH TGEKPYVCEH EGCNKAFSNA SDRAKHQNRT HSNEKPYVCK IPGCTKRYTD PSSLRKHVKT
VHGPEAHVTK KQRGDMHPRP PPPRDSGSHS QSRSPGRPTQ GAFGEQKELS NTTSKREECL QVKTVKAEKP
MTSQPSPGGQ SSCSSQQSPI SNYSNSGLEL PLTDGGSVAD LSAIDETPIM DSTISTATTA LALQARRNPA
GTKWMEHIKL ERLKQVNGMF PRLNPILPSK APAVSPLIGN GTQSNNNYSS GGPGTLLPSR SDLSGVDFTV
LNTLNRRDSN TSTISSAYLS SRRSSGISPC FSSRRSSEAS QAEGRPQNVS VADSYDPIST DASRRSSEAS
QGDGLPSLLS LTPVQQYALK AKYAAPTGGP PPTPLPHMER LSLKTKMALL GEGRDSGVTL PPVHPPRRCS
DGGGHTYRGR HLMPHDALAN SVRRDSDPVR TVSENMSLAR VQRFSSLNSF NPPNLPPSVE KRSLVLQNYT
RQESSQPRYF QASPCPPSIT ENVALEALTM DADANLNDED LLPDDVVQYL NSQNQTGYGQ QLQSGISEDS
KVAHEPEDLD LAGLPDSHVG QEYPALEQPC SEGSKTDLPI QWNEVSSGTS DLSSSKLKCG QQRPRQQPRG
FGLYNNMVVH PHNLWKVGTG PAGGYQTLGE NSSTYNGPEH FAIHSGDGLG TNGNTFHEQP FKTQQYGSQL
NRQPLTSSAL DHACGTGIQG SKLKGNSLQE NGGLLDFSLS VAPNELAGNT VNGMQTQDQM GQGYIAHQLL
SGSMQHQGPS RPGQQVLGQV GATSHINIYQ GTESCLPGTQ DNSSQPSSMA AIRGYQPCAS YGGNRRQAMP
RGNLTLQQGQ LSDMSQSSRV NSIKMEAQGQ SQQLCSTVQN YSGQFYDQTM GFSQQDRKAG SFSLSDANCL
LQGTCTENSE LLSPGANQVT STVDSFESHD LEGVQIDFDA IIDDGDHTSL MSGALSPSII QNLSHSSSRL
TTPRASLPFP IPIHGHHQHG YRGYEFFADL PCRRKQVPCS YAVGGRQGGP QTQRLK

ScanF	z	XCorr	ΔCorr	# Ions	*Gene	↓	Redun	-	Peptide
1057	3	2.764	0.480	25/76	Gli3	1			K.AVASSTTSNEDESPGQIYHR.E
1449	2	4.600	0.486	21/28	Gli3	1			R.NAITM*QPQSVQGLNK.I
470	2	1.812	0.154	11/22	Gli3	1			K.ISEEPSTSSDER.A
4478	2	3.595	0.292	18/26	Gli3	1			R.TSPNSLVTILNNSR.S
950	2	3.084	0.307	18/24	Gli3	1			R.GQQEQPEGTTLVK.E
887	2	2.717	0.370	16/24	Gli3	1			R.GQQEQPEGTTLVK.E
954	2	2.053	0.143	11/24	Gli3	1			R.GQQEQPEGTTLVK.E
637	2	2.319	0.300	13/26	Gli3	0			R.SPGRPTQGAFGEQK.E
7089	2	3.543	0.349	18/30	Gli3	0			R.SDLSGVDFTVLNTLNR.R
6376	2	2.814	0.417	13/30	Gli3	0			R.SDLSGVDFTVLNTLNR.R
1732	2	5.318	0.585	22/34	Gli3	0			R.GNLTLQQGQLSDM*SQSSR.V
1570	2	4.664	0.626	22/34	Gli3	0			R.GNLTLQQGQLSDM*SQSSR.V
1811	2	4.347	0.579	20/34	Gli3	0			R.GNLTLQQGQLSDM*SQSSR.V

Analysis of two mass spectrometry experiments from Nov 14 2007.

Repeat hits for Ski interactors

In collaboration with Wilhelm Haas

Went through the two Ski datasets (Boiling after acid elution, and the newest dataset without acid elution) to identify proteins that show up in both.

A list of proteins that appeared in both, had above-average Light to Heavy ratios, and were not obvious contaminants or FLAG-tag binders:

Presented here in order of descending signal-to-noise ratio of the first Ski IP. Only cDNA FLJ31747 had a light to heavy ratio (significantly higher than average).

reference	annotation
IPI00032003	EMERIN.
IPI00014400	DNAJ HOMOLOG SUBFAMILY B MEMBER
IPI00024642	ISOFORM 1 OF COILED-COIL DOMAIN-CONTAINING PROTEIN 47 PRECURSOR.
IPI00220739	MEMBRANE-ASSOCIATED PROGESTERONE RECEPTOR COMPONENT 1.
IPI00166785	TRANSMEMBRANE PROTEIN 32 PRECURSOR.
IPI00009320	ISOFORM 1 OF TRANSMEMBRANE PROTEIN 85
IPI00107357	ISOFORM 2 OF CLEFT LIP AND PALATE TRANSMEMBRANE PROTEIN 1.
IPI00025874	DOLICHYL-DIPHOSPHOOLIGOSACCHARIDE--PROTEIN GLYCOSYLTRANSFERASE 67 KDASUBUNIT PRECURSOR.
IPI00180956	UNCHARACTERIZED PROTEIN ENSP00000308452.
IPI00027547	DERMCIDIN PRECURSOR.
IPI00010740	ISOFORM LONG OF SPLICING FACTOR, PROLINE- AND GLUTAMINE-RICH.
IPI00009841	CDNA FLJ31747 FIS, CLONE NT2RI2007377, HIGHLY SIMILAR TO RNA-BINDING PROTEIN EWS.

SuFu phosphorylation sites: S301, S346, S349

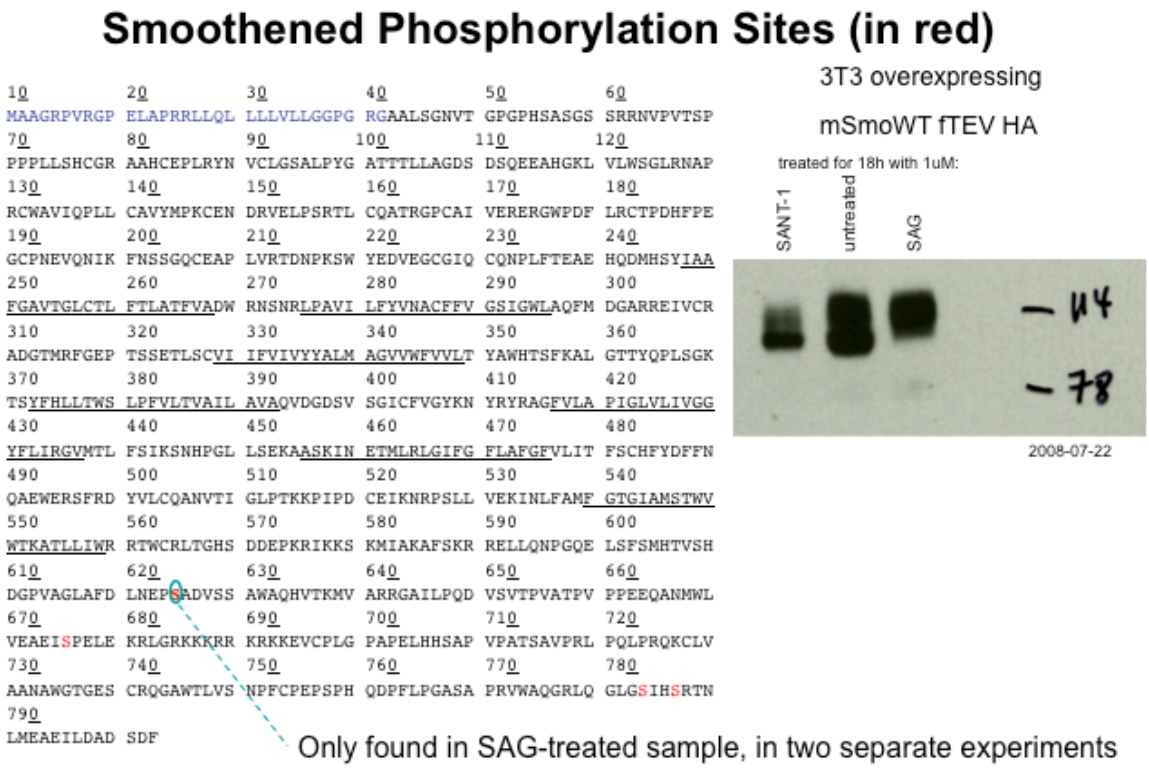

In collaboration with Wilhelm Haas